Topological Order and Universal Properties of Gapped Quantum Systems

by

Heidar Moradi

A thesis
presented to the University of Waterloo
in fulfillment of the
thesis requirement for the degree of
Doctor of Philosophy
in
Physics

Waterloo, Ontario, Canada, 2018

This thesis consists of material all of which I authored or co-authored: see Statement of Contributions included in the thesis. This is a true copy of the thesis, including any required final revisions, as accepted by my examiners.

I understand that my thesis may be made electronically available to the public.

Statement of Contributions

Chapter 2 of this thesis consists of material from the paper [1], co-authored with Xiao-Gang Wen.

Chapter 3 of this thesis consists of material from the paper [2], co-authored with Huan He and Xiao-Gang Wen.

Chapter 4 of this thesis consists of material from the paper [3], co-authored with Xiao-Gang Wen.

Chapter 5 of this thesis consists of material from the paper [4], co-authored with Wen Wei Ho, Lukasz Cincio, Davide Gaiotto, and Guifre Vidal.

Chapter 6 of this thesis consists of material from the paper [5], co-authored with Wen Wei Ho, Lukasz Cincio and Guifre Vidal.

Chapter 7 of this thesis consists of unpublished material [6], co-authored with Wen Wei Ho.

Abstract

Phases of gapped quantum liquids are topologically ordered and have very interesting physical features that are completely robust against any local perturbation that do not close the bulk energy gap. These universal properties are hidden in the ground states of these systems, as different patterns of many-body long-range entanglement. In this thesis we study the universal properties of gapped quantum liquids from various perspectives. We propose the notion of *Universal Wavefunction Overlap* as a way of extracting almost complete information about the underlying entanglement structure in a system with topological order. We propose an efficient numerical methods to use these universal wavefunction overlaps as topological order parameters and demonstrate their usefulness with concrete numerical computations. In $2 + 1D$ these overlaps correspond to known quantities and contain information about anyonic particle excitations. We show that in $3+1D$, these overlaps contain information about linked multi-string braiding processes, in particular three-string braiding.

In the second part of this thesis, we study boundary physics of systems with topological order. We investigate the correspondence between edge and entanglement spectra for non-chiral topological systems in general and with the presence of extra symmetries and dualities. We also show that by local deformations of the fixed-point wavefunction on non-chiral topological orders, all possible edge theories can be extracted from its entanglement Hamiltonian. Finally we introduce the notion of fermionic gapped boundary and see how the phase diagram of the simplest topological orders get enriched.

Acknowledgements

I would like to thank my supervisor Xiao-Gang Wen for his supervision, patience, constant support and understanding, even during hard personal times. I have been very fortunate to have had the opportunity to learn from a physicist of his caliber. His deep physical intuition is unmatched, and his enthusiasm and encouragement has benefited me a great deal. I also would like to give a very special thank you to Guifre Vidal for his collaborations, encouragement, humor and personal support when I needed it the most.

During my time at the Perimeter Institute no collaboration was closer than the one with Wen Wei Ho. We have spent countless hours on blackboards discussing physics, leaving no question undiscussed and in the process learned and developed a tremendous amount. I also would like to thank my other collaborators Huan He, Davide Gaiotto, Lukasz Cincio, Faroogh Moosavian and Apoorv Tiwari.

Very importantly I would like to thank Roger Melko as my co-supervisor for making sure that my absentmindedness did not get in the way of fulfilling the formal requirements of the university. Roger Melko, Davide Gaiotto and Anton Burkov deserve thanks for valuable advice and feedback during commitee meetings and the defence of this thesis.

I am very thankful to Marcel Franz, the external examiner of this thesis, for the time spent reading this thesis carefully and asking interesting questions during the defence.

Finally I am very grateful to the Perimeter Institute for providing a wonderful work enviroment and to all the good friends that made my time there special.

Dedication

To my family.

Table of Contents

List of Tables

List of Figures

Chapter 1

Introduction

Much of condensed matter physics and high energy physics has arguably developed on drastically opposite philosophical foundations. High energy physics, in particular particle physics, has succesfully developed pursuing a reductionistic worldview. Condensed matter physics, on the other hand, has primarily investigated the unimaginable rich physics that can emerge at low energies in systems with often boring and mundane high-energy degrees of freedom. This program of *emergent phenomena* was more concretely explicated in Philip Warren Anderson's influential essay *More is Different* [7]. The rich emergent physics arises in various phases of matter and one of the principal goals of condensed matter physics is to classify and characterize the physics of all possible phases of matter.

For a long time Landau's paradigm of spontaneous symmetry breaking [8, 9, 10, 11] was the main framework to understand different states of matter. Within this paradigm, phases of matter are characterized by local order-parameters $\vec{\phi}(x)$ and phase transitions by spontaneous breaking of some global symmetry G down to a subgroup H. For continuous symmetries, these phases will generally have gapless excitations called goldstone modes [12] and their dynamics are described by nonlinear σ-models on G/H. Futhermore, depending on space dimensionality and the topology of the target space of the order-parameter $\vec{\phi}(x)$, these systems can have topological defects such as vortices, flux tubes, hedgehogs and so on [13]. The Landau paradigm provides a rich framework where a large class of interesting phases of matter can be analyzed. This together with Landau's Fermi liquid theory [14, 15] was for a long time thought to be the almost definitive theory for phases of matter.

With the discovery of Integer Quantum Hall Effect (IQHE) [16] and later Fractional Quantum Hall Effect (FQHE) [17, 18] it became apparent that there exists states of matter that are beyond the framework provided by Landau's theory. This particular class of state

of matter was dubbed Topological Order [19] and exists in quantum systems with an energy gap in the spectrum.

Often systems with topological order are presented as very exotic states of matter with certain exotic behavior, which makes these systems appear very rare and artificial. In this thesis we will have a different perspective, we will be thinking about topological order as the most protected, robust and universal features of a system protected by nothing but an energy gap. From this point of view, topological order is not something rare and artificial but rather more appropriately something very deep and fundamental.

The main aim of this thesis is to study universal properties and invariants of gapped quantum systems from various different perspectives. In the following sections we will make a more careful definition of gapped quantum systems and introduce equivalence relations between these that will define phases of matter with topological order. It turns out that topological order belongs to a subclass of gapped systems called stable gapped quantum liquids, which arguebly contain more or less all physically interesting gapped systems. We will then discuss the entanglement properties of the ground states of gapped quantum liquids and their importance. Then we will move on to universal properties of excitations in systems with topological order. For bulk excitations, it turns out that long-range features like statistics are universal; particles in 2+1D have anyonic statistics while in higher dimensions we have anyonic strings, membranes etc. Finally we will discuss the universal boundary physics of such states of matter.

The point of the discussion below is to help the reader understand what topologial order is, starting from basic principles, and put the contributions of this thesis into context.

1.1 Gapped Quantum Systems

Any finite system naturally has gaps in the energy spectrum and therefore in order to properly define the notion of gapped and gapless systems we need to consider the thermodynamic limit. We wil primarily have spin systems (built out of qubits) in mind, but the definitions can be readily extended to much more general degrees of freedom.

Image we have a sequence of graphs (or lattices) $\mathcal{G}_{N_k}$ of N_k nodes (where $N_k \to \infty$ as $k \to \infty$, $c_1 < \frac{N_{k+1} - N_k}{N_k} < c_2$ and $c_1, c_2 > 0$) embedded on a manifold $\mathcal{M}$ with no boundary. At each node $i \in \mathcal{G}_{N_k}$ place a local Hilbert space $\mathcal{H}_i$ and construct the spaces $\mathcal{H}_{N_k}$ as

$$\mathcal{H}_{N_k} = \bigotimes_{i \in \mathcal{G}_{N_k}} \mathcal{H}_i, \tag{1.1}$$
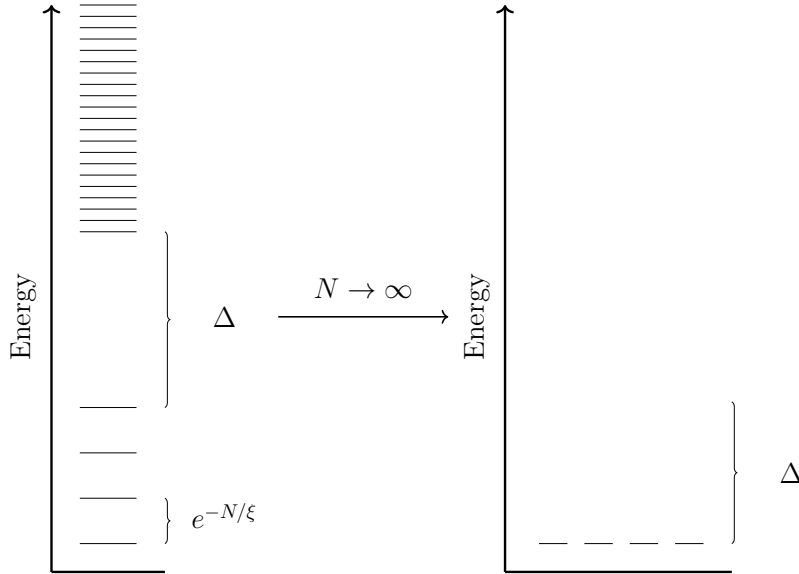
Figure 1.1: Energy spectrum of Gapped Quantum Systems in the thermodynamic limit. For finite systems, below an energy gap Δ there can exist nearly degenerate states that become exactly degenerate in the thermodynamic limit and form a ground state subspace $\mathcal{V} \subset \mathcal{H}$. The excited states above the energy gap can form a contiuum in the thermodynamic limit.

for any $k \in \mathbb{N}$. A sequence of local Hamiltonians $\{H_{N_k}\}_{k \in \mathbb{N}}$ on $\{\mathcal{H}_{N_K}\}_{k \in \mathbb{N}}$ is called a **Gapped Quantum System** if there exists a constant energy window of size Δ such that (a) there are no eigenstates in this window for any N_k and (b) the number of states below this window is constant and their energy difference approaches zero as $N_k \to \infty$ (see figure 1.1) [20]. For each system size, we will call the subspace spanned by the states under the gap Δ, for the ground state subspace $\mathcal{V}_{N_k}$ or in other words $\mathcal{H}_{N_k} = \mathcal{V}_{N_k} \oplus \cdots$.[1]

Equipped with a notion of a gapped quantum system, we would like to introduce equivalence relations that define different phases of matter. We will primarily follow the approach of [20] and [24], but also see [25] for some interesting insight into gapped quantum liquids and beyond.

Loosely speaking, imagine we have the space of all gapped quantum systems $\mathcal{G}$ which is a subset of all theories $\mathcal{G} \subset \mathcal{T}$ (which also contains gapless theories). We would like to think that each connected component of this space corresponds to a gapped quantum

---

[1]Note that a generic Hamiltonian is gapless [21] and gapped systems are in this sense rare. But even worse, the problem of proving that a system is gapped or gapless turns out to be undecidable [22, 23].
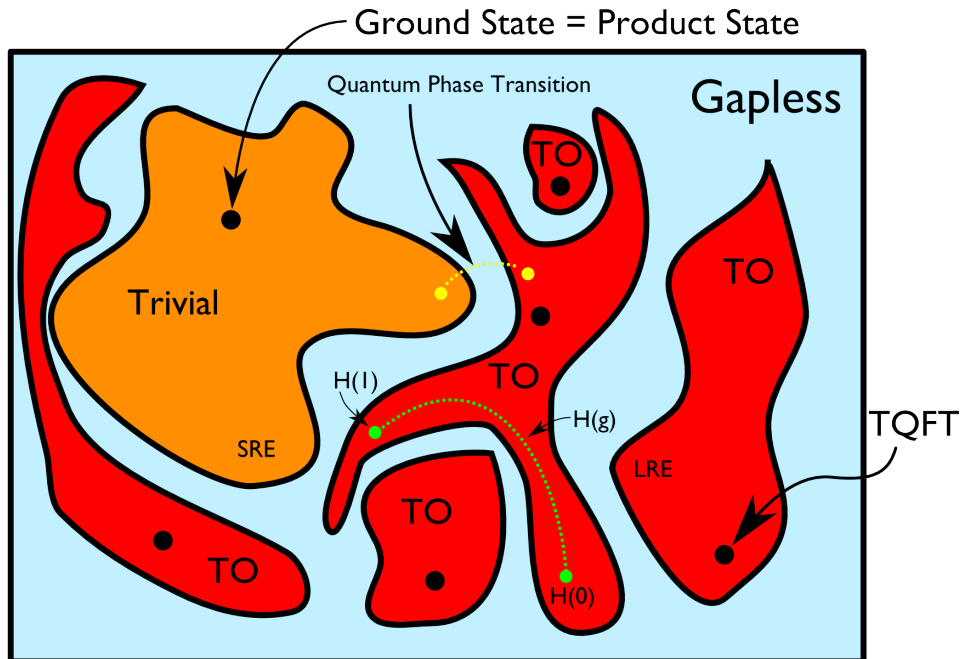
Figure 1.2: The figure illustrates the space of gapped quantum systems (more accurately, stable gapped quantum liquids) inside the space of all theories. The blue regions correspond to gapless systems, the orange region to short-range entangled systems while the red regions to long-range entangled systems. The black dots are (gapped) RG fixed points where all local degrees of freedom have been integrated out and only the universal physics is left behind. SRE systems flow to a trivial theory with product state ground states, while LRE systems are expected to flow to a Topological Quantum Field Theory (TQFT) at low energies. Each connected component corresponds to a different topological phase.

phase, and gapped phases are thus classified by $\pi_0(\mathcal{G})$ (see figure 1.2). More precisely we would like to say that two gapped Hamiltonians[2] H_0 and H_1 belong to the same phase iff there exists a path of Hamiltonians $H(\lambda)$ such that $H(0) = H_0$ and $H(1) = H_1$ and $H(\lambda)$ is a gapped quantum system for any $\lambda \in [0, 1]$. This is an equivalence relation and equivalence classes under $H_0 \sim H_1$ correspond to gapped quantum phases. We can also

---

[2]The notion of Gapped Quantum System is based on a sequence of Hamiltonians, defining the thermodynamic limit. But we will often just talk about them as a single Hamiltonian, as the meaning is clear.

think about this on the level of quantum states. Given ground states $|\psi(0)\rangle$ and $|\psi(1)\rangle$ of H_0 and H_1, respectively, there exists a (finite-time) quasi-adiabatic continuation between these states

$$|\psi(\lambda)\rangle = U(\lambda)|\psi(0)\rangle, \qquad U(\lambda) = \mathcal{T} \exp\left(-i\int_0^\lambda ds\tilde{H}(s)\right) \tag{1.2}$$

where $\mathcal{T}$ is the path-ordering operator and $\tilde{H}(s)$ is a local Hamiltonian. Again the Hamiltonian $H(\lambda) = U(\lambda)H_0U(\lambda)^\dagger$ is gapped along the path and $|\psi(\lambda)\rangle$ is its ground state. The form of $\tilde{H}(s)$ is discussed in [24, 26, 27]. This approach has the advantage of being very intuitive and connect to concepts of topology of the space of gapped quantum systems $\mathcal{G}$, but it turns out that there is a subtle step needed in order to define topological order. We will formulate the above in a slightly different way, which also connects to more physical concepts like entanglement.

It is known that a unitary finite time evolution with a local Hamiltonian can be simulated with a constant depth quantum circuit [24]. This means that we can replace the time evolution in the definition above with unitary transformations of the form

$$U_{\text{circ}} = U_{\text{pwl}}^{(1)}U_{\text{pwl}}^{(2)}\ldots U_{\text{pwl}}^{(N)}, \tag{1.3}$$

where each of the N-layers is a piecewise local unitary operator $U_{\text{pwl}}^{(a)} = \prod_i U^i$, $a = 1,\ldots,N$, where $\{U_i\}$ is a set of unitary operators that act on non-overlapping regions. A transformation of the form (1.3) is called a **Local Unitary** (LU) transformation.

1.2 Gapped Quantum Liquids

Topological order is deeply connected to patterns of long-range entanglement of gapped quantum systems, but in order to define these notions more precisely, it turns out that we need to break gapped quantum systems into smaller classes. Not all gapped quantum systems are well-behaved in the thermodynamic limit, since in the sequence $\{H_{N_k}\}_{k\in\mathbb{N}}$, Hamiltonians of different system sizes are not necessarily related to each other. We will here define a subclass that consist of, as far as I am aware, almost all examples of physically relevant gapped systems.

Starting with a Hamiltonian H_{N_k} on $\mathcal{H}_{N_k}$, define a Hamiltonian on the Hilbert space $\mathcal{H}_{N_{k+1}}$ by adding a trivial system on the new degrees of freedom

$$H_{N_k} \longrightarrow \hat{H}_{N_{k+1}} = H_{N_k} + \sum_{i=1}^{N_{k+1}-N_k} Z_i, \tag{1.4}$$

5

$$\ldots \xleftrightarrow{gLU} H_{N_k} \xleftrightarrow{gLU} H_{N_{k+1}} \xleftrightarrow{gLU} H_{N_{k+2}} \xleftrightarrow{gLU} \ldots$$

$$\big\uparrow LU \qquad\qquad \big\uparrow LU \qquad\qquad \big\uparrow LU$$

$$\ldots \xleftrightarrow{gLU} H'_{N_k} \xleftrightarrow{gLU} H'_{N_{k+1}} \xleftrightarrow{gLU} H'_{N_{k+2}} \xleftrightarrow{gLU} \ldots$$

Figure 1.3: Diagram showing the equivalence relation between two stable gapped quantum liquids $\{H_{N_k}\}_{k\in\mathbb{N}}$ and $\{H'_{N_k}\}_{k\in\mathbb{N}}$. If we ignore the condition that each layer should be related by a gLU transformation, then this defines an equivalence relation on gapped quantum systems (which includes non-liquids).

where Z_i is the Pauli Z matrix acting on site i.[3] If for a sequence $\{H_{N_k}\}_{i\in\mathbb{N}}$ for any H_{N_k}, the ground state subspace of $\hat{H}_{N_{k+1}}$ can be transformed to the ground state subspace of $H_{N_{k+1}}$ by a LU transformation, then we say that H_{N_k} and $H_{N_{k+1}}$ are connected by a **generalized Local Unitary** (gLU) transformation. We call a gapped quantum system satisfying this, a **Gapped Quantum Liquid**. A gapped quantum liquid is **stable**, if the ground state degeneracy is protected against any local perturbation.[4]

We can now modify our previous definition of gapped quantum phases: two stable gapped quantum liquid systems are equivalent $\{H_{N_k}\} \sim \{H'_{N_k}\}$ if the ground state subspace of H_{N_k} can be mapped to the ground state subspace of H'_{N_k} by a LU transformation for all N_k (see figure 1.3).[5] These equivalence classes, we will call **topological order** (TO). The class that contains a Hamiltonian with a product state ground state, such as $H = \sum_i Z_i$, will be called **trivial topological order**.

To summarize, the point of the above discussion was to point out that we are not investigating universal properties of general gapped quantum systems but gapped quantum liquids, which is not a big restriction as it contains most physically interesting gapped systems. The equivalence relation based on gLU transformations, where we allow the addition of a trivial system, is analogous to *stable equivalence* of vector bundles where instead of considering homotopy equivalence the equivalence is loosened to also allow the

---

[3]On a more general non-qubit system, one can add any gapped trivial term instead. The important thing is that the new ground state should be the old ground state tensored with a product state.

[4]It turns out that gapped quantum liquids, besides topological order, contain symmetry breaking states and other states with unstable degeneracy. The stability condition picks out the robust gapped systems. It is possible to change the gLU transformation into a so-called **generalized stocahstic local transformation** (gSL), which only captures the systems with topological degeneracy. For a more detailed discussion, see [20].

[5]This is just another way of expressing the definition that two Hamiltonian are equivalent, if they are connected along a stable gapped liquid path.

addition (Whitney summing) of trivial bundles and thus making the classification more stable. This is exacly what is used to classify topological insulators and superconductors[6], where one allows the addition of trivial bands (bundles) and thus obtains a classification based on topological K-theory [28]. The Bott periodicity of this "periodic table", is a consequence of stable equivalence.

Note that gapped non-liquids can still have some sort of well-behaved thermodynamic limit. For example if we modify (1.4) such that we add copies of the smaller system, possibly with product states too, we can then relate $H_{N_k} \leftrightarrow H_{N_{k+1}}$ via a LU transformation by dissolving such a non-trivial layer. Systems with such a thermodynamic limit, will be different from conventional topological order. It is believed that so-called *fracton topological order* [29, 30, 31, 32, 33] and systems built out of layers of lower-dimensional topological order, belong to gapped non-liquid systems [20, 25].

1.3   Long-Range Entanglement

As discussed above, we can think about the definition of topological order from the point-of-view of states in the Hilbert space. From equation (1.4) it is clear how the gLU transformation acts on the ground state subspaces $\{\mathcal{V}_{N_k}\}_{k \in \mathbb{N}}$; first the states are mapped to the larger Hilbert space by tensoring them with a product state and then they are acted upon by a LU transformation. The important point to note is that each layer of a LU transformation (1.3), separately acts on a local patch with a unitary operator. We can think of this local action as a local modification of the state's entanglement structure. Any state that can be mapped into a product state (zero entanglement) by a gLU transformation[7], we call a **short-range entangled** (SRE) state as any entanglement can be removed by locally modifying the entanglement structure, over a finite number of layers. Any state that cannot be transformed into a product state we will call a **long-range entangled** (LRE) state.

Comparing with the above discussion about topological order, we see that short-range entangled states are ground states of system with trivial topological order. While different non-trivial topological orders have ground states that differ by their patterns of long-range entanglement. This is a very interesting and significant understanding; topological order is inherently related to global many-body (long range) entanglement of ground states and

---

[6]In the language of this thesis, these correspond to free fermion SPT and (invertible) SET phases.

[7]As mentioned earlier, this is not completely accurate as gLU transformations cannot map symmetry breaking states into product states. The correct transformation to use are generalized stochastic local (gSL) transformations. For more discussion see [20].

these patterns of entanglement are responsible for all the universal physics of the stable gapped quantum liquid phase.

1.3.1 Topological Entanglement Entropy

Now the natural question is, how can we detect and distinguish different topological orders from studying their ground states? A natural quantity to study is the entanglement entropy. Consider a 2+1D topological order on a manifold of simple topology, like the two-sphere S^2. Split the Hilbert space into two spacial regions L and R, $\mathcal{H} = \mathcal{H}_L \otimes \mathcal{H}_R$, with a boundary length of L between these regions. From the pure state $\rho_{S^2} = |\psi\rangle\langle\psi|_{S^2}$ contructed from a ground state $|\psi\rangle$ on S^2, we can get a mixed state on L as $\rho_L = \mathrm{Tr}_R (\rho_{S^2})$. The entanglement entropy of ρ_{S^2} is defined as the Von Neumann entropy of ρ_L

$$S(\rho_L) = -\mathrm{Tr}\left(\rho_R \log \rho_R\right). \tag{1.5}$$

It turns out that this entanglement entropy has the following area-law scaling [34, 35, 36]

$$S = \alpha L - \gamma + \mathcal{O}(L^{-\nu}), \qquad \nu > 0. \tag{1.6}$$

This might be a surprise, as random pure states are expected to have volume-law scaling [37]. But there is a simple intuitive way to understand this result. Since gapped systems have very short-range correlations, one expects the entanglement to be fairly short range. One can make a simple (and quite trivial) toy model by tensoring valence bonds $|i,j\rangle = \frac{1}{\sqrt{2}}(|\uparrow_i\downarrow_j\rangle - |\downarrow_i\uparrow_j\rangle)$ for random sites i and j that are fairly close to each other. Now splitting the Hilbert space into L and R, it is clear that only the valence bonds crossing the boundary are "cut" and thus contribute to the entanglement entropy, hence this gives us an area-law scaling. The coefficient α is, however, clearly not universal. Note that this implies that groundstates of gapped systems belong to a tiny submanifold of Hilbert space and part of the motivation of the development of tensor networks is to parametrize this submanifold.

The constant subleading term γ is called the ***topological entanglement entropy*** [34, 35] and is universal, meaning invariant under gapped local perturbations of the system or equivalently invariant under gLU transformations.[8] This quantity turns out to be equal to $\gamma = \log \mathcal{D}$ where $\mathcal{D}$ is the total quantum dimension and directly related to physical properties of topological excitations and the ground state degeneracy [38]. This implies that long-range entanglement is like a constant entanglement over the full system, capable

---

[8]Actually it is even stronger, it is invariant under gSL transformations.

of detecting global (topological) features of the manifold the system resides on. In fact, the ground state degeneracy directly depends on the (co-)homology groups of the underlying manifold. Note that if $\gamma \neq 0$ we are guaranteed to have topological order, but even when $\gamma = 0$ we can still have topological order.[9] The topological orders with $\gamma = 0$ are called **invertible topological order** and have no topological excitations in the bulk but do have protected gapless boundary modes. It turns out that one can detect these (or gapless boundaries of so-called chiral topological order) from the **entanglement spectrum**, which is the spectrum of the entanglement Hamiltonian $H_{\text{ent.}}$ defined as [39, 40]

$$\rho_L \equiv \frac{1}{Z} \exp\left(-H_{\text{ent.}}\right). \tag{1.7}$$

The entanglement spectrum contains more information about the entanglement structure of the state $|\psi\rangle$. In chapters 5 and 6 we study the universal content of the entanglement spectrum for non-chiral topological orders.

The topological entanglement entropy can be generalized to higher dimensions [41, 42] and to topologically non-trivial bipartitions [43]. The entanglement entropy has several weaknesses, for example it contains very limited information about the universal physical properties of the system and it is hard to compute numerically.

In the next section we will discuss some very fundamental properties of the ground states of quantum liquids, in particular local indistinguishability and propose another method to extract topological information from the ground states.

1.3.2   Local Indistinguishability and the Mapping Class Group

Note that the stability condition implies that the ground states $|\psi_i\rangle$ of gapped quantum liquids are locally indistinguishable, they can only be distinguished globally. Or in other words, they form superselection sectors where

$$\langle \psi_i | \hat{\mathcal{O}} | \psi_j \rangle = C_{\mathcal{O}} \delta_{ij}, \tag{1.8}$$

---

[9]There are two competing definitions of topological order in the field, which we will call the **east-coast** and **west-coast** definitions. The east-coast definition is the one used in this thesis. The west-coast definition only considers states with $\gamma \neq 0$ as having topological order. The difference between these are so-called *invertible topological order*, which are considered to be trivial in the west-coast definition. These invertible TOs have the property that they can be made trivial by stacking them on each other. One can think of the west-coast definition as using a stronger equivalence relation, besides what we have discussed it requires that two gapped systems that are related through stacking of invertible TOs, to be considered equivalent.

in the thermodynamic limit[10] for any local operator $\hat{\mathcal{O}}$. If any local operator existed that had non-zero overlap between the different ground states, it could be used to split the degeneracy. This, however, does not have to hold for non-local operators. It turns out, as is highly plausible from the discussion so far, that the ground state degeneracy depends only on the topological structure of the underlying manifold such as the number of non-contractable homology cycles. Thus these states can be related to each other by non-local operators that act on non-contractible homology cycles (lines, surfaces etc.), signifying the non-trivial long-range entanglement hidden in these states.

A natural question is, can we extract more powerful information about the long-range entanglement structure in these states than given by the entanglement entropy? We explore this question in chapter 2. For any d-dimensional manifold M^d we can associate a group called the **_Mapping Class Group_** $\texttt{MCG}(M^d)$ that has an action on the homology cycles of M^d.[11] Any group element $A \in \texttt{MCG}(M^d)$ induces an action M_{ij}^A on the ground state subspace $\mathcal{V}$ which rotates the ground states into each other. In other words, the ground state subspace on M^d forms a representation space of the group $\texttt{MCG}(M^d)$. It is hard to implement this action on the ground state subspace for a generic gapped quantum liquid (especially on the lattice)[12], but it is easy to implement an operator $\hat{\mathcal{O}}_A$ acting on the full Hilbert space for any $A \in \texttt{MCG}(M^d)$. This will however bring us out the ground state subspace and give us a very small overlap. The question is, can we extract the universal pieace M_{ij}^A from this overlap? In chapter 2 we conjecture the following scaling behavior

$$\langle \psi_i | \hat{\mathcal{O}}_A | \psi_j \rangle = e^{-\alpha V + o(1/V)} M_{ij}^A, \tag{1.9}$$

where V is the volume of M^d. For a given topological order, we thus have mapping class group representations on essentially any compact manifold. Each of these representations constitute universal data that are not only much stronger than the topological entanglement entropy, but might provide complete set of invariants for any topological order with gappable boundary.[13]

The exponential volume-law scaling makes it very hard to compute this quantity directly, numerically. In chapters 2 and 3 we propose a simple method to compute the

---

[10]In finite systems with non-zero correlation length there might be very small off-diagonal terms, originating from the exponentially small energy-split among the states. See figure 1.1.

[11]For some intuition behind mapping class groups see section 2.B.

[12]Unless the Hamiltonian has some very special symmetries.

[13]The mapping class group is related to so-called topologically non-trivial diffeomorphisms. One could in principle detect features of gapless boundaries, like the chiral central charge, by considering Berry-phases of trivial paths of the diffeomorphism group, inducing a gravitational Chern-Simions term [44]. But these are non-trivial to implement on the lattice. Although see [45].

universal piece of this overlap from local information of a single ground state in the form of a tensor network. These universal matrices can be used as topological order parameters, detecting phase-transitions between different topological systems.

In 2+1D these quantities are well-known and directly related to physical features of topological order, such as particle statistics and fusion. In chapter 4 we study a subset of these invariants for $3 + 1D$ gapped liquids and show that they contain vital information about statistics of excitations, such as information about a braiding process containing three strings.

1.4   Topological Excitations

Having defined the notion of phases of gapped quantum liquids, discussed their ground states and their relation to entanglement, we will turn to one of the most important universal physical features of these systems, namely the unusual statistics of bulk excitations. It turns out that systems with topological order have anyonic particle-like excitations in 2+1D and higher-dimensional objects in higher dimensions.

Let us restrict the discussion to point-like excitations. Let us imagine that we have N particles on $\mathbb{R}^d$ and we will assume that particles cannot be on top of each other. If we furthermore require that all particles are indistinguishable, we must identify all points related by permutation of particles. The configuration spaces of such systems are

$$\mathcal{C}(\mathbb{R}^d, N) = \mathbb{R}^{dN} - \Delta, \qquad \mathcal{C}^{\mathrm{id}}(\mathbb{R}^d, N) = \left(\mathbb{R}^{dN} - \Delta\right)/S_N, \tag{1.10}$$

where $\Delta = \{(\mathbf{r}_1, \ldots, \mathbf{r}_N) \in \mathbb{R}^{dN} \,|\, \mathbf{r}_i = \mathbf{r}_j \text{ for some } i \text{ and } j\}$ is the set of configurations where the position of at least two particles coincide and S_N is the permutation group. The topological classification of paths in these spaces that return to the original configuration is given by [46]

$$\pi_1(\mathcal{C}(\mathbb{R}^d, N)) = \begin{cases} 0, & d \geq 3, \\ P_N, & d = 2 \end{cases}, \qquad \pi_1(\mathcal{C}^{\mathrm{id}}(\mathbb{R}^d, N)) = \begin{cases} S_N, & d \geq 3, \\ B_N, & d = 2 \end{cases}, \tag{1.11}$$

where B_N is the braid group while P_N is the colored braid group, where the strands are colored so only braids that return to their original spot are allowed. This implies that only bosons and fermions, corresponding to the symmetric and anti-symmetric one-dimensional representations of S_N, can exist for $d \geq 3$.[14]

---

[14] It turns out that any higher dimensional representations of S_N which is compatible with locality,

In 2+1D we see that the exchange statistics of indistinguishable particles are given by representations of B_N, while double exchange of two distinguishable particles correspond to representations of P_N [53, 54].[15] However, for a given gapped system with topological order there will be several types of particles. Each type with self-statistics corresponding to a whole family of representations of B_N (depending on how many particles has been created), while each pair with mutual-statistics corresponding to a family of representations of P_N. And what if a single particle encircles several other particles, which representation corresponds to this scenario? It naively appears to be very complicated to describe particle-statistics in 2+1-dimensions. However, we will below sketch how a natural algebraic theory appears for gapped quantum liquids, that takes care of all this.[16]

1.4.1 Topological Types and Fusion

Consider the energy distribution of an excited state over space. If the excited state has a higher energy density than that of the ground state only locally near a point x, we may consider that energy lump as a point-like excitation. If this excited state can be created by a local operator $\mathcal{O}_x$, $|x\rangle = \mathcal{O}_x|\psi\rangle$, we will call the particle at x for a *topologically trivial excitation* while if this is not the case we will say it is a *topologically non-trivial excitation*. In general we say that two excitations are of the same **topological type**, if we can go from one to the other by the action of local operators near the location of the excitations. Excitations of topologically trivial type are often denoted as **1**. It turns out that topologically non-trivial excitations are created by line-like operators with the end-points being the locations of the excitations. Each topological type can thus be thought of as a superselection sector [56].

We can always modify our Hamiltonian H to $H + V_{\text{trap}}$ in order to trap a few excitations locally but individually far from each other, such that the ground state of the gapped system

---

can be decomposed into tensor products of local Hilbert spaces of fermions and bosons with additional quantum numbers [47, 48, 49]. In [50] Wilczek proposed to consider projective particle statistics based on projective representations of S_N, but it was later shown to be inconsistent with locality [51]. Something similar to non-abelian statistics for (pseudo-)particles in 3+1D is however possible, called projective ribbon permutation statistics [52, 49].

[15]On topologically non-trivial manifolds we will get different results. For example, on a torus T^2 we will get the torus-braid group and as particels can now also wind around the non-contractible cyles of the torus.

[16]This discussion partially follows lectures by Xiao-Gang Wen and [55]. We will not attempt to be rigorous, but rather give an idea of how the underlying mathematical structure appears and what its physical meaning is.
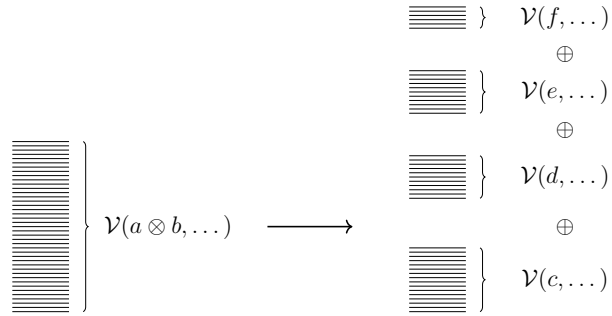
Figure 1.4: On the left we have the degenerate subspace $\mathcal{V}(a \otimes b, \dots)$, where $\dots$ represent other excitations far from a and b. The degeneracy is robust against local perturbations if a and b are far from each other. If a and b are brought near each other, or perturbations in a region containing both a and b are allowed, the degeneracy will split. The right side represents maximal splitting from a generic perturbation. Each block remain degenerate. To represent this energy splitting, we write $a \otimes b = c \oplus d \oplus e \oplus f$.

$H + V_{\text{trap}}$, is an excited state of H.[17] We will by a_i denote an excitation of topological type a at the position x_i. The ground state subspace of $H + V_{\text{trap}}$ corresponding to trapping $(a_1, b_2, \dots)$ will be denoted by $\mathcal{V}(a_1, b_2, \dots)$, called the **fusion space**, with the dimension $\dim \mathcal{V}(a_1, b_2, \dots) \geq 1$. If the degeneracy of the fusion space $\mathcal{V}(a_1, \dots)$ is robust against any local perturbations near x_1 we say that a is a **simple type** while if the degeneracy is lifted we call it a **composite type** and think of it as being composed of several simple types $a = x \oplus y \oplus \dots$. Note that the lifting of degeneracy implies the following vector space decomposition

$$\mathcal{V}(a_1 \oplus b_1, c_2, \dots) = \mathcal{V}(a_1, c_2, \dots) \oplus \mathcal{V}(b_1, c_2, \dots). \tag{1.12}$$

We will assume that we have a finite number of simple topological types, also called anyon types given by the set $\mathcal{A} = \{a, b, c, \dots\}$. If we always have that $\dim \mathcal{V}(a_1, b_2, \dots) = 1$, we say that the topological order is **abelian**, otherwise we say that it is **non-abelian**.

We can also define the notion of fusion of two anyons. Imagine a_1 and b_2 at positions x_1 and x_2, respectively, are much closer to each other than all other excitations. We will denote this by $a \otimes b$ and this can in general be considered as a composite type because by acting with local operators in a region containing both x_1 and x_2, we might be able to split the degeneracy as $\mathcal{V}(a \otimes b, \dots) = \bigoplus_{x \in \mathcal{A}} N_x^{ab} \mathcal{V}(x, \dots)$, see figure 1.4. Based on this

---

[17]Note that the system $\tilde{H} = H + V_{\text{trap}}$, while being gapped with robust degeneracy against any local perturbations, is not a quantum liquid as $\tilde{H}_{N_k}$ and $\tilde{H}_{N_{k+1}}$ are not related by a gLU [20].

13

energy splitting, we will define a **fusion ring** by the following **fusion rules**

$$a \otimes b = \bigoplus_{x \in \mathcal{A}} N_x^{ab} x, \tag{1.13}$$

where N_k^{ij} is an positive integer matrix saying how many times a given anyon type appears in the decomposition. As we can fuse particles in different orders, we need to demand associativity of the fusion product $(a \otimes b) \otimes c = a \otimes (b \otimes c)$ which gives us constraints on the fusion coefficients

$$\sum_x N_x^{ab} N_d^{xc} = \sum_x N_x^{bc} N_d^{ay}. \tag{1.14}$$

We will furthermore assume that the product (1.13) is abelian, $a \otimes b = b \otimes a$ or equivalently $N_x^{ab} = N_x^{ba}$, since there is no canonical way to define the order of fusion. This is true for $2 + 1$-dimensions and above, but in $1 + 1$-dimensions this cannot be assumed.

In [57], it was shown that topological excitations come in pairs and are created by line operators, where the end-points are the excitations. If the line is turned into a loop, the excitations annihilate. This implies that for each simple type $a \in \mathcal{A}$, we have another $\bar{a} \in \mathcal{A}$ such that a fusion channel to the vacuum (trivial type) exists: $a \otimes \bar{a} = \mathbf{1} \oplus \dots$, here $\bar{a}$ can be thought of as an anti-particle but we will call it the dual of a. The dual is unique and for simple objects they have a unique channel fusing to the vacuum. Therefore we have that $\dim \mathcal{V}(a_1, \bar{a}_2) = 1$ where the basis vector will be graphically represented as

$$|a_1, \bar{a}_2\rangle = \quad \underset{1}{\overset{a \quad b}{\bigvee}} \quad . \tag{1.15}$$

In general we can represent a fusion process by

$$\underset{c}{\overset{a \quad b}{\bigvee}}_{\mu} \quad , \tag{1.16}$$

where μ represents possible multiplicities in the fusion channel $\mu = 1, \dots, N_c^{ab}$. For notational simplicity we will here ignore these multiplicities. Therefore the basis vectors of the

14

fusion space with n excitations of type a, $\mathcal{V}(a_1, \ldots, a_n)$, is given by

$$\tag{1.17}$$

This graphical notation makes it easier to label all the states in the fusion spaces and has an intuitive physical interpretation: it is a space-time diagram showing the process of creating particles from the vacuum when read from bottom up. We can directly compute the dimension of this fusion space

$$\dim \mathcal{V}(a_1, \ldots, a_n) = \sum_{x_i} N_{x_1}^{aa} N_{x_2}^{x_1 a} \ldots N_{\mathbf{1}}^{x_{n-2} a} = \left([\mathbf{N}^a]^{n-1} \right)_{a\mathbf{1}} \sim d_a^n + O\left(1/n\right), \tag{1.18}$$

where we have defined the matrices $(\mathbf{N}^a)_{bc} = N_c^{ba}$ and d_a is the largest eigenvalue of $\mathbf{N}^a$.[18] The large n-scaling of the fusion space dimension seems to imply that we can think of each anyon of type a to be associated with a local Hilbert space of dimension d_a. However d_a is often not an integer and the d_a^n scaling is only accurate for large n. This is a very important point, as the Hilbert space does not have a standard tensor product structure but the information is rather stored non-locally among all the excitations. Only when brought near each other, can we act on this space with local operators and split the degeneracy. The number d_a is called the **quantum dimension** of anyon type a and $\mathcal{D}^2 = \sum_{a \in \mathcal{A}} d_a^2$ is the **total quantum dimension** and can be extracted from the ground state through the topological entanglement entropy $\gamma = \log \mathcal{D}$.

Imagine we chose a different basis of the fusion spaces by fusing in a different order, these must be related by a basis change. These basis changes can be built from the most basic one involving three anyons,

$$\tag{1.19}$$

---

[18]The *Perron-Frobenius theorem* ensures that a real square matrix with positive entries, has a unique largest real eigenvalue and all components of the corresponding eigenvector can be made stricly positive.

where the basis change coefficients are often called F-symbol. From this we can compute the basis change coefficient for larger number of anyons, however there might be many different ways to step by step go from one basis to another. In the case of four anyons, there are two ways to go from fusing from left to fusing from right. Since the coefficient in both cases must match, this gives us constraints of the F-symbols schematically of the form $\sum FFF = \sum FF$. This equation is known as the ***pentagon equation***. Remarkably, due the *McLane Coherence theorem* if the pentagon equation is satisfied, all other basis changes in $\mathcal{V}(a_1, b_2, \dots)$ with (1.19) will automatically be consistent.

Before turning to braiding, let us reflect over what we have done. Usually local degrees of freedom, say $s = \frac{1}{2}$ spins, carry their own local Hilbert spaces $\mathcal{H}_i$. Fusing two spins $\frac{1}{2} \otimes \frac{1}{2}$, gives rise to the "fusion" of their individual Hilbert spaces $\mathcal{H}_1 \otimes \mathcal{H}_2$. But clearly anyons do not behave the same way, the fusion space is a collective space shared among all particles and stored non-locally. Adding another anyon to the system, the fusion space changes in a highly non-trivial way. It is therefore hard to describe the anyons directly, we have instead tried to extract information about them by studying the relations between them. For example the fusion of two anyons were defined through degeneracy splitting of the fusion spaces, which is shared with many other anyons. Even though the fusion spaces do not have a nice tensor product structure like in the case of spins, the fusion rules $a \otimes b$ do give us many of the same properties. The idea of studying objects through their relationship with other objects, rather than the structure of the objects themselves is the essence of ***category theory***. What we have constructed so far is called a ***symmetric unitary fusion category***, where the objects are the anyon type $\mathcal{A}$ and the fusion states are the morphisms. The graphical notation (1.16) is literally the relation between different anyons (objects).

1.4.2 Braiding

Having discussed the algebraic theory describing topological excitations in a gapped quantum liquid, we will now turn to braiding.

Imagine we adiabatically tune V_{trap} such that the simple type a_1 at location x_1 is rotated around itself by 2π. The states in $\mathcal{V}(a_1, b_2, \dots)$ can potentially acquire a geometric phase[19] $e^{i\theta_a}$. The phase θ_a is called the ***topological spin*** of anyon type a. We can implement this in our graphical notation by giving the lines a framing and think of them as ribbons, thus whenever we undo a twist in the ribbon the corresponding state acquires a phase $e^{i\theta_a}$.

---

[19]It turns out that it is enough to assume that it is just a phase, and not a unitary matrix.

It turns out that the right way to define the data for braiding is by introducing the so-called R-symbol, defined graphically by

$$
\underset{c}{\overset{b\quad\ a}{\bigvee}} = R_c^{ba}\ \underset{c}{\overset{b\quad a}{\bigvee}}\ .
\tag{1.20}
$$

The R-matrix cannot be arbitrary and must satisfy certain non-trivial constraints which comes from consistency, one can go from one diagram to another in multiple ways giving us multiple mappings between these states and consistency requires them to be equal. Starting with three anyons, similar to the pentagon equation, we can derive a consistency relation of the schematic form $RFR = \sum FRF$ that the R and F symbols must satisfy. This is called the **hexagon equation**. Again the McLane Coherence theorem ensures that no other consistency relations are needed.

Any solution of the pentagon and hexagon equations, will give us a consistent anyon model and correspond to a particular topological order in $2+1D$. If start with the graphical notation (1.17), we can braid the anyons in any arbitrary way. By using the F and R-symbols, eq. (1.19) and (1.20), we can turn this braid diagram back into (1.17). This gives us a map on the fusion space that is nothing but the wanted Braid group representations discussed earlier.

The mathematical structure behind this is called a **modular tensor category** (MTC),[20] and $2 + 1D$ topological orders can be classified by classifying MTCs. It naively appears that the solution space of the pentagon and hexagon equations form a continuous algebraic variety, but it turns out that they also containg gauge freedoms and after a gauge fixing, the solution space becomes discrete. We say that MTCs are *rigid*, meaning that no continuos deformations are possible. The classification of MTCs is an active research direction [58].

These equations first appeared in the work of Moore and Seiberg on $1 + 1D$ Rational Conformal Field theories [59, 60] which in turn are very closely related to topological order in $2 + 1D$ [61, 62]. We will however not go into this very deep and interesting direction.

Important for this thesis are two crucial pieces of universal data in a MTC called the

---

[20]Stricly speaking, we have only presented part of the definition of a MTC here.

modular S and T matrices[21]

$$S_{ab} = \overset{a \quad b}{\bigcirc\!\!\!\bigcirc} = \frac{1}{\mathcal{D}} \sum_{x \in \mathcal{C}} N_x^{ab} d_x \frac{e^{i\theta_x}}{e^{i\theta_a} e^{i\theta_b}}, \tag{1.21}$$

$$T_{ab} = \delta_{ab} e^{i\theta_a}. \tag{1.22}$$

These matrices generate a projective representation of $SL(2,\mathbb{Z})$ and satisfy the relations,

$$(ST)^3 = e^{\frac{2\pi i}{8} c_-} C, \quad S^2 = C, \quad C^2 = 1 \tag{1.23}$$

where c_- is called the chiral central charge and is another universal quantity. Note that knowing S and T, gives us c_- mod 8, we will explain why when discussing boundary physics. For abelian topological orders with N anyons these reduce to $S_{ab} = \frac{1}{N^{1/2}} \frac{e^{i\theta_{a+b}}}{e^{i\theta_a} e^{i\theta_b}}$, $T_{ab} = \delta_{ab} e^{i\theta_a}$. Here the T matrix is just the self-statistics while the S matrix gives us the mutual particle statistics (up a normalization). Thus S and T matrices contain information about statistics of particle excitations. Despite being properties of excitations, they can be computed from the ground states by the universal wavefunction overlap (1.9) as representations of the mapping class group of the torus.

It turns out that from these matrices one can compute the fusion rules, given by the Verlinde formula [63]. Knowing the fusion rules, one can solve the pentagon and hexagon equations and potentially reconstruct the whole catagory theory. Thus until recently it was believed that the S and T matrices can be used to compute any universal quantity in the MTC, but counter examples were recently found [64, 65, 66]. New invariants were proposed, but they are also in principle computable as mapping class group representations.[22]

For more details about modular tensor categories and their application to describe anyon models, see [67, 56, 68].

A final note before we end this section. We have learned that topological excitations of gapped quantum liquids form degenerate fusion spaces that are stored non-locally and thus completely protected against local perturbations as long as the anyons are well separated. Not only that, we can act on this space using braiding of particles which is a non-local

---

[21]This diagramatic notation can be defined by introducing inner products to our current construction. In order to save space, we will not go through the details here.

[22]The smallest known examples are several rank 49 categories corresponding to discrete gauge theories $G = \mathbb{Z}_{11} \rtimes \mathbb{Z}_5$ with certain group cohomology twists $[\omega] \in H^3(\mathbb{Z}_{11} \rtimes \mathbb{Z}_5, U(1))$. The group is of order 55, and there are 5 inequivalent twists that produces a rank 49 category.

operation and thus also protected against local perturbations. These important properties has given rise to the proposal of using non-abelian anyons to do quantum computation, an idea going under the name ***topological quantum computation*** [69, 70, 71]. Thus topological order is a physical mechanism for fault tolerant error correction, rendering millions of redundant qubits, as needed in conventional error correction codes, unnecessary.

1.4.3 Excitations in 3+1D

A bosonic topological order can only have bosonic and (emergent) fermionic particle excitations in $3 + 1D$ as seen from (1.11). However, now we can also have string-like excitations[23] which opens up new and interesting possibilities. As mentioned previously, we already know an example of such a topological order, namely the S-wave superconductor. Here the string-like excitations are nothing but Abrikosov vortex strings [72] (known as Nielsen-Olesen strings in high-energy physics [73]).

In [74] it was shown that the statistics of N *unlinked* string-like excitations are governed by the ***Loop Braid Group*** LB_N. This group has two classes of generators, the first corresponds to braiding the ith and $i + 1$th string worldsheets around each other[24]

$$s_i = \qquad . \tag{1.24}$$

These generators satisfy the the following relations

$$
\begin{aligned}
s_i s_j &= s_j s_i, & &\text{for} \quad |i - j| > 1, \\
s_i s_{i+1} s_i &= s_{i+1} s_i s_{i+1}, & &\text{for} \quad 1 \le i \le N - 2, \\
s_i^2 &= 1, & &\text{for} \quad 1 \le i \le N - 1,
\end{aligned}
\tag{1.25}
$$

which forms to a permutation subgroup $S_N \subset LB_N$. This is intuitive to understand as if we shrink the strings to points, the worldsheets become the worldlines of particles and

---

[23]Actually we must have string-like excitations in order to have a non-anomalous topological order. In 2+1D we can have string-like excitations in anomalous topological systems, which are unstable unless on the boundary of a $3 + 1D$ topological system.

[24]The graphics has been borrowed from [74].

from (1.11) we know that the statistics are given by S_N. The other class of generators correspond to string excitations trading places by letting one of them go through the other

$$\sigma_i = \quad\raisebox{-2em}{\scriptsize $i \quad\ i+1$}\raisebox{-2.5em}{} \quad . \tag{1.26}$$

These generators satisfy the relations

$$
\begin{aligned}
\sigma_i\sigma_j &= \sigma_j\sigma_i, && \text{for} \quad |i-j| > 1, \\
\sigma_i\sigma_{i+1}\sigma_i &= \sigma_{i+1}\sigma_i\sigma_{i+1}, && \text{for} \quad 1 \le i \le N-2,
\end{aligned}
\tag{1.27}
$$

which interestingly form a braiding subgroup of the loop braiding group $B_N \subset LB_N$. These two subgroups are intertwined inside LB_N through the mixed relations

$$
\begin{aligned}
s_i\sigma_j &= \sigma_j s_i, && \text{for} \quad |i-j| > 1, \\
s_i s_{i+1}\sigma_i &= \sigma_{i+1} s_i s_{i+1}, && \text{for} \quad 1 \le i \le N-2, \\
\sigma_i\sigma_{i+1} s_i &= s_{i+1}\sigma_i\sigma_{i+1}, && \text{for} \quad 1 \le i \le N-2.
\end{aligned}
\tag{1.28}
$$

The loop braid group LB_N only describes braiding processes with unlinked string excitations, however in $3+1D$ we can have many other interesting braiding processes. For example we can have braiding processes of strings that are linked with each other in complicated ways. Or particle-string braiding, for example of the Aharonov-Bohm type of more nontrivial type where particle worldlines and string worldsheets form complicated links.[25]

Let us consider one particularly simple, but very important, type of linked string excitation. Imagine we have N strings of types $a, b, \ldots$ with a base string of type X threading them all, see figure 1.5. Due to the base loop X, it is clear that the other strings cannot shrink into a point and cannot perform braids of the type described by the generators s_i (1.24). Braid processes of the σ_i type (1.26) is still possible and this implies that the statistics of these loops are governed by the usual braiding group B_N. Besides braiding,

---

[25]It is very straightforward to write down $3 + 1D$ topological quantum field theories describing these linking processes. Any BF-type theory has Aharonov-Bohm type braiding, abelian three-loop braiding exist in $A \wedge A \wedge dA$ twisted theories, non-abelian three-string braiding and abelian four-string braiding in A^4 twisted theories, more complicated processes with one particle and two strings are given by $A \wedge A \wedge B$ twists. The discussing of these theories has not been included in this thesis as many related results were published by other authors before completion.
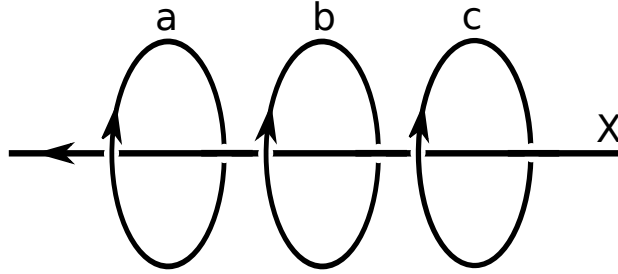
Figure 1.5: Linked string configuration with strings of type $a, b, c, \ldots$ threaded by a string of type X.

we can also fuse the strings $a \otimes_X b$, with the base loop X present, similar to $2+1D$. This implies that for this type of linked excitations we can associate fusion spaces $\mathcal{V}_X(a, b, \ldots)$ and inherit the algebraic structure from $2+1D$ such as F_X and R_X-symbols and topological spins $\theta_{a;X}$ [75]. Note that the reference to the base loop X is crucial as which MTC describing the braiding and fusion of the strings $a, b, c, \ldots$ can depend on X. This all says that the category theory describing $3+1D$ topological order $\mathcal{C}^{3D}$, must have many non-trivial MTCs $\mathcal{C}^{2D}$ "embedded" within it.

In chapter 4, using the universal wavefunction overlaps proposed in chapter 2, we extract representations of the mapping class group of the three-torus, $\text{MCG}(T^3) = SL(3, \mathbb{Z})$, from ground state wavefunctions of gapped quantum liquids. We show that these universal quantities can be used to extract the following dimensional reduction of topological orders

$$\mathcal{C}^{3D} = \bigoplus_X \mathcal{C}_X^{2D}, \tag{1.29}$$

where the sum is over string types. Here C_X^{2D} is the MTC that describes the fusion and braiding of strings $a, b, c, \ldots$ while penetrated by a base loop X. Such a linked-braiding process is called ***three-string braiding***.

This type of linked-braiding process is one of many possible in $3+1D$, where many cannot be described using dimensional reduction techniques. The construction of the proper (higher) category $\mathcal{C}^{3D}$ which provides a complete description of $3+1D$ topological orders is an active research direction.

1.4.4 Bosonic vs Fermionic Locality

The notion of "locality" and "local operators" has been crucial for most of the discussion above, but there is an important subtlety we need to point out. We usually think of our

full Hilbert space as having a tensor product decomposition $\mathcal{H} = \bigotimes_i \mathcal{H}_i$ where $\mathcal{H}_i$ is a Hilbert space for the degree of freedom located at i. Usually we think of a local operator as only having support on a small connected region and commute with local operators that have support far away. However, this excludes fermionic operators which do not commute but rather anti-commute at long-separations and in this sense seem non-local. When defining gapped quantum systems, topological type etc. it is therefore important to distinguish between bosonic and fermionic locality. In a system with fundamental bosonic degrees of freedom, like spin systems, we will only allow bosonic local operators and call the corresponding topological system for **bosonic topological order**. While in a fermionic system, like an electronic system, where the fundamental fermion appears in the spectrum we can allow fermionic local operators as we want to consider a local electron to be a trivial particle. These types of topological systems are called **fermionic topological order**.

Note that in a bosonic system we can have emergent fermions, but these are topological excitations and do not change the nature of locality. However in fermionic systems we can have a scenario where the local fermionic excitations are confined at low energies, and thus bosonic locality emerges. Fractional Quantum Hall systems are fermionic topological orders. S-wave superconductors correspond to Higgsing a $U(1)$ gauge theory to a $\mathbb{Z}_2$ gauge theory since the Higgs field, the cooper pair, has charge 2. So despite originating from fundamental fermionic degrees of freedom, superconductors are topologically ordered with emergent bosonic locality [76]. Another example is the large U limit of the Hubbard model, which is a fermionic theory, which can lead to gapped spin liquids with bosonic topological order [77].

In the discussion above (and most of this thesis), we will be working with bosonic topological order. However, in chapter 7 this distinction of locality is crucial as we argue that interfaces of different types of locality must be studied as they are relevant for experimental scenarios.

1.5 Boundary Physics

Having discussed the ground states and bulk excitations of systems with topological order, we will now discuss interesting universal features of the boundary physics. From very early on it was realized that Integer Quantum Hall systems (a fermionic invertible topological order in our nomenclature) posses quantized gapless edge modes that are completely protected against local perturbations [78]. It was later realized that Fractional Quantum Hall systems have similar properties, with boundaries forming chiral Luttinger liquids [79, 80] and the universal boundary dynamics in general described by chiral Wess-Zumino-Witten

theories. The boundary physics has also been central in the experimental studies of FQHE. It is now understood that boundaries of gapped quantum liquids are much richer yet and even useful for classifying topological orders in different dimensions.

Let us first define different types of boundaries. If we put a stable gapped quantum liquid H on a manifold with boundary M, we have to specify boundary conditions BC on ∂M. If the gapped quantum liquid remains gapped on a manifold with the boundary condition BC, we will say that the pair (H, BC) has a **gapped boundary**, otherwise we say it has a **gapless boundary**. If a gapless boundary remains gapless for *any* local perturbation near the boundary, we say that the gapped quantum liquid H has **protected** gapless boundaries, otherwise its boundary is **gappable**. For a system with gappable boundary, we can define **gapped boundary phases** as we did above but only allow for perturbations near the boundary (such that the bulk remains in the same phase).

1.5.1 Chiral and Invertible Topological Order

First we will discuss **chiral topological order**, which was the first class of systems found and includes Fractional Quantum Hall systems. As discussed above there is another universal quantity hidden in the ground state, the **chiral central charge** c_-. Systems with $c_- \neq 0$ have chiral gapless boundary modes which are protected due to their chiral nature and will generically break time-reversal symmetry. Physically these systems have a thermal Hall effect, with the thermal conductivity [81]

$$\kappa_H = c_- \frac{\pi k_B^2 T}{6}, \tag{1.30}$$

which transports energy between boundaries. The lack of energy-conservation on the boundaries are captured by (perturbative) gravitational anomalies which are directly related to c_-

$$\nabla^i T_{ij} = \frac{c_L - c_R}{96\pi} \epsilon_j^k \partial_k R, \tag{1.31}$$

where $c_- = c_L - c_R$ is the difference between the left and right central charges and R is the Ricci scalar. Here the anomaly is with respect to small diffeomorphisms, which gives rise to convervation of the boundary energy-momentum tensor (had there been no anomaly). The bulk however also has an anomaly described by the gravitational Chern-Simons term

$$S_{anom} = -\frac{c_-}{96\pi} \int \text{tr} \left(\Gamma \wedge d\Gamma + \frac{2}{3}\Gamma^3 \right), \tag{1.32}$$

23

which cancels the boundary anomaly through the usual Callan-Harvey inflow mechanism [82]. This is a consequence of the descent relations of anomalies in different dimensions [83]. Thus the universal number c_- says that the system has a thermal ("gravitational") version of the usual quantum Hall effect.

Systems with integer and fractional quantum Hall effect usually have charge conservation (when considering both bulk and boundary), due to global $U(1)$ symmetry, and usually thought of in terms of the Hall conductivity. But if we perturb these systems with charge non-conserving perturbations while preserving the bulk gap, like proximity coupling to a superconductor, does the Hall effect survive? Due to the universality of the chiral central charge, the answer is yes, even without charge conservation the thermal Hall transport remains protected. And while the statistics of the bulk anyons are protected, the fractional electric charge they carry is not under these perturbations.

It was shown in [56] that the chiral central charge only depends on the ground state and for a local lattice Hamiltonian $H = \sum_i H_i$, a formula was derived

$$c_- = -\frac{12}{\pi} \sum_{i \in A} \sum_{j \in B} \sum_{k \in C} h_{ijk}, \tag{1.33}$$

where h_{ijk} is related to thermal-averages of the commutators $[H_i, H_j]$. Interestingly this implies that any Hamiltonian which is a sum of commuting terms must have $c_- = 0$, this includes most exactly solvable models for topological order [69, 84].

Note that if we stack a chiral topological order with its time-reversed version, we will have modes with both chiralities on the boundary. Now it is possible to write interaction terms near the boundary that couples these modes and potentially gap them out, turn the system into a non-chiral topological order. Actually this construction gives rise to a large class of non-chiral topological systems often called **doubled topological order**. There are however a subset of chiral topological orders where doubling will turn the system to a trivial gapped system. These are called **invertible topological order**. This means that systems with invertible topological order, have no anyonic excitations in the bulk but do have protected gapless boundary modes. For bosonic topological order it turns out that these systems have chiral central charges given by $c_- = 8k$, $k \in \mathbb{N}$. Interestingly the derivation of this result, is closely related to lattices used in the compactification of Heterotic string theory [85, 86, 87]. This implies if one knows everything about the bulk excitations, essentially the related modular tensor category, one will only know c_- mod 8 as we can always stack the system with a invertible topological system without changing the bulk statistics. This explains equation (1.23). The simplest of these is called the E_8-state, which can be formulated as an abelian Chern-Simons theiry where the K-matrix is

the cartan matrix of the E_8 Lie algebra. The boundary of this system is described by a Wess-Zumino-Witten theory with a $(\hat{E}_8)_1$ affine Kac-Moody algebra.

1.5.2   Non-Chiral Topological Order and Gappable Boundaries

The topological orders in 2+1D with $c_- = 0$ are called ***non-chiral topological orders*** and those with gapped boundary conditions (in any dimension) are called topological orders with ***gappable boundary***. One natural question is whether there is anything universal in the boundary physics of non-chiral topological orders now the only universal boundary quantity mentioned so far is $c_- = 0$. The answer yes, but the universal features are more subtle.

In 2+1D it turns out that the number of different possible gapped boundary phases for a non-chiral topological order is universal and completely determined by the statistics of bulk anyons. Using different methods [88, 89, 90, 91], it has been shown that there is a gapped boundary phase for each ***lagrangian subgroup***. A lagrangian subgroups is a subset of anyons $\mathcal{M} \subset \mathcal{A}$ where all anyons in $\mathcal{M}$ are bosons, they all have trivial mutual statistics among each other and for any anyon outside $a \notin \mathcal{M}$ there is at least a $b \in \mathcal{M}$ such that a and b have non-trivial mutual statistics. The lagrangian subgroups represent maximal number of bulk bosons that can consistently condense on the boundary to form a gapped boundary phase. Perhaps surprisingly, there exists non-chiral topological orders with no lagrangian subgroups and thus protected gapless boundaries without chirality.

There is a different way to understand how such a thing is possible. Imagine the boundary is gapless and fine-tuned to be a conformal field theory (CFT), with equal number of right moving and left moving modes (non-chiral). It turns out that the boundary primary fields are labeled by the bulk anyons [61, 62]. In order to gap out the boundary, we need to couple the right moving and left moving modes. But in order to couple these modes consistently and be able to gap out a CFT it must be modular invariant. If it is not possible to couple the left and right moving modes such that the CFT partition function becomes modular invariant, it will be impossible to gap out the boundary modes. Whereas in the $c_- \neq 0$ case we had a perturbative gravitational anomaly, related to small diffeomorphisms, the lack of modular invariance can be thought of as a ***global gravitational anomaly***. In other words, the theory is not invariant under large diffeomorphisms (the mapping class group). Such CFTs are usually not considered well-defined and cannot exists in $1+1D$ and cannot be regularized on a lattice, but they can consistently be realized, and regularized, on the boundary of a $2 + 1D$ system.

Another very subtle universal features of $2 + 1D$ systems with gappable boundaries, is

the relation between **anyonic symmetries** of the bulk and **Kramers-Wannier dualites** on the boundary. Anyonic symmetries are a subgroups of the permutations of bulk anyons that preserves all statistics and fusions rules. It turns out that these symmetries of the bulk system, give rise to Kramers-Wannier dualities on the boundary constraining the global structures of the boundary phase diagram. In chapter 5 we see evidence of this in case of $\mathbb{Z}_2$ topological order, by studying boundary dynamics and entanglement spectrum of the ground state. We also find more non-trivial bulk-boundary relations, such as conformal defects on the boundary emerging from bulk topological physics, giving rise to interesting spectra of boundary primary fields. In chapter 7, we argue for the physical relevance of a subtle generalization of lagrangian subgroups for bosonic topological systems. With this generalizations, the $\mathbb{Z}_2$ topological order gets an enhanced effective anyonic symmetry group giving rise to non-abelian Kramers-Wannier dualities on the boundary. The boundary theory turns out to have very interesting features including lines of criticality described by orbifold CFTs and fine-tuned points with unusual symmetries, like extended supersymmetry. This relation between bulk and boundary physics will be studied further, and in higher dimensions, in [92].

We already discussed that chiral and non-chiral topological orders with protected gapless boundaries, are protected due to gravitational anomalies. These theories can only consistently exist on the boundary of a higher dimensional system. One could ask, do the gapped boundary phases also have some anomalous feature? The answer turns out to be yes. There exists anomalous topological orders which cannot be realized by a local bosonic lattice model, but can be realized as a gapped boundary of a higher dimensional topological order. It is believed that anomaly-free topological orders satisfy **the principle of remote detectability**, meaning that every excitation can be detected via some remote operation (i.e. by braiding). In section 1.4.1 we discussed fusion and fusion spaces, but if we had not assumed commutative fusion rules we would have gotten a **unitary fusion category**, which classifies the **anomalous topological orders** in $1 + 1D$. This is because particles in $1 + 1D$ cannot braid and cannot detect each other. Actually it turns out that there are no non-anomalous bosonic topological orders in $1 + 1D$. See more details in [93, 94, 95].

Thus the different gapped boundaries that are classified by lagrangian subgroups correspond to different anomalous topological orders.

Boundaries of $3 + 1D$ topological orders can be more complicated, as there are both anomalous and anomaly-free $2 + 1D$ topological orders and in general there can be an infinite number different gapped boundary phases. It turns out that there are a finite number of (anomalous) gapped boundaries if we mod out with anomaly-free topological orders and these are classified by a generalization of lagrangian subgroups. We are studying this in more detail in an ongoing work [96].

There are many topics and many very interesting details that we were not able to cover in this review of topological order, as this brief introduction is already too long. Despite the technical nature of this introduction to topological order, we hope it gives the reader enough context and background for the contributions of this thesis.

1.6   Overview of this thesis

Each chapter of this thesis is based on separate pieces of work where all except one has been published in peer reviewed journals. The chapters has been kept as much as possible close to the original published work. Therefore each chapter is largely self-containted, have its own introduction and conclusion, and can in principle be read without reading other chapters.

In chapter 2 we propose a way, called *Universal Wave Function Overlap*, to extract universal topological data from generic ground states of gapped systems in any dimensions. Those extracted topological data should fully characterize the topological orders with gapped or gapless boundary. For non-chiral topological orders in $2+1D$, this universal topological data consist of two matrices, S and T, which generate a projective representation of $SL(2,\mathbb{Z})$ on the degenerate ground state Hilbert space on a torus. For topological orders with gapped boundary in higher dimensions, this data constitutes a projective representation of the mapping class group $\texttt{MCG}(M^d)$ of closed spatial manifold M^d. For a set of simple models and perturbations in two dimensions, we show that these quantities are protected to all orders in perturbation theory. We also propose a simple and effective numerical algorithm to compute these quantities using intrinsic gauge structure of local tensors in a Projected Entangled Pair States (PEPS) tensor network.

Based on the proposal in chapter 2, in chapter 3 we introduce a systematic numerical method based on tensor networks to calculate modular S and T matrices in $2+1D$ systems, which might fully identify topological order with gapped edges. Moreover, it is shown numerically that modular matrices, including S and T matrices, are robust characterization to describe phase transitions between topologically ordered states and trivial states, which can work as topological order parameters. This method only requires local information of one ground state in the form of a tensor network, and directly provides the universal data (S and T matrices), without any non-universal contributions. Furthermore it is generalizable to higher dimensions. Unlike calculating topological entanglement entropy by extrapolating, which numerical complexity is exponentially high, this method extracts a much more complete set of topological data (modular matrices) with much lower numerical cost.

I chapter 2 we conjectured that a certain set of universal topological quantities characterize topological order in any dimension. Those quantities can be extracted from the universal overlap of the ground state wave functions. For systems with gapped boundaries, these quantities are representations of the mapping class group $\texttt{MCG}(M)$ of the space manifold M on which the systems lives. In chapter 4 we consider simple examples in $3+1$ dimensions and give physical interpretation of these quantities, related to fusion algebra and statistics of particle and string excitations. In particular, we will consider dimensional reduction from 3+1D to 2+1D, and show how the induced 2+1D topological data contains information on the fusion and the braiding of non-Abelian string excitations in 3D. These universal quantities generalize the well-known modular S and T matrices to any dimension.

In a system with chiral topological order, there is a remarkable correspondence between the edge and entanglement spectra: the low-energy spectrum of the system in the presence of a physical edge coincides with the lowest part of the entanglement spectrum (ES) across a virtual cut of the system, up to rescaling and shifting. In chapter 5, we explore whether the edge-ES correspondence extends to nonchiral topological phases. Specifically, we consider the Wen-plaquette model which has $\mathbb{Z}_2$ topological order. The unperturbed model displays an exact correspondence: both the edge and entanglement spectra within each topological sector $a(a = 1, ..., 4)$ are flat and equally degenerate. Here, we show, through a detailed microscopic calculation, that in the presence of generic local perturbations: (i) the effective degrees of freedom for both the physical edge and the entanglement cut consist of a spin-$1/2$ chain, with effective Hamiltonians H_{edge}^a and $H_{\text{ent.}}^a$, respectively, both of which have a $\mathbb{Z}_2$ symmetry enforced by the bulk topological order; (ii) there is in general no match between their low energy spectra, that is, there is no edge-ES correspondence. However, if supplement the $\mathbb{Z}_2$ topological order with a global symmetry (translational invariance along the edge/cut), i.e. by considering the Wen-plaquette model as a symmetry enriched topological phase (SET), then there is a finite domain in Hamiltonian space in which both H_{edge}^a and $H_{\text{ent.}}^a$ realize the critical Ising model, whose low-energy effective theory is the $c = 1/2$ Ising CFT. This is achieved because the presence of the global symmetry implies that both Hamiltonians, in addition to being $\mathbb{Z}_2$ symmetric, are Kramers-Wannier self-dual. Thus, the bulk topological order and the global translational symmetry of the Wen-plaquette model as a SET imply an edge-ES correspondence at least in some finite domain in Hamiltonian space.

It is well known that the bulk physics of a topological phase constrains its possible edge physics through the bulk-edge correspondence. Therefore, the different types of edge theories that a topological phase can host constitute a universal piece of data which can be used to characterize topological order. In chapter 6, we argue that, beginning from only the fixed-point wave function (FPW) of a nonchiral topological phase and by locally

deforming it, all possible edge theories can be extracted from its entanglement Hamiltonian (EH). We give a general argument, and concretely illustrate our claim by deforming the FPW of the Wen-plaquette model, the quantum double of $\mathbb{Z}_2$. In that case, we show that the possible EHs of the deformed FPW reflect the known possible types of edge theories, which are generically gapped, but gapless if translational symmetry is preserved. We stress that our results do not require an underlying Hamiltonian and thus, this lends support to the notion that a topological phase is indeed characterized by only a set of quantum states and can be studied through its FPWs.

In chapter 7 we introduce the notion of *fermionic gapped edges*, a new kind of topological gapped boundary theory of a bosonic abelian topological state. These gapped edges exist naturally if the bosonic topological order is emergent from original, local fermionic degrees of freedom, so that domain walls between the bosonic topological state and a fermionic vacuum (such as a trivial band insulator) must be considered. Using the framework of Lagrangian subgroups of [89] and [90, 91], we argue that the condition that the self-statistics of quasiparticles in a Lagrangian subgroup to be self-bosons should be removed. Physically, this implies that quasiparticles which are self-fermions can possibly condense on the boundary, leading to these fermionic gapped edges. We illustrate the presence of such a fermionic gapped edge in a system with bosonic $\mathbb{Z}_2$ topological order, and explicitly construct a microscopic model, the $\mathbb{Z}_2$ Wen-plaquette model coupled to an array of Majorana fermions (which can be considered as the ferminonic vacuum). We explore the rich phase diagram of the edge theory of this model, which can be mapped to a variant of the Ashkin-Teller model, and show that there are critical lines of $c = 1$ $\mathbb{Z}_2$-orbifold boson CFTs separating the three gapped phases, including critical points with exotic symmetries such as twisted $N = 2$ supersymmetry. We also see that the notion of fermionic gapped edge leads to an enhancement of the anyonic symmetries, as far as boundary physics is concerned, giving rise to non-abelian Kramers-Wannier Dualities on the boundary, constraining the structure of the boundary phase diagram.

Chapter 2

Universal Wave Function Overlap and Universal Topological Data from Generic Gapped Ground States

This chapter was published in [1].

2.1 Introduction

Since the discovery the fractional quantum Hall effect (FQHE)[17, 18] and theoretical study of chiral spin liquids, [97, 98] it has been known that new kind of orders beyond Landau symmetry breaking orders exist for gapped states of matter, called topological order. [99, 100] Topological order can be thought of as the set of universal properties of a gapped system, such as (a) the topology-dependent *ground state degeneracy* [99, 100] and (b) the *non-Abelian geometric phases S and T* of the degenerate ground states [19, 101, 102], which are *robust against any local perturbations* that can break any symmetries. [100] This is just like superfluid order which can be thought of as the set of universal properties: zero-viscosity and quantized vorticity, that are robust against any local perturbations that preserve the $U(1)$ symmetry. It was proposed that the non-abelian geometric phases of the degenerate ground states on the torus classify 2+1D topological orders. [19]

Interestingly, it turns out that non-trivial topological order is related to long-range quantum entanglement of the ground state [24]. These long-range patterns of entanglement are responsible for the interesting physics, such as quasiparticle excitations with exotic

statistics, completely robust edge states, as well as the universal ground state degeneracy and non-Abelian geometric phases mentioned above.

Our current understanding is that topological order in 2+1 dimensions is characterized by a unitary modular tensor category (UMTC) which encode particle statistics and gives rise to representations of the Braid group, [103] and the chiral central charge c_- which encode information about chiral gapless edge states [104, 105].

While the algebraic theory of 2+1D topological order is largely understood, it is natural to ask whether it is possible to extract topological data from a generic non-fixed point ground state.[1] One such proposal has been through using the non-Abelian geometric phase S and T [19, 101, 102, 106, 107, 108, 45]. Another is using the entanglement entropy [34, 35] which has the generic form in 2+1 dimensions $S = \alpha L - \gamma + \mathcal{O}(\frac{1}{L})$, where γ is the topological entanglement entropy (TEE). It turns out that $\gamma = \log \mathcal{D}$, where $\mathcal{D}$ is the total quantum dimension and thus a universal topological property of the gapped phase. A generalization of TEE to higher dimensions was proposed in [41]. A TQFT in the continuum limit, such as a Chern-Simons theory, captures the pure universal physics and therefore $S = -\gamma$, while for a generic dynamical theory non-universal contributions are non-zero. The topological entanglement entropy, however, only captures a small piece of the data needed to characterize the topological order of a ground state. The question is, can we from a non-fixed point ground state extract more data that could characterize the underlying TQFT more fully?

Here, we would like to propose a simple way to extract data from non-fixed point ground states, that could potentially fully characterize the underlying TQFT. We conjecture that for a system on a d-dimensional manifold M^d of volume V with the set of degenerate ground states $\{|\psi_\alpha\rangle\}_{\alpha=1}^N$, the overlaps of the degenerate ground states have the following form [109, 94]

$$\langle \psi_\alpha | \hat{\mathcal{O}}_A | \psi_\beta \rangle = e^{-\alpha V + o(1/V)} M_{\alpha,\beta}^A, \tag{2.1}$$

where $\hat{\mathcal{O}}_A$, labeled by index A, are transformations of the wave functions induced by the automorphism transformations of the space $M^d \to M^d$, α is a non-universal constant, and M^A is an *universal* unitary matrix (upto an overall $U(1)$ phase). M^A form a projective representation of the automorphism group of the space M^d – $\mathtt{AMG}(M^d)$, which is robust against any perturbations. We propose that *such projective representations for different space topologies are universal topological data and that they might fully characterize topological orders with finite ground state degeneracy.* The disconnected components of the automorphism group is the mapping class group: $\mathtt{MCG}(M^d) \equiv \pi_0[\mathtt{AMG}(M^d)]$. We propose

---

[1]Here, generic non-fixed point ground states refers to ground states of any generic gapped Hamiltonian, not necessarily ideal fixed point Hamiltonians with special properties.

that *projective representations of the mapping class group for different space topologies are universal topological data and that they might fully characterize topological orders with gapped boundary.* (For a more general and a more detailed discussion, see Ref. [94].) For some more intuition behind our conjecture, we refer to the supplemental material.

For a 2D torus T^2 the mapping class group $\texttt{MCG}(T^2) = SL(2, \mathbb{Z})$ is generated by a $90°$ rotation $\hat{S}$ and a Dehn twist $\hat{T}$. The corresponding M^A are the unitary matrices S, T which generate a projective representation of $SL(2, \mathbb{Z})$. Compared to the proposal in Ref. [19, 101, 102], here we do not need to calculate the geometric phase for a family of ground states and only have to consider a much simpler calculation – a particular overlap (with the cost of a non-universal contribution with volume scaling). We will calculate this for the simple example of $\mathbb{Z}_N$ topological state studied in Refs. [110, 111, 112, 113, 114] and investigate the universality of this under perturbations such as adding string tension.

We note that a UMTC that describe the statistics of the excitations in $2 + 1$D, can also gives rise to a projective representation of $SL(2, \mathbb{Z})$. We propose that the universal wave function overlap eqn. (2.1) computes this projective representation. The representation is generated by two elements S and T satisfying the relations

$$(ST)^3 = e^{\frac{2\pi i}{8}c_-} C, \quad S^2 = C, \tag{2.2}$$

where C is a so-called charge conjugation matrix and satisfy $C^2 = 1$. Furthermore we have that $\frac{1}{\mathcal{D}} \sum_a d_a^2 \theta_a = e^{\frac{2\pi i}{8}c_-}$, where d_a and θ_a are the quantum dimension and topological spin of quasiparticle a, respectively. This shows that the UMTC, or particle statistics, fixes the chiral central charge mod 8. [2] This constitutes a projective representation of $SL(2, \mathbb{Z})$ on the groundstate subspace on a torus, which encode how the groundstates transform under large automorphisms $\texttt{MCG}(T^2)$. We believe that our higher dimensional universal quantities (2.1) also encode information about the topological order in the ground state.

---

[2]The ambiguity of c_- can be understood by the existence of the so-called E_8 state, which can be realized by a Chern-Simons theory where the K matrix is the Cartan matrix of E_8. This theory has only trivial bulk excitations since $\det K = 1$ but boundary theory given by the affine Lie algebra $(\hat{E}_8)_1$, which has $c_- = 8$. Thus there is always the ambiguity of adding a E_8 state to a topological order without changing the bulk excitations, but shifting the chiral central charge by 8. The chiral central charge is related to perturbative gravitational anomalies on the edge, which signals lack of energy conservation, or a gravitational parity anomaly from the bulk perspective. Physically, this corresponds to a thermal Hall effect by the Callan-Harvey inflow mechanism [82] and is a consequence of the descent relations of anomalies in different dimensions. Note that in the case $c_- = 0$, the edge states are not chiral but they can however still be completely robust. [89] This is related to global gravitational anomalies, ie modular anomaly on the edge.

2.2 Construction of degenerate set of ground states from local tensor networks

Since topological order exist even on topologically trivial manifolds, all its properties should be available from a local wave function. But we need to sharpen what we mean by a local wave functions, since wave functions typically depend on global data such as boundary conditions. Amazingly, there exist a surprisingly simple local representation of globally entangled states using tensor network language. In particular, a tensor network state (TNS) known as PEPS, is given by associating a tensor $T^{[i]}_{\sigma_i}(\alpha\beta\gamma\dots)$ to each site i, where σ_i is a physical index associated to the local Hilbert space, and α, β, γ are inner indices and connect to each other to form a graph. Using this representation, the wave function is given by

$$|\psi\rangle = \sum_{\{\sigma_i\}} \text{tTr}\left(T^{[1]}_{\sigma_1} T^{[2]}_{\sigma_2}\dots\right)|\sigma_1, \sigma_2, \dots\rangle, \tag{2.3}$$

where $\text{tTr}(\dots)$ contracts the tensor indices in the tensor product network. By choosing the dimension of the inner indices large enough, one can approximate any state arbitrarily well. This particular representation is especially interesting for the study of gapped states since it automatically satisfies the area law, a property gapped ground states are known to have [115, 116]. One can think of TNS as parametrization of the interesting sub-manifold of the Hilbert space, where ground states of local gapped Hamiltonians live.

Local tensor representation of wave functions is however not enough, it must be equipped with a gauge structure [117]. Surprisingly, local variations of a tensor do not always correspond to local perturbations of the Hamiltonian and can change the global topological order. In order to approximate the ground state of a Hamiltonian with topological order with gauge group G, it is important to search within the set of variational tensors with symmetry G. Arbitrarily small G breaking variations, might lead to tensor networks which can approximate local properties of a system well but give wrong predictions about the global properties.

In [118] a few concepts were introduced to characterize the symmetry structure of a TNS. In particular d_{space}-IGG, which is the group of intrinsically d_{space}-dimensional gauge transformations on the inner indices that leave the tensors invariant. It was in particular shown that in the case of the two-dimensional $\mathbb{Z}_2$ topological state we have 2-IGG $= \mathbb{Z}_2$. Furthermore it was shown that 2-IGG contains information about string operators and can be used to construct the full set of degenerate ground states on the torus from a local tensor representation. [3]

---

[3] A related concept for a finite group G, is G-injective PEPS [119]. A G-injective tensor is a tensor

The point of this discussion is the following. Imagine one is interested in probing whether a 2D local gapped Hamiltonian has topological order described by gauge group G. It is then important to search within the set of variational tensors with 2-IGG= G and keep this symmetry intact during all variations and along renormalization group flows. This is a necessary symmetry condition to probe the topological order [117]. If the ground state of the system has topological order with gauge group G, how can we find out which kind of topological order it has? For example, for $G = \mathbb{Z}_2$ there are two theories with topological order, the universality classes corresponding to the $\mathbb{Z}_2$ toric code and the double semion model.

This can be decided if one knows the corresponding modular S and T matrices. First one can construct the set of ground states on a torus from the local tensor, by exploiting its gauge structure as in [118]. Now one can extract the S and T matrices by considering the overlaps (2.1). This will also fix the chiral central charge c_-, modulo 8.

Thus the local data we need is = local tensor + gauge structure. From this gauge structure we can twist the tensor to get the full set of ground states on a torus [118, 119, 120]. We shall call the natural basis we get from such a procedure for twist basis.

We will in the following consider the $\mathbb{Z}_N$ topological state. We can construct a local tensor for this state in the following way. Let the physical spins live on the links of the lattice, and give each link an orientation as in figure 2.1(b). Put a tensor $T^{(\sigma_1\sigma_2\sigma_3\sigma_4)}_{\alpha\beta\gamma\delta}$ on each site and require that

$$T^{(\alpha\beta\gamma\delta)}_{\alpha\beta\gamma\delta} = 1 \quad \text{if } \beta + \gamma - \alpha - \delta = 0 \mod N, \tag{2.4}$$

otherwise $T^{(\sigma_1\sigma_2\sigma_3\sigma_4)}_{\alpha\beta\gamma\delta} = 0$. This tensor has a $\mathbb{Z}_N$ symmetry given by the tensors (see figure 2.1(c))

$$\xrightarrow{\alpha}\text{(A)}\xrightarrow{\beta} = \delta_{\alpha\beta}e^{\frac{2\pi i}{N}\alpha}, \quad \xrightarrow{\alpha}\text{(B)}\xrightarrow{\beta} = \delta_{\alpha\beta}e^{\frac{-2\pi i}{N}\alpha}. \tag{2.5}$$

---

which is invariant under a G-action on all inner indices simultaneously, together with the property that one can achieve any action on the virtual indices by acting on the physical indices. It was shown that these tensors are ground states of a parent Hamiltonian with TEE $\gamma = \log|G|$. This class of PEPS describe the universality class of quantum double models $D(G)$. Recently this was generalized to (G, ω)-injective PEPS [120], where the action of G is twisted by a 3-cocycle of ω of G. It was shown that these PEPS describes topological order in the university class of Dijkgraaf-Witten TQFT's [121] and only depend on the cohomology class $[\omega] \in H^3(G, U(1))$ of ω.
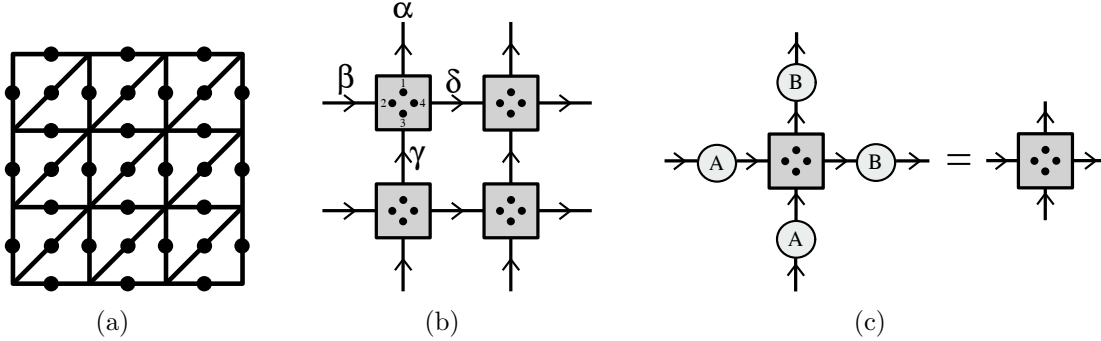
Figure 2.1: (a) Lattice under consideration, with the spins living on the links. (b) Tensor network for $\mathbb{Z}_N$ gauge theory. The lattice is chosen with the orientation shown. The tensors live on the lattice sites and the dots represent the physics indices. (c) Symmetry of the $\mathbb{Z}_N$ tensor.

2.3 $\mathbb{Z}_N$ Topological Order

Equipped with the ground states of from local tensors, one can calculate the overlap (2.1) to extract the universal topological properties.

As a simple example, let us calculate the overlap (2.1) for the case of $\mathbb{Z}_N$ topological state on the lattice in figure 2.1(a). For this simple example we will not use tensor product representation for simplicity, since it can be calculated directly. See [2] for calculation of (2.1) using tensor network and gauge structure.

Let there be a local Hilbert space $\mathcal{H}_a \approx \mathbb{C}[\mathbb{Z}_N] \approx \mathbb{C}^N$ associated to each link $a \in \Omega$ with basis $\{|\sigma_a\rangle\}_{\sigma_a=0}^{N-1}$.

We will represent a spin configuration $|\sigma_{a_1}\sigma_{a_2}\ldots\rangle$ using a string picture, where the state on link $a \in \Omega$ is represented by an oriented string of type $\sigma_a \in \mathbb{Z}_N$ with a chosen orientation, and $|0\rangle$ corresponds to no string. There is a natural isomorphism $\mathcal{H}_a \xrightarrow{\sim} \mathcal{H}_{a^\star}$ for link a and its reversed orientation $a^\star$ by $|\sigma_a\rangle \mapsto |\sigma_{a^\star}\rangle = |-\sigma_a\rangle$.

The ground state Hilbert space of the $\mathbb{Z}_N$ topological order consists of an equal superposition of all closed-string configurations that satisfy the $\mathbb{Z}_N$ fusion rules.

The string-net ground state Hilbert space on T^2 can be algebraically constructed in the following way. Let $\Lambda_{\triangle}^\star$ denote the set of triangular plaquettes and for each $p \in \Lambda_{\triangle}^\star$ define the string operator $B_p^{\triangle}$ which act on the links bounding p, with clockwise orientation, by $|\sigma\rangle \mapsto |\sigma+1 \bmod N\rangle$. The set of all contractable closed loop configurations can be thought

of as the freely generated group $G_{\text{free}} = \left\langle \{B_p^\triangle\}_{p \in \Lambda_\triangle^\star} \right\rangle$, modulo the relations $\left(B_p^\triangle\right)^N \sim 1$, $\prod_{p \in \Lambda_\triangle^\star} B_p^\triangle \sim 1$ and $B_p^\triangle B_q^\triangle \sim B_q^\triangle B_p^\triangle$, denoted as $G_\triangle^{00} = G_{\text{free}}/\sim$. Similarly we let the subgroup $G_\square^{00} \subset G_\triangle^{00}$ correspond to closed loop configurations on the square lattice links. For the ground states on the torus, we need to introduce two new operators W_x and W_y, corresponding to non-contractable loops along the two cycles of T^2. These satisfy $(W_i)^N = 1$, $i = x, y$. With these, we can construct the group $G_\triangle^{\alpha\beta}$, corresponding to closed string configurations with (α, β) windings around the cycle (x, y), modulo N. Similarly, let $G_\triangle$ be the group of all possible closed string configurations on the torus. These states are orthonormal $\langle g_{\alpha\beta} | \bar{g}_{\bar\alpha\bar\beta} \rangle = \delta_{g_{\alpha\beta}, \bar{g}_{\bar\alpha\bar\beta}}$.

The N^2-dimensional ground state Hilbert space is then spanned by the following vectors $|\alpha, \beta\rangle = |G_\triangle^{\alpha\beta}|^{-1/2} \sum_{g_{\alpha\beta} \in G_\triangle^{\alpha\beta}} |g_{\alpha\beta}\rangle$, where $\alpha, \beta = 0, \ldots, N-1$. The construction can trivially be extended to higher-genus surfaces.

This is the string-net basis for the $\mathbb{Z}_N$ gauge theory. The ground states in the twist basis corresponding to the tensor (2.4), are just the eigenbasis the operators W_x and W_y. These are given by

$$|\psi_{ab}\rangle = \frac{1}{\sqrt{|G_\triangle|}} \sum_{g \in G_\triangle} \gamma^{a\omega_x(g) + b\omega_y(g)} |g\rangle, \qquad (2.6)$$

where $\gamma = e^{-\frac{2\pi i}{N}}$ and ω_i count how many times the string configuration g wraps around the i'th cycle. Note that $W_x|\psi_{ab}\rangle = e^{\frac{2\pi i}{N}a}|\psi_{ab}\rangle$ and $W_y|\psi_{ab}\rangle = e^{\frac{2\pi i}{N}b}|\psi_{ab}\rangle$. For later use, note that $|G_\triangle^{\alpha\beta}| = N^{|\Lambda_\triangle^\star|-1} = N^{2L^2-1}$, $|G_\square^{\alpha\beta}| = N^{|\Lambda_\square^\star|-1} = N^{L^2-1}$, $|G_\triangle| = N^2|G_\triangle^{\alpha\beta}|$ and $|G_\square| = N^2|G_\square^{\alpha\beta}|$.

2.3.1 Modular S and T-matrix from the ground state

We can now define two non-local operators on our Hilbert space $\hat{\mathcal{O}}_S, \hat{\mathcal{O}}_T : \mathcal{H} \to \mathcal{H}$ as in figure 2.2, mimicking the generators of the torus mapping class group in the continuum. Here $\hat{\mathcal{O}}_S$ maps any spin configuration, to the 90 degree rotated configuration. $\hat{\mathcal{O}}_T$ corresponds to shear transformation and is defined as in figure 2.2. It is clear that since we are on the lattice, these operators will not preserve the subspace of closed string configurations.

We can easily calculate the matrix elements of $\hat{\mathcal{O}}_T$ and $\hat{\mathcal{O}}_S$ between ground states. In both cases, only $|G_\square|$ configurations have a non-zero overlap with the un-deformed ground state. For the S transformation we find the overlap

$$\langle \psi_{ab} | \hat{\mathcal{O}}_S | \psi_{\bar{a}\bar{b}} \rangle = \delta_{a,\bar{b}} \delta_{b,-\bar{a}} \frac{|G_\square|}{|G_\triangle|} = S_{ab,\bar{a}\bar{b}} e^{-\log(N)L^2}, \qquad (2.7)$$
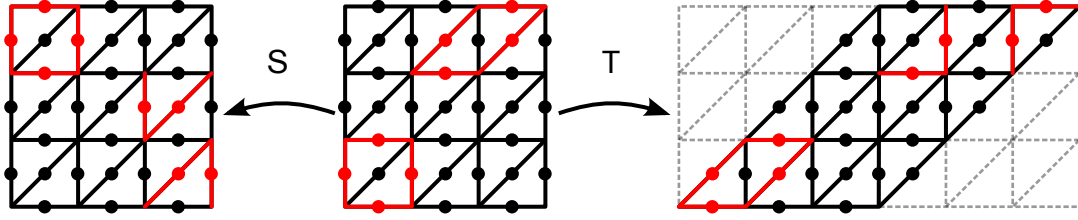
Figure 2.2: Definition of S and T transformations. The S transformation corresponds to rotating configurations 90 degrees, while T corresponds to a shear transformation. Note that this transformation does not leave the space of closed loop configurations invariant.

where we have defined the modular S matrix $S_{ab,\bar{a}\bar{b}} = \delta_{a,\bar{b}}\delta_{b,-\bar{a}}$. Similarly we have $\langle\psi_{ab}|\hat{\mathcal{O}}_T|\psi_{\bar{a}\bar{b}}\rangle = T_{ab,\bar{a}\bar{b}}e^{-\log(N)L^2}$, where the modular T matrix is given by $T_{ab,\bar{a}\bar{b}} = \delta_{a+b,\bar{a}}\delta_{b,\bar{b}}$. One can readily check that these satisfy eq. (2.2) with $c_- = 0 \mod 8$ and $C_{ab,\bar{a}\bar{b}} = \delta_{a,-\bar{a}}\delta_{-b,\bar{b}}$. Thus this forms a projective representation of the modular group $SL(2,\mathbb{Z})$.

In order to use Verlinde's formula and generate the relevant UMTC, we need to put the modular matrices in the quasi-particle basis[4]. This is done as follows, for the $\mathbb{Z}_N$ theory there are non-contractable magnetic operators on the dual lattice satisfying $(\Gamma_i)^N = 1$, and with the commutation relations $W_x\Gamma_y = e^{-\frac{2\pi i}{N}}\Gamma_y W_x$ and $W_y\Gamma_x = e^{-\frac{2\pi i}{N}}\Gamma_x W_y$. The basis we are after corresponds to having a well-defined magnetic and electric flux through one direction of the torus. In the eigenbasis of W_y and Γ_y, $|\phi_{mn}\rangle$, we find

$$S_{mn,\bar{m}\bar{n}} = \frac{1}{N}e^{-\frac{2\pi i}{N}(m\bar{n}+n\bar{m})}, \quad T_{mn,\bar{m}\bar{n}} = \delta_{m,\bar{m}}\delta_{n,\bar{n}}e^{\frac{2\pi i}{N}mn}, \tag{2.8}$$

the well-known modular matrices for the $\mathbb{Z}_N$ model.

2.3.2 Perturbed $\mathbb{Z}_N$ model

We will now consider a local perturbation to the $\mathbb{Z}_N$ topological state. One interesting perturbation is to add a magnetic field of the form $\frac{J}{2}\sum_{a\in\Omega}(Z_a + Z_a^\dagger)$, where Z_a is a local operator defined as $Z_a|\sigma_a\rangle = e^{\frac{2\pi i}{N}\sigma_a}|\sigma_a\rangle$ [5]. This perturbation breaks the exact solvability of the model, but essentially corresponds to introducing string tension to each closed string

---

[4]In general we do not have a gauge theory and need another way to find the modular matrices in the right basis. One way is to find a basis which satisfy certain special properties. In [122] it was shown for several examples, that this basis is unique and leads to the right form of S and T.

[5]See [113] for analysis of models of this type.
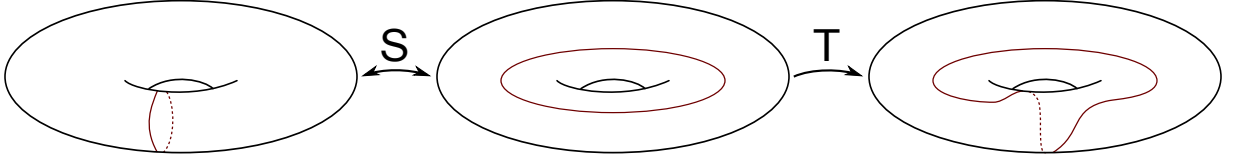
Figure 2.3: In the string-net basis, a modular S transformation flips the topological sectors $(\alpha, \beta) \rightarrow (\beta, -\alpha \mod N)$, while a T transformation has the effect $(\alpha, \beta) \rightarrow (\alpha, \alpha + \beta \mod N)$.

configuration. This can be implemented by local deformation of the ground states of the form

$$|\psi_{ab}\rangle_{\mathcal{A}} = \frac{1}{\sqrt{|G_{\triangle}|}} \sum_{g \in G_{\triangle}} \mathcal{A}^{-\mathcal{L}(g)/2} \gamma^{a\omega_x(g)+b\omega_y(g)} |g\rangle, \qquad (2.9)$$

where $\mathcal{A}$ is a variational parameter. Furthermore $\mathcal{L}(g) = \sum_{a \in \Omega} \frac{1}{2}[1 - \cos(\frac{2\pi}{N}\sigma_a)]$, which is just the total string length for $N = 2$.

Performing a S transformation, we find the overlap

$$_{\mathcal{A}}\langle \psi_{ab}|\hat{\mathcal{O}}_S|\psi_{\bar{a}\bar{b}}\rangle_{\mathcal{A}} = \frac{1}{|G_{\triangle}|} \sum_{\alpha\beta=0}^{N-1} \gamma^{(\bar{b}-a)\alpha-(b+\bar{a})\beta} \sum_{g \in G_{\square}^{\alpha\beta}} \mathcal{A}^{-\mathcal{L}(g)} \qquad (2.10)$$

If we view strings as domain walls of a $\mathbb{Z}_N$ clock model on square lattice described by the following Hamiltonian $H = \sum_{\langle ij \rangle} \frac{1}{2} \left[1 - \cos\left(\frac{2\pi}{N}[\sigma_i - \sigma_j] \right) \right], \sigma_i, \sigma_j = 0, 1, \cdots, N-1$, we find that $N \sum_{g \in G_{\square}^{00}} \mathcal{A}^{-\mathcal{L}(g)} = \sum_{\{\sigma_i\}} e^{-\beta H}$ can be viewed as the partition function of the $\mathbb{Z}_N$ clock model, where $\beta = \log(\mathcal{A})$. In the appendix below we show that in the disordered phase of the $\mathbb{Z}_N$ clock model,

$$Z(\beta) = \sum_{\{\sigma_i\}} e^{-\beta H} = e^{L^2 \log(N) - f(\beta)L^2 + o(L^{-1})} \qquad (2.11)$$

to all orders in perturbation theory in β, where $f(\beta)$ is a function of β only. Since $N \sum_{g \in G_{\square}^{\alpha\beta}} \mathcal{A}^{-\mathcal{L}(g)}$ can be viewed as the partition function of the $\mathbb{Z}_N$ clock model with twisted boundary condition, we find that

$$\left| \log \frac{N \sum_{g \in G_{\square}^{\alpha\beta}} \mathcal{A}^{-\mathcal{L}(g)}}{N \sum_{g \in G_{\square}^{00}} \mathcal{A}^{-\mathcal{L}(g)}} \right| < hLe^{-L/\xi}, \qquad (2.12)$$

38

where h and ξ are L independent constants. This is because the total free energies of the $\mathbb{Z}_N$ clock model with twisted and untwisted boundary condition can only differ by $hLe^{-L/\xi}$ at most. Putting everything together, we find that

$$_{\mathcal{A}}\langle \psi_{ab}|\hat{\mathcal{O}}_S|\psi_{\bar{a}\bar{b}}\rangle_{\mathcal{A}} = S_{ab,\bar{a}\bar{b}}e^{-[\log N + f(\beta)]L^2 + o(L^{-1})} \tag{2.13}$$

The universal quantity, $S_{ab,\bar{a}\bar{b}}$ is protected, to all orders in β.

2.4   3D Topological States and $SL(3,\mathbb{Z})$

According to our conjecture (2.1) there are similar universal quantities in higher dimensions and it would be interesting to consider a simple example in three dimensions. For example, the mapping class group of the 3-torus is $\texttt{MCG}(T^3) = SL(3,\mathbb{Z})$. This group is generated by two elements of the form [123] $\hat{\tilde{S}} = \begin{pmatrix} 0 & 1 & 0 \\ 0 & 0 & 1 \\ 1 & 0 & 0 \end{pmatrix}$ and $\hat{\tilde{T}} = \begin{pmatrix} 1 & 0 & 0 \\ 1 & 1 & 0 \\ 0 & 0 & 1 \end{pmatrix}$. These matrices act on the unit vectors by $\hat{\tilde{S}} : (\hat{\boldsymbol{x}}, \hat{\boldsymbol{y}}, \hat{\boldsymbol{z}}) \mapsto (\hat{\boldsymbol{z}}, \hat{\boldsymbol{x}}, \hat{\boldsymbol{y}})$ and similarly $\hat{\tilde{T}} : (\hat{\boldsymbol{x}}, \hat{\boldsymbol{y}}, \hat{\boldsymbol{z}}) \mapsto (\hat{\boldsymbol{x}} + \hat{\boldsymbol{y}}, \hat{\boldsymbol{y}}, \hat{\boldsymbol{z}})$. Thus $\tilde{S}$ corresponds to a rotation, while $\tilde{T}$ is shear transformation in the xy-plane. In the case of 3D $\mathbb{Z}_N$ model, we can directly compute these generators in a basis with well-defined flux in one direction as [3]

$$\tilde{S}_{abc,\bar{a}\bar{b}\bar{c}} = \frac{1}{N}\delta_{b,\bar{c}}e^{\frac{2\pi i}{N}(\bar{a}c - a\bar{b})}, \quad \tilde{T}_{abc,\bar{a}\bar{b}\bar{c}} = \delta_{a,\bar{a}}\delta_{b,\bar{b}}\delta_{c,\bar{c}}e^{\frac{2\pi i}{N}ab}. \tag{2.14}$$

These matrices contain information about self and mutual statistics of particle and string excitations above the ground state [3].

In the 2D limit where one direction is taken to be very small, the operator creating a non-contractable loop along this direction is now essentially local. By such a local perturbation, one can break the GSD from N^3 down to N^2. One can directly show that the generators for an $SL(2,\mathbb{Z}) \subset SL(3,\mathbb{Z})$ subgroup exactly reduce to the 2D S and T matrices. [3]

2.5   Conclusion

In this chaper we have conjectured a universal wave function overlap (2.1) for gapped systems in d dimensions, which give rise to projective representations of the mapping class

group $\texttt{MCG}(M^d)$, for any manifold M^d. These quantities contain more information than the topological entanglement entropies [34, 35, 41], and might characterize the topological order completely, like in two dimensions [19]. In the paper [2], we numerically study the overlaps (2.1) for simple two-dimensional models and show that the universal quantities are very robust against perturbations and unambiguously characterize phase transitions. In [3] we study the universal quantities (2.1) for three-dimensional systems.

Appendices

2.A   Appendix A: Cumulant Expansion

Consider the following expansion, which only converges in the disordered phase

$$Z(\beta) = \sum_{\{\sigma_i\}} e^{-\beta H} = \exp\left(\log Z(\beta)\right)$$

$$= \exp\Bigg(\log Z(0) + \frac{Z'(0)}{Z(0)}\beta$$

$$+ \frac{1}{2}\left[-\left(\frac{Z'(0)}{Z(0)}\right)^2 + \frac{Z''(0)}{Z(0)}\right]\beta^2 + o(\beta^3)\Bigg)$$

$$= \exp\left(\log NL^2 + \sum_{n=1}^{\infty} \frac{(-1)^n}{n!}\mu_n\beta^n\right), \tag{2.15}$$
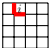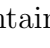
where μ_n is the n'th cumulant of the moment of H. In particular $\mu_1 = \langle H\rangle_0$, $\mu_2 = \langle H^2\rangle_0 - \langle H\rangle_0^2$, $\mu_3 = \langle H^3\rangle_0 - 3\langle H\rangle_0\langle H^2\rangle_0 + 2\langle H\rangle_0^3$ and so on. All averages are evaluated at $\beta = 0$, $\langle\mathcal{O}\rangle_0 = \frac{1}{Z(0)}\sum_{\{\sigma_i\}}\mathcal{O}$. Since the averages are taken in the extreme disordered limit (infinite temperature), we have $\langle H\rangle_0 = 2L^2\langle E(\sigma_i,\sigma_j)\rangle_N = L^2$, where each of the $2L^2$ bonds contribute with the average energy $\langle E(\sigma_i,\sigma_j)\rangle_N = \frac{1}{2}$.

More generally, consider the total energy to the n'th power

$$H^n = \sum_{i_1\ldots i_n} \sum_{\alpha_1,\ldots,\alpha_n = x,y} E_{i_1}(\alpha_1)\ldots E_{i_n}(\alpha_n), \tag{2.16}$$

where $E_i(\alpha) = E(\sigma_i - \sigma_{i+\alpha}) = \frac{1}{2}\left[1 - \cos\left(\frac{2\pi}{N}[\sigma_i - \sigma_{i+\alpha}]\right)\right]$. From here we find

$$\langle H^n\rangle_0 = \frac{1}{Z(0)}\sum_{\{\sigma_i\}} H^n =$$

$$\frac{1}{Z(0)}\sum_{\{\sigma_i\}}\left(\sum_i \boxed{} + \sum_{i\neq j}\boxed{} + \sum_{i\neq j\neq k}\boxed{} + \ldots\right), \tag{2.17}$$

where $\boxed{}$ contain all possible terms where all $E_i(\alpha)$ are at site i, while $\boxed{}$ contain all possible terms where all $E_i(\alpha)$ are at i and j, and so on. The first term is given by

$$\sum_i \boxed{} = \sum_i \sum_{q=0}^{n} \binom{n}{q} E_i^q(x)E_i^{n-q}(y) \equiv \sum_i \mathcal{M}_i(n). \tag{2.18}$$

41

Similarly, the next two terms are given by

$$\sum_{i_1 \neq i_2} \boxed{} = \frac{1}{2} \sum_{i_1 \neq i_2} \sum_{k=1}^{n-1} \binom{n}{k} \mathcal{M}_{i_1}(k) \mathcal{M}_{i_2}(n-k), \tag{2.19}$$

and

$$\sum_{i_1 \neq i_2 \neq i_3} \boxed{} = \frac{1}{3!} \sum_{i_1 \neq i_2 \neq i_3} \sum_{k_1+k_2+k_3=n}^{1 \leq k_i \leq n-2} \binom{n}{k_1, k_2, k_3} \\ \times \mathcal{M}_{i_1}(k_1) \mathcal{M}_{i_2}(k_2) \mathcal{M}_{i_3}(k_3), \tag{2.20}$$

where the symbol $\binom{n}{k_1, k_2, \ldots, k_m} = \frac{n!}{k_1! k_2! \ldots k_m!}$ is the multinomial coefficient. One can verify that in general the expectation value takes the form

$$\langle H^n \rangle_0 = \frac{1}{Z(0)} \sum_{\{\sigma_i\}} \sum_{p=1}^{n} \frac{1}{p!} \sum_{i_1 \neq \cdots \neq i_p} \sum_{k_1+\cdots+k_p=n}^{1 \leq k_i \leq n-p+1} \binom{n}{k_1, \ldots, k_p} \\ \times \mathcal{M}_{i_1}(k_1) \ldots \mathcal{M}_{i_p}(k_p) \\ = \frac{1}{Z(0)} \sum_{p=1}^{n} \frac{1}{p!} \sum_{i_1 \neq \cdots \neq i_p} \sum_{\{\sigma\}_{i_1, \ldots, i_p}} \sum_{k_1+\cdots+k_p=n}^{1 \leq k_i \leq n-p+1} \binom{n}{k_1, \ldots, k_p} \tag{2.21} \\ \times \left[\sum_{\sigma_{i_1} \sigma_{i_1+x} \sigma_{i_1+y}} \mathcal{M}_{i_1}(k_1) \right] \ldots \left[\sum_{\sigma_{i_p} \sigma_{i_p+x} \sigma_{i_p+y}} \mathcal{M}_{i_p}(k_p) \right].$$

The notation $\{\sigma\}_{i_1, \ldots, i_p}$ stands for the set of σ_i for all i, except $\sigma_{i_1}, \sigma_{i_1+x}, \sigma_{i_1+y}, \ldots, \sigma_{i_p}, \sigma_{i_p+x}, \sigma_{i_p+y}$. This sum is therefore $\sum_{\{\sigma\}_{i_1, \ldots, i_p}} 1 = N^{L^2-3p}$. The other sum can be rewritten as follows

$$\sum_{\sigma_i \sigma_{i+x} \sigma_{i+y}} \mathcal{M}_i(k) = \sum_{q=0}^{k} \binom{k}{q} \sum_{\sigma_i \sigma_{i+x} \sigma_{i+y}} E^q(\sigma_i - \sigma_{i+x}) E^{k-q}(\sigma_i - \sigma_{i+y}) \\ = N^3 \sum_{q=0}^{k} \binom{k}{q} \langle E^q \rangle_N \langle E^{k-q} \rangle_N \equiv N^3 \tilde{\mathcal{M}}(k). \tag{2.22}$$

Here we have defined the link-averages $\langle E^q \rangle_N \equiv \frac{1}{N} \sum_A E^q(A)$ and the second line follows from changing variables in the σ sums. The N^3 factors together with the fact that $Z(0) =$

N^{L^2} cancel the N^{L^2-3p} factor. Now, since $\tilde{\mathcal{M}}(k)$ does not depend on the site i any more we get another factor of $\sum_{i_1 \neq \cdots \neq i_p} 1 = (L^2)_p$, where

$$(L^2)_p = \frac{\Gamma(L^2+1)}{\Gamma(L^2-p+1)} = L^2(L^2-1)\ldots(L^2-p+1) \tag{2.23}$$

is the descending Pochhammer symbol. Collecting all this together, we find the following simplified expression for the total energy moments

$$\langle H^n \rangle_0 = \sum_{p=1}^{n} C_p(n)(L^2)_p, \tag{2.24}$$

with the coefficients

$$C_p(n) = \frac{1}{p!} \sum_{k_1+\cdots+k_p=n}^{1 \leq k_i \leq n-p+1} \binom{n}{k_1 \ldots, k_p} \tilde{\mathcal{M}}(k_1)\ldots\tilde{\mathcal{M}}(k_p). \tag{2.25}$$

The usefulness of (2.24) comes from the fact that the L^2 dependence is explicitly factorized.

We note that the total energy moments in equation (2.24) goes as $o(L^2)$ in the volume, and in particular do not contain any constant terms. The cumulants μ_n are just sums and differences of these moments, and are therefore of order $o(L^2)$. Thus the cumulants do not have any constant terms at all.

Furthermore, it is well known from statistical physics that the free energy $F(\beta) = \log Z(\beta)$ is an extensive quantity and scales as volume in the thermodynamic limit. This implies that all the moments also scale as L^2 and the higher order terms must cancel out (this can directly be verified for the first few moments using (2.24)). Thus we conclude that

$$Z(\beta) = e^{\log N L^2 - f_N(\beta)L^2 + o(L^{-1})}, \tag{2.26}$$

in particular there is no constant term to all orders of β. As a few examples, we can use (2.24) to calculate

$$f_2(\beta) = \beta - \frac{\beta^2}{4} + \frac{\beta^4}{96} - \frac{\beta^6}{1440} + o(\beta^7),$$

$$f_3(\beta) = \beta - \frac{\beta^2}{8} - \frac{\beta^3}{96} + \frac{\beta^4}{512} + \frac{\beta^5}{2048} - \frac{7\beta^6}{245760} + o(\beta^7), \tag{2.27}$$

$$f_4(\beta) = \beta - \frac{\beta^2}{8} + \frac{\beta^4}{768} - \frac{\beta^6}{46080} + o(\beta^7).$$

2.B Appendix B: Mapping Class Groups

In this appendix we will give a bit of intuition behind the conjecture in this chapter, based on eq. (2.1). The discussion will be intuitive, rather than rigorous.

Topological order can be understood as patterns of long-range entanglement of ground states, which are responsible for the protected physical properties of the systems such as anyonic quasiparticle statistics and protected chiral edge modes.

Due to the patterns of long-range entanglement, the ground state degeneracy $GSD(\mathcal{M})$ on any manifold $\mathcal{M}$, is known to only depend on the topology of $\mathcal{M}$ and is completely robust against any local perturbations that do not induce a phase transition. These states $\{|\psi_\alpha\rangle\}_{\alpha=1}^{GSD(\mathcal{M})}$ are locally completely indistinguishable, but globally distinguishable. In order to distinguish them from each other, non-local operators must be used which usually are of string, or higher dimensional p-brane type that wrap around non-trivial cycles of $\mathcal{M}$.

The question is, how can we probe for the universal global pattern of long-range entanglement and thereby extract the topological physics?

One way to do this is to study how the ground states (topological sectors) map into each other under certain *non-local transformations* of the manifold that act on the global degrees of freedom.

In order to give some intuition for what we mean, consider a gapped system on a two-torus $\mathcal{M} = T^2$. By transformation on the torus we mean maps $f : T^2 \to T^2$ which preserve certain structures, for example we want them to be invertible and continuous. Meaning that any set of points connected continuously to each other, map to points connected continuously to each other, but the map, however, can be very non-local (see fig. 2.B.1). The set of such maps we call $\mathtt{AMG}(T^2)$, the group of automorphisms of T^2. This is a group since it contains the identity map $id \in \mathtt{AMG}(T^2)$, defined by $id(p) = p \in T^2$ and group multiplication is given by composition of maps.

Note that the group $\mathtt{AMG}(T^2)$ is not connected; some maps $f \in \mathtt{AMG}(T^2)$ can be continuously deformed to the identity map $f \sim id$, while others cannot (see fig. 2.B.2). The key thing to note is that, maps that are not continuously connected to the identity act nontrivially on global degrees of freedom and will map different ground states into each other.

Let $\mathtt{AMG}_0(T^2)$ be the connected component containing the identity map. The object of interest is therefore the group of all connected components $\mathtt{MCG}(T^2) = \mathtt{AMG}(T^2)/\mathtt{AMG}(T^2)_0 = \pi_0[\mathtt{AMG}(T^2)]$, where maps that differ by an element in $\mathtt{AMG}_0(T^2)$ are identified. This group
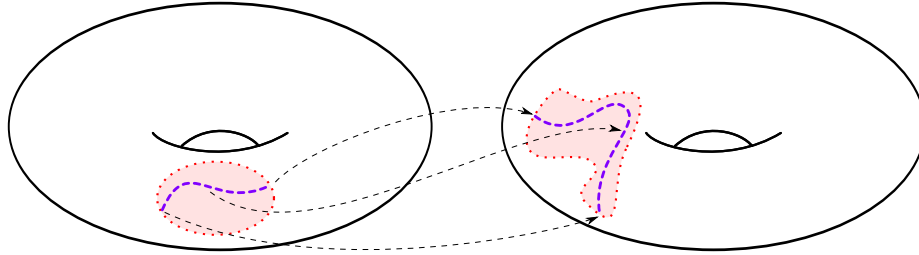
Figure 2.B.1: Locally, elements $f \in \mathtt{AMG}(T^2)$ map points to other points in a continuous fashion. The figure shows an example where points in a small local region is mapped onto other points, where following some curve (blue dashed line) continuously we get a new continuous curve. The map has to be continuous like this, globally. Doing this patch by patch, we can both create elements in $\mathtt{AMG}(T^2)$, that either can or cannot be continuously deformed to the identity map.
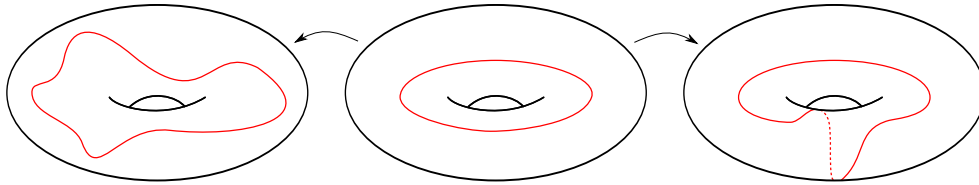
Figure 2.B.2: Some maps $f \in \mathtt{AMG}(T^2)$ belong to the connected component containing the identity $\mathtt{AMG}_0(T^2) \subset \mathtt{AMG}(T^2)$, while others do not. One way to see the difference, is to draw some closed loops and see where the loop is mapped to. It is easy to see that for the map to the left, the image of the curve can be continuously deformed to the original curve. While for the map to the right this cannot be done, thus the map does not belong to $\mathtt{AMG}_0(T^2)$ but to a non-trivial class in $\mathtt{MCG}(T^2)$.

is usually called the mapping class group, and in the case of a two-torus one can show that it is isomorphic to $\mathtt{MCG}(T^2) \approx SL(2, \mathbb{Z})$. Thus each element in $\mathtt{MCG}(T^2)$ corresponds to a class of globally non-trivial maps, while the identity element corresponds to the class of maps in $\mathtt{AMG}_0(T^2)$.

Each transformation $A \in \mathtt{MCG}(T^2)$, will induce a transformation of the ground states $|\psi_\alpha\rangle \rightarrow M^A_{\alpha,\beta}|\psi_\beta\rangle$. The set of matrices M^A for all A, form a representation of $\mathtt{MCG}(T^2)$ on the ground state subspace, and probes the global patterns of long-range entanglement, thus contain information about the topological physics of the phase. Naively, these matrix elements are given by computing the overlaps $\langle\psi_\alpha|\hat{\mathcal{O}}_A|\psi_\beta\rangle$, where $\hat{\mathcal{O}}_A$ are very non-local maps acting on the full Hilbert space and induced by $A \in \mathtt{MCG}(T^2)$.

However in general the maps $\hat{\mathcal{O}}_A$ do not leave the ground state subspace invariant (unless we have ground-states of ideal TQFT's), since the ground states contain local non-universal information (short-range entanglement). Therefore the overlap of $\hat{\mathcal{O}}_A|\psi_\beta\rangle$ with the ground states $\langle\psi_\alpha|$ will be a very small number and the question is: how can we extract the universal matrices M^A from the overlaps $\langle\psi_\alpha|\hat{\mathcal{O}}_A|\psi_\beta\rangle$?

This is precisely the content of our conjecture in eq. (2.1). Further justification for this conjecture will be given in future work.

Chapter 3

Modular Matrices as Topological Order Parameter by Gauge Symmetry Preserved Tensor Renormalization Approach

This chapter was published in [2]

3.1   Introduction

The most basic question in condensed matter is to classify all different states and phases. Landau symmetry breaking theory is the first successful step to classify all phases [9, 10, 11]. However, the experimental discovery of Integer Quantum Hall Effect [16] and Fractional Quantum Hall Effect [17] led condensed matter physics to a new era that goes beyond Landau theory, in which the most fundamental concept is topological order [99, 100, 124]. Topological order is characterized/defined by a new kind of "topological order parameter": (a) the topology-dependent *ground state degeneracy* [99, 100] and (b) the *non-Abelian geometric phases S and T* of the degenerate ground states [124, 101, 102], where both of them are *robust against any local perturbations* that can break any symmetries [100]. This is just like superfluid order being characterized/defined by zero-viscosity and quantized vorticity that are robust against any local perturbations that preserve the $U(1)$ symmetry.

Recently, it was found that, microscopically, topological order is related to long-range

47

entanglement [35, 34]. In fact, we can regard topological order as pattern of long-range entanglement [24] defined through local unitary (LU) transformations.[84, 125, 126] Chiral spin liquids, [97, 98] integral/fractional quantum Hall states [16, 17, 18], $\mathbb{Z}_2$ spin liquids, [110, 111, 127] non-Abelian fractional quantum Hall states, [128, 129, 130, 131] are examples of topologically ordered phases. Topological order and long-range entanglement are truly new phenomena, which require new mathematical language to describe them. It appears that tensor category theory [132, 84, 24, 133, 134] and simple current algebra [128, 135, 136, 137] (or pattern of zeros [138, 139, 140, 141, 142, 143, 144, 145, 146]) may be part of the new mathematical language. For 2+1D topological orders (with gapped or gapless edge) that have only Abelian statistics, we find that we can use integer K-matrices to classify them.[147, 148, 149, 150, 151, 88]

As proposed in Ref. [124, 101, 102], the non-Abelian geometric phases of the degenerate ground states, *i.e.* the Modular matrices generated by Dehn twist and 90 degree rotation, are effective "topological order parameters" that can be used to characterize topological order. Refs. [106, 45, 108, 107] makes the first step to calculate numerically modular matrices using various methods. Actually, the relation of tensor network states (TNS) and topological order has already been investigated by several papers [152, 153]. Ref. [154, 155, 119, 120] concluded that gauge-symmetry structure of TNS will give rise to information of topological order. Unlike calculating topological entanglement entropy which in principle needs to calculate the reduced density matrix with exponentially high computational cost, extracting topological data through the gauge-symmetry structure of TNS has acceptable lower cost.

In this chapter, we will give a systematical approach to calculate modular matrices, using the wave-function overlap method proposed in Ref. [109, 1]. Our approach is based on TNS and gauge-symmetry preserved tensor renormalization group. Gauge-symmetry preserved RG differs from original tensor RG (TRG) in the sense that every step of TRG will keep the gauge-symmetry structure invariant and manifest. The chapter is organized as follows: I) we will first review the basic ideas of modular matrices and TRG; II) we will explain the systematical method to calculate modular matrices based on TRG; III) we will show the numerical results of modular matrices for the toric code and double-semion topological orders,[110, 111, 127, 132, 84] which clearly identifies the correct topological order and characterizes phase transitions.

3.2 Review of Modular Matrices

Modular matrices, or T- and S-matrices, are generated respectively by Dehn twist (twist) and $90°$ rotation on torus. The operation of twist can be defined by cutting up a torus along one axis, twisting the edge by $360°$ and glueing the two edges back.

The elements of the universal T- and S-matrices are given by: [109, 1]

$$\begin{aligned} \langle \psi_i | \hat{T} | \psi_j \rangle &= e^{-A/\xi^2 + o(1/A)} T_{ij} \\ \langle \psi_i | \hat{S} | \psi_j \rangle &= e^{-A/\xi^2 + o(1/A)} S_{ij} \end{aligned} \tag{3.1}$$

where $|\psi_i\rangle$ form a set of orthonormal basis for degenerate ground space; and $\hat{T}$ and $\hat{S}$ are the operators that generate the twist and the rotation on torus. A is the area of the system and ξ is of order of correlation length which is not universal.

The T- and S-matrices encode all the information of quasi-particles statistics and their fusion.[103, 55] It was also conjectured that the T- and S-matrices form a complete and one-to-one characterization of topological orders with gapped edge [124, 101, 102] and can replace the fixed-point tensor description to give us a more physical label for topological order.

3.3 Review of Tensor Renormalization Group

To be specific, TRG here means double tensor renormalization group [156]. Essentially, a translation invariant TNS can be written by definition as

$$|\psi\rangle = \sum_{m_1 m_2 ..} \mathrm{tTr}(T^{m_1} T^{m_2} ... T^{m_N}) |m_1\rangle |m_2\rangle ... |m_N\rangle \tag{3.2}$$

where T^{m_i}'s are local tensors with physical index m_i defined either on links or vertices; and m_i's are local Hilbert space basis. (Sometimes m_i is not written out explicitly if there is no ambiguity). tTr means contracting over all internal indices of local tensors pair by pair. The norm of the state is given by

$$\langle \psi | \psi \rangle = \mathrm{tTr}(\boldsymbol{T} \boldsymbol{T} ... \boldsymbol{T}) \tag{3.3}$$

where, $\boldsymbol{T}$ is the local double tensor, which is formed by $T^\star$ and T tracing out physical degree freedom.

$$\boldsymbol{T} = \sum_{m_i} T^{m_i \star} T^{m_i} \tag{3.4}$$

The essence of double TRG is to find fewer double tensors $\boldsymbol{T}'$, which keeps the norm approximately invariant. I.e.,

$$\langle\psi|\psi\rangle \simeq \text{tTr}(\boldsymbol{T}'\boldsymbol{T}'...\boldsymbol{T}') \tag{3.5}$$

This approximation can be done non-uniquely. And SVD TRG approach shall be utilized in this chapter for its convenience and low cost. The procedure of SVD RG approach is graphically explained in the Fig. 3.3.1 (c) and (d). Step (c) is to perform local SVD to decompose double tensor $\boldsymbol{T}$ into $\boldsymbol{T}_1$ and $\boldsymbol{T}_2$. In order to prevent the bond dimension of internal indices from growing exponentially, only finite number D_{cut} of singular values are kept. Step (d) is to do coarse graining, the tensors on new smaller square will form a new double tensor $\boldsymbol{T}'$. After step (c) and (d), half of tensors will be contracted. For a translation invariant TNS, after enough steps of SVD TRG, the double tensor will flow to the fixed point double tensor, $\boldsymbol{T}_{fp}$, which plays an essential role in the next section. Topological data can be extracted from $\boldsymbol{T}_{fp}$.

Note that the above TRG approach suffers from the necessary symmetry condition [154]. If the gauge symmetry is not preserved in each step of TRG, the approach will be ruined by errors. And more importantly, the RG flow will arrive at some wrong fixed point tensors. Gauge-Symmetry Preserved TRG is introduced in the next section in order to prevent this happening. Another reason that normal TRG is not suitable here is that during TRG, the gauge symmetry information is lost. So that in order to reproduce all topological data, the gauge symmetry should be preserved.

3.4 Modular Matrices by Gauge-Symmetry Preserved Tensor Renormalization Group

In refs. [155, 119, 120], the gauge structure of TNS is analyzed. It was concluded that by inserting gauge transformation tensors to TNS, a set of basis for the degenerate ground space will be obtained. More specifically, the ground states could be labeled as $|\psi(g,h)\rangle$, where g, h are gauge tensors acting on internal indices in two directions. Different ground states can be transformed to each other by applying gauge tensors on internal indices of a TNS. Therefore it is natural to think that since all ground states could be obtained, by calculating all overlaps $\langle\psi_i|\hat{T}|\psi_j\rangle$ and $\langle\psi_i|\hat{S}|\psi_j\rangle$, the whole modular matrices could be calculated. However, it is difficult to compute the overlap directly and keep track of the non-universal contributions. See EQ. 3.1.
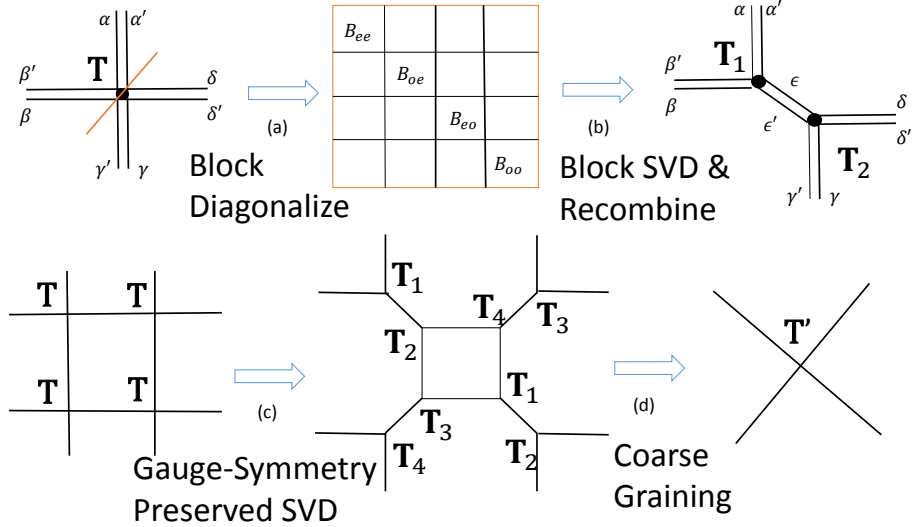
Figure 3.3.1: Illustration for Symmetry Preserved Tensor Renormalization Group. First (a) before SVD, block diagonalize double tensor $\boldsymbol{T}$ according to the $\mathbb{Z}_2$ symmetry rule, $\alpha + \beta + \gamma + \delta$ and $\alpha' + \beta' + \gamma' + \delta'$ are both even numbers. Therefore the indices of each block matrices $B_{ee}, B_{eo}, B_{oe}, B_{oo}$ represent whether $\alpha + \beta$ and $\alpha' + \beta'$ are even or odd. (b) Perform SVD in each block matrices and recombine the tensors coming out of SVD into tensor $\boldsymbol{T}_1$ and $\boldsymbol{T}_2$, according to the rule $\alpha + \beta + \epsilon'$, $\alpha' + \beta' + \epsilon$, $\gamma + \delta + \epsilon'$ and $\gamma' + \delta' + \epsilon$ are all even numbers. I.e., tensor $\boldsymbol{T}_1$ and $\boldsymbol{T}_2$ both obey $\mathbb{Z}_2$ gauge symmetry. (c) and (d) are the same procedures as TRG. (c) is to use SVD to decompose $\boldsymbol{T}$ into $\boldsymbol{T}_1$ and $\boldsymbol{T}_2$. Only D_{cut} numbers of singular values will be kept. (d) is coarse graining. The four tensors on the small square will form a new double tensor $\boldsymbol{T}'$. Note that T_3 and T_4 are outcoming tensors that are cut in another direction.

TRG will help reduce the difficulty, since one fixed point double tensor essentially represents the whole lattice. Calculating on one double tensor is much easier and size effects do not appear. However, normal TRG is not suitable here since gauge symmetry needs to be preserved through every tensor RG step in order to insert gauge transformation tensors.

To be more specific, let us consider the case of $\mathbb{Z}_2$ topological order, which also makes it clear in the next section. As already known in the refs. [155, 119, 120], tensor network representation for $\mathbb{Z}_2$ topological state has $\mathbb{Z}_2$ gauge symmetry. The double tensor $\boldsymbol{T}_{\alpha\alpha^\star\beta\beta^\star\gamma\gamma^\star\delta\delta^\star}$ will have a $\mathbb{Z}_2 \times \mathbb{Z}_2$ gauge symmetry, where $\alpha, \alpha^\star, \beta, \beta^\star, \gamma, \gamma^\star, \delta, \delta^\star = 0, 1$, and

$\alpha, \beta, \gamma, \delta$ are indices coming from T while $\alpha^\star, \beta^\star, \gamma^\star, \delta^\star$ are indices coming from $T^\star$. So the double tensor with $\mathbb{Z}_2$ gauge symmetry satisfies

$$\begin{aligned}
\boldsymbol{T}_{\alpha'\alpha^{\star\prime}\beta'\beta^{\star\prime}\gamma'\gamma^{\star\prime}\delta'\delta^{\star\prime}} &= \boldsymbol{T}_{\alpha\alpha^\star\beta\beta^\star\gamma\gamma^\star\delta\delta^\star} \times \\
&A_{\alpha\alpha'}A_{\beta\beta'}A_{\gamma\gamma'}A_{\delta\delta'}B_{\alpha^\star\alpha^{\star\prime}}B_{\beta^\star\beta^{\star\prime}}B_{\gamma^\star\gamma^{\star\prime}}B_{\delta^\star\delta^{\star\prime}}
\end{aligned} \tag{3.6}$$

where repeated indices imply summation and tensor A, $B \in \{I, \sigma_z\}$ generate the $\mathbb{Z}_2 \times \mathbb{Z}_2$ gauge symmetry on both layer of double tensor, which only act on internal indices. If a double tensor has such a gauge symmetry, its elements are nonzero only when $\alpha + \beta + \gamma + \delta$ and $\alpha^\star + \beta^\star + \gamma^\star + \delta^\star$ are both even. [1]

In order to keep $\mathbb{Z}_2 \times \mathbb{Z}_2$ gauge symmetry manifest at each RG step, we develop *gauge-symmetry preserved tensor RG* (GSPTRG). Essentially, it differs from normal TRG only when we do SVD. The double tensor needs to be block diagonalized by even or odd of its indices, and then SVD is performed in each block and recombine the tensors coming out of SVD into one tensor, just as the way to block diagonalize it. In each block, the tensor elements have the same even or odd indices, which therefore is key to preserve $\mathbb{Z}_2$ symmetry manifest. The procedures are also explained in the Fig. 3.3.1.

After several steps of GSPTRG (c.f. Fig. 3.5.1), double tensor will flow to the gauge-symmetry preserved fixed point tensor. Equivalent to calculate the overlap by brute force, we can obtain the modular matrices by the following three steps:

1) inserting gauge symmetry tensors into double tensor; 2) performing rotation and twist on one layer of fixed point double tensor; 3) tracing out rest indices.

The procedures are also explained in the Fig. 3.4.1. Actually the innerproduct of ground states ($\langle \psi(g', h')|\psi(g, h)\rangle$) (each ground state is obtained by inserting gauge tensors on boundary) in topological phase will be diagonal with each element modulo 1. The elements of T- and S-matrices are just reshuffle of elements ($\langle \psi(g', h')|\psi(g, h)\rangle$). More explicitly for the $\mathbb{Z}_2$ topological state

$$\langle \psi(g', h')|\hat{T}|\psi(g, h)\rangle = \langle \psi(g', h')|\psi(g, gh)\rangle \tag{3.7}$$

$$\langle \psi(g', h')|\hat{S}|\psi(g, h)\rangle = \langle \psi(g', h')|\psi(h, g^{-1})\rangle \tag{3.8}$$

---

[1]For general $\mathbb{Z}_N$ model, the generators are $\{(A)_{\alpha\beta} = e^{i\frac{2\pi}{N}c\beta}\delta_{\alpha\beta}\}_{c=0}^{N-1}$. And due to $\mathbb{Z}_N$ gauge symmetry, the tensor will satisfy that only the components which summation of indices equal to 0 (mod N) will be nonzero.
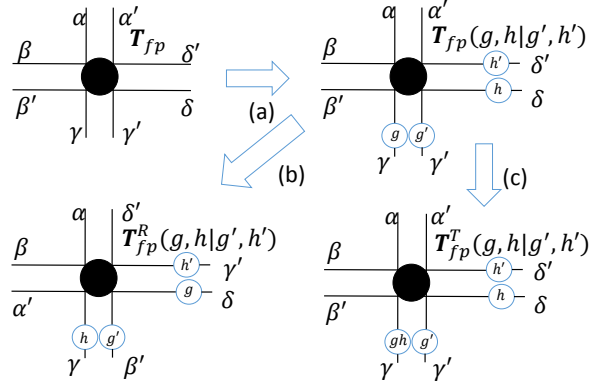
Figure 3.4.1: Modular matrices from the fixed point double tensor $\boldsymbol{T}_{fp}$. Eight legs of $\boldsymbol{T}_{fp}$ will all be traced over because of torus geometry. (a) By inserting $\mathbb{Z}_2$ gauge tensors g, h, g', h' into $\boldsymbol{T}_{fp}$, $\boldsymbol{T}_{fp}(g, h|g', h')$ is obtained; and tracing over eight legs of $\boldsymbol{T}_{fp}(g, h|g', h')$ will give rise to overlaps of $\langle \psi(g', h') | \psi(g, h) \rangle$, where $|\psi(g, h)\rangle$ labels different ground states with gauge symmetry on boundary. The elements of T- and S-matrices are just reshuffling of $\langle \psi(g', h') | \psi(g, h) \rangle$, as illustrated in the Fig. (b) and (c). Fig. (b) represents 90° rotation and Fig. (c) represents twist.

3.5 Modular Matrices for $\mathbb{Z}_2$ topological order

Toric code model [69] is the simplest model that realize the $\mathbb{Z}_2$ topological order [110, 111]. Local physical states are defined on every link with spin up and down. In the notation of string-net states, spin up represents a string while spin down represents no-string. Essentially, the $\mathbb{Z}_2$ topological state can be written as equal superposition of all closed string loops:

$$|\psi_{TC}\rangle = \sum_X |X\rangle \tag{3.9}$$

where X represents a closed loop, and normalization factor is implicity in the above equation.

When putting the $\mathbb{Z}_2$ topologically ordered state on a torus, the ground state degeneracy is four and the quasi-particles are usually labeled by $\{1, e, m, em\}$. T- and S-matrices in the twist basis[1] are given in Fig. 3.5.1c for $g > 0.802$.

It is easy to represent $|\psi_{TC}\rangle$ in terms of a tensor network. For the sake of convenience, we replace local physical states $|1\rangle$ and $|0\rangle$ with $|11\rangle$ and $|00\rangle$ respectively. And combine each $|1\rangle$ and $|0\rangle$ to its nearest sites. So local physical states now are on vertices without
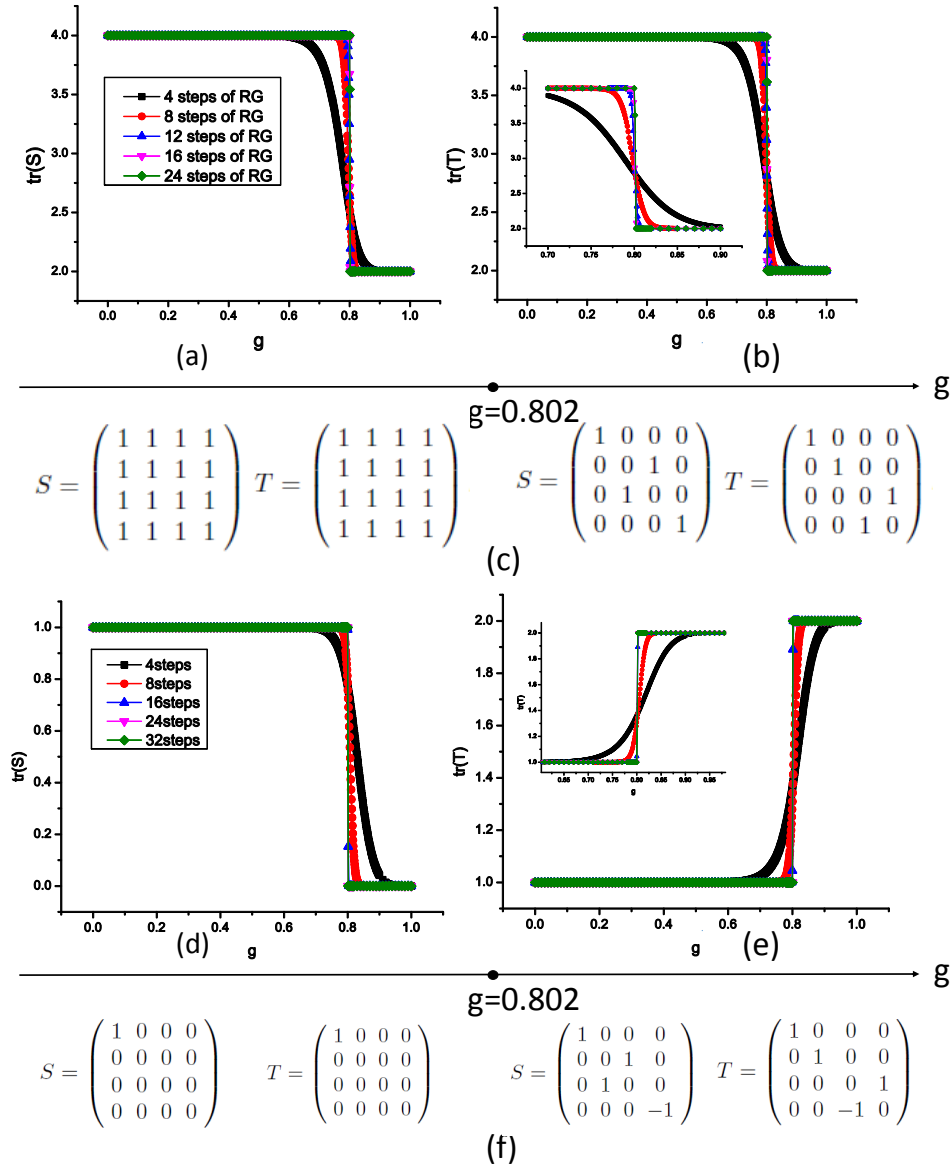
Figure 3.5.1: The trace of modular matrices S and T as functions of g display a very sharp phase transition at critical point g_c as increasing RG steps, for both $\mathbb{Z}_2$ and double-semion topological order. The $\mathbb{Z}_2$ topological order transition point coincides exactly with the results in Ref. [24] by another characterization.
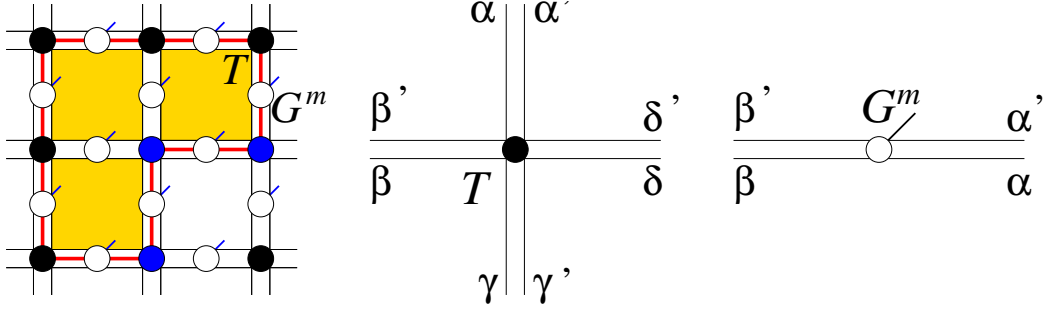
Figure 3.5.2: The T tensor and the G^m tensor that describes the ground state wave function of the double semion model. The "virtual qubits" are in the "1" state in the shaded squares and in the "0" state in other squares. The red line is the domain wall (string) between "0" and "1" states of the virtual qubits. The blue (black) dots represent $t_{\alpha\beta\gamma'\delta'} = -1$ ($t_{\alpha\beta\gamma'\delta'} = 1$).

extending Hilbert space. Here we choose the parameterization of $\mathbb{Z}_2$ topological state utilized in Ref. [24]

$$T^{(\alpha\beta\gamma\delta)}_{\alpha\beta\gamma\delta} = g^{\alpha+\beta+\gamma+\delta} \text{when} \quad \alpha + \beta + \gamma + \delta \quad \text{even}$$

$$\text{Rest elements of T are zeros.}$$

When $g = 1$, it is $|\psi_{TC}\rangle$ while when g=0, it is a trivial state $|0000....0\rangle$. Of course, when g is driven from 0 to 1, it must undergo a phase transition.

We calculate T- and S-matrices along g. We find that when $0 \leq g < 0.802$, all components of T- and S-matrices are 1, because the gauge twisting does not produce other ground states in the trivial phase. When $0.802 \leq g < 1$, it belongs to $\mathbb{Z}_2$ topological phase, since the T- and S-matrices for each $g \in (0.802, 1]$ agrees with that of $\mathbb{Z}_2$ topological phase[1] (see Fig. 3.5.1c).

3.6 Modular Matrices for Double-semion model

The double-semion model[132, 84, 157] is another topologically ordered state with two semions of statistics $\theta = \pm\pi/2$. In the notation of string-net states, the double-semion ground state can also be written as superposition of all closed string loops:

$$|\psi_{DS}\rangle = \sum_X (-)^{N_{loops}}|X\rangle \tag{3.10}$$

where X represents a closed loop, and N_{loops} the number of loops. The above double-semion state can be described by a TNS with the following tensors T and G^m at $g = 1$ (see Fig. 3.5.2):

$$
\begin{aligned}
T_{(\alpha\alpha')(\beta\beta')(\gamma\gamma')(\delta\delta')} &= t_{\alpha\beta\gamma'\delta'}\delta_{\alpha\beta'}\delta_{\beta\gamma}\delta_{\gamma'\delta}\delta_{\delta'\alpha'}, \\
t_{1000} &= t_{1101} = -1, \quad \text{other } t_{\alpha\beta\gamma'\delta'} = 1; \\
G^m_{(\alpha\alpha')(\beta\beta')} &= g^m_{\alpha\alpha'}\delta_{\alpha\beta}\delta_{\alpha'\beta'}, \\
g^1_{10} &= g^1_{01} = g, \quad g^0_{00} = g^0_{11} = 1, \\
g^1_{00} &= g^1_{00} = g^0_{10} = g^0_{01} = 0.
\end{aligned}
\tag{3.11}
$$

Note that if we view $\alpha = \beta'$, $\beta = \gamma$, $\gamma' = \delta$, and $\delta' = \alpha'$ as indices that label "virtual qubits" in the squares, then the strings can be viewed as domain wall between the "0" and "1" states of the qubits. Also if we choose $t_{\alpha\beta\gamma'\delta'} = 1$, the above tensors will describe the $\mathbb{Z}_2$ topologically ordered state discussed previously.

The $\mathbb{Z}_2$ gauge symmetry is generated by $\sigma^x \otimes \sigma^x$ acting on each internal indices $(\alpha\alpha')$ followed by a transformation generated by $u^i_{\alpha\alpha'}$, $i = t, l, b, r$ acting on the links of the four orientations. Here $u^i_{\alpha\alpha'}$ must satisfy

$$
f_{\alpha\beta\gamma'\delta'} = u^t_{\beta\gamma'}u^b_{\alpha\delta'}u^l_{\beta\alpha}u^r_{\gamma'\delta'}
\tag{3.12}
$$

where

$$
f_{1000} = f_{0111} = f_{0010} = f_{1101} = -1, \quad \text{others } f_{\alpha\beta\gamma'\delta'} = 1.
\tag{3.13}
$$

Furthermore $u^i_{\alpha\alpha'}$ must also satisfy

$$
\begin{aligned}
g^m_{\alpha\alpha'} &= (u^t_{\alpha\alpha'})^* g^m_{\alpha\alpha'} (u^b_{\alpha\alpha'})^* \\
g^m_{\alpha\alpha'} &= (u^l_{\alpha\alpha'})^* g^m_{\alpha\alpha'} (u^r_{\alpha\alpha'})^*.
\end{aligned}
\tag{3.14}
$$

We find that

$$
u^t = u^b = \begin{pmatrix} 1 & -1 \\ 1 & 1 \end{pmatrix}, \quad u^r = u^l = \begin{pmatrix} 1 & 1 \\ -1 & 1 \end{pmatrix},
\tag{3.15}
$$

See [120] for a general analysis of twisted gauge structures.

After the GSPTRG calculation, we find a phase transition at $g_c = 0.802$. The S- and T-matrices for the nontrivial phase with $g \in (0.802, 1]$ are given by Fig. 3.5.1, which agree with the modular matrices for the double semion model in string basis [158]. For the trivial phase near $g = 0$, the modular matrices become $T_{\alpha\beta} = S_{\alpha\beta} = \delta_{\alpha,0}\delta_{\beta,0}$.

3.7 Conclusion

We have developed a systematic approach, *gauge-symmetry preserved tensor renormalization*, to calculate modular matrices from a generic many-body wave function described by a tensor network. The modular matrices can be viewed as very robust "topological order parameters" that only change at phase transitions. The tensor network approach gives rise to S and T matrices in a particular basis which is different from the standard quasiparticle basis.[124, 101, 103, 102, 106, 45, 108, 107, 55] The trivial phase will result in trivial modular matrices $S = 1$ and $T = 1$ (since there is no degeneracy on a torus), and the topological phase will give rise to nontrivial modular matrices, which contain topological informations, such as quasi-particles information, like statistic angle, fusion rule, quantum dimension, etc.

In particular, a general algorithm can be developed: the tensor network ansatz can be imposed with gauge symmetry G (or MPO symmetry, see below) in the beginning, and the corresponding update algorithm, which is used to find ground states, also preserves such a gauge symmetry. Therefore if the topological phase indeed has such a gauge theory description, the ansatz obviously is better than the normal tensor network ansatz. In Appendix B we perform such a benchmark computation using the $\mathbb{Z}_2$ phase of the Kitaev honeycomb model [56]. There we prepare an arbitrary tensor with $\mathbb{Z}_2$ symmetry, find the ground state (locally) numerically by gauge-symmetry preserved update and from there compute the modular matrices. A similar tensor network computation of Kitaev honeycomb model is developed in Ref. [159] where $\mathbb{Z}_2$ gauge structure is also imposed but expressed by Grassmann tensor network. The energy and nearest neighbor correlation are computed there.

After the completion and publication of the preprint of this chapter, the notion of (twisted) G-injectivity of [119, 120] was generalized to the matrix product operator (MPO) case in [160] and it was shown that any string-net model is included with this generalization. The method developed in this chapter can thus similarly be generalized to any MPO symmetry and does not need any group structure (and thus not restricted to twisted discrete gauge theories).

The universal wave function overlap [1] (3.1) applies to any dimension and have already been investigated in exactly solvable models in 3+1D [161, 3, 162]. The method outlined in this chapter can similarly be generalized to higher dimensions to extract universal topological information from generic gapped ground states.

Finally we note that although the universal wave function overlap [1] works for any topological order, the machinery developed in this chapter in 2+1D only works for non-

chiral topological order (gapped boundaries) as formulated here. This is only because the tensor network techniques used are best understood for non-chiral topological order, but a generalization for chiral topological order would be both interesting and important.

After the publication of the work presented in the previous and current chapter, lots of interesting work has been generated using these ideas. Some related to numerically detecting topological order and others related to 3+1D topological systems (see next chapter). In particular, I would like to mention [163]. There the ideas of this chapter was developed to study a much more realistic system that has been studied theoretically and experimentally for many years, namely the Heisenberg model on the Kagome lattice. It was shown that the modular matrices computed in this fashion, are a very sensitive probe of a gap above the ground-state. They find that the Heisenberg model is a gapped spin liquid with $\mathbb{Z}_2$ topological order and with a correlation length $\xi \sim 10$ unit cells. This long correlation length explains the gapless behavior observed in many simulations on smaller systems.

Appendices

3.A   Appendix A: Robustness of modular matrices under $\mathbb{Z}_2$ perturbations

In the phase diagram Fig. 3.5.1, it already demonstrates that T- and S-matrices are very robust characterization of topological order, which only depend on the phase. In order to address on this issue more explicitly, we will perturb $\mathbb{Z}_2$ topological state at $g = 1$, while the perturbation also respects internal $\mathbb{Z}_2$ gauge symmetry, i.e., the perturbation tensor T' is written as:

$$T'^{\alpha'\beta'\gamma'\delta'}_{\alpha\beta\gamma\delta} = \epsilon r \ \ when \ \ \alpha + \beta + \gamma + \delta \ \ even \tag{3.16}$$

where r is a uniform distributed random number ranging from $[-1, 1]$ depending on α', β', γ', δ', α, β, γ, δ; and ϵ represents perturbation strength starting from zero. The initial tensor before RG will be $T + T'$.

As already shown in Ref. [24], $\mathbb{Z}_2$ topological phase is robust under tensor perturbations which respect the $\mathbb{Z}_2$ gauge symmetry, while fragile under perturbations breaking the $\mathbb{Z}_2$ gauge symmetry. Here we start from perturbed tensor $T + T'$ and calculate modular matrices for different ϵ's, which will demonstrate the robustness of this topological characterization3.A.1.

Numerically it demonstrates that when $0 \leq \epsilon \leq 0.35$, T- and S-matrices are always eqn. 3.10. However, when $\epsilon > 0.35$, the perturbations will possibly break the topological phase (and possibly not). In this case, T- and S-matrices have three possibilities as shown in the figure. Anyway, this calculation clearly demonstrates modular matrices are robust characterization of topological phase.

3.B   Appendix B: Gauge-Symmetry Preserved Update

For a typical tensor network algorithm, there are two main steps: updating local tensors to lower the energy to ground state energy and contracting all local tensors to compute physical quantities and norms. Here we only point out some details in gauge-symmetry preserved update algorithm, since the details in contraction have already been reviewed in the main text to some extent.

$$T = \begin{pmatrix} 1 & 0 & 0 & 0 \\ 0 & 1 & 0 & 0 \\ 0 & 0 & 0 & 1 \\ 0 & 0 & 1 & 0 \end{pmatrix}$$

$\epsilon = 0.35$ ϵ

$$S = \begin{pmatrix} 1 & 0 & 0 & 0 \\ 0 & 0 & 1 & 0 \\ 0 & 1 & 0 & 0 \\ 0 & 0 & 0 & 1 \end{pmatrix}$$

Figure 3.A.1: Phase diagram under perturbation

We choose Kitaev honeycomb model as a benchmark. Kitaev honeycomb model is defined on the honeycomb lattice with spins on each site and different interactions along the three different links connected to each site

$$H = -J_x \sum_{x-\text{links}} \sigma_i^x \sigma_j^x - J_y \sum_{y-\text{links}} \sigma_i^y \sigma_j^y - J_z \sum_{z-\text{links}} \sigma_i^z \sigma_j^z. \tag{B.1}$$

J_γ are coupling constants along the $\gamma-$link. For simplicity we will assume they are all positive. For the coupling constants J_γ satisfying $J_x + J_y < J_z$ (or other permutations), a gapped phase will be acquired that indeed is a toric code phase by perturbation analysis [56].

We impose $\mathbb{Z}_2$ gauge symmetry on our tensor network ansatz. I.e., local tensors should satisfy

$$T_{ijk}^m = 0, \quad \text{if} \quad i + j + k \text{ odd}. \tag{B.2}$$

Other elements of tensors are random in the initial states before simple update. Gauge-symmetry preserved update differs from simple update only when we do SVD. Again, what we need to do in SVD approach is the following three steps: block diagonalization according to gauge symmetry, SVD in each block and rearrange the outcoming tensors back to the original form. Note that the gauge symmetry only acts on internal indices, so that block diagonalization only happens for internal indices. The procedure is also summarized in the figure B.1.
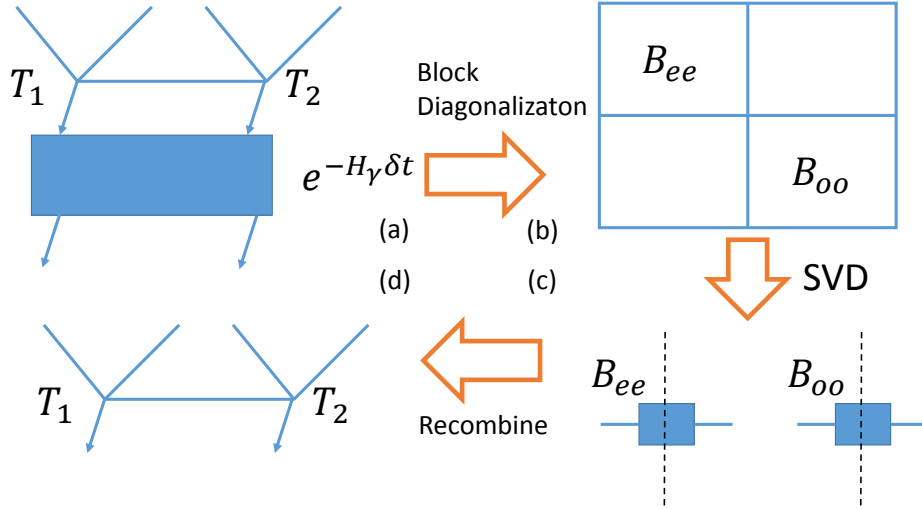
Figure B.1: Illustration of gauge-symmetry preserved simple update. (a) shows that tenor T_1 and T_2 are contracted and acted with local imaginary evolution operator represented by the blue box. The legs with arrow are physical indices while legs without arrows are internal indices. (b) Block diagonalization according to internal indices. B_{ee} and B_{oo} represent the matrices with both legs even and odd. (c) B_{ee} and B_{oo} are SVD-ed. (d) The outcoming matrices are recombined into the original form as in figure (a).

We randomly pick up a few points in the gapped phase of Kitaev honeycomb model, use gauge-symmetry preserved update to obtain the ground states by $\mathbb{Z}_2$ symmetric ansatz B.2. Modular matrices are calculated by the method explained in the main text, and the result is exactly the same matrices found in the main text:

$$
S = \begin{pmatrix} 1 & 0 & 0 & 0 \\ 0 & 0 & 1 & 0 \\ 0 & 1 & 0 & 0 \\ 0 & 0 & 0 & 1 \end{pmatrix}, \qquad T = \begin{pmatrix} 1 & 0 & 0 & 0 \\ 0 & 1 & 0 & 0 \\ 0 & 0 & 0 & 1 \\ 0 & 0 & 1 & 0 \end{pmatrix}. \tag{B.3}
$$

Chapter 4

Universal Topological Data for Gapped Quantum Liquids in Three Dimensions and Fusion Algebra for Non-Abelian String Excitations

This chapter was published in [3]

4.1 Introduction

For more than two decades exotic quantum states[16, 17, 18, 97, 98, 110, 111, 127, 128, 129, 130, 131] have attracted a lot attention from the condensed matter community. In particular gapped systems with non-trivial topological order,[99, 100, 124] which is a reflection of long-range entanglement[24] of the ground state, have been studied intensely in $2+1$ dimensions. Recently, people started to work on a general theory of topological order in higher than $2+1$ dimensions.[84, 164, 1, 165, 166]

In a recent work Ref. [1], we conjectured that for a gapped system on a d-dimensional manifold $\mathcal{M}$ of volume V with the set of degenerate ground states $\{|\psi_\alpha\rangle\}_{\alpha=1}^N$ on $\mathcal{M}$, we have the following overlaps

$$\langle\psi_\alpha|\hat{\mathcal{O}}_A|\psi_\beta\rangle = e^{-\alpha V + o(1/V)} M_{\alpha,\beta}^A, \tag{4.1}$$

where $\hat{\mathcal{O}}_A$ are transformations on the wave functions induced by the automorphisms $A :$ $\mathcal{M} \to \mathcal{M}$, α is a non-universal constant and M^A is a universal matrix up to an overall $U(1)$ phase. Here M^A form a projective representation of the automorphism group $\texttt{AMG}(\mathcal{M})$, which is robust against *any* local perturbations that do not close the bulk gap.[124, 101] In Ref. [1] we conjectured that such projective representations for different space manifold topologies fully characterize topological orders with finite ground state degeneracy in any dimension. Furthermore, we conjectured that projective representations of the mapping class groups $\texttt{MCG}(\mathcal{M}) = \pi_0[\texttt{AMG}(\mathcal{M})]$ classify topological order with gapped boundaries.[124, 101] These quantities can be used as order parameters for topological order and detect transitions between different phases [2].

In this chapter we will study these universal quantities further in 3-dimensions for one of the most simple manifolds, the 3-torus $\mathcal{M} = T^3$. The mapping class group of the 3-torus is $\texttt{MCG}(T^3) = SL(3, \mathbb{Z})$. This group is generated by two elements of the form [123]

$$\hat{\tilde{S}} = \begin{pmatrix} 0 & 1 & 0 \\ 0 & 0 & 1 \\ 1 & 0 & 0 \end{pmatrix}, \qquad \hat{\tilde{T}} = \begin{pmatrix} 1 & 0 & 0 \\ 1 & 1 & 0 \\ 0 & 0 & 1 \end{pmatrix}. \tag{4.2}$$

These matrices act on the unit vectors by $\hat{\tilde{S}} : (\hat{\boldsymbol{x}}, \hat{\boldsymbol{y}}, \hat{\boldsymbol{z}}) \mapsto (\hat{\boldsymbol{z}}, \hat{\boldsymbol{x}}, \hat{\boldsymbol{y}})$ and similarly $\hat{\tilde{T}} :$ $(\hat{\boldsymbol{x}}, \hat{\boldsymbol{y}}, \hat{\boldsymbol{z}}) \mapsto (\hat{\boldsymbol{x}} + \hat{\boldsymbol{y}}, \hat{\boldsymbol{y}}, \hat{\boldsymbol{z}})$. Thus $\tilde{S}$ corresponds to a rotation, while $\tilde{T}$ is shear transformation in the xy-plane.

In this chapter, we will study the $SL(3, \mathbb{Z})$ representations generated by a very simple class of $\mathbb{Z}_N$ models in detail and then consider models for any finite group G, which are 3-dimensional versions of Kitaevs quantum double models [69]. One can also generalize into twisted versions of these based on the group cohomology $H^4(G, U(1))$ by direct generalization of Ref. [167] into 3+1D, which has been done for some simple groups in Ref. [166, 168].

We will consider dimensional reduction of a 3D topological order $\mathcal{C}^{3D}$ to 2D by making one direction of the 3D space into a small circle. In this limit, the 3D topologically ordered states $\mathcal{C}^{3D}$ can be viewed as several 2D topological orders $\mathcal{C}_i^{2D}$, $i = 1, 2, \cdots$ which happen to have degenerate ground state energy. We denote such a dimensional reduction process as

$$\mathcal{C}^{3D} = \bigoplus_i \mathcal{C}_i^{2D}. \tag{4.3}$$

We can compute such a dimensional reduction using the representation of $SL(3, \mathbb{Z})$ that we have calculated.

We consider $SL(2,\mathbb{Z}) \subset SL(3,\mathbb{Z})$ subgroup and the reduction of the $SL(3,\mathbb{Z})$ representation R^{3D} to the $SL(2,\mathbb{Z})$ representations R_i^{2D}:

$$R^{3D} = \bigoplus_i R_i^{2D}. \tag{4.4}$$

We will refer to this as branching rules for the $SL(2,\mathbb{Z})$ subgroup. The $SL(3,\mathbb{Z})$ representation R^{3D} describes the 3D topological order $\mathcal{C}^{3D}$ and the $SL(2,\mathbb{Z})$ representations R_i^{2D} describe the 2D topological orders $\mathcal{C}_i^{2D}$. The decomposition (4.4) gives us the dimensional reduction (4.3).

Let us use $\mathcal{C}_G$ to denote the topological order described by the gauge theory with the finite gauge group G. Using the above result, we find that

$$\mathcal{C}_G^{3D} = \bigoplus_{n=1}^{|G|} \mathcal{C}_G^{2D} \tag{4.5}$$

for Abelian G where $|G|$ is the number of the group elements. For non-Abelian group G

$$\mathcal{C}_G^{3D} = \bigoplus_C \mathcal{C}_{G_C}^{2D} \tag{4.6}$$

where $\bigoplus_C$ sums over all different conjugacy classes C of G, and G_C is a subgroup of G which commutes with an element in C. The results for $G = \mathbb{Z}_N$ were mentioned in the paper [1] (chapter 2 of this thesis).

We also found that the reduction of $SL(3,\mathbb{Z})$ representation, eqn. (4.4), encodes all the information about the three-string statistics discussed in Ref. [165] for Abelian groups. For non-Abelian groups, we will have a "non-Abelian" string braiding statistics and a non-trivial string fusion algebra. We also have a "non-Abelian" three-string braiding statistics and a non-trivial three-string fusion algebra. Within the dimension reduction picture, the 3D strings reduces to particles in 2D, and the (non-Abelian) statistics of the particles encode the (non-Abelian) statistics of the strings.

4.2 $\mathbb{Z}_N$ Model in 3-Dimensions

In this section we will define and study the excitations of a $\mathbb{Z}_N$ model in detail[1] and compute the 3-torus universal matrices, eq. (4.1).

---

[1]Two-dimensional version of this model has previously been studied in for example Ref. [113].
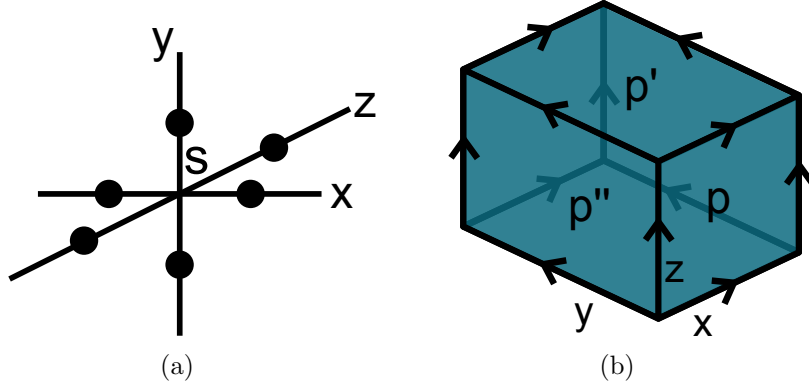
Figure 4.2.1: (a) Lattice site of 3D cubic lattice. A_s act on spins connected to site s. (b) 2D plaquettes. B_p acts on the four spins surrounding p. Choose a righthanded (x, y, z) frame, and let all links be oriented wrt. to these directions. This associates a natural orientation to $2D$ plaquettes on the dual lattice.

Consider a simple cubic lattice with a local Hilbert space on each link isomorphic to the group algebra of $\mathbb{Z}_N$, $\mathcal{H}_i \approx \mathbb{C}[\mathbb{Z}_N] \approx \mathbb{C}^N \approx \mathrm{span}_{\mathbb{C}}\{|\sigma\rangle | \sigma \in \mathbb{Z}_N\}$. Give the links on the lattice an orientation as in figure 4.2.1 and let there be a natural isomorphism $\mathcal{H}_i \xrightarrow{\sim} \mathcal{H}_{i^\star}$ for link i and its reversed orientation $i^\star$ as $|\sigma_i\rangle \mapsto |\sigma_{i^\star}\rangle = |-\sigma_i\rangle$. Let this basis be orthonormal. Define two local operators

$$Z_i|\sigma_i\rangle = \omega^{\sigma_i}|\sigma_i\rangle, \qquad X_i|\sigma_i\rangle = |\sigma_i - 1\rangle, \tag{4.7}$$

where $\omega = e^{\frac{2\pi i}{N}}$. These operators have the important commutation relation $X_i Z_i = \omega Z_i X_i$. Note that these operators are unitary and satisfy $X_i^N = Z_i^N = 1$. For each lattice site s and plaquette p define

$$A_s = \prod_{i \in s_+} Z_i \prod_{j \in s_-} Z_j^\dagger, \quad B_p = \prod_{i \in \partial p_+} X_i^\dagger \prod_{j \in \partial p_-} X_j. \tag{4.8}$$

Here s_+ is the set of links pointing into s, while s_- is the set of links pointing away from s. B_p creates a string around plaquette p with orientation given by the normal direction using the right hand thumb rule. Then $\partial p_\pm$ are the set of links surrounding plaquette p with the same or opposite orientation as the lattice. One can directly check that all these operators commute for all sites and plaquettes.

We can now define the $\mathbb{Z}_N$ model by the Hamiltonian

$$H_{3D,\mathbb{Z}_N} = -\frac{J_e}{2}\sum_s \left(A_s + A_s^\dagger\right) - \frac{J_m}{2}\sum_p \left(B_p + B_p^\dagger\right), \tag{4.9}$$

65

where we will assume $J_e, J_m \geq 0$ throughout. Since $\text{eigen}(A_s + A_s^\dagger) = \{2\cos(\frac{2\pi}{N}q)\}_0^{N-1}$, and the similar for $B_p + B_p^\dagger$, the ground state is the state satisfying

$$A_s|GS\rangle = |GS\rangle, \qquad B_p|GS\rangle = |GS\rangle, \qquad (4.10)$$

for all s and p. We can easily construct hermitian projectors to the state with eigenvalue 1 for all vertices and plaquettes

$$\rho_s = \frac{1}{N}\sum_{k=0}^{N-1} A_s^k, \qquad \rho_p = \frac{1}{N}\sum_{k=0}^{N-1} B_p^k. \qquad (4.11)$$

The ground state is thus $|GS\rangle = \prod_s \rho_s \prod_p \rho_p|\psi\rangle$, for any reference state $|\psi\rangle$ such that $|GS\rangle$ is non-zero. For the choice $|\psi\rangle = |00\ldots0\rangle \equiv |0\rangle$, the ρ_s is trivial and the ground state is thus

$$|GS\rangle = \prod_p \left(\frac{1}{N}\sum_{k=0}^{N-1} B_p^k\right)|0\rangle = \mathcal{N}\sum_{\mathbb{Z}_N \text{ string nets}} |\text{loops}\rangle. \qquad (4.12)$$

The first condition in equation (4.10) requires that the ground state consists of $\mathbb{Z}_N$ string-nets, while the second requires that these appear with equal superpositions. Note that if we had used eigenstates of X_i instead, we would find that the ground state is a membrane condensate on the dual lattice.

String and Membrane Operators

Now let l_{ab} denote a curve on the lattice from site a to b, with the orientation that it points from a to b. And let $\Sigma_\mathcal{C}$ denote an oriented surface on the dual lattice with $\partial\Sigma_\mathcal{C} = \mathcal{C}$. Using these, define string and membrane operators

$$W[l_{ab}] = \prod_{i\in l_{ab}^-} X_i \prod_{j\in l_{ab}^+} X_j^\dagger, \quad \Gamma[\Sigma_\mathcal{C}] = \prod_{i\in\Sigma_\mathcal{C}^-} Z_i^\dagger \prod_{j\in\Sigma_\mathcal{C}^+} Z_j. \qquad (4.13)$$

Again $l_{ab}^\pm$ and $\Sigma_\mathcal{C}^\pm$ are defined wrt. the orientation of the lattice. Note that $B_p = W[\partial p]$, where ∂p denotes a closed loop around plaquette p with right hand thumb rule orientation wrt. the normal direction. Similarly, $A_s = \Gamma[\text{star}(s)]$, where $\text{star}(s)$ is the closed surface on the dual lattice surrounding site s with inward orientation.

It is clear that the following operators commute

$$\left[W[l_{ab}], B_p\right] = 0, \quad \forall p, \quad \text{and} \quad \left[\Gamma[\Sigma_\mathcal{C}], A_s\right] = 0, \quad \forall s. \qquad (4.14)$$

66
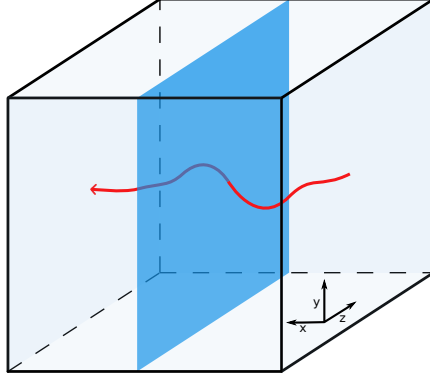
Figure 4.2.2: The cube represents the 3-torus T^3, where the sides are appropriately identified. The red string represents l_x, a closed non-contractable loop wrapping around the x-cycle of the torus (orientation along the x-axis). Similarly two other non-contractable strings, l_y and l_z can be defined. The blue surface Σ_x (orientation of normal along x-axis), is a non-contractable surface with topology of T^2. Similarly Σ_y and Σ_z surfaces can be defined.

Furthermore it is easy to show that

$$\left[W[l_{ab}], A_s\right] = 0, \quad s \neq a, b, \qquad \left[\Gamma[\Sigma_{\mathcal{C}}], B_p\right] = 0, \quad p \notin \mathcal{C}, \tag{4.15}$$

while

$$A_a W[l_{ab}] = \omega^{-1}\, W[l_{ab}]A_a, \qquad A_b W[l_{ab}] = \omega\, W[l_{ab}]A_b, \tag{4.16}$$

and

$$B_p \Gamma[\Sigma_{\mathcal{C}}] = \omega^{\pm 1}\, \Gamma[\Sigma_{\mathcal{C}}]B_p, \quad p \in \mathcal{C}, \tag{4.17}$$

where $\pm$ depends on the orientation of $\Sigma_{\mathcal{C}}$.

Ground States on 3-Torus

The ground state degeneracy depends on the topology of the manifold on which the theory is defined, take for example the 3-torus T^3. Let l_x, l_y and l_z be non-contractible loops along the three cycles on the lattice, with the orientation of the lattice. Similarly, let Σ_x, Σ_y and Σ_z be non-contractible surfaces along the three-directions, with the orientation of the dual lattice (see figure 4.2.2). We can define the operators

$$W_i \equiv W[l_i] = \prod_{j \in l_i} X_j^\dagger, \quad \Gamma_i \equiv \Gamma[\Sigma_i] = \prod_{j \in \Sigma_i} Z_i, \quad i = x, y, z. \tag{4.18}$$

These operators have the commutation relations

$$W_i \Gamma_i = \omega^{-1} \Gamma_i W_i, \qquad i = x, y, z. \tag{4.19}$$

We can thus find three commuting (independent) non-contractible operators to get N^3 fold ground state degeneracy. For example $|\alpha, \beta, \gamma\rangle = (W_x)^\alpha (W_y)^\beta (W_z)^\gamma |GS\rangle$, where $\alpha, \beta, \gamma = 0, \ldots, N-1$. This basis correspond to eigenstates of the surface operators $\Gamma_i |\alpha_1, \alpha_2, \alpha_3\rangle = \omega^{\alpha_i} |\alpha_1, \alpha_2, \alpha_3\rangle$. Note that on the torus we get the extra set of constraints $\prod_s A_s = 1$, $\prod_p B_p = 1$. Let G be the group generated by B_p for all p, modulo $B_p B_{p'} = B_{p'} B_p$, $B_p^N = 1$ and $\prod_p B_p = 1$. Furthermore define the groups $G_{\alpha\beta\gamma} \equiv (W_x)^\alpha (W_y)^\beta (W_z)^\gamma G$, then we can write the ground states as

$$|\alpha, \beta, \gamma\rangle = \frac{1}{\sqrt{|G_{\alpha\beta\gamma}|}} \sum_{g \in G_{\alpha\beta\gamma}} |g\rangle, \tag{4.20}$$

where $|g\rangle \equiv g|0\rangle$.

In 2D, the quasiparticle basis corresponds to the basis in which there is well-defined magnetic and electric flux along one cycle of the torus. We can try to do the same in three-dimensions. Γ_x, W_y, W_z all commute with each other and we can consider the basis which diagonalizes all of them. This basis is given by

$$|\psi_{abc}\rangle = \frac{1}{N} \sum_{\beta\gamma} \omega^{-\beta b - \gamma c} |a, \beta, \gamma\rangle, \tag{4.21}$$

where $a, b, c = 0, \ldots, N-1$. These are clearly eigenstates of Γ_x, and furthermore we have that $W_y |\psi_{abc}\rangle = \omega^b |\psi_{abc}\rangle$ and $W_z |\psi_{abc}\rangle = \omega^c |\psi_{abc}\rangle$. This basis is a 3D version of minimum entropy states (MES).[106]

Excitations

Now lets go back to, say, this theory on S^3 and look at elementary excitations of our model. An excitation correspond to a state in which the conditions (4.10) are violated in a small region. Using the string operators, we can create a pair of particles by $|-q_e, q_e\rangle = W[l_{ab}]^{q_e} |GS\rangle$ with the electric charges

$$A_a|-q_e, q_e\rangle = \omega^{-q_e}|-q_e, q_e\rangle, \quad A_b|-q_e, q_e\rangle = \omega^{q_e}|-q_e, q_e\rangle. \tag{4.22}$$

68
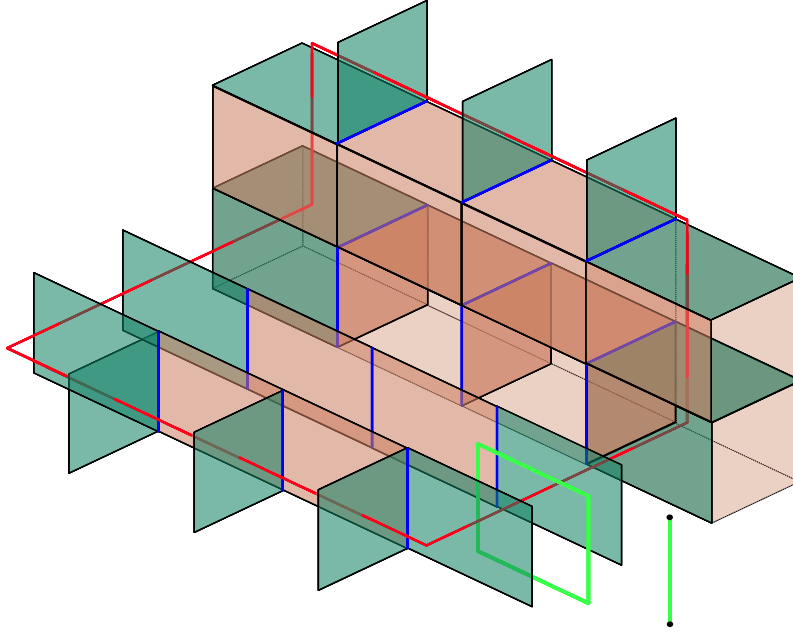
Figure 4.2.3: String and particle excitations. The red curve is the boundary of a membrane on the dual lattice and correspond to a string excitation. The blue links are the ones affected by the membrane operator and the green plaquettes are the ones on which B_p can measure the presence of the string excitation. The green line correspond to a string operator on the lattice, in which the end point are particles. Mutual statistics between strings and particles can be calculated by creating a particle-antiparticle pair from the vacuum, moving one particle around the string excitation and annihilating the particles.

This excitation has an energy cost of $\Delta E_{\text{particles}} = 2J_e[1 - \cos(\frac{2\pi}{N}q_e)]$. Furthermore we have oriented string excitations by using the membrane operators $|\mathcal{C}, q_m\rangle = \Gamma[\Sigma_{\mathcal{C}}]^{q_m}|GS\rangle$, with the magnetic flux

$$B_p|\mathcal{C}, q_m\rangle = \omega^{\pm q_m}|\mathcal{C}, q_m\rangle, \quad p \in \mathcal{C}, \tag{4.23}$$

where the $\pm$ depend on the orientation of $\mathcal{C}$. This excitation comes with the energy penalty $\Delta E_{\text{string}} = \text{Lenght}(\mathcal{C})J_m[1 - \cos(\frac{2\pi}{N}q_m)]$.

One can easily show that all the particles have trivial self and mutual statistics, and the same with the strings. Mutual statistics between particles and strings can be non-trivial however, taking a charge q_e particle through a flux q_m string gives the anyonic phase $\omega^{\pm q_e q_m}$, where the $\pm$ depend on the orientations. See figure 4.2.3.

69

4.3 Representations of $\texttt{MCG}(T^3) = SL(3, \mathbb{Z})$

Let us now go back to T^3 and consider the universal quantities as defined in (4.1). In the $|\alpha, \beta, \gamma\rangle$ basis, the representation of the $SL(3, \mathbb{Z})$ generators (4.2) is given by

$$\tilde{S}_{\alpha\beta\gamma,\alpha'\beta'\gamma'} = \delta_{\alpha,\beta'}\delta_{\beta,\gamma'}\delta_{\gamma,\alpha'}, \tag{4.24}$$

and

$$\tilde{T}_{\alpha\beta\gamma,\alpha'\beta'\gamma'} = \delta_{\alpha,\alpha'}\delta_{\beta,\alpha'+\beta'}\delta_{\gamma,\gamma'}. \tag{4.25}$$

In the 3D quasiparticle basis (4.21) these are given by

$$\tilde{S}_{abc,\bar{a}\bar{b}\bar{c}} = \frac{1}{N}\delta_{b,\bar{c}}e^{\frac{2\pi i}{N}(\bar{a}c - a\bar{b})}, \quad \tilde{T}_{abc,\bar{a}\bar{b}\bar{c}} = \delta_{a,\bar{a}}\delta_{b,\bar{b}}\delta_{c,\bar{c}}e^{\frac{2\pi i}{N}ab}. \tag{4.26}$$

For example in the simplest case $N = 2$, which is the 3D Toric code, we have

$$\tilde{T} = \begin{pmatrix} 1 & & & & & & & \\ & 1 & & & & & & \\ & & 1 & & & & & \\ & & & -1 & & & & \\ & & & & 1 & & & \\ & & & & & 1 & & \\ & & & & & & 1 & \\ & & & & & & & -1 \end{pmatrix},$$

and

$$\tilde{S} = \frac{1}{2}\begin{pmatrix} 1 & 1 & 0 & 0 & 1 & 1 & 0 & 0 \\ 1 & 1 & 0 & 0 & -1 & -1 & 0 & 0 \\ 1 & -1 & 0 & 0 & 1 & -1 & 0 & 0 \\ 1 & -1 & 0 & 0 & -1 & 1 & 0 & 0 \\ 0 & 0 & 1 & 1 & 0 & 0 & 1 & 1 \\ 0 & 0 & 1 & 1 & 0 & 0 & -1 & -1 \\ 0 & 0 & 1 & -1 & 0 & 0 & 1 & -1 \\ 0 & 0 & 1 & -1 & 0 & 0 & -1 & 1 \end{pmatrix}.$$

Interpretation of $\tilde{T}$

These matrix elements in this particular ground state basis, actually contain some physical information about statistics of excitations. In order to see this, we can associate a collection of excitations to each ground state on the 3-torus.

Figure 4.3.1: The result of cutting open the 3-torus along the x-axis, can be represented by a hollow solid cylinder where the inner and outer surfaces are identified, but there are two boundaries along x. In the above, the compactified direction is y and the radial direction is z, while the open direction is x. We can see the N^3 possible excitations on the boundaries which give rise to 3-torus ground states uppon gluing. The four first states correspond to $|\mathbf{1}\rangle$, $|e_a\rangle$, $|m_{y,c}\rangle$ and $|m_{z,b}\rangle$.

First cut the 3-torus along the x-axis such that it now has two boundaries. We can measure the presence of excitations on the boundary using the operators Γ_x, W_y and W_z. First take the state with no particle, $|\mathbf{1}\rangle = \frac{1}{N}\sum_{\beta\gamma}|\beta,\gamma\rangle$, in which all operators have eigenvalue 1. Here $|\beta,\gamma\rangle$ are states with β and γ non-contractible electric loops along the y and z axis, respectively. Now add excitations on the boundary using open string and membrane operators (see fig. 4.3.1) $|e_a\rangle = (W[l_{12}])^a|\mathbf{1}\rangle$, $|m_{y,c}\rangle = (\Gamma[\Sigma_{\mathcal{C}_y}])^c|\mathbf{1}\rangle$, $|m_{z,b}\rangle = (\Gamma[\Sigma_{\mathcal{C}_z}])^b|\mathbf{1}\rangle$, $|e_a m_{y,c}\rangle = (W[l_{12}])^a(\Gamma[\Sigma_{\mathcal{C}_y}])^c|\mathbf{1}\rangle$, $|e_a m_{z,b}\rangle = (W[l_{12}])^a(\Gamma[\Sigma_{\mathcal{C}_z}])^b|\mathbf{1}\rangle$, $|m_{y,c}m_{z,b}\rangle = (\Gamma[\Sigma_{\mathcal{C}_y}])^c(\Gamma[\Sigma_{\mathcal{C}_z}])^b|\mathbf{1}\rangle$ and $|e_a m_{y,c} m_{z,b}\rangle = (W[l_{12}])^a(\Gamma[\Sigma_{\mathcal{C}_y}])^c(\Gamma[\Sigma_{\mathcal{C}_z}])^b|\mathbf{1}\rangle$, where $a, b, c = 1, \dots, N-1$. Or more compactly, $|e_a m_{y,c} m_{z,b}\rangle$, where $a, b, c = 0, \dots, N-1$. Here l_{12} is a curve from one edge to the other, $\Sigma_{\mathcal{C}_y}$ is a membrane between edges wrapping along the y-cycle and $\Sigma_{\mathcal{C}_z}$ is a membrane between edges wrapping along z-cycle. All these have the same orientation as the (dual) lattice. These states have well-defined electric and

71

magnetic flux wrt. Γ_x, W_y and W_z. Here m_y and m_z correspond to the strings on the boundaries, wrapping around the y and z cycles, respectively.

If we now glue the two boundaries together, we see that for each of these excitations we have a 3-torus ground state

$$
\begin{aligned}
|\mathbf{1}\rangle &= |\psi_{000}\rangle, & |e_a m_{1,c}\rangle &= |\psi_{a0c}\rangle, \\
|e_a\rangle &= |\psi_{a00}\rangle, & |e_a m_{2,b}\rangle &= |\psi_{ab0}\rangle, \\
|m_{1,c}\rangle &= |\psi_{00c}\rangle, & |m_{1,c} m_{2,b}\rangle &= |\psi_{0bc}\rangle, \\
|m_{2,b}\rangle &= |\psi_{0b0}\rangle, & |e_a m_{1,c} m_{2,b}\rangle &= |\psi_{abc}\rangle.
\end{aligned}
$$

We can add other string excitations on the boundary, however they will not give rise to new 3-torus ground states after gluing. We thus see a generalization of the situation in 2D, where there is a direct relation between number of excitation types and GSD on the torus.

Now lets to back to the open boundaries, and consider making a 2π twist of one of the boundaries, which will give some kind of 3D analogue of *topological spin*. It can be seen that most states will be invariant under such an operation by appropriately deforming and reconnecting the string and membrane operators. For example $|e_a\rangle \to |e_a\rangle$, which implies that the particles e_a are bosons. However we pick up a factor of ω^{ab} for $|e_a m_{2,b}\rangle$ and $|e_a m_{1,c} m_{2,b}\rangle$, since the string corresponding to particle e_a has to cross the membrane corresponding to $m_{2,b}$. Physically this is a consequence of mutual statistics of the particle and string excitation. We can consider these as 3D analogue of topological spin.

Now notice that this operation precisely corresponds to the $\tilde{T}$ Dehn twist on the 3-torus by gluing the boundaries (see fig.4.3.2). Thus $\tilde{T}$, as calculated from the ground state, should contain information about statistics of excitations. Writing $\tilde{T}_{abc,\bar{a}\bar{b}\bar{c}} = \delta_{a,\bar{a}}\delta_{b,\bar{b}}\delta_{c,\bar{c}}e^{\frac{2\pi i}{N}ab} \equiv \delta_{a,\bar{a}}\delta_{b,\bar{b}}\delta_{c,\bar{c}}\tilde{T}_{abc}$, we get the following 3D *topological spins*

$$
\begin{aligned}
\tilde{T}_{\mathbf{1}} = \tilde{T}_{000} &= 1, & \tilde{T}_{e_a} = \tilde{T}_{a00} &= 1, \\
\tilde{T}_{m_{1,c}} = \tilde{T}_{00c} &= 1, & \tilde{T}_{m_{2,b}} = \tilde{T}_{0b0} &= 1, \\
\tilde{T}_{e_a m_{1,c}} = \tilde{T}_{a0c} &= 1, & \tilde{T}_{e_a m_{2,b}} = \tilde{T}_{ab0} &= e^{\frac{2\pi i}{N}ab}, \\
\tilde{T}_{m_{1,c} m_{2,b}} = \tilde{T}_{0bc} &= 1, & \tilde{T}_{e_a m_{1,c} m_{2,b}} = \tilde{T}_{abc} &= e^{\frac{2\pi i}{N}ab}.
\end{aligned}
$$

This exactly match the properties of the excitations. Thus the universal quantity $\tilde{T}$ calculated from the ground state alone, contain direct physical information about statistics of excitations in the system. Note that elements like $\tilde{T}_{m_{1,c} m_{2,b}}$ can be non-trivial in theories with non-trivial string-string statistics.

72
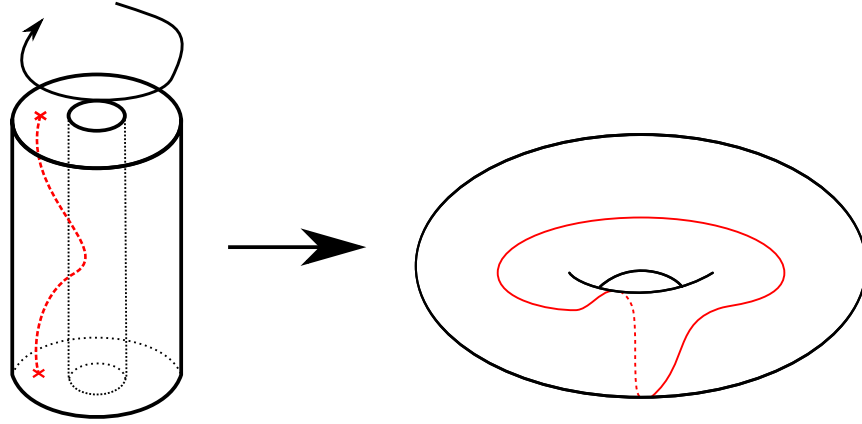
Figure 4.3.2: The Dehn twist $\tilde{T}$ is along the $x - y$ plane, thus it is natural to think of T^3 as a solid hollow 2-torus where the inner and outer boundaries are identified, here the thickened direction is z. In this picture, we can think of $\tilde{T}$ just as a usual Dehn twist of a 2-torus.

$3D \rightarrow 2D$ Dimensional Reduction

We can actually relate these universal quantities to the well-known S and T matrices in two dimensions. Consider now the $SL(2,\mathbb{Z})$ subgroup of $SL(3,\mathbb{Z})$ generated by

$$\hat{T}^{yx} \equiv \begin{pmatrix} 1 & 0 & 0 \\ 1 & 1 & 0 \\ 0 & 0 & 1 \end{pmatrix} \qquad \text{and} \qquad \hat{S}^{yx} \equiv \begin{pmatrix} 0 & 1 & 0 \\ -1 & 0 & 0 \\ 0 & 0 & 1 \end{pmatrix} \tag{4.27}$$

One can directly compute the representation of this subgroup for the above $\mathbb{Z}_N$ model, which is given by

$$S^{yx}_{abc,\bar{a}\bar{b}\bar{c}} = \frac{1}{N}\delta_{c,\bar{c}}e^{-\frac{2\pi i}{N}(a\bar{b}+\bar{a}b)}, \quad T^{yx}_{abc,\bar{a}\bar{b}\bar{c}} = \delta_{a,\bar{a}}\delta_{b,\bar{b}}\delta_{c,\bar{c}}e^{\frac{2\pi i}{N}ab}. \tag{4.28}$$

Note that $S_{\mathbb{Z}_N}^{3D} = \bigoplus_{n=1}^{N} S_{\mathbb{Z}_N}^{2D}$ and $T_{\mathbb{Z}_N}^{3D} = \bigoplus_{n=1}^{N} T_{\mathbb{Z}_N}^{2D}$. In particular, for the toric code $N = 2$ we have

$$
S^{yx} = \frac{1}{2}
\begin{pmatrix}
1 & 1 & 1 & 1 & & & & \\
1 & 1 & -1 & -1 & & & & \\
1 & -1 & 1 & -1 & & & & \\
1 & -1 & -1 & 1 & & & & \\
& & & & 1 & 1 & 1 & 1 \\
& & & & 1 & 1 & -1 & -1 \\
& & & & 1 & -1 & 1 & -1 \\
& & & & 1 & -1 & -1 & 1
\end{pmatrix},
$$

and

$$
T^{yx} =
\begin{pmatrix}
1 & & & & & & & \\
& 1 & & & & & & \\
& & 1 & & & & & \\
& & & -1 & & & & \\
& & & & 1 & & & \\
& & & & & 1 & & \\
& & & & & & 1 & \\
& & & & & & & -1
\end{pmatrix}.
$$

These N blocks are distinguished by eigenvalues of W_z. Consider the 2D limit of the three-dimensional $\mathbb{Z}_N$ model where the x and y directions are taken to be very large compared to the z direction. In this limit a non-contractible loop along the z-cycle becomes very small and the following perturbation is essentially local

$$
H = H_{3D,\mathbb{Z}_N} - \frac{J_z}{2} \left(W_z + W_z^\dagger \right), \tag{4.29}
$$

where W_z creates a loop along z. Since this perturbation commutes with the original Hamiltonian, besides the conditions (4.10) the ground state must also satisfy $W_z|GS\rangle = |GS\rangle$. Thus the N^3-fold degeneracy is not stable in the 2D limit and the N^2 remaining ground states are now $|2D, a, b\rangle \equiv |\psi_{ab0}\rangle$. The gap to the state $|\psi_{abc}\rangle$ is $\Delta E_c = J_c[1 - \cos(\frac{2\pi}{N}c)]$.

It is easy to see that S_{yx} and T_{yx} on this set of ground states exactly correspond the two dimensional $\mathbb{Z}_N$ modular matrices and can be used to construct the corresponding UMTC. Thus the 3D $\mathbb{Z}_N$ model and our universal quantities exactly reduce to the 2D versions in this limit. Furthermore, the 3D quasiparticle basis also directly reduce to the 2D quasiparticle basis.

4.4 Quantum Double Models in Three-Dimensions

In this section we will construct exactly soluble models in three-dimensions for any finite group G. These are nothing but a natural generalization of Kitaev's quantum double models [69] to three-dimensions and are closely related to discrete gauge theories with gauge group G. These models will have the above $\mathbb{Z}_N$ models as a special case, but formulated in a slightly different way.

Consider a simple cubic lattice [2] with the orientation used above. Let there be a Hilbert space $\mathcal{H}_l \approx \mathbb{C}[G]$ on each link l, where G is a finite group, and let there be an isomorphism $\mathcal{H}_l \xrightarrow{\sim} \mathcal{H}_{l^\star}$ for the link l and its reverse orientation $l^\star$ as $|g_l\rangle \mapsto |g_{l^\star}\rangle = |g_l^{-1}\rangle$. Furthermore let the natural basis of the group algebra be orthonormal. The following local operators will be useful

$$
\begin{aligned}
L_+^g|z\rangle = |gz\rangle, && T_+^h|z\rangle = \delta_{h,z}|z\rangle, \\
L_-^g|z\rangle = |zg^{-1}\rangle, && T_-^h|z\rangle = \delta_{h^{-1},z}|z\rangle.
\end{aligned}
\tag{4.30}
$$

To each two dimensional plaquette p, associate an orientation wrt. to the lattice orientation using the right-hand rule. For such a plaquette, define the following operator

$$
B_h(p) \left| z_L \begin{array}{c} z_U \\ \boxed{p} \\ z_D \end{array} z_R \right\rangle = \delta_{z_U z_R^{-1} z_D^{-1} z_L, h} \left| z_L \begin{array}{c} z_U \\ \boxed{p} \\ z_D \end{array} z_R \right\rangle,
\tag{4.31}
$$

and similar for other orientations of plaquettes. Note that the order of the product is important for non-Abelian groups. To each lattice site s, define the operator

$$
A_g(s) = \prod_{l_-} L_-^g(l_-) \prod_{l_+} L_+^g(l_+),
\tag{4.32}
$$

where l_- are the set of links pointing into s while l_+ are the links pointing away from s. In particular we have that

$$
A_g(s) \left| \begin{array}{c} z_2 \quad y_2 \\ x_1 \quad s \quad x_2 \\ y_1 \quad z_1 \end{array} \right\rangle = \left| \begin{array}{c} gz_2 \quad gy_2 \\ x_1 g^{-1} \quad s \quad gx_2 \\ y_1 g^{-1} \quad z_1 g^{-1} \end{array} \right\rangle.
\tag{4.33}
$$

---

[2] The model can easily be defined on arbitrary triangulations, but for simplicity we will consider the cubic lattice.

From these we have two important operators

$$A(s) = \frac{1}{|G|} \sum_{g \in G} A_g(s), \tag{4.34}$$

and $B(p) \equiv B_1(p)$, where $1 \in G$ is the identity element. One can show that both these operators are hermitian projectors. Furthermore one can check that they all commute together

$$
\begin{aligned}
\big[A(s), B(p)\big] &= 0, & \forall s, p, \\
\big[B(p), B(p')\big] &= 0, & \forall p, p', \\
\big[A(s), A(s')\big] &= 0, & \forall s, s'.
\end{aligned}
$$

We can now define the Hamiltonian of the three-dimensional quantum double model as

$$H = -J_e \sum_s A(s) - J_m \sum_p B(p). \tag{4.35}$$

Since the Hamiltonian is just a sum of commuting projectors, the ground states of the system must satisfy
$$A(s)|GS\rangle = B(p)|GS\rangle = |GS\rangle, \tag{4.36}$$

for all s and p. The ground state can be constructed using the following hermitian projector $\rho_{GS} = \prod_s A(s) \prod_p B(p)$. If we take as reference state $|1\rangle = |1_{l_1} 1_{l_2} \dots\rangle$, we can write
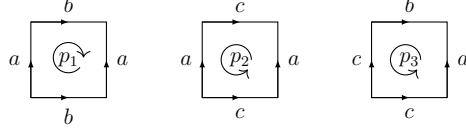
$$|GS\rangle = \rho_{GS}|1\rangle = \prod_s A(s)|1\rangle. \tag{4.37}$$

4.4.1 Ground states on T^3

The easiest way to construct the ground states on the three-torus is to consider the minimal torus, which is just a single cube where the boundaries are identified. The minimal torus has one site s
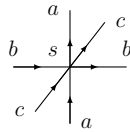
and three plaquettes p_1, p_2, p_3

One can readily show that the subspace $\mathcal{H}^{B=1}$ satisfying $B(p)|GS\rangle \overset{!}{=} |GS\rangle$ for $p = p_1, p_2, p_3$, is spanned by the vectors $|a, b, c\rangle$ such that $ab = ba$, $bc = cb$ and $ac = ca$. The last condition is $A(s)|GS\rangle = |GS\rangle$ where on the basis vectors

$$A(s)|a, b, c\rangle = \frac{1}{|G|} \sum_{g \in G} |gag^{-1}, gbg^{-1}, gcg^{-1}\rangle. \tag{4.38}$$

In the case of Abelian groups G, this condition is clearly trivial and then we have $GSD = |G|^3$. In general we can find the ground state degeneracy by taking the trace of the projector $A(s)$ in $\mathcal{H}^{B=1}$. This is given by

$$\begin{aligned}
GSD &= \sum_{\{a,b,c\}} \langle a, b, c|A(s)|a, b, c\rangle \\
&= \frac{1}{|G|} \sum_{g \in G} \sum_{\{a,b,c\}} \delta_{ag,ga}\delta_{bg,gb}\delta_{cg,gc},
\end{aligned} \tag{4.39}$$

where $\{a, b, c\}$ is triplets of commuting group elements. One can actually easily check that the following vectors span the ground state subspace

$$|\psi_{[a,b,c]}\rangle = \frac{1}{|G|} \sum_{g \in G} |gag^{-1}, gbg^{-1}, gcg^{-1}\rangle, \tag{4.40}$$

where $[a, b, c] = \{(\tilde{a}, \tilde{b}, \tilde{c}) \in G \times G \times G \,|\, (\tilde{a}, \tilde{b}, \tilde{c}) = (gag^{-1}, gbg^{-1}, gcg^{-1}), g \in G\}$ is the three-element conjugacy class and a, b, c are representatives of the class.

4.4.2   3D $\tilde{S}$ and $\tilde{T}$ matrices and the $SL(2, \mathbb{Z})$ subgroup

We can now readily compute the overlaps (4.1) for the above model for any group G. We find the following representations of $\texttt{MCG}(T^3) = SL(3, \mathbb{Z})$

$$\tilde{S}_{[a,b,c],[\bar{a},\bar{b},\bar{c}]} = \langle \psi_{[a,b,c]}|\, \tilde{S}\, |\psi_{[\bar{a},\bar{b},\bar{c}]}\rangle = \delta_{[a,b,c],[\bar{b},\bar{c},\bar{a}]} \tag{4.41}$$

and

$$\tilde{T}_{[a,b,c],[\bar{a},\bar{b},\bar{c}]} = \langle \psi_{[a,b,c]}| \, \tilde{T} \, |\psi_{[\bar{a},\bar{b},\bar{c}]}\rangle = \delta_{[a,b,c],[\bar{a},\bar{a}b,\bar{c}]}, \tag{4.42}$$

since $\tilde{S}|\psi_{[a,b,c]}\rangle = |\psi_{[b,c,a]}\rangle$ and $\tilde{T}|\psi_{[a,b,c]}\rangle = |\psi_{[a,ab,c]}\rangle$.

Once again we can consider the subgroup $SL(2,\mathbb{Z}) \subset SL(3,\mathbb{Z})$ generated by (4.27). The representation of this subgroup can be directly computed and is given by

$$S^{yx}_{[a,b,c],[\bar{a},\bar{b},\bar{c}]} = \langle \psi_{[a,b,c]}| \, S^{yx} \, |\psi_{[\bar{a},\bar{b},\bar{c}]}\rangle = \delta_{[a,b,c],[\bar{b},\bar{a}^{-1},\bar{c}]} \tag{4.43}$$

and

$$T^{yx}_{[a,b,c],[\bar{a},\bar{b},\bar{c}]} = \langle \psi_{[a,b,c]}| \, T^{yx} \, |\psi_{[\bar{a},\bar{b},\bar{c}]}\rangle = \delta_{[a,b,c],[\bar{a},\bar{a}b,\bar{c}]}. \tag{4.44}$$

Note that since c is not independent of a and b, in general we don't have the decomposition $S^{3D}_G = \bigoplus_{n=1}^{|G|} S^{2D}_G$ and $T^{3D}_G = \bigoplus_{n=1}^{|G|} T^{2D}_G$, unless the group is Abelian.

4.4.3 Branching Rules and Dimensional Reduction

With the above formulas, we can directly compute the $\tilde{S}$ and $\tilde{T}$ generators for any group G. In the limit where one direction of the 3-torus is taken to be very small, we can view the 3D topological order as several 2D topological orders.

The branching rules (4.3) for the dimensional reduction can be directly computed by studying how a representation of $SL(3,\mathbb{Z})$ decomposes into representations of the subgroup $SL(2,\mathbb{Z}) \subset SL(3,\mathbb{Z})$. For example, for some of the simplest non-Abelian finite groups we find the branching rules

$$\begin{aligned}
\mathcal{C}^{3D}_{S_3} &= \mathcal{C}^{2D}_{S_3} \oplus \mathcal{C}^{2D}_{\mathbb{Z}_3} \oplus \mathcal{C}^{2D}_{\mathbb{Z}_2}, \\
\mathcal{C}^{3D}_{D_4} &= 2\,\mathcal{C}^{2D}_{D_4} \oplus 2\,\mathcal{C}^{2D}_{D_2} \oplus \mathcal{C}^{2D}_{\mathbb{Z}_4}, \\
\mathcal{C}^{3D}_{D_5} &= \mathcal{C}^{2D}_{D_5} \oplus 2\,\mathcal{C}^{2D}_{\mathbb{Z}_5} \oplus \mathcal{C}^{2D}_{\mathbb{Z}_2}, \\
\mathcal{C}^{3D}_{S_4} &= \mathcal{C}^{2D}_{S_4} \oplus \mathcal{C}^{2D}_{D_4} \oplus \mathcal{C}^{2D}_{D_2} \oplus \mathcal{C}^{2D}_{\mathbb{Z}_4} \oplus \mathcal{C}^{2D}_{\mathbb{Z}_3}.
\end{aligned} \tag{4.45}$$

In general we find the following branching in the dimensional reduction $\mathcal{C}^{3D}_G = \bigoplus_C \mathcal{C}^{2D}_{G_C}$, where $\bigoplus_C$ sums over all different conjugacy classes C of G, and G_C is the centralizer subgroup of G for some representative $g_C \in C$. Similar to the $G = \mathbb{Z}_N$ case above (4.29), the degeneracy between the different sectors can be lifted by a perturbation creating Wilson loops along the small non-contractible cycle of T^3, which is essentially a local perturbation in the 2D limit.

We like to remark that the above branching result for dimensional reduction can be understood from a "gauge symmetry breaking" point of view. In the dimensional reduction, we can choose to insert gauge flux through the small compactified circle. The different choices of the gauge flux is given by the conjugacy classes C of G. Such gauge flux break the "gauge symmetry" from G to G_C. So, such a compactification leads to a 2D gauge theory with gauge group G_C and reduces the 3D topological order $\mathcal{C}_G^{3D}$ to a 2D topological order $\mathcal{C}_{G_C}^{2D}$. The different choices of gauge flux lead to different degenerate 2D topological ordered states, each described by $\mathcal{C}_{G_C}^{2D}$ for a certain G_C. This gives us the result eqn. (4.6). It is quite interesting to see that the branching (4.4) of the representation of the mapping class group $SL(3, \mathbb{Z}) \to SL(2, \mathbb{Z})$ is closely related to the "gauge symmetry breaking" in our examples.

In order to gain a better understanding of the information contained in these branching rules, we will consider a simple example.

$\otimes$	$\mathbf{1}$	A^1	A^2	B	B^1	C	C^1	C^2
$\mathbf{1}$	$\mathbf{1}$	A^1	A^2	B	B^1	C	C^1	C^2
A^1	A^1	$\mathbf{1}$	A^2	B^1	B	C	C^1	C^2
A^2	A^2	A^2	$\mathbf{1} \oplus A^1 \oplus A^2$	$B \oplus B^1$	$B \oplus B^1$	$C^1 \oplus C^2$	$C \oplus C^2$	$C \oplus C^1$
B	B	B^1	$B \oplus B^1$	$\mathbf{1} \oplus A^2 \oplus C \oplus C^1 \oplus C^2$	$A^1 \oplus A^2 \oplus C \oplus C^1 \oplus C^2$	$B \oplus B^1$	$B \oplus B^1$	$B \oplus B^1$
B^1	B^1	B	$B \oplus B^1$	$A^1 \oplus A^2 \oplus C \oplus C^1 \oplus C^2$	$\mathbf{1} \oplus A^2 \oplus C \oplus C^1 \oplus C^2$	$B \oplus B^1$	$B \oplus B^1$	$B \oplus B^1$
C	C	C	$C^1 \oplus C^2$	$B \oplus B^1$	$B \oplus B^1$	$\mathbf{1} \oplus A^1 \oplus C$	$C^2 \oplus A^2$	$C^1 \oplus A^2$
C^1	C^1	C^1	$C \oplus C^2$	$B \oplus B^1$	$B \oplus B^1$	$C^2 \oplus A^2$	$\mathbf{1} \oplus A^1 \oplus C^1$	$C \oplus A^2$
C^2	C^2	C^2	$C \oplus C^1$	$B \oplus B^1$	$B \oplus B^1$	$C^1 \oplus A^2$	$C \oplus A^2$	$\mathbf{1} \oplus A^1 \oplus C^2$

Table 4.4.1: Fusion rules of two-dimensional $D(S_3)$ model. Here B and C correspond to pure flux excitations, A^1 and A^2 pure charge excitations, $\mathbf{1}$ the vacuum sector while B^1, C^1 and C^2 are charge-flux composites. If we add the subscript $3D$, the table becomes a list of the 3D particle/string excitations, and their fusion rules.

4.5 Example: $G = S_3$

4.5.1 Two-Dimensional $D(S_3)$

Let us consider the simplest non-Abelian group $G = S_3$. Let us first recall the 2D quantum double models. The excitations of these models are given by irreducible representations of the Drinfeld Quantum Double $D(G)$. The states can be labelled by $|C, \rho\rangle$, where C denote a conjugacy class of G while ρ is a representation of the centralizer subgroup $G_C \equiv Z(a) = \{g \in G | ag = ga\}$ of some element in $a \in C$ (note that $Z(a) \approx Z(gag^{-1})$).

The symmetric group $G = S_3$ consists of the elements $\{(), (23), (12), (123), (132), (13)\}$, where $(\ldots)$ is the standard notation for cycles (cyclic permutations). There are three conjugacy classes $A = \{()\}$, $B = \{(12), (13), (23)\}$ and $C = \{(123), (132)\}$, with the corresponding centralizer subgroups $G_A = S_3$, $G_B = \mathbb{Z}_2$, $G_C = \mathbb{Z}_3$. The number of irreducible representations for each group is equal to the number of conjugacy classes, 3 for G_A and G_C while 2 for G_B. For simplicity we will label the particles corresponding to the three different conjugacy classes by $(\mathbf{1}, A^1, A^2)$, (B, B^1) and (C, C^1, C^2). Here the particles without a superscript, B and C, are pure fluxes (trivial representation), A^1 and A^2 are pure charges (trivial conjugacy class), while B^1, C^1 and C^2 are charge-flux composites. The fusion rules for the two-dimensional $D(S_3)$ model is given in table 4.4.1.

4.5.2 Three-Dimensional $G = S_3$ Model

In three dimensions, the S_3 model has two point-like topological excitations, which are pure charge excitations that can be labelled by A^1_{3D} and A^2_{3D}. Here A^1 is the one-dimensional irreducible representation of S_3 and A^2 the two-dimensional irreducible representation of S_3. Under the dimensional reduction to 2D, they become the 2D charge particles labelled by A^1 and A^2. The S_3 model also has two string-like topological excitations, labelled by the non-trivial conjugacy classes B_{3D} and C_{3D}. Under the dimensional reduction to 2D, they become the 2D particles with pure fluxes described by B and C. (For details, see the discussion below.) We can also add a 3D charged particle to a 3D string and obtain a so called mixed string-charge excitation. Those mixed string-charge excitations are labelled by B^1_{3D}, C^2_{3D}, and C^3_{3D}, and, under the dimensional reduction, become the 2D particles B^1, C^2, and C^3 (see Table 4.4.1).

We like to remark that, since a 3D string carries gauge flux described by a conjugacy class B or C, the S_3 "gauge symmetry" is broken down to $G_B = \mathbb{Z}_2$ on the B_{3D} string, and down to $G_C = \mathbb{Z}_3$ on the C_{3D} string.

Under the symmetry breaking $S_3 \to \mathbb{Z}_2$, the two irreducible representations A^1 and A^2 of S_3 reduce to the irreducible representations 1 and e of $\mathbb{Z}_2$: $A^1 \to e$ and $A^2 \to 1 \oplus e$. Thus fusing the S_3 charge A^1_{3D} to a B_{3D} string give us the mixed string-charge excitation B^1_{3D}. But fusing the S_3 charge A^2_{3D} to a B_{3D} string gives us a composite mixed string-charge excitation $B_{3D} \oplus B^1_{3D}$. (The physical meaning of the composite topological excitations $B_{3D} \oplus B^1_{3D}$ is explained in Ref. [55].) So fusing the two non-trivial S_3 charges to a B_{3D} string only give us one mixed string-charge excitation B^1_{3D}.

Under the symmetry breaking $S_3 \to \mathbb{Z}_3$, the two irreducible representations A^1 and A^2 of S_3 reduce to the irreducible representations 1, e_1 and e_2 of $\mathbb{Z}_3$: $A^1 \to 1$ and $A^2 \to e_1 \oplus e_2$.
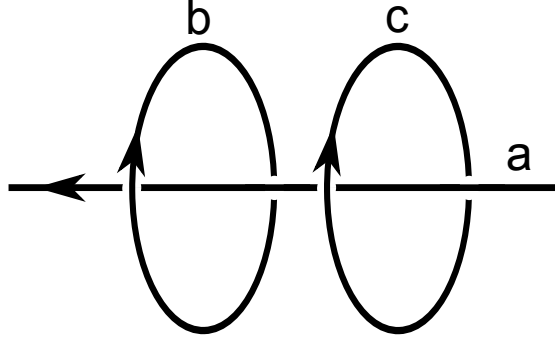
Figure 4.5.1: Three string configuration, where two loops of type b and c are threaded by a string of type a.

Thus fusing the S_3 charge A^1 to a C_{3D} string still gives us the string excitation C_{3D}. But fusing the S_3 charge A_{3D}^2 to a C_{3D} string gives us a composite mixed string-charge excitation $C_{3D}^1 \oplus C_{3D}^2$. So fusing the two non-trivial S_3 charges to a C string give us two mixed string-charge excitations C_{3D}^1 and C_{3D}^2. We see that the fusion between point S_3 charges and the strings is consistent with fusion of the corresponding 2D particles.

Now, we would like to understand the fusion and braiding properties of the 3D strings B_{3D} and C_{3D}. To do that, let us consider the dimension reduction $\mathcal{C}_{S_3}^{3D} = \mathcal{C}_{S_3}^{2D} \oplus \mathcal{C}_{\mathbb{Z}_3}^{2D} \oplus \mathcal{C}_{\mathbb{Z}_2}^{2D}$. Let us choose the gauge flux through the small compactified circle to be B. In this case $\mathcal{C}_{S_3}^{3D} \to \mathcal{C}_{\mathbb{Z}_2}^{2D}$. $\mathcal{C}_{\mathbb{Z}_2}^{2D}$ is a $\mathbb{Z}_2$ topological order in 2D and contains four particle-like topological excitations $\mathbf{1}$, e, m, f, where $\mathbf{1}$ is the trivial excitations. e is the $\mathbb{Z}_2$ charge and m the $\mathbb{Z}_2$ vortex, which are both bosons. f is the bound state of e and m which is a fermion. The trivial 2D excitation $\mathbf{1}$ comes from the trivial 3D excitation $\mathbf{1}_{3D}$, and the $\mathbb{Z}_2$ charge e comes from the 3D charge excitation A^1. The 3D string excitations B and B^1, wrapping around the small compactified circle, give rise to two particle-like excitations in 2D – the $\mathbb{Z}_2$ vortex m and the fermion f. In the dimensional reduction, the gauge flux B through the small compactified circle forbids the 3D string excitations C_{3D}, C_{3D}^1, and C_{3D}^2 to wrap around the small compactified circle. So there is no 2D excitations that correspond to the 3D string excitations C_{3D}, C_{3D}^1, and C_{3D}^2. Because of the symmetry breaking $S_3 \to \mathbb{Z}_2$ caused by the gauge flux B, the 3D particle A_{3D}^2 reduces to $\mathbf{1} \oplus e$ in 2D.

The above results have a 3D understanding. Let us consider the situation where two loops, b and c, are threaded by string a (see Fig. 4.5.1). If the a-string is the type-B_{3D} string, then the b and c-strings must also be the type-B_{3D} string. So the type B_{3D} string in the center forbids the 3D strings C_{3D}, C_{3D}^1, and C_{3D}^2 to loop around it. This is just like the gauge flux B through the small compactified circle forbids the 3D string excitations

81

C_{3D}, C_{3D}^1, and C_{3D}^2 to wrap around the small compactified circle. So the type-B_{3D} string in the center corresponds to the gauge flux B through the small compactified circle.

The fusion and braiding of the 2D particle e is very simple: it is an boson with fusion $e \otimes e = \mathbf{1}$. This is consistent with the fact that the corresponding 3D particle A_{3D}^1 is a boson with fusion $A_{3D}^1 \otimes A_{3D}^1 = \mathbf{1}_{3D}$. The fusion and braiding of the 2D particle m is also very simple, since it is also an boson $m \otimes m = \mathbf{1}$. This suggests that the 3D type-B_{3D} string excitations has a simple fusion and braiding property, *provided that those 3D string excitations are threaded by a type-B_{3D} string going through their center* (see Fig. 4.5.1). For example, from the 2D fusion rule $m \otimes m = \mathbf{1}$, we find that the fusion of two type-B_{3D} loops give rise to a trivial string

$$B_{3D} \otimes B_{3D} = \mathbf{1}_{3D}. \tag{4.46}$$

As suggested by the 2D braiding of two m particles, when a type-B_{3D} string going around another type-B_{3D} string, the induced phase is zero (*i.e.* the mutual braiding "statistics" is trivial).

Similarly, we can choose the gauge flux through the small compactified circle to be C. In this case $\mathcal{C}_{S_3}^{3D} \to \mathcal{C}_{\mathbb{Z}_3}^{2D}$, and $\mathcal{C}_{\mathbb{Z}_3}^{2D}$ is a $\mathbb{Z}_3$ topological order in 2D which has 9 particle types: $\mathbf{1}$, e_1, e_2, m_1, m_2, $e_i m_j|_{i,j=1,2}$. In this case, the gauge flux C through the small compactified circle forbids the 3D string excitations B_{3D} and B_{3D}^1 to wrap around the small compactified circle. So there is no 2D excitations that correspond to the 3D string excitations B_{3D} and B_{3D}^1. The 3D string excitation C_{3D} wrapping around the small compactified circle gives rise to a composite $\mathbb{Z}_3$ vortex $m_1 \oplus m_2$ in 2D. (This is because there are two non-trivial group elements in S_3 that commute with a group element in the conjugacy class C). Also, from the $S_3 \to \mathbb{Z}_3$ symmetry breaking: $A^1 \to 1$ and $A^2 \to e_1 \oplus e_2$, we see that the 3D A_{3D}^1 charge reduces to type-$\mathbf{1}$ particle in 2D, and the 3D A_{3D}^2 charge reduce to a composite particle $e_1 \oplus e_2$ in 2D.

The fusion of the composite 2D particle $c = m_1 \oplus m_2$ is given by

$$c \otimes c = 2\mathbf{1} \oplus c. \tag{4.47}$$

This leads to the corresponding fusion rule for the 3D type-C_{3D} loops

$$C_{3D} \otimes C_{3D} = 2\mathbf{1}_{3D} \oplus C_{3D} \text{ or } \mathbf{1}_{3D} \oplus A_{3D}^1 \oplus C_{3D}, \tag{4.48}$$

provided that those 3D loops are threaded by a type-C_{3D} string going through their center (see Fig. 4.5.1). (The ambiguity arises because the 3D charge A_{3D}^1 reduces to $\mathbf{1}$ in 2D.)

Now, let us choose the gauge flux through the small compactified circle to be trivial. In this case $\mathcal{C}_{S_3}^{3D} \to \mathcal{C}_{S_3}^{2D}$, which has 8 particle types: $\mathbf{1}$, A^1, A^2, B, B^1, C, C^1, C^2. The 3D

82

string excitation B_{3D} and C_{3D} wrapping around the small compactified circle gives rise to the 2D excitation B and C. The fusion of the 2D particle C is given by

$$C \otimes C = \mathbf{1} \oplus A^1 \oplus C. \tag{4.49}$$

This leads to the corresponding fusion rule for the 3D type-C_{3D} loops

$$C_{3D} \otimes C_{3D} = \mathbf{1}_{3D} \oplus A^1_{3D} \oplus C_{3D}, \tag{4.50}$$

provided that those 3D loops are not threaded by any non-trivial string. The above fusion rule implies that when we fusion two C_{3D} loops, we obtain three accidentally degenerate states: the first one is a non-topological excitation, the second one is a S_3 charge A^1_{3D}, and the third one is a S_3 string C_{3D}.

Similarly, the fusion of the 2D particle B is given by

$$B \otimes B = \mathbf{1} \oplus A^2 \oplus C \oplus C^1 \oplus C^2. \tag{4.51}$$

This leads to the corresponding fusion rule for the 3D type-B_{3D} loops

$$B_{3D} \otimes B_{3D} = \mathbf{1}_{3D} \oplus A^2_{3D} \oplus C_{3D} \oplus C^1_{3D} \oplus C^2_{3D}. \tag{4.52}$$

This way, we can obtain the fusion algebra between all the 3D excitations A^1_{3D}, A^2_{3D}, B_{3D}, B^1_{3D}, C_{3D}, C^1_{3D}, C^2_{3D} (see Table 4.4.1).

On the other hand, since the above 3D string loops are not threaded by any non-trivial string, we can shrink a single loop into a point. So we should be able to compute the fusion of 3D loops by shrinking them into a points. Mathematically we will define shrinking operation $\mathcal{S}$, which describes the shrinking process of loops.

Let $\mathcal{E}$ denote the set of 3D particle and string excitations. We would like to make sure that the shrinking operation is consistent with the fusion rules, ie $\mathcal{S}(a \otimes b) = \mathcal{S}(a) \otimes \mathcal{S}(b)$ for $a, b \in \mathcal{E}$. One can indeed check that this is the case for the following shrinking operations

$$\begin{aligned}
\mathcal{S}(C_{3D}) &= \mathbf{1}_{3D} \oplus A^1_{3D}, \quad \mathcal{S}(C^1_{3D}) = A^2_{3D}, \quad \mathcal{S}(C^2_{3D}) = A^2_{3D}, \\
\mathcal{S}(B_{3D}) &= \mathbf{1}_{3D} \oplus A^2_{3D}, \qquad \mathcal{S}(B^1_{3D}) = A^1_{3D} \oplus A^2_{3D}.
\end{aligned} \tag{4.53}$$

So indeed, we can compute the fusion of 3D loops by shrinking them into points. In particular, we find that the topological degeneracy for N type-C_{3D} loops is $2^N/2$. The topological degeneracy for two type-B_{3D} loops is 2. The topological degeneracy for N type-B_{3D} loops is of order 3^N in large N limit.

a	A	B	C
Symmetry Breaking	$S_3 \to S_3$	$S_3 \to \mathbb{Z}_2$	$S_3 \to \mathbb{Z}_3$
$\mathbf{1}_{3D} \to$	$\mathbf{1}$	$\mathbf{1}$	$\mathbf{1}$
$A^1_{3D} \to$	A^1	e	$\mathbf{1}$
$A^2_{3D} \to$	A^2	$\mathbf{1} \oplus e$	$e_1 \oplus e_2$
$B_{3D} \to$	B	m	-
$B^1_{3D} \to$	B^1	em	-
$C_{3D} \to$	C	-	$m_1 \oplus m_2$
$C^1_{3D} \to$	C^1	-	$e_1 m_1 \oplus e_1 m_2$
$C^2_{3D} \to$	C^2	-	$e_2 m_1 \oplus e_2 m_2$

Table 4.5.1: The situation of figure 4.5.1, where strings are wrapped around another string of type $a = A, B, C$. Depending on a, fusion algebra and braiding statistics of each string will be related to a particle of some 2D topological order, as computed from the branching rules (4.6). See the text for more details.

The above example suggests the following. Given a topological order in 3D, $\mathcal{C}^{3D}$, one may want to consider the situation illustrated in figure 4.5.1 where two loops b and c are threaded with a string a, and ask about the three-string braiding statistics. One way to compute this is to put the system on a 3-torus and compute the quantities (4.1), which give rise to a $SL(3, \mathbb{Z})$ representation. Then by finding the branching rules of this representation wrt. to the subgroup $SL(2, \mathbb{Z}) \subset SL(3\,\mathbb{Z})$, one finds how the systems decomposes in the 2D limit $\mathcal{C}^{3D} = \bigoplus_i \mathcal{C}^{2D}_i$, where there will be a sector i for each string type. The three-string statistics with string a in the middle, will be related to the 2D topological order $\mathcal{C}^{2D}_a$. To summarize:

- The representation branching rule (4.4) for $SL(3, \mathbb{Z}) \to SL(2, \mathbb{Z})$ leads to the dimension reduction branching rule (4.3).

- The number of the $SL(2, \mathbb{Z})$ representations (or the number of induced 2D topological orders) is equal to the number of 3D string types in the 3D topological order $\mathcal{C}^{3D}$.

- The $SL(2, \mathbb{Z})$ representations also contains information about two-string/three-string fusion, as described by eqns. (4.46,4.48,4.50,4.52). The two-string/three-string braiding can be obtained directly from the correspond 2D braiding of the corresponding particles.

4.6 Some general considerations

To calculate the braiding statistics of strings and particles, we first need to know the topological degeneracy D in the presence of strings and particles before they braid. This is because the unitary matrix that describe the braiding is D by D matrix. To compute the topological degeneracy D, we need to know the topological types of strings and the particles since the topological degeneracy D depends on those types.

We have seen that, from the branching rules of $SL(3,\mathbb{Z})$ representation under $SL(3,\mathbb{Z}) \to SL(2,\mathbb{Z})$ (see eqn. (4.4)) we can obtain the number of the string types. How to obtain the number of the particle types?

To compute the number of the particle types, we start with a 3D sphere S^3, and then remove two small balls from it. The remaining 3D sphere will have two S^2 surfaces. This two surfaces may surround a particle and anti-particle. So the number of the particle types can be obtained by calculating the ground state degeneracy. But there is one problem with this approach, the two surfaces may carry gapless boundary excitations or some irrelevant symmetry breaking states.

To fix this problem, we note that the 3D space $S^2 \times I$ also have have two S^2 surfaces, where I is the 1D segment: $I = [0,1]$. We can glue the space $S^2 \times I$ onto the 3D sphere S^3 with two balls removed, along the two 2D spheres S^2. The resulting space is $S^2 \times S^1$. This way, we show that the topological degeneracy on $S^2 \times S^1$ is equal to the number of the particle types.

For the gauge theory of finite gauge group G, the topologically degenerate ground states on $S^2 \times S^1$ are labelled by the group elements $g \in G$ (which describe the monodromy along the non-contractible loop in $S^2 \times S^1$), but not in an one-to-one fashion. Two elements g and $g' = h^{-1}gh$ label the same ground state since g and g' are related by a gauge transformation. So the topological degeneracy on $S^2 \times S^1$ is equal to the number of conjugacy classes of G. The number of conjugacy classes is equal to the number of irreducible representations of G, which is also the number of the particle types, a well known result for gauge theory.

Once we know the types of particles and strings, the simple fusion and braiding of those excitations can be obtained from the dimensional reduction as described in this chapter.

4.7 Conclusion

In a recent work Ref. [1], we proposed that for a gapped d-dimensional theory on a manifold $\mathcal{M}$, the overlaps (4.1) give rise to a representation of $\texttt{MCG}(\mathcal{M})$ and that these are robust

against any local perturbation that do not close the energy gap. In this chapter we studied a simple class of $\mathbb{Z}_N$ models on $\mathcal{M} = T^3$ and computed the corresponding representations of $\texttt{MCG}(T^3) = SL(3, \mathbb{Z})$. We argued that, similar to in 2D, the $\tilde{T}$ generator contains information about particle and string excitations above the ground state, although computed from the ground states. In an independent work Ref. [166], the authors studied the matrices (4.1) using some Abelian models on T^3. They argued that the generator $\tilde{S}$ contains information about braiding processes involving three loops.

Furthermore we studied a dimensional reduction process in which the 3D topological order can be viewed as several 2D topological orders $\mathcal{C}^{3D} = \bigoplus_i \mathcal{C}_i^{2D}$. This decomposition can be computed from branching rules of a $SL(3, \mathbb{Z})$ representation into representations of a $SL(2, \mathbb{Z}) \subset SL(3, \mathbb{Z})$ subgroup. Interestingly, this reduction encodes all the information about three-string statistics discussed in Ref. [165] for Abelian groups. This approach, however, also provide information about fusion and braiding statistics of non-Abelian string excitations in 3D.

We also discussed how to obtain information about particles by putting the theory on $S^2 \times S^1$. All this lends support for our conjecture[1], that the overlaps (4.1) for different manifold topologies $\mathcal{M}$, completely characterize topological order with finite ground state degeneracy in any dimension.

Chapter 5

Edge-Entanglement Spectrum Correspondence in a Nonchiral Topological Phase and Kramers-Wannier duality

This chapter was published in [4]

5.1 Introduction

Quantum entanglement has been found to be very useful in characterizing topological states of matter, which is not possible with conventional local order parameters. In particular, the entanglement spectrum (ES)[39] is one such tool, and has been applied to many systems, such as quantum Hall fluids[39, 169, 170, 171, 172, 173, 174, 175], topological order[176, 40, 177], topological insulators [178, 179, 180], fractional Chern insulators[181], symmetry-protected topological phases [182, 183], quantum spin chains[184, 185, 186, 187] and ladders [188, 189, 190, 191, 192, 193], and other spin and fermionic systems.

5.1.1 Entanglement spectrum and edge-ES correspondence

The ES is defined as follows. Given a system's ground state $|\Psi\rangle$, together with a bipartition of the full Hilbert space $\mathcal{H}$ into parts L and R, so that $\mathcal{H} = \mathcal{H}_L \otimes \mathcal{H}_R$, one forms the reduced

density matrix $\rho_L := \text{Tr}_R|\Psi\rangle\langle\Psi|$ on L. Because of hermiticity and positivity, the reduced density matrix can be written in the thermal form $\rho_L \equiv \frac{1}{Z}e^{-H_{\text{ent.}}}$, where $H_{\text{ent.}}$ is the so-called entanglement Hamiltonian and $Z = \text{Tr}(e^{-H_{\text{ent.}}})$. The ES is then simply the eigenenergies of the entanglement Hamiltonian.

This definition of the ES is an operational one. However, there exists a remarkable observation made by Li and Haldane [39] for quantum Hall systems and by others in subsequent works for $(2+1)$-d topological phases: in the cases where the system possesses low energy states living near an open boundary of the manifold the system is placed on (i.e. edge states), it was found that the low-lying edge spectrum of the physical boundary Hamiltonian on L are in one-to-one correspondence with the low-lying spectrum of $H_{\text{ent.}}$, a so-called edge-ES correspondence. (This correspondence should not be confused with the more established bulk-edge correspondence [78, 79, 80] also used in the context of topological phases).

Analytic proofs of the edge-ES correspondence have been proposed, for example in Ref. [40] for $(2+1)$-d topological states whose edge states are described by a $(1+1)$-d CFT. In that work, a 'cut and glue' approach and methods of boundary CFT were used, and it was claimed that the edge and entanglement spectra should be equal up to rescaling and shifting in the low energy limit. However, this method is only applicable to chiral topological phases, where there are protected, physical chiral edge states appearing at an actual spatial boundary of a system. For the case of a non-chiral topological phase, it is unclear as to what information the ES will yield, or even if there is any form of the edge-ES correspondence that exists[194].

5.1.2   Edge-ES correspondence in non-chiral topological order

It is thus the purpose of this chapter to explore the edge-ES correspondence in non-chiral topological phases. Specifically we consider the $\mathbb{Z}_2$ Wen-plaquette model [195] (unitarily equivalent to Kitaev's toric code model [69] in the bulk), and ask if some form of correspondence exists. We choose to work on an infinite cylinder with a bipartition into two semi-infinite cylinders terminated with smooth edges. The model on this geometry has four topological sectors a ($a = 1, \cdots, 4$) with four locally indistinguishable ground states (these are states with well-defined anyonic flux), and therefore the edge theory on the semi-infinite cylinder and ES of the full cylinder can be unambiguously defined within each topological sector. For the unperturbed Wen-plaquette model, there is in fact an *exact* edge-ES correspondence because the edge and entanglement spectra in each a-sector are flat and equally degenerate; thus, the two spectra agree perfectly up to rescaling and shifting. However,

this correspondence is potentially lost in the presence of perturbations. Here, we present a detailed microscopic derivation of the edge and entanglement Hamiltonians of the Wen-plaquette model deformed by generic local perturbations, which allows us to compare the two spectra and hence explore the edge-ES correspondence. This calculation constitutes the main result of this chapter.

From our calculation, we find the following.

(i) Our calculation shows that the edge states (belonging to the lowest energy eigenspace) of the unperturbed Wen-plaquette model on the semi-infinite cylinder are generated by so-called boundary operators, which can be mapped to $\mathbb{Z}_2$ symmetric operators acting on a finite length (spin-1/2) spin chain, the effective low-energy degrees of freedom. The effects of generic local perturbations to the Wen-plaquette model are to lift this degeneracy - we find that the effective Hamiltonian in each topological sector a acting on these edge states, H_{edge}^a, is a $\mathbb{Z}_2$ symmetric Hamiltonian acting on the spin chain. The $\mathbb{Z}_2$ symmetry can be understood as arising from the bulk topological order: it is generated by a Wilson loop operator wrapping around the cylinder.

(ii) We also find that the entanglement Hamiltonian $H_{\text{ent.}}^a$ in each a-sector acts on a (spin-1/2) spin chain of equal length, and is generated in part by the edge Hamiltonians $(H_{\text{edge},L}^a + H_{\text{edge},R}^a)$ of the two halves of the bipartition (L and R) and in part by V_{LR}, a perturbation spanning the cut. It is also $\mathbb{Z}_2$ symmetric. However, $H_{\text{ent.}}^a$ is in general not equal to the edge Hamiltonians, being different in some arbitrary way. Thus, there is in general no edge-ES correspondence for generic perturbations, even in the low energy limit, i.e. the low lying values of the edge and entanglement spectra do not match.

(iii) We do find a mechanism in which an edge-ES correspondence is established, though. If we consider the Wen-plaquette model as a symmetry enriched topological phase (SET), by supplementing the $\mathbb{Z}_2$ topological order with a global translational symmetry along the edge/entanglement cut, achieved by restricting perturbations to those that respect the symmetry, then there is a finite domain in Hamiltonian space in which both H_{edge}^a and $H_{\text{ent.}}^a$ realize the critical $(1+1)$-d Ising model, which has the $c = 1/2$ Ising CFT as its low energy effective theory. It is in this context that we have observed, in concrete examples, the edge-ES correspondence being realized. This happens because the global translational symmetry implies that the effective degrees of freedom of both the edge and entanglement cut are governed by Kramers-Wannier self-dual Hamiltonians, in addition to them being $\mathbb{Z}_2$ symmetric, which is imposed by the topological order. The fact that the Hamiltonians have $\mathbb{Z}_2$ symmetry and Kramers-Wannier self-duality then further guarantees that all perturbations about the $c = 1/2$ Ising CFT must be irrelevant, giving us the result

that the low lying values of the edge and entanglement spectra match upon shifting and rescaling. We therefore see that by considering the Wen-plaqeutte model as a SET, the topological order in the bulk together with the translation invariance of the perturbations along the edge/cut guarantee an edge-ES correspondence at least in some finite domain in Hamiltonian space.

It should be noted that there have been studies of the edge theories and ES of two-dimensional spin systems within the framework of projected entangled pair state models (PEPs)[196, 197], but this work uses standard techniques in perturbation theory and therefore offers a complementary approach to probing the edge-ES correspondence.

5.1.3   Structure of chapter

The rest of the chapter is organized as follows. In Sec. 5.2, we introduce the Wen-plaquette model and solve for its edge theory on the semi-infinite cylinder by identifying boundary operators and mapping them to $\mathbb{Z}_2$ symmetric operators acting on a finite length (spin-1/2) spin chain. We also calculate the entanglement spectra on the infinite cylinder by deriving an effective spin ladder Hamiltonian whose ground states equal the ground states on the infinite cylinder. Next, in Sec. 5.3, we consider the effects of perturbations to the Wen plaquette model. We present a quick summary of the Schrieffer-Wolff (SW) transformation, central to the derivation of our results. Then, we derive the edge theory and solve for the entanglement spectrum. This allows us to compare the edge-ES correspondence for the perturbed Wen-plaquette model. Then, in Sec. 5.4, we identify the mechanism to establish an edge-ES correspondence: we consider the Wen-plaquette model as a symmetry enriched topological phase (SET) with a global translational symmetry along the edge/entanglement cut, which forces the edge and entanglement Hamiltonians to be additionally Kramers-Wannier self-dual, resulting in the edge-ES correspondence. We also provide a numerical example of the correspondence where the perturbations are uniform magnetic fields acting on single spins. Lastly, in Sec. 5.5, we discuss the implications of our findings and conclude. Appendix 5.A presents the Schrieffer-Wolff transformation and necessary formulas, appendix 5.B presents the perturbation theory calculations for the entanglement Hamiltonian, specifically, Λ', defined in Sec. 5.3.3, while Appendix 5.C presents the derivation of the edge and entanglement Hamiltonians of the Wen-plaquette model on an infinite cylinder perturbed by uniform single-site magnetic fields, as considered in Sec. 5.4.

5.2 Exact Wen-plaquette model

5.2.1 Edge theory on semi-infinite cylinder

We first consider the unperturbed $\mathbb{Z}_2$ Wen-plaquette model on a semi-infinite cylinder, L (left), terminated with a smooth boundary, with the periodic direction along the y-axis. The Hamiltonian is the sum of commuting plaquette terms,

$$H_L = -g\left(\sum_{\text{plaq.}} \mathcal{O}_{\text{plaq.}} - c\right) = -\sum_{\text{pl.}} \fbox{pl.} - c, \tag{5.1}$$

where $\mathcal{O}_{\text{plaq.}} = \fbox{pl.} = Z_1 X_2 Z_3 X_4$ is the four-spin plaquette operator, and $\{X_i, Y_i, Z_i\}$ the set of Pauli matrices acting on site i. The energy scale g has been set to 1 and c is a shift in energy such that the ground state energy of $H_L = 0$. The number of sites L_y along y is taken to be even, in order to avoid having a twist defect line (i.e. a consistent checkerboard coloring of the plaquettes can be made so that the elementary excitations e and m live on plaquettes of different colors). Figure 5.2.1 shows the semi-infinite cylinder with a checkerboard coloring.

Note that this is a choice of the Hamiltonian acting on the semi-infinite cylinder that we have made, as we need to also specify boundary conditions on the edge of the manifold. In particular, in eqn. (5.1), we have chosen free boundary conditions - we have simply taken the Wen-plaquette model on a semi-infinite cylinder to be the sum of plaquette operators with no additional commuting boundary Hamiltonian operators. The choice of different boundary conditions - the addition of boundary operators - will naturally affect the edge-ES correspondence, but we will only restrict our analysis to the case of free boundary conditions in this chapter.

It will be useful to introduce the following graphical notation: we represent the Pauli operators as red string operators $Z_i =$ ⟋$_i$, $X_i =$ ⟍$_i$ if the strings live on the grey plaquettes ($\tilde{p}$); while we represent them as blue string operators $Z_i =$ ⟋$_i$, $X_i =$ ⟍$_i$ if they live on the white plaquettes (p). For example, the *white* plaquette operator is given by $\boxed{p}$ since the strings live on the *grey* plaquettes neighboring it.

Topological sectors of ground state subspace. The ground state subspace $\mathcal{V}_{0,L}$ of the Wen-plaquette model (defined by the plaquette condition $\fbox{pl.} = +1$) on an semi-infinite cylinder, similar to that of the infinite cylinder and of the torus, has four topological sectors
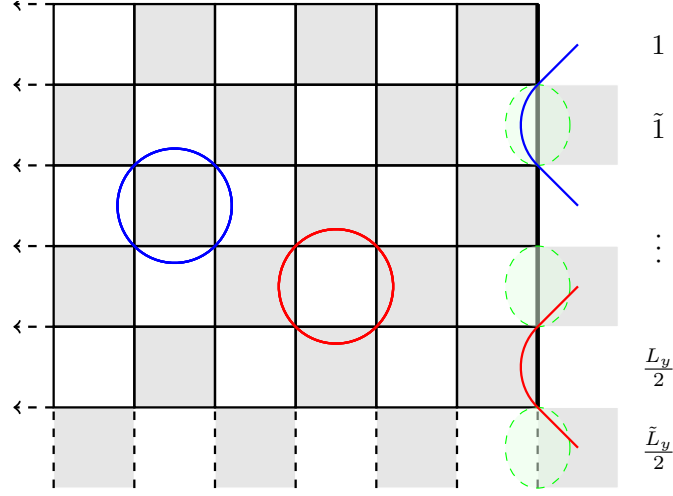
Figure 5.2.1: Semi-infinite cylinder that terminates in the x-direction, with the periodic direction along y. The grey plaquette and white plaquette operators are shown as blue and red circles respectively. The boundary operators (BO) can be thought of as half of the plaquette operators in the bulk (acting on the white (p) or grey ($\tilde{p}$) plaquettes). The green ellipses on the edge correspond to the virtual, boundary spin degree of freedom. The blue BO acts on a single virtual spin, while the red BO acts on a pair of nearest-neighbor virtual spins.

a ($\mathcal{V}_{0,L} = \oplus_{a=1}^{N=4} \mathcal{V}_{0,L}^a$). They are distinguished by the eigenvalues of the two non-contractible Wilson loop operators around the cylinder $\tilde{\Gamma}_L = \left.\begin{array}{c}\end{array}\right\}_L$ and $\Gamma_L = \left.\begin{array}{c}\end{array}\right\}_L$, where $\tilde{\Gamma}_L$ is the string operator $Z_1 X_2 Z_3 \cdots X_{L_y}$ living on the grey plaquettes, acting on the spins on the boundary, as defined using the graphical notation above and similarly for Γ_L for the white plaquettes. These operators commute with all $\mathcal{O}_{\text{plaq.}}$, square to $\mathbb{1}$, and thus have eigenvalues $\tilde{Q}_L$ and Q_L respectively taking values ± 1 each, giving the four topological sectors $a \simeq (\tilde{Q}_L, Q_L)$. States within each topological sector a are said to have well-defined anyonic flux with respect to $\tilde{\Gamma}_L$ and Γ_L.

Ground state degeneracy. The ground state subspace $\mathcal{V}_{0,L}$ is however not four-dimensional. To find the ground state degeneracy, we need to find a maximal set of commuting and independent operators in addition to the plaquette operators. Besides $\tilde{\Gamma}_L$ and Γ_L we can have boundary operators (BO) $S_{p,L} = \boxed{}\begin{array}{c} p \\ L \end{array}$; $S_{\tilde{p},L} = \boxed{}\begin{array}{c} \tilde{p} \\ L \end{array}$, where $S_{p,L} = Z_{2p-1} X_{2p}$ and $S_{\tilde{p},L} = Z_{2\tilde{p}} X_{2\tilde{p}+1}$ are half-plaquette operators or string operators acting on the spins on the boundary. The strings thus start and terminate outside the boundary of the semi-infinite

92

cylinder (see Fig. 5.2.1). There are $L_y/2$ of each kind of operators. The BOs individually commute with $\mathcal{O}_{\text{plaq.}}$, Γ and $\tilde{\Gamma}$. However, $[S_{p,L}, S_{\tilde{p},L}] \neq 0$ if p neighbors $\tilde{p}$, so a choice of a maximal set of commuting and independent operators on the L semi-infinite cylinder is

$$\left\{ \mathcal{O}_p, \ \mathcal{O}_{\tilde{p}}, \ S_{\tilde{p}}, \ \tilde{\Gamma} \right\}_L = \left\{ \boxed{p}, \ \boxed{\tilde{p}}, \ \boxed{\tilde{p}}, \ \Big\} \right\}_L . \tag{5.2}$$

Note that Γ_L is not included in the set because it can be formed by the boundary operators: $\Gamma_L = \prod_{\tilde{p}} S_{\tilde{p},L}$. Thus $\mathcal{V}_{0,L}$ has four topological sectors a, such that $\mathcal{V}_{0,L} = \oplus_{a=1}^4 \mathcal{V}_{0,L}^a$, each with $L_y/2 - 1$ states labeled by the eigenvalues of $S_{\tilde{p},L}$, for a total dimensionality $\dim(\mathcal{V}_{0,L}) = 2^{L_y/2+1}$. Physically, these states can be thought of as having pairs of anyons (e or m) that condense on the boundary - this process does not cost energy and thus the ground state degeneracy is given by the number of ways we can condense the anyons on the boundary. For this reason, these ground states can also be understood as edge states, and from now on, the terms 'lowest-energy states' and 'edge states' will be used interchangeably with 'ground states'. We will also define the projector $P_{0,L}^a$ onto the eigenspace $\mathcal{V}_{0,L}^a$ for future use.

At this point, we introduce a mapping of the boundary operators $S_{p,L}$ and $S_{\tilde{p},L}$ to local operators acting on a finite length (spin-1/2) spin chain. This mapping will be important as it elucidates the tensor product structure of the edge theory on the semi-infinite cylinder. Consider the Wilson loop operator $\Big\}_L$ partitioning $\mathcal{V}_{0,L}$ into two: $\mathcal{V}_{0,L} = \oplus_{\tilde{Q}=\pm1} \mathcal{V}_{0,L}^{\tilde{Q}_L}$, labeled by $\tilde{Q}_L$. Each $\tilde{Q}_L$ sector has dimension $2^{L_y/2}$, which is isomorphic to a spin-1/2 chain of length $L_y/2$. Let us therefore associate a virtual spin-1/2 degree of freedom for each $\tilde{p}$-plaquette (see Fig. 5.2.1). Here, we see that a (not unique) representation of the operators $S_{p,L}$ and $S_{\tilde{p},L}$ acting on the L spin-1/2 chain for each $\tilde{Q}_L$ can be found:

$$\begin{aligned} \boxed{\tilde{p}} &\simeq \tau_{\tilde{p},L}^x \text{ for } 1 \leq \tilde{p} \leq \tilde{L}_y/2, \\ \boxed{p} &\simeq \tau_{\tilde{p},L}^z \tau_{\tilde{p}-1,L}^z \text{ for } 2 \leq \tilde{p} \leq \tilde{L}_y/2, \end{aligned} \tag{5.3}$$

and $\boxed{1} \simeq \tilde{Q}_L \times \tau_{1,L}^z \tau_{\tilde{L}_y/2,L}^z$, i.e. toroidal boundary conditions. One can check that the Pauli spin operators reproduce the canonical anticommutation algebra of $S_{p,L}$ and $S_{\tilde{p},L}$ and that $\Big\}_L = \tilde{Q}_L$ is satisfied. Note that the Wilson loop $\Big\}_L$ is mapped to the global spin-flip operator $\hat{Q}_L := \prod_{\tilde{p}} \tau_{\tilde{p},L}^x$, with eigenvalues $Q_L = \pm1$. A similar representation can be found for the operators $S_{p,R}$ and $S_{\tilde{p},R}$ acting on the spin-1/2 chain of R.

Higher energy subspaces. Higher energy subspaces $\mathcal{V}_{\alpha>0,L}$ are spanned by states for which the plaquette condition $\boxed{\text{pl.}} = +1$ is violated. As such, there is a spectral gap of

at least $+1$ separating the ground state subspace from the higher energy subspaces. These violations are generated by string operators that have at least one end point in the bulk.

For each higher subspace $\mathcal{V}_{\alpha>0,L}$, we can further define a notion of topological sectors a, where $a = 1, \cdots 4$, in the following way: the subspace $\mathcal{V}_{\alpha>0,L}^a$, is the space spanned by all states in $\mathcal{V}_{0,L}^a$ which are acted upon by all possible products of finite-length (i.e. local) string operators such that the number of end-points of these string operators in the bulk of L is α. These sectors are called topological because the matrix element of generic local operators using states belonging to different topological sectors vanishes.

Edge theory. The edge theory in each topological sector a is defined to be the Hamiltonian $H_{\text{edge},L}^a$ acting on the $2^{L_y/2-1}$ edge states of the subspace $\mathcal{V}_{0,L}^a$ that give rise to the different states' energy levels. However, all states in $\mathcal{V}_{0,L}$ have the exact same energy, and hence the edge Hamiltonian for the exact Wen-plaquette model in each topological sector is identically 0.

Let us summarize what we have learned:

• The effective low energy degrees of freedom $(\mathcal{V}_{0,L}^{\tilde{Q}_L})$ at the boundary of the L semi-infinite cylinder of length L_y is a spin chain made of $L_y/2$ virtual spin-1/2 degrees of freedom, for each topological $\tilde{Q}_L$ sector. The spin chain is generated by the boundary operators $S_{p,L}$ and $S_{\tilde{p},L}$ which are half-plaquette operators in the bulk. In the effective spin chain language, these boundary operators are mapped to $\mathbb{Z}_2$ symmetric spin-operators $\tau_{\tilde{p},L}^z \tau_{\tilde{p}-1,L}^z$ and $\tau_{\tilde{p},L}^x$. Without perturbations, $H_{\text{edge},L}^a$ is identically 0. With perturbations, there will be dynamics on this effective spin chain, generated by these boundary operators. A similar situation arises for the R semi-infinite cylinder.

5.2.2 Entanglement spectrum

Let us now solve for the four ground states of the exact Wen-plaquette model on the infinite cylinder, and compute their entanglement spectrum for a bipartition of the infinite cylinder into two semi-infinite cylinders. We can do this by putting two semi-infinite cylinders L and R together, and gluing them with the plaquette terms that act on the strip of plaquettes spanning the two cylinders. That is, we solve:

$$H = H_L + H_R + H_{LR}, \tag{5.4}$$

where H_L is given by eqn. (5.1) (and correspondingly for H_R), acting on the L and R semi-infinite cylinders respectively, while $H_{LR} = -\sum_{\text{plaq.}\in\text{strip}} \mathcal{O}_{\text{plaq.}}$. The entanglement
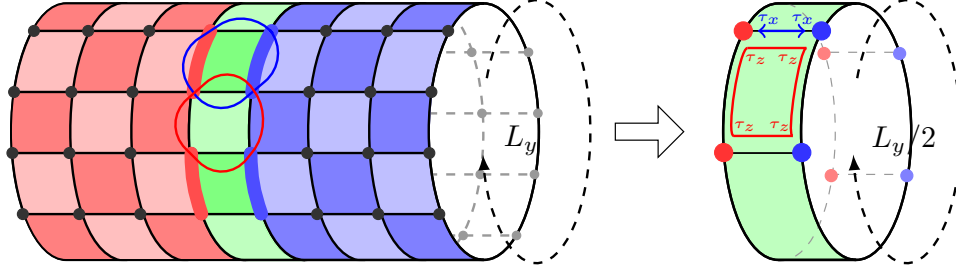
Figure 5.2.2: (Left) Gluing two semi-infinite cylinders of circumference L_y together. The L semi-infinite cylinder is colored red, the R semi-infinite cylinder is colored blue, while the plaquette terms belonging to the strip are colored green. The entanglement cut is naturally taken to be the divisor through the strip so that the system is bipartitioned into the L and R semi-infinite cylinders. A checkerboard coloring has been made on the infinite cylinder, and the $L_y/2$ effective virtual spin-1/2 degrees of freedom are denoted by red and blue ellipses living on the boundaries of the semi-infinite cylinders. (Right) The mapping, eqn. (5.3), gives rise to an effective Hamiltonian acting on the spin-ladder system, with each spin chain having $L_y/2$ sites, which were previously the red and blue ellipses. The red and blue plaquette operators have been mapped to z-rung and x-rung operators respectively. The effective Hamiltonian's ground states correspond to the ground states of the infinite cylinder.

cut is naturally taken to be through the strip of plaquettes that divides the system into the L and R subsystems, such that the full Hilbert space $\mathcal{H}$ is the tensor product of the two semi-infinite cylinders: $\mathcal{H} = \mathcal{H}_L \otimes \mathcal{H}_R$. Figure 5.2.2 shows the gluing process.

Now, $\mathcal{H}$ can also be written as $\mathcal{H} = \bigoplus_{\alpha,\beta=0}^{\infty} \mathcal{V}_{\alpha,L} \otimes \mathcal{V}_{\beta,R}$. Note that a plaquette operator in H_{LR} is comprised of two matching boundary operators acting on the L and R cylinders, for example $\mathcal{O}_{\text{plaq.}\in\text{strip.}}(p) = S_{p,L} \otimes S_{p,R}$ (note that p is the same for L and R) and similarly for $\tilde{p}$, which implies that its action must be such that the tensor product structure is preserved, $H_{LR} : \mathcal{V}_{\alpha,L} \otimes \mathcal{V}_{\beta,R} \to \mathcal{V}_{\alpha,L} \otimes \mathcal{V}_{\beta,R}$. Since H_{LR} is the sum of mutually commuting terms, we can simply focus on its action on the $\mathcal{V}_{0,L} \otimes \mathcal{V}_{0,R}$ sector because that is where the ground states of the infinite cylinder live in.

Next, we employ the fact that there are topological sectors a and a' in $\mathcal{V}_{0,L}$ and $\mathcal{V}_{0,R}$ to further narrow down the subspace of the Hilbert space where the ground states reside in. Consider the subspace given by tensoring subspaces of L and R with $\tilde{Q}_L \neq \tilde{Q}_R$: $\mathcal{V}_{0,L}^{\tilde{Q}_L} \otimes \mathcal{V}_{0,R}^{\tilde{Q}_R}$. In this space, $\left\{_L \otimes \right\}_R = -1$, which means that one of the plaquette conditions of the

plaquettes in H_{LR} is violated. Thus, the ground states cannot live in this space. Conversely it means that the ground states must have $\tilde{Q}_L = \tilde{Q}_R \equiv \tilde{Q}$.

A similar argument can be made for $\begin{smallmatrix} \\ \end{smallmatrix}_L$ (with eigenvalues $Q_L = \pm 1$), which would yield $Q_L = Q_R \equiv Q$ for the ground states. This would imply that $a = a'$ for the ground states (or equivalently $a \simeq (\tilde{Q}_L, Q_L) = (\tilde{Q}_R, Q_R) \simeq a'$ as there is a one-to-one map between a and $(\tilde{Q}_L, Q_L)$). Let us therefore first consider projecting H_{LR} into the $\tilde{Q}$-sector subspace $\mathcal{V}_{0,L}^{\tilde{Q}} \otimes \mathcal{V}_{0,R}^{\tilde{Q}}$ by the projector $P_{0,L}^{\tilde{Q}} \otimes P_{0,R}^{\tilde{Q}}$.

Using the mapping, eqn. (5.3), one possible representation of the strip-plaquette operators upon projection into $\mathcal{V}_{0,L}^{\tilde{Q}} \otimes \mathcal{V}_{0,R}^{\tilde{Q}}$, is of operators acting on two spin chains (of length $L_y/2$ each) for the left and right cylinders:

$$
\begin{aligned}
\mathcal{O}_{\tilde{p}} = \; \textcircled{$\tilde{p}$} \; &\to \tau_{\tilde{p},L}^x \tau_{\tilde{p},R}^x \\
\mathcal{O}_p = \; \boxed{p} \; &\to \tau_{\tilde{p},L}^z \tau_{\tilde{p}-1,L}^z \tau_{\tilde{p},R}^z \tau_{\tilde{p}-1,R}^z,
\end{aligned}
\tag{5.5}
$$

for both $\tilde{Q}$. These operators are called "x-rung" and "z-rung" operators respectively.

The effective Hamiltonian, i.e. the projection of H_{LR} into $\mathcal{V}_{0,L}^{\tilde{Q}} \otimes \mathcal{V}_{0,R}^{\tilde{Q}}$, is therefore

$$
H_{\text{eff}} = - \sum_{\tilde{p}=1}^{\tilde{L}_y/2} \left(\tau_{\tilde{p},L}^x \tau_{\tilde{p},R}^x + \tau_{\tilde{p},L}^z \tau_{\tilde{p}-1,L}^z \tau_{\tilde{p},R}^z \tau_{\tilde{p}-1,R}^z \right).
\tag{5.6}
$$

This is a spin-ladder system (see Fig. 5.2.2), of length $L_y/2$, with $\mathcal{O}_p$ and $\mathcal{O}_{\tilde{p}}$ coupling the two chains. It also has a $\mathbb{Z}_2$ symmetry generated by the global spin flip operator $\hat{Q}_L := \prod_{\tilde{p}} \tau_{\tilde{p},L}^x$ (whose eigenvalue is Q_L). Solving eqn. (5.6) for both $\tilde{Q}$ will give us all four ground states of the system.

Let us fix a $\tilde{Q}$. Define the (unique) state $| \uparrow \rangle_L$ as the state that is a ground state of H_L with $\tilde{Q}_L = \tilde{Q}$ and furthermore satisfies $\tau_{\tilde{p},L}^z = +1$. Then we see that the other $2^{\tilde{L}_y/2}$ states spanning $\mathcal{V}_{0,L}^{\tilde{Q}}$ comprise of all other possible spin configurations $| \tau \rangle_L$, generated by $\tau_{\tilde{p},L}^x$ acting on $| \uparrow \rangle_L$. The same is also true for R. The ground state of eqn. (5.6), or equivalently of the full Hamiltonian, in this $\tilde{Q}$ sector with $Q = Q_L = Q_R$ is therefore given

by

$$|\tilde{Q}, Q\rangle = \mathcal{N} \prod_{\tilde{p}} \left(\frac{\mathbb{1} + \tau_{\tilde{p},L}^x \tau_{\tilde{p},R}^x}{2} \right) \left(|\uparrow\rangle_L |\uparrow\rangle_R + Q\hat{Q}_L |\uparrow\rangle_L |\uparrow\rangle_R \right)$$

$$= \frac{1}{\sqrt{2^{\tilde{L}_y/2}}} \frac{1}{\sqrt{2}} \sum_{\tau} \left(|\tau\rangle_L |\tau\rangle_R + Q|\bar{\tau}\rangle_L |\tau\rangle_R \right) \qquad (5.7)$$

$$= \frac{1}{\sqrt{2^{\tilde{L}_y/2-1}}} \sum_{\tau} \mathbb{P}_{Q,L} |\tau\rangle_L |\tau\rangle_R,$$

where $\mathbb{P}_{Q,L} := (\mathbb{1} + Q_L \hat{Q}_L)/2$ is the $\mathbb{Z}_2$ projector onto the $Q_L = Q$ sector in the L chain. Thus, in total, there are four ground states on the infinite cylinder as claimed, each with well-defined anyonic flux through the cylinder.

Lastly, from eqn. (5.7), it can be readily seen that the entanglement spectrum of $|\tilde{Q}, Q\rangle$ is flat: the reduced density matrix on L is

$$\rho_L^{a \simeq (\tilde{Q}, Q)} := \text{Tr}_R |\tilde{Q}, Q\rangle\langle\tilde{Q}, Q| = \frac{1}{2^{\tilde{L}_y/2-1}} \mathbb{P}_{Q,L}, \qquad (5.8)$$

with $2^{\tilde{L}_y/2-1}$ non-zero eigenvalues all of value $1/2^{\tilde{L}_y/2-1}$. The entanglement Hamiltonian $H_{ent.}^a \equiv -\ln(\rho_L^a)$ is therefore also flat and acts on a virtual spin chain of length $L_y/2$.

In summary:

• The entanglement Hamiltonian of the exact Wen-plaquette model in topological sector a is flat and acts on a virtual spin-1/2 spin chain of length $L_y/2$, similar to the case of the edge Hamiltonian. Each entanglement Hamiltonian gives an ES with $2^{L_y/2-1}$ finite values. The entanglement Hamiltonians can be derived by considering an effective Hamiltonian acting on a spin-ladder system with length $L_y/2$, for each $\tilde{Q} = \tilde{Q}_L = \tilde{Q}_R$ sector. Solving the effective Hamiltonian in each $\tilde{Q}$ sector gives two ground states distinguished by the eigenvalue $Q = Q_L = Q_R$, for a total of four ground states overall.

5.2.3   Edge-ES correspondece

Since the edge Hamiltonian is identically 0, and the entanglement Hamiltonian flat, the edge-ES correspondence is exact in this case: the two spectra are equal up to rescaling and shifting. However, that is not to say that the flat entanglement spectrum is uninteresting:

for example, the entanglement entropy in each topological sector can be readily calculated, yielding

$$S_a = \text{Tr}(\rho_L^a \ln \rho_L^a) = \left(\tilde{L}_y/2 - 1 \right) \ln 2. \tag{5.9}$$

From there the topological entanglement entropy[35, 34] γ_a, defined to be the universal sub-leading piece of the entanglement entropy, $S_a = \alpha_a L - \gamma_a + \cdots$, can be extracted:

$$\gamma_a = \ln 2, \tag{5.10}$$

in agreement with the fact that $|\tilde{Q}, Q\rangle$ are the so-called minimum entangled states[198] on the infinite cylinder.

We conclude:

• The edge-ES correspondence for the exact Wen-plaquette model is exact: all $2^{L_y/2-1}$ levels of the edge and entanglement spectra in a topological sector a conincide with a shift and rescaling that is common to all sectors a.

5.3 Perturbed Wen-plaquette model

In this section, we perturb the Wen-plaquette model and derive both the edge theory on the semi-infinite cylinder and entanglement spectrum of the ground states on the infinite cylinder. We shall be precise as to what we mean by the edge theory in this case. The general perturbed Wen-plaquette model on the full cylinder is

$$H = H_L + H_R + H_{LR} + \epsilon(V_L + V_R + V_{LR}), \tag{5.11}$$

where $H_L + H_R + H_{LR}$ is as before, in eqn. (5.4), while V_L and V_R are perturbations acting on each respective semi-infinite cylinder, and V_{LR} is a perturbation that spans the cut. We assume that for weak enough perturbations, the lowest energy subspaces of H_L and $H_L + \epsilon V_L$ are adiabatically connected. Thus, energy levels in the highly degenerate subspace $\mathcal{V}_{0,L}$ of $\mathcal{H}_L$ acquire dispersions due to the perturbations, and split. The edge theory or edge Hamiltonian $H_{\text{edge},L}$ is then defined to be the Hamiltonian acting on the states in the lowest energy eigenspace of $H_L + \epsilon V_L$ that generates the dynamics and hence the dispersion.

The key to deriving this edge Hamiltonian and subsequently, the entanglement spectrum of the four ground states of eqn. (5.11), is the Schrieffer-Wolff (SW)[199] transformation. This is a transformation which perturbatively block diagonalizes a Hamiltonian if its

original, unperturbed Hamiltonian was block-diagonal to begin with, which is the case for the Wen-plaquette model. We begin this section by introducing the SW transformation before then applying it to finding the edge and the entanglement Hamiltonians.

5.3.1 Mathematical preliminaries: Schrieffer-Wolff transformation

We present a concise but necessary introduction to the Schrieffer-Wolff (SW) transformation[199]. See Ref. [200] for all precise definitions and theorems concerning the SW transformation.

Let us be given a Hamiltonian H_0 that has a low-energy eigenspace $\mathcal{V}_0$ and a high-energy eigenspace $\mathcal{V}_1$ separated by a spectral gap. Then H_0 can be written as

$$H_0 = P_0 H_0 P_0 + P_1 H_0 P_1, \tag{5.12}$$

where P_α are projectors to $\mathcal{V}_\alpha$, $\alpha = 0, 1$. Let us now add a small perturbation to the system ϵV that does not commute with H_0. We assume that the perturbations are weak enough such that the new Hamiltonian can be written as

$$H = H_0 + \epsilon V = \tilde{P}_0 H \tilde{P}_0 + \tilde{P}_1 H \tilde{P}_1, \tag{5.13}$$

where there are still low-energy $\tilde{\mathcal{V}}_0$ and high-energy $\tilde{\mathcal{V}}_1$ subspaces separated by the spectral gap. $\mathcal{V}_\alpha$ and $\tilde{\mathcal{V}}_\alpha$ are assumed to have the same dimensionality, and have significant overlap. Then, we can find a unique direct rotation (i.e. unitary) U between the old and new subspaces ($U\tilde{P}_\alpha U^\dagger = P_\alpha$) such that we can rotate H to a new Hamiltonian H' with eigenspaces V_α:

$$H' := UHU^\dagger = P_0 UHU^\dagger P_0 + P_1 UHU^\dagger P_1. \tag{5.14}$$

This is the so-called Schrieffer-Wolff transformation[199, 200]. It will be useful that U can be written uniquely as $U = e^S$, where S is an antihermitian and block off-diagonal (in both $\mathcal{V}_\alpha$ and $\tilde{\mathcal{V}}_\alpha$) operator, and can be constructed perturbatively in ϵ: $S = \sum_{n \geq 1} \epsilon^n S_n$, $S_n^\dagger = -S_n$. The exact formulas for S_n can be found in Ref. [200], and we reproduce them in Appendix 5.A.

Though our discussion above has been limited to Hamiltonians with only two invariant subspaces (low and high), the SW transformation can be readily generalized to Hamiltonians that have many invariant subspaces each separated by a spectral gap, such that the Hilbert space $\mathcal{H} = \bigoplus_{\alpha \geq 0} \mathcal{V}_\alpha$, see Ref. [201]. S will still be block-off-diagonal.

The generalized Schrieffer-Wolff transformation is also referred to as the effective Hamiltonian method[202]. To second order in perturbation theory, H', which by construction is block-diagonal in $\mathcal{V}_\alpha$, is given explicitly by

$$\langle i, \alpha | H' | j, \alpha \rangle = E_i^\alpha \delta_{ij} + \epsilon \langle i, \alpha | V | j, \alpha \rangle + \frac{\epsilon^2}{2} \sum_{\substack{k \\ \beta \neq \alpha}}$$

$$\langle i, \alpha | V | k, \beta \rangle \langle k, \beta | V | j, \alpha \rangle \left(\frac{1}{E_i^\alpha - E_k^\beta} + \frac{1}{E_j^\alpha - E_k^\beta} \right), \qquad (5.15)$$

where $|i, \alpha\rangle \in \mathcal{V}_\alpha$, $|j, \beta\rangle \in \mathcal{V}_\beta$ and E_i^α is the energy of $|i, \alpha\rangle$. See appendix 5.A for the full perturbative series of the effective Hamiltonian.

5.3.2 Edge theory on semi-infinite cylinder

As mentioned before, the SW transformation is suitable for use on the perturbed Wen-plaquette model on the semi-infinite cylinder, $H_L + \epsilon V_L$, because the unperturbed Hamiltonian H_L is block-diagonal with spectral gaps separating the different energy eigenspaces. To find the edge theory, $H_{\text{edge},L}$, we want to evaluate eqn. (5.15) (with $V \to V_L$) for the L semi-infinite cylinder with states belonging to $\mathcal{V}_{0,L}$, the lowest energy subspace. Furthermore, we can make use of the fact that states with different $\tilde{Q}_L$ do not mix at any order in perturbation theory, as the perturbations are local and cannot generate a global term that mixes $\tilde{Q}_L$ sectors, so we can consider eqn. (5.15) restricted to states belonging to $\mathcal{V}_{0,L}^{\tilde{Q}_L}$.

However, since by construction $H_{\text{edge},L}^{\tilde{Q}_L}$ acts only on $\mathcal{V}_{0,L}^{\tilde{Q}_L}$, $H_{\text{edge},L}^{\tilde{Q}_L}$ is generated solely from virtual processes in the perturbative series (eqn. (5.15)) that map states in the ground state subspace back to itself. These virtual processes are simply products of boundary operators and plaquette operators on L.

To clarify this statement, let us show this for a particular second order term in a fixed $\tilde{Q}_L$ sector. Let $v_{1,L}$ and $v_{2,L}$ be two local perturbations, each of which are not sums of perturbations, coming from V_L (which is generally a sum of local perturbations) that give rise to a non-zero contribution in the matrix element, i.e., $\langle i, 0 | v_{1,L} | k, \beta \rangle \langle k, \beta | v_{2,L} | j, 0 \rangle \neq 0$ for some i, j, k, β. $v_{2,L}$ is comprised of products of string operators with end points in the bulk of the L semi-infinite cylinder. The number of end points in L determines β, i.e. $v_{2,L}$ can link a ground state to a state with β excitations in L. This is a state which lives in $\mathcal{V}_{\beta,L}$. Furthermore, this state is unique. Indeed, $|k, \beta\rangle = v_{2,L} |j, 0\rangle$, and so $\langle l, \gamma | v_{2,L} | j, 0 \rangle = 0$ for any other state such that $|l, \gamma\rangle \neq |k, \beta\rangle$. Now, since $\langle i, 0 | v_{1,L} | k, \beta \rangle \neq 0$, $v_{1,L}$ must be

such that it creates the same bulk excitations as $v_{2,L}$, in order to cancel out the excitations of $|k, \beta\rangle$, modulo products of plaquette and boundary operators. The presence of the boundary operators makes $|i, 0\rangle$ potentially not equal to $|j, 0\rangle$. Putting all these facts together, we see that replacing $|k, \beta\rangle\langle k, \beta|$ with the sum over all possible states in the Hilbert space, i.e. $\sum_{l,\gamma} |l, \gamma\rangle\langle l, \gamma| = \mathbb{1}$ for this $v_{1,L}, v_{2,L}$ does not change the value of the matrix element, yielding the desired assertion:

$$\langle i, 0|v_{1,L}|k, \beta\rangle\langle k, \beta|v_{2,L}|j, 0\rangle = \langle i, 0|v_{1,L}\mathbb{1}v_{2,L}|j, 0\rangle =$$
$$\langle i, 0| \prod_{\substack{\{\text{pl.},p,\tilde{p}\} \\ \text{of } v_{1,L}v_{2,L}}} \text{\small(pl.)} \times \boxed{}\!\!\!\diagdown\!\!\!\text{\small(} p \times \boxed{}\!\!\!\diagdown\!\!\!\text{\small(} \tilde{p} \ \ |j, 0\rangle. \tag{5.16}$$

A similar argument can be made for terms of other orders in perturbation theory.

Since $\text{\small(pl.)} = +1$ for the ground states, we therefore see that $H^{\tilde{Q}_L}_{\text{edge},L}$ must be a function of products of $S_{p,L}$ and $S_{\tilde{p},L}$ projected down into $\mathcal{V}^{\tilde{Q}_L}_{0,L}$:

$$H^{\tilde{Q}_L}_{\text{edge},L} = f_{\tilde{Q}_L,L}\left(\boxed{}\!\!\!\diagdown\!\!\!\text{\small(} p \ , \ \boxed{}\!\!\!\diagdown\!\!\!\text{\small(} \tilde{p} \right). \tag{5.17}$$

However, recall the mapping given by eqn. (5.3), which allows us to interpret the edge Hamiltonian in terms of a more physical picture: a Hamiltonian acting on a spin chain.

The edge Hamiltonian in a $\tilde{Q}_L$-sector at finite order in perturbation theory is therefore a local Hamiltonian acting on a spin-1/2 chain of length $L_y/2$:

$$H^{\tilde{Q}_L}_{\text{edge},L} = f_{\tilde{Q}_L,L}(\tau^x_{\tilde{p},L}, \tau^z_{\tilde{p},L}\tau^z_{\tilde{p}-1,L}), \tag{5.18}$$

with toroidal boundary conditions given by $\tilde{Q}_L$ (i.e. $\tau^z_{0,L} = \tilde{Q}_L\tau^z_{\tilde{L}_y/2,L}$). Since it is constructed perturbatively, it generically appears at order ϵ. Importantly, we also see that the edge Hamiltonian is always $\mathbb{Z}_2$ symmetric regardless of the type of perturbation. This is not a surprising result because the two sectors of $\mathbb{Z}_2$ in the spin language, given by the generator $\hat{Q}_L := \prod_{\tilde{p}} \tau^x_{\tilde{p},L}$, correspond to the two topological sectors $Q_L = \pm 1$ of the Wilson loop $\text{\small$\lessgtr$}_L$, which are preserved under any local perturbations. The edge Hamiltonian in each topological sector a then arises from projecting $H^{\tilde{Q}_L}_{\text{edge},L}$ into the relevant Q sector: $H^a_{\text{edge},L} \equiv \mathbb{P}_{Q,L}H^{\tilde{Q}_L}_{\text{edge},L}\mathbb{P}_{Q,L}$.

In summary:

- The edge Hamiltonian of the perturbed Wen-plaquette model for the L semi-infinite cylinder is given by $H^{\tilde{Q}_L}_{\text{edge},L}$, eqn. (5.18), in each $\tilde{Q}_L$ sector. At any finite order in perturbation theory, it is a $\mathbb{Z}_2$ symmetric local Hamiltonian on the virtual spin chain. This is guaranteed if the perturbations of the Wen-plaquette model are themselves local on the cylinder. To further find the edge Hamiltonians in each topological sector $a \simeq (\tilde{Q}_L, Q_L)$, we project into the Q_L sector:

$$H^a_{\text{edge},L} \equiv \mathbb{P}_{Q,L} H^{\tilde{Q}_L}_{\text{edge},L} \mathbb{P}_{Q,L}, \tag{5.19}$$

where $\mathbb{P}_{Q,L} = (\mathbb{1} + Q_L \hat{Q}_L)/2$. A similar result holds for the R semi-infinite cylinder.

5.3.3 Entanglement spectrum

We now find the ground states in each topological sector a of the perturbed Wen-plaquette model on the infinite cylinder,

$$H = H_L + H_R + H_{LR} + \epsilon(V_L + V_R + V_{LR}). \tag{5.20}$$

The precise definition of each term can be found in eqn. (5.11).

Let us fix a sector $a \simeq (\tilde{Q}, Q)$. There will now be corrections to the ground state leading to a ES with dispersion. However, there now exists a difficulty in comparing the edge and entanglement spectra. From eqn. (5.19), we see that H^a_{edge} still has $2^{L_y/2-1}$ eigenvalues; but, there will be many more entanglement energies than the $2^{L_y/2-1}$ finite ones as found in eqn. (5.7). What does it mean to compare the two spectra then? The resolution can be found by looking at the general form of the perturbed ground state. Dropping the normalization constant for now, for a fixed $\tilde{Q}$, the perturbed ground state can be written as

$$
\begin{aligned}
|\tilde{Q}, Q\rangle = &\sum_{\tau',\tau} (\mathbb{P}_Q - \Lambda)_{\tau',\tau} |\tau'\rangle_L |\tau\rangle_R + \\
&\sum_{\tau,i,\alpha \geq 1} \left(\Theta_{\tau,\{i,\alpha\}} |\tau\rangle_L |i,\alpha\rangle_R + \Xi_{\{i,\alpha\},\tau} |i,\alpha\rangle_L |\tau\rangle_R \right) \\
&+ \sum_{\substack{i,\alpha \geq 1 \\ j,\beta \geq 1}} \Omega_{\{i,\alpha\},\{j,\beta\}} |i,\alpha\rangle_L |j,\beta\rangle_R,
\end{aligned}
\tag{5.21}
$$

where $(\mathbb{P}_Q)_{\tau',\tau}$ are the matrix elements of the matrix $\mathbb{P}_Q = (\mathbb{1} + Q \prod_i \tau_i^x)/2$, written in the τ^z basis. $\Lambda, \Theta, \Xi, \Omega$ are coefficient matrices linking a state in L with another state in R

and are small in magnitude (ϵ or higher). Here $|\tau'\rangle_L \in \mathcal{V}_{0,L}^{\tilde{Q}}$, and $|i,\alpha\rangle \in \mathcal{V}_{\alpha,L}$ for $\alpha \geq 1$. The same holds true for states in R.

We have written the ground state in a way to emphasize the change in the entanglement structure. Our claim is that for generic local perturbations, Λ has the form

$$\Lambda = \mathbb{P}_Q \Lambda' \mathbb{P}_Q, \tag{5.22}$$

which is an order ϵ correction which is related to $H_{\text{ent.}}^a$. Here we have implicitly defined the central object of interest, Λ', which we will argue is related to the entanglement Hamiltonian.

Furthermore, Λ is generated by the terms $H_{\text{edge},L}^a$, $H_{\text{edge},R}^a$, and $(P_{0,L}^a \otimes P_{0,R}^a)V_{LR}(P_{0,L}^a \otimes P_{0,R}^a)$. We see that $\mathbb{P}_Q \Lambda' \mathbb{P}_Q$ is a $2^{L_y/2}$ by $2^{L_y/2}$ matrix with $2^{L_y/2-1}$ eigenvalues that have eigenvectors with $\mathbb{P}_Q = 1$, linking states in $\mathcal{V}_{0,L}^{\tilde{Q}}$ with $\mathcal{V}_{0,R}^{\tilde{Q}}$ which is spanned by $|\tau'\rangle_L \otimes |\tau\rangle_R$. Θ and Ξ are generically order ϵ corrections and links states in $\mathcal{V}_{0,L}^{\tilde{Q}}$ with $\mathcal{V}_{\alpha \geq 0,R}$ and $\mathcal{V}_{\alpha \geq 0,L}$ with $\mathcal{V}_{0,R}^{\tilde{Q}}$ respectively. Ω represents order ϵ corrections to the ground state in the space $\mathcal{V}_{\alpha \geq 0,L} \otimes \mathcal{V}_{\beta \geq 0,R}$.

We sketch here why $\Lambda = \mathbb{P}_Q \Lambda' \mathbb{P}_Q$ is related to the entanglement Hamiltonian. If we form the un-normalized reduced density matrix on L, $\rho_L^a = \text{Tr}_R |\tilde{Q}, Q\rangle\langle\tilde{Q}, Q|$, it will have a dominant piece that looks like

$$(\rho_L^a)_{\text{dom.}} = \sum_{\tau',\tau} \left(\mathbb{P}_Q - \mathbb{P}_Q(\Lambda' + \Lambda'^\dagger)\mathbb{P}_Q + \cdots \right)_{\tau',\tau} |\tau'\rangle_L\langle\tau|_L, \tag{5.23}$$

where $\cdots$ refers to higher order terms. Since in a suitable basis $\mathbb{P}_Q = \mathbb{1}_a$ (for a fixed $\tilde{Q}$), the expression above can be approximated with an exponential ($1 - x \approx \exp(-x)$ for small x), and so the entanglement Hamiltonian is unitarily equivalent to $\mathbb{P}_Q(\Lambda' + \Lambda'^\dagger)\mathbb{P}_Q$.

The original, flat, non-zero $2^{L_y/2-1}$ eigenvalues of $\mathbb{P}_Q$ therefore become the non-zero $2^{L_y/2-1}$ eigenvalues of $\exp[-\mathbb{P}_Q(\Lambda' + \Lambda'^\dagger)\mathbb{P}_Q]$, i.e.

$$1 \to \text{eig}(\exp[-\mathbb{P}_Q(\Lambda' + \Lambda'^\dagger)\mathbb{P}_Q]), \tag{5.24}$$

which are near 1 in magnitude. The entanglement spectrum $\xi_{\text{ent.}}$ associated with these eigenvalues is then calculated by taking -1 times the logarithm of the eigenvalues of the reduced density matrix: $\xi_{\text{ent.}} = \text{eig}(\mathbb{P}_Q(\Lambda' + \Lambda'^\dagger)\mathbb{P}_Q)$. Of course, there will be other levels in the entanglement spectrum coming from the sub-dominant part of ρ_L^a, but they 'flow down from infinity', as those $\xi_{\text{ent.}} \sim -\ln(\epsilon) \sim \infty$. These are not the levels of interest and
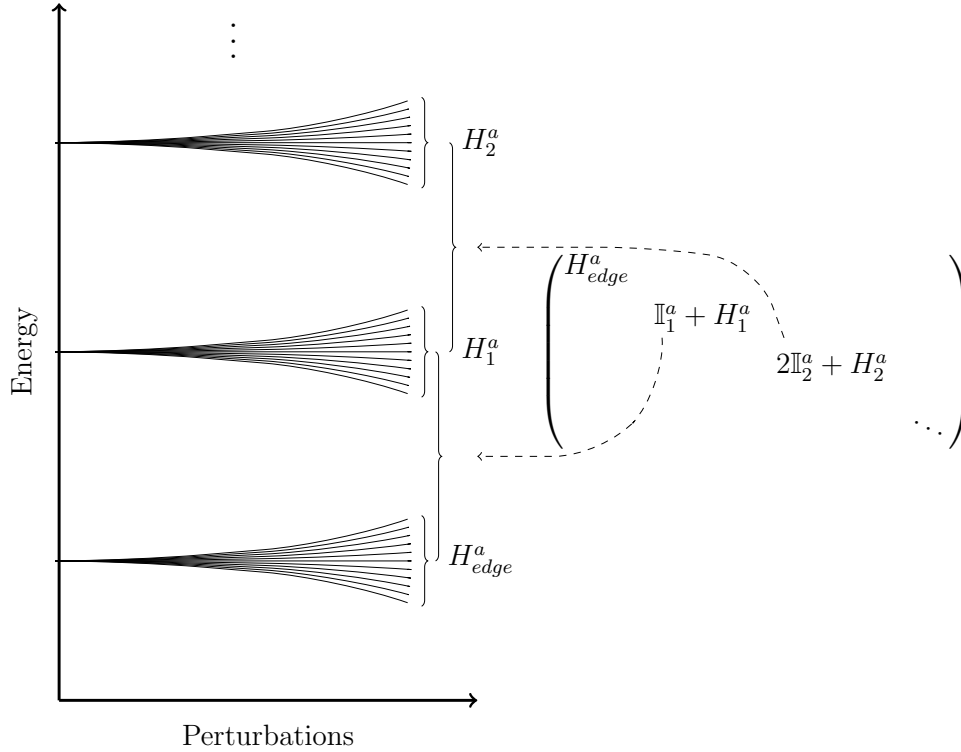
Figure 5.3.1: Illustration of the terms appearing in the first line of eqn. (5.26). The Schrieffer-Wolff transformation rotates the perturbed Hamiltonian into a Hamiltonian that is block diagonal in the old eigenspaces (so that $P_\alpha^a = \mathbb{I}_\alpha^a$), and adds small dynamics due to the perturbation on top of each space ($H_\alpha^a \simeq \mathcal{O}(\epsilon)$).

will therefore be ignored. Thus, we aim to derive only the new eigenvalues of the reduced density matrix that are perturbed from the original *non-zero* values, up to *leading order* corrections. These values are defined to be the ones that give rise to the relevant part of the entanglement spectrum, and are the values of interest when comparing the edge to the ES in the edge-ES correspondence.

Of course, the discussion above was to sketch the flow of the logic of our argument, and we have to be rigorous in our derivation. They key step to solve for the ground states of the perturbed system is to rewrite eqn. (5.11) in a way which makes obtaining the form of eqn. (5.21) manifest - in other words, we want to reorder the perturbative series which gives the tensor product structure automatically. The key is the Schrieffer-Wolff transformation. We can rewrite $H_L + \epsilon V_L$ within each topological sector (letting $a \simeq (\tilde{Q}_L, Q_L)$ also refer to

104

the topological sector on the L semi-infinite cylinder) as:

$$e^{-S_L^a} e^{S_L^a} P_L^a (H_L + \epsilon V_L) P_L^a e^{-S_L^a} e^{S_L^a}, \tag{5.25}$$

where $P_L^a = \sum_{\alpha \geq 0} P_{\alpha,L}^a$, a projector onto the topological sector a. $P_{\alpha,L}^a$ are the projectors onto $\mathcal{V}_{\alpha,L}^a$ (see Sec. 5.2.1). This can be done since local perturbations do not connect topological sectors a at any order in perturbation theory.

The BCH expansion then allows us to expand it as

$$
\begin{aligned}
&e^{-S_L^a}(H_{\text{edge},L}^a + P_{1,L}^a + H_{1,L}^a + 2P_{2,L}^a + H_{2,L}^a + \cdots)e^{S_L^a} \\
&= \underbrace{\sum_{\alpha \geq 1} \alpha P_{\alpha,L}^a}_{\text{large}} + \underbrace{H_{\text{edge},L}^a + \sum_{\alpha \geq 1} H_{\alpha,L}^a + \sum_{\alpha \geq 1}[-S_L^a, \alpha P_{\alpha,L}^a] +}_{\text{small}} \\
&\underbrace{[-S_L^a, H_{\text{edge},L}^a] + \sum_{\alpha \geq 1}[-S_L^a, H_{\alpha,L}^a]}_{\text{small}} \\
&+ \underbrace{\frac{1}{2}\sum_{\alpha \geq 1}[-S_L^a, [-S_L^a, \alpha P_{\alpha,L}^a]]}_{\text{small}} + \cdots,
\end{aligned}
\tag{5.26}
$$

and similarly for the theory on the R semi-infinite cylinder, $H_R + \epsilon V_R$, using $a' \simeq (\tilde{Q}_R, Q_R)$ as the topological sector label. $H_{\alpha,L}^a$ are (at least) order ϵ effective Hamiltonians acting in $\mathcal{V}_{\alpha,L}^a$ that generate the dynamics over $\alpha P_{\alpha,L}^a$ upon the addition of perturbations ϵV_L to the system. All terms labeled 'large' are of order 1, while all terms labeled 'small' are at least of order ϵ. To help illustrate the meaning of the terms that appear in the first line of the equation above between the exponentials, we have schematically plotted the energy spectrum of the Wen-plaquette model under perturbations in Fig. 5.3.1. The Schrieffer-Wolff transformation simply rotates the perturbed Hamiltonian into a Hamiltonian that is block diagonal in the old eigenspaces (so that $P_\alpha^a = \mathbb{I}_\alpha^a$), and adds small dynamics due to the perturbation on top of each space ($H_\alpha^a \simeq \mathcal{O}(\epsilon)$).

Now, we see that $H_0 = H_{LR} + \sum_{\alpha \geq 1} \alpha (\sum_a P_{\alpha,L}^a + \sum_{a'} P_{\alpha,R}^{a'})$ is nothing but the original, unperturbed Wen-plaquette Hamiltonian on the full cylinder [c.f. eqn. (5.4)] whose ground states are given by eqn. (5.7), with $a = a' \equiv (\tilde{Q}, Q)$ (hence justifying the use of a single label a). The small terms in eqn. (5.26) (and similarly for R) can therefore be thought of as perturbations to the large Hamiltonian, H_0, and their corrections to the non-degenerate ground state (within each a sector) can be calculated in normal non-degenerate wavefunction perturbation theory.

Similarly, we can decompose ϵV_{LR} as

$$\epsilon V_{LR} = \epsilon \sum_{\substack{\alpha \geq 0 \\ \tilde{Q}_L, \tilde{Q}_R}} (P_{\alpha,L}^{\tilde{Q}_L} \otimes P_{\alpha,L}^{\tilde{Q}_R}) V_{LR} (P_{\alpha,L}^{\tilde{Q}_L} \otimes P_{\alpha,L}^{\tilde{Q}_R}) \qquad (5.27)$$

because V_{LR} is local and cannot mix different $\tilde{Q}_L$ sectors (and similarly for $\tilde{Q}_R$).

This decomposition allows us to identify the origins of the corrections of Λ, Θ, Ξ and Ω, at least to the first order process to the corrections to the ground states, eqn. (5.7). For a fixed topological sector a, standard non-degenerate wavefunction perturbation theory tells us to correct the ground states in the first order process as

$$|\tilde{Q}, Q\rangle = |\tilde{Q}, Q\rangle_0 + \sum_{\text{exc.}} \frac{\langle \text{exc.}|O_{\text{small}}|\tilde{Q}, Q\rangle_0}{\Delta E} |\text{exc.}\rangle, \qquad (5.28)$$

where O_{small} are small corrections to the unperturbed Hamiltonian, $|\text{exc.}\rangle$ excited eigenstates of the exact Wen-plaquette model, and ΔE the energy difference of the excited and ground states, which is always negative.

Thus we see that since $H_{\text{edge},L}^a + H_{\text{edge},R}^a : \mathcal{V}_{0,L}^a \otimes \mathcal{V}_{0,R}^a \to \mathcal{V}_{0,L}^a \otimes \mathcal{V}_{0,R}^a$, it gives rise to part of the correction Λ. The other correction in Λ comes from $(P_{0,L}^{\tilde{Q}} \otimes P_{0,R}^{\tilde{Q}}) V_{LR} (P_{0,L}^{\tilde{Q}} \otimes P_{0,R}^{\tilde{Q}})$. Furthermore, both terms which contribute are symmetric under the $\mathbb{Z}_2$ generators $\hat{Q}_L$ and $\hat{Q}_R$ and so do not mix the Q_L and Q_R topological sectors. Together, Λ must be therefore Q symmetric, i.e. $\Lambda = \mathbb{P}_Q \Lambda' \mathbb{P}_Q$, for some Λ', as claimed. The exact derivation of Λ' is left to Appendix 5.B. It turns out that Λ' is a Hermitian matrix, so that $\Lambda' = \Lambda'^\dagger$.

Next, since S_L^a is block diagonal, $[-S_L^a, nP_{n,L}^a] : \mathcal{V}_{0,L}^a \otimes \mathcal{V}_{0,R}^a \to \mathcal{V}_{n,L}^a \otimes \mathcal{V}_{0,R}^a$, and generates Ξ (the R equivalent generates Θ). Similarly, other terms in the decomposition of V_{LR} also contribute to Θ, Ξ and Ω.

Obviously, it is impossible to compute corrections to the ground state exactly for arbitrary local perturbations. However, it is still possible to say something concrete for generic arbitrary perturbations. In general, Λ is of order ϵ. We can then ignore Θ and Ξ as they give rise to ϵ^2 corrections in the eigenvalues of the reduced density matrix. Since we are only concerned about corrections to the ground state which give the leading order corrections to the entanglement energies (which are order ϵ from Λ), we only need to keep corrections in the dominant part of the reduced density matrix. The perturbed wavefunction, considered to leading order, is then

$$|\tilde{Q}, Q\rangle = \frac{1}{\sqrt{Z}} \sum_{\tau', \tau} (\mathbb{P}_Q - \mathbb{P}_Q \Lambda' \mathbb{P}_Q)_{\tau', \tau} |\tau'\rangle_L |\tau\rangle_R, \qquad (5.29)$$

Z being a normalization factor. The reduced density matrix to leading order is then given by eqn. (5.23),

$$\begin{aligned} \rho_L^a &\equiv \frac{1}{Z} \exp\left[-H_{\text{ent.}}^a\right] = \text{Tr}_R |\tilde{Q}, Q\rangle\langle\tilde{Q}, Q| \\ &\approx \frac{1}{Z}\left(\mathbb{P}_Q - 2\mathbb{P}_Q\Lambda'\mathbb{P}_Q\right) \\ &\approx \frac{1}{Z}\exp\left[-2\mathbb{P}_Q\Lambda'\mathbb{P}_Q\right], \end{aligned} \tag{5.30}$$

leading to the identification

$$H_{\text{ent.}}^a \equiv 2\mathbb{P}_Q\Lambda'\mathbb{P}_Q. \tag{5.31}$$

The entanglement spectrum, $\xi_{\text{ent.}}^a$, is given by

$$(\xi_{\text{ent.}}^a)_n = 2\text{eig}(\mathbb{P}_Q\Lambda'\mathbb{P}_Q)_n \tag{5.32}$$

where $n = 1, 2, \cdots, 2^{L_y/2-1}$ label the eigenvalues of eigenvectors that have $\mathbb{P}_Q = 1$.

To conclude:

• The entanglement Hamiltonian, $H_{\text{ent.}}^a$, generically appearing at order ϵ, is given by eqn. (5.31), where Λ' is generated at lowest order by $H_{\text{edge},L}^a + H_{\text{edge},R}^a$ and V_{LR} (see Appendix 5.B). It is $\mathbb{Z}_2$ symmetric and acts on a virtual spin chain of $L_y/2$ sites, similar to the edge Hamiltonians.

5.3.4 Edge-ES correspondence

From the calculation of Λ' in Appendix 5.B and eqn. (5.32), we see that within each topological sector a, the edge Hamiltonian $H_{\text{edge},L}^a + H_{\text{edge},R}^a$ and the entanglement Hamiltonian $H_{\text{ent.}}^a$ differ from each other in two ways: (i) terms in the edge Hamiltonian are reproduced in the entanglement Hamiltonian but with term-dependent rescaling factors, and (ii) additional terms arising from V_{LR} appear in the entanglement Hamiltonian. Since this means that $H_{\text{edge},L}^a + H_{\text{edge},R}^a$ and $H_{\text{ent.}}^a$ can differ in a potentially arbitrary fashion, there is no reason to expect that the edge spectrum will match the entanglement spectrum, even for the low energy values. We therefore conclude that there is no edge-ES correspondence in general.

However, we note that both Hamiltonians have remarkably similar structure: they both act on a spin-1/2 chain of length $L_y/2$, and are $\mathbb{Z}_2$ invariant, i.e. they commute with the

global spin flip operator $\prod_i \tau_i^x$, which is the Wilson loop operator in the bulk. The $\mathbb{Z}_2$ symmetry can therefore be understood as being enforced by the bulk topological order.

To summarize:

- There is no edge-ES correspondence, even in the low energy limit, for generic local perturbations. However, both the edge and entanglement Hamiltonians are $\mathbb{Z}_2$ symmetric and act on a virtual spin chain of $L_y/2$ sites.

5.3.5   Remarks

One might ask: what happens if Λ appears at order ϵ^n, $n \geq 2$ instead of at order ϵ? Of course, this situation is a result of fine-tuning the perturbations to the system. For example, perturbing the Wen-plaquette model with only single-site magnetic fields (so that $V_{LR} = 0$) will yield an edge Hamiltonian at order ϵ^2, and therefore Λ at order ϵ^2 as well. One has to now account for the additional contributions from Θ, Ξ in eqn. (5.21) as they will lead to ϵ^2 corrections in the dominant part of the reduced density matrix, thereby potentially modifying the entanglement spectrum.

However, the procedure to account for these additional contributions is clear: we simply perform non-degenerate wavefunction perturbation theory on $|\tilde{Q}, Q\rangle$ to a desired order consistently in the reduced density matrix, using the decomposition eqn. (5.26) and eqn. (5.27).

An explicit example showing how this is done is given in the next section (also refer to appendix 5.C), where we consider a mechanism to achieve an edge-ES correspondence in the low energy limit. We look at the case of uniform single-site magnetic fields as perturbations and present the perturbative calculations to order ϵ^2 explicitly. In that case, we will see that the terms Θ, Ξ simply lead to a constant shift in the entanglement energies of the entanglement spectrum, and so the relation that $H_{\text{ent.}}^a \equiv 2\mathbb{P}_Q \Lambda' \mathbb{P}_Q$ still holds up to a constant shift.

5.4   Mechanism for correspondence: Translational symmetry and Kramers-Wannier duality

In this section, we present a mechanism that ensures an edge-ES correspondence, at least in a finite domain in Hamiltonian space. We consider the Wen-plaquette model as a symmetry

enriched topological phase (SET) with the global symmetry being translational invariance along the edge/entanglement cut. That is, we restrict ourselves to perturbations that are translationally invariant along the width of the cylinder. In that case, both the edge and entanglement Hamiltonians will be Kramers-Wannier (KW) self-dual.

It is not difficult to understand why this is so for the edge Hamiltonian. For the Wen-plaquette model and for an even L_y cylinder, we have assigned a consistent checkerboard coloring of the plaquettes (see Fig. 5.2.1), in which e quasiparticles live on one color and m quasiparticles live on the other color. However, this coloring is not unique, and we could have swapped the two colors, effectively exchanging $e \leftrightarrow m$ quasiparticles, a so-called electromagnetic duality. One can check that the fusion rules obeyed by the anyons are invariant under this swap. This swap can also be thought of being effected by simplying translating the Wen-plaquette model by one site around the circumference of the cylinder, while keeping the underlying checkerboard coloring.

In terms of boundary operators, one sees that this swaps $S_{p,L}$ with $S_{\tilde{p},L}$, which necessarily leaves the physics of the edge or entanglement Hamiltonian invariant. However, recall that in the spin chain language $S_{p,L} \simeq \tau^x_{\tilde{p},L}$ with $S_{\tilde{p},L} \simeq \tau^z_{\tilde{p},L}\tau^z_{\tilde{p}-1,L}$. These two operators are precisely the Kramers-Wannier duals of each other. Translation by one site in the Wen-plaquette model thereby effects a KW transformation in the spin chain.

Thus, if we restrict to translationally invariant perturbations, then a term that appears in the edge Hamiltonian must also have its Kramers-Wannier dual appear in the edge Hamiltonian with the same coefficient, since $S_p \leftrightarrow S_{\tilde{p}}$ leaves the physics invariant. Thus, the edge Hamiltonian is Kramers-Wannier self-dual. It also follows that Λ, and therefore the entanglement Hamiltonian is also Kramers-Wannier self-dual, as claimed.

Let us now analyze the edge and entanglement Hamiltonians in different $\tilde{Q}$ sectors, $H^{\tilde{Q}}_{\text{edge}}$ and $H^{\tilde{Q}}_{\text{ent.}} = 2\Lambda'$, respectively. These are local, Kramers-Wannier self-dual, $\mathbb{Z}_2$ symmetric Hamiltonians on a finite length spin chain, with $\tilde{Q}$ giving the boundary conditions: $\tilde{Q} = +1$ corresponds to periodic boundary conditions and $\tilde{Q} = -1$ to anti-periodic boundary conditions. We claim that these Hamiltonians must be sitting at a phase transition.

First we argue the following. *Let us be given a local gapped $\mathbb{Z}_2$ symmetric spin Hamiltonian acting on an infinite spin chain. Let us assume that it spontaneously breaks the $\mathbb{Z}_2$ symmetry. Its Kramers-Wannier dual is another local gapped Hamiltonian which does not break spontaneously the dual $\mathbb{Z}_2$ symmetry. The reverse is true if the original Hamiltonian does not break the $\mathbb{Z}_2$ symmetry; then, its KW dual will spontaneously break the dual $\mathbb{Z}_2$ symmetry* .

The proof goes as follows. Consider the Hamiltonian on a finite spin chain. Since it is

$\mathbb{Z}_2$ symmetric, it must be a function of τ_i^x and $\tau_i^z \tau_{i+1}^z$ only. The Hilbert space associated with this spin chain be be split into the ± 1 eigenvalues of the $\mathbb{Z}_2$ symmetry which is effected by the global spin-flip operator $\mathcal{S} \equiv \prod_i \tau_i^x$. We also have to assign boundary conditions, of which there are two kinds: periodic bondary conditions (PBC) and anti-periodic boundary conditions (APBC). Defining $\mathcal{T} \equiv \prod_i \tau_i^z \tau_{i+1}^z$ gives us $\mathcal{T} = +1$ for PBC and $\mathcal{T} = -1$ for APBC. We can consider a mapping between this quantum system and another quantum system whose Hilbert space comprises of spins (labeled by $i+\frac{1}{2}$) placed on the links (labeled by $(i, i + 1)$) of the original spin chain, i.e. a dual spin chain. Clearly, the two Hilbert spaces' dimensions are equal. Then, we can write down a dual Hamiltonian with the same spectrum as the original Hamiltonian, with the identification that the dual Hamiltonian is formed from the old Hamiltonian with $\tilde{\tau}_{i+\frac{1}{2}}^x \equiv \tau_i^z \tau_{i+1}^z$ and $\tilde{\tau}_{i-\frac{1}{2}}^z \tilde{\tau}_{i+\frac{1}{2}}^z \equiv \tau_i^x$. This works because the new operators defined above give a representation of the algebra of the old set of operators. We see that this is nothing but the Kramers-Wannier transformation.

However, note that the KW transformation maps $\mathcal{T} \leftrightarrow \tilde{\mathcal{S}}$ and $\mathcal{S} \leftrightarrow \tilde{\mathcal{T}}$, where $\tilde{\mathcal{S}}$ is the dual $\mathbb{Z}_2$ symmetry generator $\prod_i \tilde{\tau}_i^x$ and $\tilde{\mathcal{T}}$ the dual boundary condition selector $\prod_i \tilde{\tau}_i^z \tilde{\tau}_{i+1}^z$. Now, if we assume that the original Hamiltonian with $\mathcal{T} = +1$ spontaneously breaks the $\mathbb{Z}_2$ symmetry $\mathcal{S}$, then it has two ground states that can be labeled by $\mathcal{S} = \pm 1$ which are close in energy. The order at which the ground state degeneracy is broken is at order e^{-mL} for some mass scale m. Conversely, the Hamiltonian with $\mathcal{T} = -1$ will have a ground state with a domain wall between the above two vacua, and will thus have higher energy than the ground states on the system with $\mathcal{T} = +1$, with an energy difference on the order of the mass gap. On the other hand, for a $\mathbb{Z}_2$ preserving theory on $\mathcal{T} = \pm 1$, then there will only be a single ground state with $\mathcal{S} = +1$. The difference in energies of these ground states with $\mathcal{T} = \pm 1$ will be exponentially small.

Now, let us take the limit as the length of the chain becomes infinite. In this limit, the boundary conditions do not matter, and we should only consider sectors with different $\mathcal{S}$ of the original Hilbert space and different $\tilde{\mathcal{S}}$ of the dual Hilbert space. From our exposition above, if the original Hamiltonian breaks the $\mathbb{Z}_2$ symmetry, then it will have two degenerate ground states labeled by $\mathcal{S} = \pm 1$ with some energy E. However, after the KW transformation, the dual Hamiltonian will now have only one state near E (it has $\tilde{\mathcal{S}} = +1$) - all other states have higher energies, with an energy difference of at least the mass gap. Thus we see that the dual Hamiltonian does not break the dual $\mathbb{Z}_2$ symmetry. Similarly, if the original Hamiltonian does not break the $\mathbb{Z}_2$ symmetry, it has only one state with $\mathcal{S} = +1$ that has lowest energy E'; all other states are separated in energy by the mass gap. However, its dual Hamiltonian will have two states near energy E', with $\tilde{\mathcal{S}} = \pm 1$. Thus, we see that the dual Hamiltonian spontaneously breaks the dual $\mathbb{Z}_2$ symmetry. This thereby concludes the proof of our claim.

Next, let us be given a Kramers-Wannier $\mathbb{Z}_2$ symmetric self-dual Hamiltonian H_0, and deform it by a small $\mathbb{Z}_2$ symmetric perturbation H_1 which is odd under KW duality:

$$H = H_0 + hH_1, \tag{5.33}$$

where a KW transformation maps $h \to -h$. If the deformed Hamiltonian H is gapped and breaks the $\mathbb{Z}_2$ symmetric spontaneously for some sign of h, it will not break it for the opposite sign, and viceversa. Thus the theory must have a phase transition at $h = 0$! This therefore concludes the proof that $H_{\text{edge}}^{\tilde{Q}}$ and $H_{\text{ent.}}^{\tilde{Q}}$ must be sitting at a phase transition.

Furthermore, it is natural to expect the phase transition to be generically of second order. If that was the case, the KW self-dual Hamiltonians would be gapless (i.e. critical). Now, a stronger statement can be made: if the dominant part of $H_{\text{edge}}^{\tilde{Q}}$ and $H_{\text{ent.}}^{\tilde{Q}}$ are the transverse field Ising model $((1 + 1)$-d Ising model), then the low energy spectra of both Hamiltonians must be that of the $c = 1/2$ Ising CFT. This is guaranteed because there are no relevant deformations to the critical $(1 + 1)$-d Ising model that are both $\mathbb{Z}_2$ invariant and KW-even. To see this is true, list all relevant operators in the theory (i.e. with scaling dimension $\Delta < 2$): the spin primary field σ and the energy density primary field ϵ. Now σ is $\mathbb{Z}_2$ even, so this deformation does not appear in the edge and entanglement Hamiltonians. On the other hand, ϵ is $\mathbb{Z}_2$ even but is KW-odd, so it cannot appear either. Any deformations in the edge and entanglement Hamiltonians must therefore be irrelevant - all renormalization flows are towards the $c = 1/2$ Ising CFT.

This therefore shows that there is a finite domain in Hamiltonian space such that the edge and entanglement Hamiltonians both realize the $c = 1/2$ Ising CFT as their low energy effective theory. It is therefore seen that in this case, the Wen-plaquette model, considered as an SET with the global symmetry being translational invariance along the edge/entanglement cut, realizes an edge-ES correspondence: the low lying values of both the edge and entanglement spectra will match.

However, a note of caution should be pointed out here. There is no guarantee that the edge and entanglement Hamiltonians will be both near the critical $(1 + 1)$-d Ising models, even though it is natural to assume they should be. There are other models which are also $\mathbb{Z}_2$ symmetric and Kramers-Wannier self-dual, such as the tricritical Ising model or even $\mathbb{Z}_2$ symmetric Hamiltonians which break the KW-duality spontaneously (i.e. the model realizes a first order transition, which the critical Ising model and tricritical Ising model do not).

Thus, one cannot conclude that the edge and entanglement Hamiltonians must *both* be the $c = 1/2$ Ising CFT. For example, it could be that the edge Hamiltonian is a critical

Ising model while the entanglement Hamiltonian is instead a tricritical Ising model. In that case, there is no edge-ES correspondence in the way that we have defined, as the low energy spectra clearly do not match. However, what is still guaranteed with the global translational symmetry is that both the edge and entanglement Hamiltonians will be $\mathbb{Z}_2$ symmetric and Kramers-Wannier dual; thus, a weaker form of edge-ES correspondence holds in which both Hamiltonians belong to the same *class* of Hamiltonians, whether or not the specific form of the Hamiltonian is the critical Ising, tricritical Ising, or a first order phase transition Hamiltonian.

In summary:

• Considered as an SET, the symmetry protection (translational invariant perturbations) and the bulk topological order ensure that the edge and entanglement Hamiltonians of the Wen-plaquette model are Kramers-Wannier self-dual and are $\mathbb{Z}_2$ symmetric. If both theories are close to the critical $(1+1)$-d Ising model, then since there are no relevant KW-even and $\mathbb{Z}_2$ symmetric perturbations to the model, this implies that there is a finite domain in Hamiltonian space in which their low energy physics is a $c = 1/2$ Ising CFT. There is, therefore, an edge-ES correspondence in such a scenario (the low energy spectra match). However, there is no guarantee that both Hamiltonians will always be critical Ising models, as there are other $\mathbb{Z}_2$ symmetric models which realize the Kramers-Wannier self-duality, such as the tricritical Ising model or a Hamiltonian sitting at a first order phase transition. Thus, a weaker form of the edge-ES correspondence instead holds, in which both the edge and entanglement Hamiltonians belong to the same class of Kramers-Wannier even and $\mathbb{Z}_2$ symmetric Hamiltonians.

5.4.1 Analytical example: uniform single-site magnetic fields

We present an analytic and numerical illustration of our claim of the edge-ES correspondence, in which both the edge and entanglement Hamiltonians realize the critical $(1+1)$-d Ising models and thus have the $c = 1/2$ Ising CFT as their low energy effective theory. Let us consider the case of perturbations being uniform single-site magnetic fields:

$$\epsilon V = \epsilon \sum_i h_X X_i + h_Y Y_i + h_Z Z_i, \tag{5.34}$$

where (h_X, h_Y, h_Z) is a vector with entries of order 1. This perturbation is translationally invariant along the edge/cut of the cylinder. On physical grounds it is the simplest possible local perturbation of the toric code, and on theoretical grounds, it is the deformation of

the Toric code that is the most well studied, see existing literature on the subject, e.g. Ref. [203, 204, 205].

Such a uniform single-site magnetic field generates an edge and entanglement Hamiltonian with the critical $(1+1)$-d Ising model as their dominant term at order ϵ^2: eqn. (5.19) (Appendix 5.C.1 gives the detailed calculations) tells us that the edge Hamiltonians of each topological sector are the critical periodic ($\tilde{Q} = +1$) /antiperiodic ($\tilde{Q} = -1$) transverse field Ising Hamiltonians projected into the $\mathbb{Z}_2$ sectors ($Q = \pm 1$). Explicitly, the critical $(1+1)$-d Ising model on a spin chain of length $\tilde{L}_y/2$, also called the transverse field Ising model (TFIM), is given by

$$H_{\text{TFIM}}^{\tilde{Q}} = -\sum_{\tilde{p}=1}^{\tilde{L}_y/2} \left(\tau_{\tilde{p}}^z \tau_{\tilde{p}-1}^z + \tau_{\tilde{p}}^x \right), \tag{5.35}$$

with toroidal boundary conditions $\tau_0 = \tilde{Q}\tau_{\tilde{L}_y/2}$, and its decomposition into its $\mathbb{Z}_2$ charge sectors as follows:

$$H_{\text{TFIM},Q}^{\tilde{Q}} \equiv \mathbb{P}_Q H_{\text{TFIM}}^{\tilde{Q}} \mathbb{P}_Q, \tag{5.36}$$

where $\mathbb{P}_Q = \prod_{\tilde{p}=1}^{\tilde{L}_y/2} \tau_{\tilde{p}}^x$. This model is the *lattice realization* of the $c = 1/2$ Ising CFT.

On the other hand, for the entanglement Hamiltonians (refer to Appendix 5.C.2 for the calculation of the entanglement Hamiltonians), up to rescaling and shifting, we have the following identification between states in the topological phase (left) and their entanglement Hamiltonians to leading order (ϵ^2) (right):

$$\begin{aligned} |\mathbb{0}\rangle &\leftrightarrow H_{\text{TFIM},+1}^{+1}, \\ |e\rangle &\leftrightarrow H_{\text{TFIM},-1}^{+1}, \\ |m\rangle &\leftrightarrow H_{\text{TFIM},+1}^{-1}, \\ |\varepsilon\rangle &\leftrightarrow H_{\text{TFIM},-1}^{-1}, \end{aligned} \tag{5.37}$$

where the label $\{\mathbb{0}, e, m, \varepsilon = e \times m\}$ indicates that the states carry the corresponding anyonic flux.

Thus, we see that there is an edge-ES correspondence in this case: both the edge and entanglement Hamiltonians have the $c = 1/2$ Ising CFT as their low energy effective theory.

5.4.2 Numerical example: uniform single-site magnetic fields

To check our predictions, we numerically solve for the ground states of the Wen-plaquette model on an infinite cylinder with even L_y sites on its circumference, $L_y = 20$, with
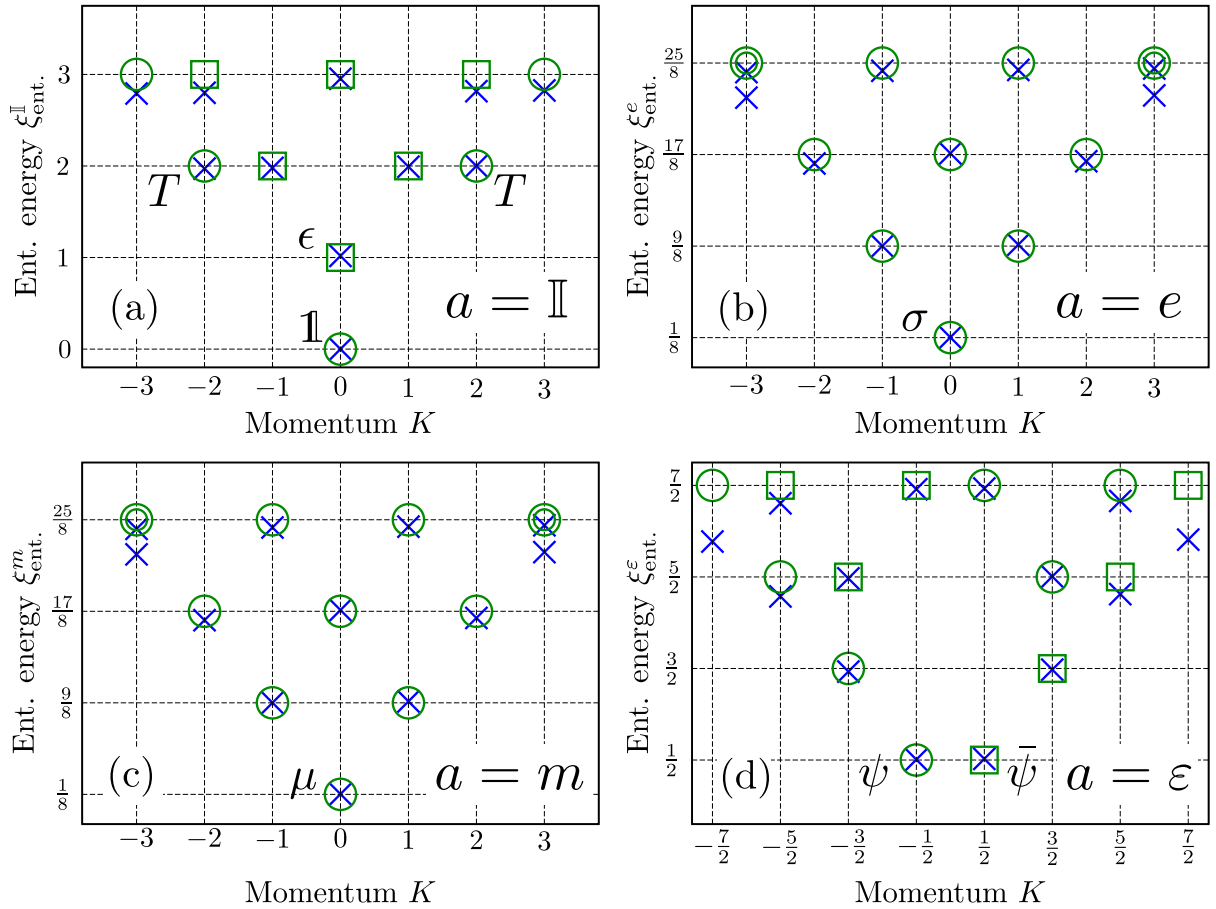
Figure 5.4.1: Rescaled and shifted entanglement spectra in each topological sector a for Wen-plaquette model on an $L_y = 20$ (even), infinite cylinder, for $\epsilon h_X = -0.01$, $\epsilon h_Y = -0.015$ and $\epsilon h_Z = -0.02$. The data points are marked by blue crosses. We have also plotted the $c = 1/2$ Ising CFT spectra in each sector for comparison (scaling dim. versus momenta), with the identification that entanglement energy equals scaling dimension. They are given by the green squares and circles. Squares and circles represent conformal towers labeled by different primaries at the bottom of the towers, and double circles denote two-fold degenerate states. (a) The ES of the ground state $|\tilde{\mathbb{1}}\rangle$ with the identity anyonic flux through the cylinder. This corresponds to the $(\tilde{Q}, Q) = (+1, +1)$ sector of the TFIM, whose low energy effective theory is the $c = 1/2$ Ising CFT in the sector that the identity primary $\mathbb{1}$ & its descendants (green circles), and energy density primary ϵ & its descendants (green squares) belong to. The two points labeled T are the holomorphic and antiholomorphic stress-energy tensors. (b) ES of $|e\rangle$, the state with the electric anyonic flux. This gives the $(\tilde{Q}, Q) = (+1, -1)$ sector of the TFIM. This corresponds to the sector of Ising CFT which the spin primary σ and its descendants belong to (green circles). (c) ES of $|m\rangle$, the state with the magnetic anyonic flux. This gives the $(\tilde{Q}, Q) = (-1, +1)$ sector of the TFIM, which in turn corresponds to the sector of the Ising CFT (with a D_ϵ defect insertion[206, 207, 208]) which the disorder primary μ and its descendants belong to (green circles). The spectra of the conformal families from σ and μ conincide, and so do the entanglement spectra. (d) ES of $|\varepsilon\rangle$, the state with the fermionic anyonic flux. This gives the $(\tilde{Q}, Q) = (-1, -1)$ sector of the TFIM. This corresponds to the sector of the Ising CFT (with a D_ϵ defect insertion) which the two Majorana fermion primaries $\psi, \bar{\psi}$ and their descendants belong to (green squares and circles).
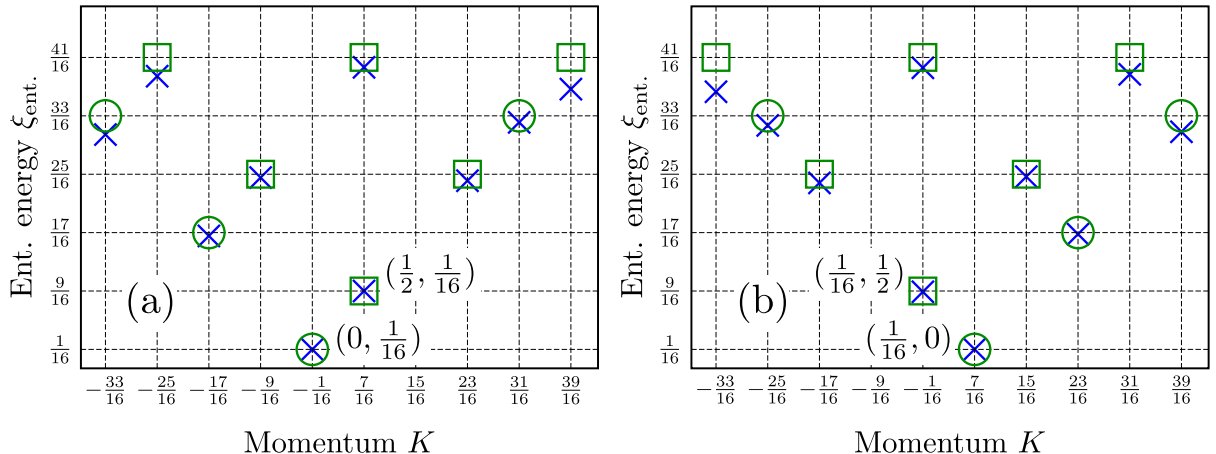
114

Figure 5.4.2: Rescaled and shifted entanglement spectra in each topological sector for the perturbed Wen-plaquette model on an $L_y = 19$ (odd), infinite cylinder. Shown also are the $c = 1/2$ CFT spectra with a conformal duality defect D_σ (see Fig. 5.4.1 for details on labels). (a) The ES corresponds to the spectrum of the duality-twisted Ising model with primary fields $(0, 1/16), (1/2, 1/16)$. (b) The ES corresponds to the spectrum of the duality-twisted Ising model with primary fields $(1/16, 0), (1/16, 1/2)$.

perturbations of the form eqn. (5.34), using DMRG for infinite cylinders[209, 107]. Here, $\epsilon h_X = -0.01$, $\epsilon h_Y = -0.015$ and $\epsilon h_Z = -0.02$. Starting from a random initialization of the MPS, it was found that the DMRG algorithm converged to four orthonormal states, which are the four ground states with well-defined anyonic flux through the cylinder. We then find the entanglement spectrum associated with each ground state, and plot it against momenta around the cylinder. Figure 5.4.1 shows the entanglement spectra in each topological sector a of the Wen-plaquette model with the parameters described above.

Each spectrum has been (i) shifted and then (ii) rescaled by the same value across all topological sectors a. The shift has been chosen so that the lowest entanglement energy across all entanglement spectra is at entanglement energy 0, and the rescaling chosen so that in the topological sector which contains the lowest overall entanglement energy, the lowest entanglement energy at momentum $K = \pm 2$ is at entanglement energy 2. In doing so, we fix the identity primary (scaling dimension $\Delta = 0$, momentum $K = 0$) and the holomorphic and antiholomorphic stress-energy tensors (scaling dimension $\Delta = 2$, momentum $K = \pm 2$), which are always present in a CFT without defects. Remarkably, this common shift and rescaling of the entanglement spectra across topological sectors a reproduces the $c = 1/2$ Ising CFT spectra in the different charge sectors accurately; from Fig. 5.4.1(a), we can identify the identity primary $\mathbb{1}$ [conformal weights $(h, \bar{h}) = (0, 0)$] and the energy-density primary $\epsilon \sim (1/2, 1/2)$ with its descendants, which belong to the $(\tilde{Q}, Q) = (+1, +1)$ charge sector of the TFIM. In the CFT language this is the $\mathbb{Z}_2 = +1$ sector of the usual diagonal

115

$c = 1/2$ Ising CFT. From Fig. 5.4.1(b), we identify the spin primary $\sigma \sim (1/16, 1/16)$ with its descendants, which belong to the $(\tilde{Q}, Q) = (+1, -1)$ sector of the TFIM. This corresponds to the $\mathbb{Z}_2 = -1$ sector of the Ising CFT. From Fig. 5.4.1(c), we identify the disorder primary $\mu \sim (1/16, 1/16)$ with its descendants, which is identical to the spectrum of σ, belonging to the $(\tilde{Q}, Q) = (-1, +1)$ sector of the TFIM. In this case, this corresponds to the $\mathbb{Z}_2 = +1$ sector of $c = 1/2$ Ising CFT with anti-periodic boundary conditions. Lastly, we identify the Majorana fermions $\psi \sim (1/2, 0)$ and $\bar{\psi} \sim (0, 1/2)$ and its descendants which belong to the $(\tilde{Q}, Q) = (-1, -1)$ sector of the TFIM. This corresponds to the $\mathbb{Z} = -1$ sector of the Ising CFT with anti-periodic boundary conditions. This is in agreement with the theoretical prediction from our calculation, eqn. (5.37).

Lastly, even though our analysis in this chapter was restricted to the Wen-plaquette model on an infinite cylinder with even L_y circumference, we numerically solve for the ground states of the perturbed Wen-plaquette model on an infinite cylinder with odd L_y circumference. The perturbation is as before, eqn. (5.34), with values as in the even cylinder case. We take $L_y = 19$. In this case, a consistent checkerboard coloring of the plaquettes cannot be done. If one insists on placing a checkerboard coloring on the cylinder, there is necessarily a line of topological defects where an e quasiparticle (as measured locally) transmutes into an m quasiparticle upon crossing the line defect[210].

In this case, we obtain two ground states. This makes sense as the only Wilson loop operator that exists is a string that wraps around the cylinder twice. The two ground states can be taken to be eigenvectors of this Wilson loop operator. Figure 5.4.2 shows the plots of the entanglement energies against momenta along a $L_y = 19$ cylinder for both ground states, with a common shifting and rescaling as follows. We shift the spectra of the two ground states so that the lowest entanglement energy of one sector is at $1/16$, and we rescale both ES so that the next lowest entanglement energy in that sector is at $9/16$. The two ES exactly match the spectrum of the boundary theory computed directly using perturbation theory

$$H_\pm = -\left(\sum_{i=1}^{N-1} \tau_i^x + \sum_{i=1}^{N-1} \tau_i^z \tau_{i+1}^z \pm \tau_N^y \tau_1^z \right), \tag{5.38}$$

with $N = \frac{L_y+1}{2}$, which is the Ising model with *duality-twisted* boundary conditions[211]. We see that H_+ and H_- are related by complex conjugation, thus they have the same energy spectrum but with opposite momenta which can also be seen from the numerical data. Figure 5.4.2(a) shows the ES which corresponds to the spectrum of the duality-twisted Ising model with primary fields $(0, 1/16), (1/2, 1/16)$, while figure 5.4.2(b) shows the ES which corresponds to the spectrum of the duality-twisted Ising model with primary fields $(1/16, 0), (1/16, 1/2)$.

All these results can be understood from a CFT point-of-view, using the language of conformal defects. The $c = 1/2$ Ising CFT can be given different twisted boundary conditions by insertions of conformal defect lines X, where the spectrum is then given by the *generalized twisted partition function*[206] $Z_X = \text{tr}\left(X\, q^{L_0-c/24} q^{\bar{L}_0-c/24}\right)$. In order to be able to move the defects around without energy cost, we need X to commute with the energy-momentum tensor, or equivalently $[L_n, X] = [\bar{L}_n, X] = 0$ where L_n and $\bar{L}_n$ are the Virasoro algebra generators. The conformal defects are then classified by representations of the Virasoro algebra, for the $c = 1/2$ CFT we have three defects: $D_{\mathbb{1}}$, D_ϵ and D_σ. Crossing the D_ϵ defect σ goes to $-\sigma$ and it thus implement anti-periodic boundary conditions, while for D_σ we have $\sigma \to \mu$ which is nothing but the Kramers-Wannier duality. The spectra with these defect insertions are given by[206, 207, 208]

$$
\begin{aligned}
Z_{\mathbb{1}} &= |\chi_0|^2 + |\chi_{\frac{1}{2}}|^2 + |\chi_{\frac{1}{16}}|^2, \\
Z_\epsilon &= |\chi_{\frac{1}{16}}|^2 + \chi_0 \bar{\chi}_{\frac{1}{2}} + \chi_{\frac{1}{2}} \bar{\chi}_0, \\
Z_\sigma &= (\chi_0 + \chi_{\frac{1}{2}})\bar{\chi}_{\frac{1}{16}} + \chi_{\frac{1}{16}}(\bar{\chi}_0 + \bar{\chi}_{\frac{1}{2}}).
\end{aligned}
\tag{5.39}
$$

The spectra in Fig. 5.4.1(a) and 5.4.1(b) correspond to the insertion of the trivial (identity) conformal defect $D_{\mathbb{1}}$ in the partition function, while the spectra in Figs. 5.4.1(c) and 5.4.1(d) correspond to the insertion of the conformal epsilon defect D_ϵ. These two cases are distinguished by the absence and presence of a Wilson flux line in the ground states of the bulk respectively, as measured by ⟨. This Wilson flux line terminates at the boundary and is responsible for implementing anti-periodic BC, and thus can be thought of as 'inserting' the conformal defect D_ϵ which has the same function. Next, the spectra in Fig. 5.4.2 correspond to the insertion of the conformal duality defect D_σ in the partition function. This duality defect is nothing but the endpoint of the topological line defect in the bulk which comes from electro-magnetic duality. Thus this is completely consistent with the following correspondence between bulk and boundary: *electro-magnetic duality ↔ Kramers-Wannier duality*, as seen several times in this chapter. Perhaps this hints that one can understand defects in a CFT as arising from defects in a topological phase of one higher dimension, which has the CFT as its boundary theory[212]?

Lastly, if one can find a mechanism to protect the edge-ES correspondence in such cases, then one can construct lattice realizations of CFTs with defects, by constructing the low-energy effective edge Hamiltonian using the Schrieffer-Wolff transformation and identifying a mapping from boundary operators acting in the bulk to local operators acting on some effective low-energy degrees of freedom. In particular, for the case of the Wen-plaquette model on the odd cylinder, we find by direct perturbative calculations the lattice realization of a duality-twisted Ising model, which was only written down very recently by Ref. [211],

eqn. (5.38).

5.5   Conclusion and discussion

In this chapter, we have studied the edge-ES correspondence in a non-chiral topological phase, specifically concentrating on a phase with $\mathbb{Z}_2$ topological order, the Wen-plaquette model on an infinite cylinder. The main result of this chapter is a detailed, microscopic calculation of both the edge and entanglement Hamiltonians, which exhibits the mechanism for the absence or presence of the correspondence. We find through our calculation that the correspondence, i.e., that the edge and entanglement spectra agree in the low energy limit up to rescaling and shifting, is exact for the unperturbed Wen-plaquette model. However, for generic local perturbations, there is no edge-ES correspondence.

We have managed to identify a mechanism to establish the edge-ES correspondence though, by considering the Wen-plaquette model as a SET with the global symmetry being translational invariance along the edge/entanglement cut. That is, if we deform the Wen-plaquette model by perturbations that are restricted to be invariant under translation by one site along the edge/cut, then both the edge and entanglement Hamiltonians are Kramers-Wannier self-dual. There is then a finite domain in Hamiltonian space such that both the edge and entanglement Hamiltonians have the $c = 1/2$ Ising CFT as their low energy effective theory, as there are no KW-even and $\mathbb{Z}_2$ symmetric perturbations to the critical $(1 + 1)$-d Ising model that are relevant. Thus, the edge-ES correspondence is achieved in such a scenario. However, there is no guarantee that both the edge and entanglement Hamiltonians will be near the critical Ising models, as there are other models which are Kramers-Wannier even and $\mathbb{Z}_2$ symmetric as well. Thus, a weaker form of the edge-ES correspondence holds, in which both Hamiltonians belong to the same class of Hamiltonians, even though the low energy spectra do not match.

Our approach of deriving an effective spin ladder Hamiltonian spanning the entanglement cut can potentially be extended to prove some form of the edge-ES correspondence in other non-chiral topological phases that are defined by a fixed point Hamiltonian consisting of a sum of mutually commuting local terms. One would have to find a set of maximally commuting operators on one half of the system, and also find a representation of the algebra of the operators acting on the edge to derive an analogous spin ladder system. In particular, we note that the extension of our calculations to the direct generalization of $\mathbb{Z}_2$ topological phases, $\mathbb{Z}_N$ topological phases, is straightforward, and we leave it to future work to explore the edge-ES correspondence in those cases.

Appendices

5.A Schrieffer-Wolff transformation

In this appendix we introduce the Schrieffer-Wolff transformation which reproduces the work of Ref. [200].

Let H_0 be a Hamiltonian that has a low-energy eigenspace $\mathcal{V}_0$ and a high-energy eigenspace $\mathcal{V}_1$ separated by a spectral gap. H_0 can be written as

$$H_0 = P_0 H_0 P_0 + P_1 H_0 P_1, \tag{5.40}$$

where P_α are projectors onto $\mathcal{V}_\alpha$, where $\alpha = 0, 1$. Let us add a small perturbation ϵV which does not commute with H_0. Assuming the perturbation is weak enough, the new Hamiltonian will still have low and high-energy eigenspaces, $\tilde{\mathcal{V}}_0$ and $\tilde{\mathcal{V}}_1$, which have the same dimension as $\mathcal{V}_0$ and $\mathcal{V}_1$ respectively. That is,

$$H = H_0 + \epsilon V = \tilde{P}_0 H \tilde{P}_0 + \tilde{P}_1 H \tilde{P}_1. \tag{5.41}$$

Then there exists a unique direct rotation (i.e. unitary) U that rotates the old and new subspaces

$$U \tilde{P}_\alpha U^\dagger = P_\alpha. \tag{5.42}$$

By direct rotation, we mean the "minimal" rotation that maps $\tilde{P}_\alpha$ to P_α: among all unitary operators U' satisfying $U' \tilde{P}_\alpha U'^\dagger = P_\alpha$, the direction rotation U differs least from the identity in the Frobenius norm. See Ref. [200] for the construction of a direct rotation. In that case, we can rotate H to a new Hamiltonian H' with eigenspaces $\mathcal{V}_\alpha$:

$$H' := U H U^\dagger = P_0 U H U^\dagger P_0 + P_1 U H U^\dagger P_1. \tag{5.43}$$

This is the so-called Schrieffer-Wolff transformation.

There exists a unique antihermitian and block-off diagonal (in both $\mathcal{V}_\alpha$ and $\tilde{\mathcal{V}}_\alpha$) operator S such that $U = e^S$ and $||S|| < \pi/2$. It is constructed perturbatively as follows.

First we introduce some notation. Decompose an operator X on the Hilbert space in its block-diagonal X_{d} and block off-diagonal X_{od} parts:

$$\begin{aligned} X_{\mathrm{d}} &= P_0 X P_0 + (1 - P_0) X (1 - P_0), \\ X_{\mathrm{od}} &= P_0 X (1 - P_0) + (1 - P_0) X P_0. \end{aligned} \tag{5.44}$$

Also given Y, an operator acting on the Hilbert space, define the linear map which is the adjoint action of Y on other operators X that act on the Hilbert space:

$$\hat{Y}(X) = [Y, X]. \tag{5.45}$$

Lastly, define

$$\mathcal{L}(X) = \sum_{i,j} \frac{\langle i | X_{\text{od}} | j \rangle}{E_i - E_j} |i\rangle\langle j|, \tag{5.46}$$

where $|i\rangle$ is an eigenvector of H_0 with eigenvalue E_i and similarly for j. Note that $\mathcal{L}(X)$ is by construction block off-diagonal.

Now, S can be written perturbatively as

$$S = \sum_{n=1}^{\infty} \epsilon^n S_n, \quad S_n^\dagger = -S_n, \tag{5.47}$$

where

$$\begin{aligned}
S_1 &= \mathcal{L}(V_{\text{od}}), \\
S_2 &= -\mathcal{L}\hat{V}_{\text{d}}(S_1), \\
S_n &= -\mathcal{L}\hat{V}_{\text{d}}(S_{n-1}) + \sum_{j \geq 1} a_{2j} \mathcal{L}\hat{S}^{2j}(V_{\text{od}})_{n-1}, \text{ for } n \geq 3.
\end{aligned} \tag{5.48}$$

Here the coefficients a_m come from the Taylor series

$$x \coth(x) = \sum_{n=0}^{\infty} a_{2n} x^{2n}, \quad a_m = \frac{2^m B_m}{m!}, \tag{5.49}$$

where B_m are the Bernoulli numbers. We have also used the shorthand

$$\hat{S}^k(V_{\text{od}})_m = \sum_{\substack{n_1, \cdots, n_k \geq 1 \\ n_1 + \cdots + n_k = m}} \hat{S}_{n_1} \cdots \hat{S}_{n_k}(V_{\text{od}}). \tag{5.50}$$

From here, the low-energy effective Hamiltonian of H' is given by

$$H_{\text{eff}} := P_0 H' P_0 = P_0 H_0 P_0 + \epsilon P_0 V P_0 + \sum_{n=2}^{\infty} \epsilon^n H_{\text{eff},n}, \tag{5.51}$$

where

$$H_{\text{eff},n} = \sum_{j\geq 1} b_{2j-1} P_0 \hat{S}^{2j-1} (V_{\text{od}})_{n-1} P_0. \tag{5.52}$$

b_{2j-1} are the Taylor coefficients of $\tanh(x/2)$, i.e.

$$\tanh(x/2) = \sum_{n=1}^{\infty} b_{2n-1} x^{2n-1}, \quad b_{2n-1} = \frac{2(2^{2n} - 1)B_{2n}}{(2n)!}. \tag{5.53}$$

To second order in perturbation theory, and with a basis of states $|i,\alpha\rangle \in \mathcal{V}_\alpha$, the matrix elements of H' projected into $\mathcal{V}_\alpha$ is given explicitly

$$\langle i, \alpha | H' | j, \alpha \rangle = E_i^\alpha \delta_{ij} + \epsilon \langle i, \alpha | V | j, \alpha \rangle + \frac{\epsilon^2}{2} \sum_{\substack{k \\ \beta \neq \alpha}}$$

$$\langle i, \alpha | V | k, \beta \rangle \langle k, \beta | V | j, \alpha \rangle \left(\frac{1}{E_i^\alpha - E_k^\beta} + \frac{1}{E_j^\alpha - E_k^\beta} \right), \tag{5.54}$$

where E_i^α is the energy of $|i,\alpha\rangle$.

The generalized Schrieffer-Wolff transformation to Hamiltonians that have many invariant subspaces, each separated by a spectral gap to the next subspace, such that the Hilbert space $\mathcal{H} = \bigoplus_{\alpha \geq 0} V_\alpha$, is given in Ref. [201]. The generator of rotation S is still a block off-diagonal hermitian operator, with its first term in its expansion given by

$$S_1 = \sum_{\substack{i,j,\alpha,\beta \\ \alpha \neq \beta}} \frac{\langle i, \alpha | V_{\text{od}} | j, \beta \rangle}{E_i^\alpha - E_j^\beta} |i, \alpha\rangle \langle j, \beta|, \tag{5.55}$$

where $|i,\alpha\rangle \in \mathcal{V}_\alpha$, $|j,\beta\rangle \in \mathcal{V}_\beta$ and E_i^α is the energy of $|i,\alpha\rangle$. We will use this term in the derivation of the entanglement Hamiltonian.

5.B Calculation of Λ' of the entanglement spectrum

In this appendix, we calculate Λ', [see Sec. 5.3.3 eqn. (5.21)], obtained from standard non-degenerate wavefunction perturbation theory. Our starting point is the perturbed Wen-plaquette Hamiltonian on the infinite cylinder, $H = H_L + H_R + H_{LR} + \epsilon(V_L + V_R + V_{LR})$,

written according to the decompositions given by eqn. (5.26) and eqn. (5.27) using the Schrieffer-Wolff transformation. This reorganizes the perturbative series to make the tensor product structure of the new ground state manifest. We have:

$$
H = \underbrace{H_{LR} + \sum_{\alpha \geq 1} \alpha \Big(\sum_a P_{\alpha,L}^a + \sum_{a'} P_{\alpha,R}^{a'} \Big)}_{\text{large}}
$$
$$
+ \sum_a \Bigg(H_{\text{edge},L}^a + [-S_L^a, H_{\text{edge},L}^a] + \cdots + \sum_{\alpha \geq 1} \Big(H_{\alpha,L}^a +
$$
$$
[-S_L^a, \alpha P_{\alpha,L}^a] + [-S_L^a, H_{\alpha,L}^a] + \frac{1}{2}[-S_L^a, [-S_L^a, \alpha P_{\alpha,L}^a]] + \cdots \Big) \Bigg) \tag{5.56}
$$
$$
+ \sum_{a'} \Big(\cdots R \text{ terms} \cdots \Big)
$$
$$
+ \epsilon \sum_{\substack{\alpha \geq 0 \\ \tilde{Q}_L, \tilde{Q}_R}} (P_{\alpha,L}^{\tilde{Q}_L} \otimes P_{\alpha,L}^{\tilde{Q}_R}) V_{LR} (P_{\alpha,L}^{\tilde{Q}_L} \otimes P_{\alpha,L}^{\tilde{Q}_R}),
$$

where the large part is simply the unperturbed Wen-plaquette model $H_L + H_R + H_{LR}$, and the other part is small (order ϵ or higher) which comes from the perturbations $\epsilon(V_L + V_R + V_{LR})$.

From section 5.2.2, it suffices to solve H_{LR} for the four ground states of the Wen-plaquette model. The projection of H_{LR} onto a $\tilde{Q}$ sector, under the mapping given by eqn. (5.3), becomes a spin-ladder Hamiltonian:

$$
H_{\text{eff}} = -\sum_{\tilde{p}=1}^{\tilde{L}_y/2} (\tau_{\tilde{p},L}^x \tau_{\tilde{p},R}^x + \tau_{\tilde{p},L}^z \tau_{\tilde{p}-1,L}^z \tau_{\tilde{p},R}^z \tau_{\tilde{p}-1,R}^z), \tag{5.57}
$$

whose ground states (in each topological sector $a \simeq (\tilde{Q}, Q)$) are given by eqn. (5.7):

$$
|\tilde{Q}, Q\rangle = \frac{1}{\sqrt{2^{\tilde{L}_y/2-1}}} \sum_\tau \mathbb{P}_Q |\tau\rangle_L |\tau\rangle_R, \tag{5.58}
$$

where $|\tau\rangle_L \in V_{0,L}^{\tilde{Q}}$ is a spin configuration on the L spin chain. A similar statement holds for $|\tau\rangle_R$ on the R spin chain. Let us call the operator $\tau_{\tilde{p},L}^x \tau_{\tilde{p},R}^x$ the 'x-rung' operator and $\tau_{\tilde{p},L}^z \tau_{\tilde{p}-1,L}^z \tau_{\tilde{p},R}^z \tau_{\tilde{p}-1,R}^z$ the 'z-rung' operator.

For each topological sector a, we wish to calculate the corrections to the ground state of eqn. (5.57) in its $\mathcal{V}_{0,L}^{\tilde{Q}} \otimes \mathcal{V}_{0,R}^{\tilde{Q}}$ tensor product structure, generated by the small part of eqn. (5.56). To leading order in ϵ, the relevant terms in H for each $\tilde{Q}$ sector that generate the changes in the two ground states of $\tilde{Q}$ are

$$H_{\text{edge},L}^{\tilde{Q}} + H_{\text{edge},R}^{\tilde{Q}} + \epsilon(P_{0,L}^{\tilde{Q}} \otimes P_{0,L}^{\tilde{Q}})V_{LR}(P_{0,L}^{\tilde{Q}} \otimes P_{0,L}^{\tilde{Q}}). \tag{5.59}$$

From the mapping to virtual spin operators acting on the two spin chains, we can rewrite the above as

$$\begin{aligned} &f_{\tilde{Q},L}(\tau_{\tilde{p},L}^x, \tau_{\tilde{p},L}^z\tau_{\tilde{p}-1,L}^z) + f_{\tilde{Q},R}(\tau_{\tilde{p},R}^x, \tau_{\tilde{p},R}^z\tau_{\tilde{p}-1,R}^z)+ \\ &g_{\tilde{Q}}(\tau_{\tilde{p},L}^x, \tau_{\tilde{p},L}^z\tau_{\tilde{p}-1,L}^z, \tau_{\tilde{p},R}^x, \tau_{\tilde{p},R}^z\tau_{\tilde{p}-1,R}^z), \end{aligned} \tag{5.60}$$

where $f_{\tilde{Q},L}$ and $f_{\tilde{Q},R}$ are as in eqn. (5.18) and $g_{\tilde{Q}}$ the function associated with $(P_{0,L}^{\tilde{Q}} \otimes P_{0,L}^{\tilde{Q}})V_{LR}(P_{0,L}^{\tilde{Q}} \otimes P_{0,L}^{\tilde{Q}})$. There are also toroidal boundary conditions for both chains given by $\tilde{Q}_L$ (i.e. $\tau_{0,L}^z = -\tau_{\tilde{L}_y/2,L}^z$) on the L chain and similarly for the R chain.

Since both the original, unperturbed Hamiltonian eqn. (5.57) and the perturbation eqn. (5.60) are symmetric under $\mathbb{Z}_2 \times \mathbb{Z}_2$, generated by $\hat{Q}_L = \prod_{\tilde{p}} \tau_{\tilde{p},L}^x$ and $\hat{Q}_R = \prod_{\tilde{p}} \tau_{\tilde{p},R}^x$, it suffices to perform standard, non-degenerate wavefunction perturbation theory to the ground states eqn. (5.58), which have $Q_L = Q_R = Q$. We therefore need to solve for all the eigenstates of H_{eff}.

Eigenstates of H_{eff}. H_{eff} is exactly solvable because all terms in it commute. However there is one constraint: $\prod_{\tilde{p}=1}^{\tilde{L}_y/2} \tau_{\tilde{p},L}^z\tau_{\tilde{p}-1,L}^z\tau_{\tilde{p},R}^z\tau_{\tilde{p}-1,R}^z = \mathbb{1}$, and one term, $\hat{Q}_L$, not present in H_{eff} that commutes with it. Thus, all eigenstates of H_{eff} can be uniquely labeled by the eigenvalues of the set of commuting operators

$$\left\{ \{\tau_{\tilde{p},L}^x\tau_{\tilde{p},R}^x\}_{\tilde{p}=1}^{\tilde{L}_y/2}, \{\tau_{\tilde{p},L}^z\tau_{\tilde{p}-1,L}^z\tau_{\tilde{p},R}^z\tau_{\tilde{p}-1,R}^z\}_{\tilde{p}=2}^{\tilde{L}_y/2}, \hat{Q}_L \right\}. \tag{5.61}$$

Note the choice of the z-rung operators from $\tilde{p} = 2$ to $\tilde{L}_y/2$ only. The ground states of H_{eff} satisfy $\tau_{\tilde{p},L}^x\tau_{\tilde{p},R}^x = +1$ and $\tau_{\tilde{p},L}^z\tau_{\tilde{p}-1,L}^z\tau_{\tilde{p},R}^z\tau_{\tilde{p}-1,R}^z = +1$. There are two ground states given by eqn. (5.58) with $Q = Q_L$.

Now consider the excited states of H_{eff} that we will need in perturbation theory. Such states can be built up from the ground states by acting products of the following mutually commuting operators on them (they also commute with $\hat{Q}_L$):

$$\begin{aligned} s_{\tilde{p}}^z &:= \tau_{\tilde{p},R}^z, \text{ for } \tilde{p} = \tilde{1}, \cdots, \tilde{L}_y/2 \text{ and} \\ s_{\tilde{p}}^x &:= \prod_{\tilde{2}\leq\tilde{q}\leq\tilde{p}} \tau_{\tilde{p},L}^x \text{ for } \tilde{p} = \tilde{2}, \cdots, \tilde{L}_y/2, \end{aligned} \tag{5.62}$$

to give $\prod \left(s_{\tilde{p}}^{z/x} \right) |\tilde{Q}, Q\rangle$. These s-operators violate the x-rung or z-rung $= +1$ conditions with an energy cost of $2g$ and $4g$ above the ground states respectively.

Ground state perturbation; calculation of Λ'. We are now ready to find the four perturbed ground states of the Wen-plaquette model on the infinite cylinder. Let us find the correction to the ground state $|\tilde{Q}, Q\rangle$ for fixed $(\tilde{Q}, Q)$.

Consider first the contribution from $H_{\text{edge},L}^a = \mathbb{P}_{Q,L} f_{\tilde{Q},L}(\tau_{\tilde{p},L}^x, \tau_{\tilde{p},L}^z \tau_{\tilde{p}-1,L}^z) \mathbb{P}_{Q,L}$ first. $f_{\tilde{Q},L}$ contains products of $\tau_{L,\tilde{p}}^x$ and $\tau_{L,\tilde{p}}^z \tau_{L,\tilde{p}-1}^z$. Let us consider a generic first order term in $f_{\tilde{Q},L}$ given by $\epsilon \left(c \prod \tau_{\tilde{p},L}^x \prod \tau_{\tilde{p},L}^z \tau_{\tilde{p}-1,L}^z \right)$, where c is the coefficient of the term (necessarily making it hermitian). From the first order *process* in perturbation theory, the correction to the ground state from this term is an order ϵ correction given by

$$\epsilon \, c \sum_{\text{prod}}^{\prime} \frac{\langle \tilde{Q}, Q | \prod s^{z/x} \left(\prod \tau_{\tilde{p},L}^x \prod \tau_{\tilde{p},L}^z \tau_{\tilde{p}-1,L}^z \right) |\tilde{Q}, Q\rangle}{\Delta(\prod s^{z/x})} \times \tag{5.63}$$
$$\prod s^{z/x} |\tilde{Q}, Q\rangle.$$

An explanation is in order. The sum is over all possible products $\prod s^{z/x}$ which generate all possible excited states $\prod s^{z/x} |\tilde{Q}, Q\rangle$ (in the same topological sector), with the prime denoting the exclusion of the trivial product. $\Delta(\prod s^{z/x})$ is the energy gap between the ground state $|Q\rangle$ and the excited state defined by the product, which is always negative: $\Delta < 0$. We have also made use of the fact that $\mathbb{P}_{Q,L} = 1$ on the particular ground state we are working with.

It is not hard to see that the only contributions arise if $\left(\prod s^{z/x} \right) \left(\prod \tau_{\tilde{p},L}^x \prod \tau_{\tilde{p},L}^z \tau_{\tilde{p}-1,L}^z \right) = \mathbb{1}$ or $\hat{Q}_L$. That is, the excited states cancel the excitations over the ground states from $H_{\text{edge},L}^{\tilde{Q}}$. In other words, we have

$$\prod s^{z/x} = \prod \tau_{\tilde{p},L}^x \prod \tau_{\tilde{p},L}^z \tau_{\tilde{p}-1,L}^z \text{ or}$$
$$\prod s^{z/x} = \hat{Q}_L \left(\prod \tau_{\tilde{p},L}^x \prod \tau_{\tilde{p},L}^z \tau_{\tilde{p}-1,L}^z \right). \tag{5.64}$$

For the first case, the matrix element is 1, and so the excitation induced from $H_{\text{edge},L}^{\tilde{Q}}$ on the ground state is reproduced in the correction to the ground state, up to a negative rescaling that depends on the energy difference of this excited state with the ground state. For the second case, the matrix element is Q (since $Q_L = Q$), and the correction to the

ground state is

$$
\begin{aligned}
&\hat{Q}_L \left(\prod \tau^x_{\tilde{p},L} \prod \tau^z_{\tilde{p},L} \tau^z_{\tilde{p}-1,L} \right) |\tilde{Q}, Q\rangle \\
=&\hat{Q}_L \left(\prod \tau^x_{\tilde{p},L} \prod \tau^z_{\tilde{p},L} \tau^z_{\tilde{p}-1,L} \right) Q\hat{Q}_L |\tilde{Q}, Q\rangle \\
=&Q \left(\prod \tau^x_{\tilde{p},L} \prod \tau^z_{\tilde{p},L} \tau^z_{\tilde{p}-1,L} \right) |\tilde{Q}, Q\rangle,
\end{aligned}
\tag{5.65}
$$

where in the second equality we have commuted $\hat{Q}_L$ past the excitations. The Q from the matrix element cancels the Q from the correction to the ground statement, and so this correction once again reproduces the excitation induced from $H^{\tilde{Q}}_{\text{edge},L}$ on the ground state, up to a negative rescaling $1/\Delta(\prod s^{z/x})$.

Interestingly, we therefore see that *each* term in the edge Hamiltonian $H^{\tilde{Q}}_{\text{edge},L}$ is reproduced as excitations to the ground state *acting on the L spin chain*, albeit with a negative term-dependent rescaling $1/\Delta(\prod s^{z/x}) < 0$. That is,

$$
\begin{aligned}
H^a_{\text{edge},L} \xrightarrow{\text{induces corr.}} &-\left(\bar{H}^{\tilde{Q}}_{\text{edge,L}} \right)_L |\tilde{Q}, Q\rangle \\
=&-\sum_{\tau',\tau} \left(\mathbb{P}_Q \bar{H}^{\tilde{Q}}_{\text{edge,L}} \mathbb{P}_Q \right)_{\tau',\tau} |\tau'\rangle_L |\tau\rangle_R,
\end{aligned}
\tag{5.66}
$$

where the the bar on $\bar{H}^{\tilde{Q}}_{\text{edge},L}$ signifies that we reproduce each term in $H^{\tilde{Q}}_{\text{edge},L}$ but with each term scaled by a positive rescaling: $1/|\Delta(\prod s^{z/x})|$.

In the above, we have introduced notation using double subscripts (two Ls). The L in $\bar{H}^{\tilde{Q}}_{\text{edge},L}$ corresponds to the *form* of the Hamiltonian acting on the L semi-infinite cylinder, while the L of the parenthesis around it corresponds to operators acting on the L spin-chain. Explicitly this means

$$
\left(\bar{H}^{\tilde{Q}}_{\text{edge},\zeta} \right)_\xi := \bar{H}^{\tilde{Q}}_{\text{edge},\zeta}(\tau^z_{\tilde{p},\xi}\tau^z_{\tilde{p}-1,\xi}, \tau^x_{\tilde{p},\xi}),
\tag{5.67}
$$

where $\zeta, \xi \in \{L, R\}$, and in the above case we have $\zeta = \xi = L$. We will use this notation below.

It will be helpful to provide examples of both cases to make our discussion concrete. Consider an example of the first case: a term $\tau^x_{\tilde{p},L}$ of $H^{\tilde{Q}}_{\text{edge},L}$ such that $\tilde{p} \neq \tilde{1}$. Then, there exists either a single operator $(s^x_{\tilde{2}})$ or a product of two adjacent operators $(s^x_{\tilde{p}} s^x_{\tilde{p}-1})$ which is the inverse of $\tau^x_{\tilde{p},L}$, i.e. itself. The energy difference Δ is -4 in this case. Consider next

125

an example of the second case: $\tau^x_{L,\tilde{1}}$ in $H^{\tilde{Q}}_{\text{edge},L}$. One needs to multiply by $s^x_{\tilde{L}_y/2}$ to get $\hat{Q}_L$. Now, $\langle \tilde{Q}, Q | \hat{Q}_L | \tilde{Q}, Q \rangle s^x_{\tilde{L}_y/2} | \tilde{Q}, Q \rangle_L = Q^2_L \left(s^x_{\tilde{L}_y/2} \hat{Q}_L \right) | \tilde{Q}, Q \rangle = \tau^x_{\tilde{1},L} | \tilde{Q}, Q \rangle$. The excited state involved in the process also has an energy difference of $\Delta = -4$ from the ground state. Concluding, we have the result that *any* $\tau^x_{\tilde{p},L}$ term that appears in $H^{\tilde{Q}}_{\text{edge},L}$ shows up also in the correction to the ground states:

$$\tau^x_{\tilde{p},L} \xrightarrow{\text{induces corr.}} -\frac{1}{4} \left(\tau^x_{\tilde{p},L} \right)_L | \tilde{Q}, Q \rangle$$
$$= -\frac{1}{4} \sum_{\tau',\tau} \left(\mathbb{P}_Q \tau^x_{\tilde{p},L} \mathbb{P}_Q \right)_{\tau',\tau} | \tau' \rangle_L | \tau \rangle_R \tag{5.68}$$

Next let us consider the corrections from $H^{\tilde{Q}}_{\text{edge},R}$. By making use of the fact the ground states satisfy the x-rung and z-rung operators $= +1$, we can convert $H^{\tilde{Q}}_{\text{edge},R}$ acting on the R *spin chain* to it acting on the L *spin chain*: $\prod \tau^x_{\tilde{p},R} \prod \tau^z_{\tilde{p},R} \tau^z_{\tilde{p}-1,R} | \tilde{Q}, Q \rangle = \prod \tau^x_{\tilde{p},L} \prod \tau^z_{\tilde{p},L} \tau^z_{\tilde{p}-1,L} | \tilde{Q}, Q \rangle$, and our above analysis holds.

We therefore have

$$H^a_{\text{edge},R} \xrightarrow{\text{induces corr.}} -\left(\bar{H}^{\tilde{Q}}_{\text{edge},R} \right)_L | \tilde{Q}, Q \rangle$$
$$= -\sum_{\tau',\tau} \left(\mathbb{P}_Q \bar{H}^{\tilde{Q}}_{\text{edge},R} \mathbb{P}_Q \right)_{\tau',\tau} | \tau' \rangle_L | \tau \rangle_R, \tag{5.69}$$

where we remind the reader once again that it is the modified (term-dependent rescaled) R edge Hamiltonian acting on the L spin degrees of freedom of the ground state.

Lastly, consider the contribution from $\epsilon(P^{\tilde{Q}}_{0,L} \otimes P^{\tilde{Q}}_{0,L}) V_{LR} (P^{\tilde{Q}}_{0,L} \otimes P^{\tilde{Q}}_{0,L})$, which can be written as $g_{\tilde{Q}}(\tau^x_{\tilde{p},L}, \tau^z_{\tilde{p},L} \tau^z_{\tilde{p}-1,L}, \tau^x_{\tilde{p},R}, \tau^z_{\tilde{p},R} \tau^z_{\tilde{p}-1,R})$ in the spin chain language. Like above, if $g_{\tilde{Q}}$ acts on the ground state $| \tilde{Q}, Q \rangle$, then we can convert terms that act on the R spin chain to act on the L spin chain, so that the overall contributions from V_{LR} act only on the L spin chain. For example, $\tau^z_{\tilde{p},L} \tau^z_{\tilde{p}-1,L} \tau^x_{\tilde{p},R} | \tilde{Q}, Q \rangle = \tau^z_{\tilde{p},L} \tau^z_{\tilde{p}-1,L} \tau^x_{\tilde{p},L} | \tilde{Q}, Q \rangle$.

Thus,

$$V_{LR} \xrightarrow{\text{induces corr.}} -\left(\bar{V}_{LR} \right)_L | \tilde{Q}, Q \rangle$$
$$= -\sum_{\tau',\tau} \left(\mathbb{P}_Q \bar{V}_{LR} \mathbb{P}_Q \right)_{\tau',\tau} | \tau' \rangle_L | \tau \rangle_R, \tag{5.70}$$

where $\left(\bar{V}_{LR} \right)_L$ is a term-dependent rescaled, $R \to L$ operators swapped version of V_{LR}.

Therefore, we have calculated Λ and hence Λ':

$$\Lambda = \mathbb{P}_Q(\bar{H}^{\tilde{Q}}_{\text{edge,L}} + \bar{H}^{\tilde{Q}}_{\text{edge,R}} + \bar{V}_{LR})\mathbb{P}_Q \equiv \mathbb{P}_Q\Lambda'\mathbb{P}_Q. \tag{5.71}$$

$\left(\bar{H}^{\tilde{Q}}_{\text{edge,L}} + \bar{H}^{\tilde{Q}}_{\text{edge,R}} + \bar{V}_{LR}\right)_L$ differs from $\left(H^{\tilde{Q}}_{\text{edge,L}} + H^{\tilde{Q}}_{\text{edge,R}}\right)_L$ in two ways: the term dependent rescaling $|\Delta(\prod s^{z/x})|$, and also in a potentially arbitrary fashion from $\bar{V}_{LR}$. Thus, there is no reason to expect that the two spectra should match in the low-energy limit, leading to the conclusion that there is no edge-ES correspondence in general.

5.C Derivation of $H^a_{\text{edge},L}$ and $H^a_{\text{ent.}}$ for uniform magnetic fields as perturbations

In this appendix we calculate $H^a_{\text{edge},L}$ and $H^a_{\text{ent.}}$ for the case of perturbations being uniform single-site magnetic fields:

$$\epsilon V = \epsilon \sum_i h_X X_i + h_Y Y_i + h_Z Z_i. \tag{5.72}$$

This can be written as $V = V_L + V_R$ where V_L are the perturbations acting on the L semi-infinite cylinder and V_R are the perturbations acting on the R semi-infinite cylinder.

5.C.1 Calculation of $H^a_{\text{edge},L}$

We calculate $H^a_{\text{edge},L}$ of the L semi-infinite cylinder according to the Schrieffer-Wolff transformation, eqn. (5.51) and eqn. (5.54), for the perturbation V_L, to lowest non-trivial order.

The zeroth order term is identically 0, since the unperturbed Wen-plaquette model on the semi-infinite cylinder has a flat edge theory. Next, the first order (ϵ) term of the edge Hamiltonian in each topological sector, $\epsilon P^a_{0,L} V_L P^a_0$, is also identically 0 because single site magnetic fields cannot connect states in $\mathcal{V}^a_{0,L}$ to $\mathcal{V}^a_{0,L}$. Thus, we have to go to second order in ϵ.

At this order, there can now be virtual processes that connect $\mathcal{V}^a_{0,L}$ to $\mathcal{V}^a_{0,L}$. They are mediated by excited states that are one unit of energy above the ground states. We can

therefore simplify the the notation in eqn. (5.54) for the case of the Wen-plaquette model, in each $\tilde{Q}$ sector:

$$\langle i, 0, \tilde{Q}|H'|j, 0, \tilde{Q}\rangle = -\epsilon^2 \sum_k \langle i, 0, \tilde{Q}|V_L|k, 1\rangle\langle k, 1|V_L|j, 0, \tilde{Q}\rangle$$
$$= -\epsilon^2 \langle i, 0, \tilde{Q}|V_L V_L|j, 0, \tilde{Q}\rangle, \tag{5.73}$$

for $|i, 0, \tilde{Q}\rangle \in \mathcal{V}_{0,L}^{\tilde{Q}}$ and $|k, 1\rangle \in \mathcal{V}_{1,L}$.

Now, there are only two ways in which the above matrix element is non-zero. The first case is when a term in the first V_L annihilates a term in the second V_L. However, this simply contributes to a diagonal matrix element whose value is the same for all states. In other words, such a process just renormalizes the energy of the system. We will hence disregard the contributions of this matrix element. The second case is when a term in the first V_L combines with a term in the second V_L to form a boundary operator $S_{p,L}$ or $S_{\tilde{p},L}$. This is now not a diagonal matrix element, and gives the lowest order non-trivial dynamics to the edge Hamiltonian. Dropping the label $\{0\}$ for notational convenience, the edge Hamiltonian to second order in ϵ^2 simplifies to

$$\langle i, \tilde{Q}|H'|j, \tilde{Q}\rangle = -\epsilon^2 h_Z h_X \sum_{l=1}^{L_y} \times$$
$$\left(\langle i, \tilde{Q}|Z_l X_{l+1}|j, \tilde{Q}\rangle + \langle i, \tilde{Q}|X_{l+1} Z_l|j, \tilde{Q}\rangle\right)$$
$$= -2\epsilon^2 h_Z h_X \sum_{l=1}^{L_y} \langle i, \tilde{Q}|Z_l X_{l+1}|j, \tilde{Q}\rangle$$
$$= -2\epsilon^2 h_Z h_X \langle i, \tilde{Q}| \left(\sum_{p=1}^{L_y/2} \left(\square^{\,p} \right)_L + \sum_{\tilde{p}=1}^{\tilde{L}_y/2} \left(\square^{\,\tilde{p}} \right)_L \right) |j, \tilde{Q}\rangle. \tag{5.74}$$

From the mapping, eqn. (5.3), we can read off the edge Hamiltonian in each $\tilde{Q}$ sector at order ϵ^2:

$$H_{\text{edge},L}^{\tilde{Q}} = -2\epsilon^2 h_Z h_X \sum_{\tilde{p}=1}^{\tilde{L}_y/2} \left(\tau_{\tilde{p},L}^z \tau_{\tilde{p}-1,L}^z + \tau_{\tilde{p},L}^x \right), \tag{5.75}$$

with toroidal boundary conditions $\tau_{0,L} = \tilde{Q}\tau_{\tilde{L}_y/2,L}$. This is nothing but the critical periodic ($\tilde{Q} = +1$) or antiperiodic ($\tilde{Q} = -1$) $(1+1)$-d Ising model, which is $\mathbb{Z}_2$ symmetric and is clearly at the Kramers-Wannier self-dual point.

The edge Hamiltonian in each topological sector a is then found by projecting the Ising model down into the relevant $\mathbb{Z}_2 = Q_L$ sector:

$$H^{a \simeq (\tilde{Q}, Q)}_{\text{edge}, L} = \mathbb{P}_{Q,L} H^{\tilde{Q}}_{\text{edge}, L} \mathbb{P}_{Q,L}, \tag{5.76}$$

where $\mathbb{P}_Q = (\mathbb{1} + Q_L \hat{Q}_L)/2$, $\hat{Q}_L := \prod_{\tilde{p}} \tau^x_{\tilde{p}, L}$.

The edge Hamiltonian on the R semi-infinite cylinder at ϵ^2, $H^a_{\text{edge}, R}$ is identical, except with the replacement $\vec{\tau}_{\tilde{p}, L}$ with $\vec{\tau}_{\tilde{p}, R}$.

5.C.2 Calculation of $H^a_{\text{ent.}}$

We calculate $H^a_{\text{ent.}}$ of the ground states of the Wen-plaquette model perturbed by uniform single-site magnetic fields to lowest order in ϵ. We start with the calculation of Λ' in eqn. (5.71) of Appendix 5.B. Firstly note that $V_{LR} = 0$, so $\tilde{V}_{LR} = 0$ as well. Secondly note that as discussed in Appenix 5.B, each term in the both edge Hamiltonians is reproduced in Λ', acting on the L spin degrees of freedom, with a term-dependent rescaling that depends on the energy difference between the ground state of H_{eff} in eqn. (5.57) and the excited states of H_{eff} generated by the edge Hamiltonians. However, both edge Hamiltonians only contain the terms $\tau^x_{\tilde{p}, L/R}$ and $\tau^z_{\tilde{p}, L/R} \tau^z_{\tilde{p}-1, L/R}$, and the excited states generated by these terms acting on the ground states $|\tilde{Q}, Q\rangle$ give an energy difference of -4 (they violate 2 z-rung operators or 2 x-rung operators respectively). Thus, in this case, the term-dependent rescaling becomes a single, overall rescaling, and we have the result

$$\Lambda' = \frac{1}{4} \left(H^{\tilde{Q}}_{\text{edge}, L} + H^{\tilde{Q}}_{\text{edge}, R} \right)_L = \frac{1}{2} \left(H^{\tilde{Q}}_{\text{edge}, L} \right)_L, \tag{5.77}$$

where in the second equality we made use of the fact that $(H^{\tilde{Q}}_{\text{edge}, R})_L = (H^{\tilde{Q}}_{\text{edge}, L})_L$.

At this point, it would be tempting to conclude from eqn. (5.31) and eqn. (5.32) that the entanglement Hamiltonian is then precisely proportional to the edge Hamiltonian in the lowest order in ϵ. However, the identification $H^a_{\text{ent.}} \equiv 2\mathbb{P}_Q \Lambda' \mathbb{P}_Q$ is only valid if Λ' appears at order ϵ. In the case we are considering here, it appears at order ϵ^2, and so we cannot directly identify the entanglement Hamiltonian.

To be consistent, we want to calculate all ϵ^2 corrections to the reduced density matrix ρ^a_L. This implies that in eqn. (5.21), we have to calculate Λ to second order in ϵ, and Θ and Ξ to first order in ϵ. Thus our calculation of Λ' in eqn. (5.77) is not entirely correct as it is only a part of the ϵ^2 correction. Also, it might be the case that Θ and Ξ give rise

129

to undesirable ϵ^2 contributions in the dominant part of the reduced density matrix that modifies the entanglement spectrum from that of the spectrum of the edge Hamiltonians. However, we will show that in this case, (i) the other contribution to Λ' is simply a constant, (ii) the contributions from Θ and Ξ simply contribute shift the entanglement Hamiltonian. This calculation also explicitly shows how to perform calculations in our perturbative framework to order ϵ^2, and by extension, to arbitrary order in ϵ.

Result. We first state the result. To order ϵ^2,

$$\Lambda = \mathbb{P}_{Q,L} \Lambda' \mathbb{P}_{Q,L} = \mathbb{P}_{Q,L} \left(\frac{1}{2} \left(H_{\text{edge},L}^{\tilde{Q}} \right)_L + \mathcal{O}(\epsilon^2) \right) \mathbb{P}_{Q,L}$$

$$\Theta = \epsilon \mathbb{P}_{Q,L} \otimes \vec{w}_1^\dagger$$
$$\Xi = \epsilon \mathbb{P}_{Q,L} \otimes \vec{w}_2$$
$$\Omega \sim \mathcal{O}(\epsilon^2) \Omega' \tag{5.78}$$

where $\vec{w}_1$ and $\vec{w}_2$ are (long) column vectors of unit strength denoting coefficients in front of a state $|\tau\rangle_L |i, \alpha\rangle_R$ ($\alpha \geq 1$), and $|i, \alpha\rangle_L |\tau\rangle_R$ respectively. The exact expression or length of $\vec{w}_1$ and $\vec{w}_2$ are unimportant here. Ω is a matrix that appears at ϵ^2 as it requires at least a second order virtual process to create an excitation to the ground state outside of the space of two spin chains $\mathcal{V}_{0,L}^{\tilde{Q}} \otimes \mathcal{V}_{0,R}^{\tilde{Q}}$.

With this result, let us form the reduced density matrix $\rho_L^a = \text{Tr}_R |\tilde{Q}, Q\rangle \langle \tilde{Q}, Q|$. To order ϵ^2, we have the unnormalized reduced density matrix

$$\rho_L^a = \sum_{\tau',\tau} \left(\left(1 + \mathcal{O}(\epsilon^2) + \vec{w}_1^\dagger \vec{w}_1 \right) \mathbb{P}_{Q,L} \right.$$

$$\left. - \mathbb{P}_{Q,L} \left(H_{\text{edge},L}^{\tilde{Q}} \right)_L \mathbb{P}_{Q,L} \right)_{\tau',\tau} |\tau'\rangle_L \langle \tau|_L$$

$$+ \sum_{\tau,i,\alpha \geq 1} \left(\mathbb{P}_{Q,L} \otimes \vec{w}_2 |\tau\rangle_L \langle i, \alpha|_L + \text{h.c.} \right)$$

$$+ \sum_{\substack{i,\alpha \geq 1 \\ j,\beta \geq 1}} \cdots \mathcal{O}(\epsilon^2) \cdots |i, \alpha\rangle_L \langle j, \beta|_L. \tag{5.79}$$

To extract the entanglement spectrum, we find the eigenvalues of ρ_L^a. This can be calculated

130

in standard matrix perturbation theory, yielding the unnormalized eigenvalues

$$\text{eig.}(\rho_L^a) =$$
$$\left(1 + \mathcal{O}(\epsilon^2) + \vec{w}_1^\dagger \vec{w}_1 + \vec{w}_2^\dagger \vec{w}_2 \right) - \text{eig.}\left(\mathbb{P}_{Q,L} \left(H_{\text{edge},L}^{\tilde{Q}} \right)_L \mathbb{P}_{Q,L} \right). \tag{5.80}$$

Since $\vec{w}_1^\dagger \vec{w}_1$ and $\vec{w}_2^\dagger \vec{w}_2$ are just numbers of order ϵ^2, we see that we can absorb the order ϵ^2 constants in the first term of the above expression into a constant shift of the second term, which is nothing but the entanglement Hamiltonian. Thus, we have

$$H_{\text{ent.}}^a = \mathbb{P}_{Q,L} \left(H_{\text{edge},L}^{\tilde{Q}} \right)_L \mathbb{P}_{Q,L} + \text{const.}, \tag{5.81}$$

at order ϵ^2. Therefore, it is clear that in this case

$$H_{\text{ent.}}^a = H_{\text{edge},L}^a \tag{5.82}$$

up to shifting and rescaling, at order ϵ^2 - an edge-ES correspondence. The edge/ES Hamiltonians calculated in this case are the critical $(1+1)$-d Ising models, or the transverse field Ising model, eqn. (5.35), projected into the different charge sectors ($\mathbb{Z}_2$ labeled by Q and toroidal boundary conditions labeled by $\tilde{Q}$). We have the following identification between states in the topological phase (left) and their edge/ES Hamiltonians (right):

$$|\mathbb{0}\rangle \leftrightarrow H_{\text{TFIM},+1}^{+1}$$
$$|e\rangle \leftrightarrow H_{\text{TFIM},-1}^{+1}$$
$$|m\rangle \leftrightarrow H_{\text{TFIM},+1}^{-1}$$
$$|\varepsilon\rangle \leftrightarrow H_{\text{TFIM},-1}^{-1}, \tag{5.83}$$

where the label $\{\mathbb{0}, m, \varepsilon = e \times m\}$ indicates that the states carry the corresponding anyonic flux.

Proof. We present the proof of our assertion, eqn. (5.78). First let us find the order ϵ corrections in Θ and Ξ. We identify the relevant terms in eqn. (5.56) that contribute. Let us concentrate on the contribution from perturbations on the right semi-infinite cylinder, V_R. The term that contributes is $[-S_R^a, \alpha P_{\alpha,R}^a]$, specifically, the order-ϵ term of S_L^a, which is given by eqn. (5.55). By virtue of the fact that V_R is a sum of single-site magnetic fields which can only connect the subspace $\mathcal{V}_{0,R}^a$ to $\mathcal{V}_{1,R}^a$ through a single virtual process, we can further distill the relevant term:

$$-\epsilon(P_{0,R}^a V_R P_{1,R}^a + \text{h. c.}) \tag{5.84}$$

131

is the term that contributes to Θ to order ϵ. The correction induced is

$$\epsilon \sum_{\tau,i} \langle\tau|_L \langle i,\alpha|_R P_{1,R} V_R P_{0,R} |\tilde{Q},Q\rangle \times |\tau\rangle_L |i,\alpha\rangle_R$$

$$= \epsilon \sum_{\tau,i} \langle\tau|_L \langle i,\alpha|_R V_R \left(\sum_\sigma \mathbb{P}_{Q,L} |\sigma\rangle_L |\sigma\rangle_R \right) \times |\tau\rangle_L |i,\alpha\rangle_R$$

$$= \epsilon \sum_{\tau,\sigma,i} (\mathbb{P}_{Q,L})_{\tau,\sigma} \langle i,\alpha|_R V_R |\sigma\rangle_R \times |\tau\rangle_L |i,\alpha\rangle_R. \tag{5.85}$$

where $\alpha = 1$. Now, $V_R = \sum_s (w_1^*)_s v_R^s$, where v_R^s are single-site magnetic fields. For each v_R^s, v_R^s acting on $|\sigma\rangle_R$ creates a unique excited state $v_R^s |\sigma\rangle_R \in \mathcal{V}_1$ which is unique - there is no other $v_R^{s'}$ such that $v_R |\sigma\rangle_R = v_R^{s'} |\sigma\rangle_R$. Thus, the label s identifies a unique excited state $|\sigma_s^e\rangle_R \equiv v_R^s |\sigma\rangle_R$. Using this result, we can write the correction as

$$\epsilon \sum_{\tau,s} (\mathbb{P}_{Q,L})_{\tau,\sigma} (w_1^*)_s |\tau\rangle_L |\sigma_s^e\rangle_R, \tag{5.86}$$

from which we read off

$$\Theta = \epsilon \mathbb{P}_{Q,L} \otimes \vec{w}_1^\dagger, \tag{5.87}$$

as claimed. A similar analysis for the contributions from the perturbation V_L on the L semi-infinite cylinder will yield

$$\Xi = \epsilon \mathbb{P}_{Q,L} \otimes \vec{w}_2. \tag{5.88}$$

Next, we show that Λ has the asserted form. We have already accounted for the $H_{\text{edge},L}^{\tilde{Q}}$ term, as it appears from the edge Hamiltonians, and so we only have to account for the $\mathcal{O}(\epsilon^2)$ shift in Λ' of eqn. (5.78).

This $\mathcal{O}(\epsilon^2)$ shift arises from the second order *process* in perturbation theory. This second order process corrects the state $|n^{(0)}\rangle$ as

$$\left(\sum_{\substack{k\neq n \\ l\neq n}} |k^{(0)}\rangle \frac{\langle k^{(0)}|V|l^{(0)}\rangle \langle l^{(0)}|V|k^{(0)}\rangle}{(E_n^{(0)} - E_k^{(0)})(E_n^{(0)} - E_l^{(0)})} \right.$$

$$- \sum_{k\neq n} |k^{(0)}\rangle \frac{\langle n^{(0)}|V|n^{(0)}\rangle \langle k^{(0)}|V|n^{(0)}\rangle}{(E_n^{(0)} - E_k^{(0)})^2}$$

$$\left. - \frac{1}{2}|n^{(0)}\rangle \sum_{k\neq n} \frac{\langle n^{(0)}|V|k^{(0)}\rangle \langle k^{(0)}|V|n^{(0)}\rangle}{(E_n^{(0)} - E_k^{(0)})^2} \right), \tag{5.89}$$

132

where $|k^{(0)}\rangle$ refers to eigenstates of the unperturbed Hamiltonian. As it is a process which involves two Vs it gives rise to contributions of at least order ϵ^2. In our case, the unperturbed Hamiltonian is the exact Wen-plaquette model $H_L + H_R + H_{LR}$, and $|n^{(0)}\rangle$ is the ground state of the exact Wen-plaquette model on the infinite cylinder in each topological sector, eqn. (5.58). Note that the second term evaluates to 0 because $\langle n^{(0)}|V|n^{(0)}\rangle = 0$.

Now, there are two contributions to $\mathcal{O}(\epsilon^2)$. The third term in eqn. (5.89) simply rescales $|n^{(0)}\rangle = |\tilde{Q}, Q\rangle$ - this gives one source of the shift $\mathcal{O}(\epsilon^2)$ in Λ'. The other source comes from the $[-S_L^a, [-S_L^a, \alpha P_{\alpha,L}^a]]$ term in eqn. (5.56) (and also the R term), specifically with the first order term S_1 of S_L^a and S_R^a. Expanding the two commutators and focusing on the relevant term on the R cylinder gives us

$$[-S_R^a, [-S_R^a, \alpha P_{\alpha,R}^a]] \sim \epsilon^2 P_{0,R}^a V_R P_{1,R}^a V_R P_{0,R}^a. \tag{5.90}$$

However making use of the fact that the each term in $V_R = \sum_s (w_1^*)_s v_R^a$ creates a unique excited state above any given state in $\mathcal{V}_{0,R}^a$, it must be that the above term is simply proportional (at order ϵ^2) to $P_{0,R}^a$, i.e.

$$[-S_R^a, [-S_R^a, \alpha P_{\alpha,R}^a]] \sim \epsilon^2 P_{0,R}^a. \tag{5.91}$$

This then contributes $\sim \epsilon^2 |\tilde{Q}, Q\rangle$ in perturbation theory as well. A similar story holds for the L term. Thus, we have identified the sources of the $\mathcal{O}(\epsilon^2)$ shift in Λ' of eqn. (5.78).

This concludes the proof of our claim.

Chapter 6

Universal Edge Information from Wave Function Deformation

This chapter was published in [5]

6.1 Introduction

Topological order (TO) in a gapped $(2 + 1)$-dimensional quantum many-body system is believed to be characterized entirely by universal properties of its ground state(s) [213, 19, 214, 35]. For instance, a nonzero topological entanglement entropy γ in the ground state indicates the presence of TO and is a measure of the total quantum dimension of the underlying anyonic system [34, 35]. The braiding statistics of anyons in the theory is another such universal property and can be extracted from the $\mathcal{S}$ and $\mathcal{T}$ matrices, computed by measuring the overlap between the ground states transformed by modular matrices on a torus [198, 107, 1, 215].

The different kinds of edge theories that a topological phase can support, when placed on a manifold with a boundary, constitute another universal piece of data that we will be concerned with in this chapter. It is well-known from the bulk-edge correspondence that the topological physics of the bulk constrains the possible types of edge theories [78, 79, 80, 216]. For example, in Abelian topological phases, it is understood that the number of topologically distinct gapped edges is in one-to-one correspondence with the number of Lagrangian subgroups of the anyonic model in the bulk, each of which is a set of quasiparticles that obey certain braiding statistics within and without the set [89,

90, 91]. One very useful way of studying the edge theory of a given bulk is to look at the entanglement spectrum [ES] (or entanglement Hamiltonian [EH]) of its ground state $|\Psi\rangle$, through the edge-ES (or edge-EH) correspondence [217]. The EH $H_{\text{ent.}}$ is defined as follows. For a given bipartition of the system into two parts L and R, such that the entanglement cut mimics the geometry of the physical edge in question, the EH is obtained from $\rho_L \equiv \frac{1}{Z}e^{-H_{\text{ent.}}}$, where $Z = \text{Tr}(e^{-H_{\text{ent.}}})$ and $\rho_L := \text{Tr}_R|\Psi\rangle\langle\Psi|$ is the reduced density matrix on L. The ES is then simply the eigenvalues of the EH. The edge-ES correspondence states that the ES typically reproduces the universal, low-energy spectrum of the edge [218, 4]. It is natural to conjecture that this correspondence applies not just to the spectrum but also to the Hamiltonians in an edge-EH correspondence – such a view is indeed supported by the recent work of Ref. [4].

However, here a quandary arises. A single quantum state gives a unique EH, i.e. a single instance of an edge theory. Yet, as mentioned before, the universal features of topological order, which include the *set* of possible edge theories, should all be contained within a quantum state. Thus, a natural question that arises is: can one extract all possible edge theories starting from only one quantum state (or a microscopically few number of quantum states) believed to host the TO?

In this chapter, we argue that this is indeed the case: by locally deforming only one (or a few) quantum state(s), one can extract the edge theories of the TO, at least perturbatively. Concretely, we work with nonchiral topological phases, where the natural quantum states that characterize the TO are the so-called fixed-point wave functions (FPWs), $|\psi_{\text{FPW}}\rangle$ [219, 220, 26, 84]. These are special quantum states obtained at the fixed-point of an entanglement renormalization group flow in the space of quantum states, after all nonuniversal, short-ranged entanglement has been removed. We consider deforming the FPW as such:

$$|\psi_{\text{FPW}}\rangle \to |\psi'\rangle \equiv \bigotimes_i (\mathbb{1}_i + \epsilon V_i)|\psi_{\text{FPW}}\rangle. \qquad (6.1)$$

Here i is a region localized in space (not necessarily single-site), ϵ a small parameter and V_i some chosen operator with support on i. Our claim is that all edge theories of a topological phase, obtained perturbatively from a fixed-point limit (more precisely, the fixed-point Hamiltonian), can be extracted by studying the EH of the deformed FPW $|\psi'\rangle$. Furthermore, we can restrict the set of operators V_i to have support only in L, so that we can also study the edge theories through deformations of the reduced density matrix

directly:

$$\rho_L \to \rho'_L = \left[\bigotimes_{i \in L}(\mathbb{1}_i + \epsilon V_i)\right] \rho_L \left[\bigotimes_{i \in L}(\mathbb{1}_i + \epsilon V_i)\right]. \qquad (6.2)$$

Note that there is no bulk Hamiltonian involved in this approach of studying edge theories - thus, wave-function deformation lends even more support to the view that TO is characterized by only a small set of quantum states.

At first sight, the possibility of extracting universal edge information simply from deformations of the FPWs is a rather surprising claim. This is so because the nth-Rényi entropies of ρ_L are all equal for the FPW, so one would expect that beyond the topological entanglement entropy, no further universal data about the edge can be extracted from $|\psi_{\mathrm{FPW}}\rangle$, which was indeed claimed in Ref. [221]. On the other hand, TO is characterized by the "pattern of entanglement" in the wave function [84], and so all universal data including that of the edge should be contained within the structure of the FPW.

In the rest of this chapter, we present both theoretical analysis and numerical evidence to support the latter point of view. For the sake of exposition, we first illustrate our claim in a specific model: the Wen-plaquette model [195], a quantum double of $\mathbb{Z}_2$ with TO similar to the toric code. We present a perturbative analysis to derive the EHs of the Wen-plaqutte model from local deformations to its FPWs, comparing this to known results about its edges theories. We also numerically confirm our analysis by showing that we can reproduce and distinguish the two topologically distinct gapped edge theories that are well known to exist for a system with $\mathbb{Z}_2$-toric code TO, by measuring a nonlocal order parameter. Then, we present a perturbative argument for the validity of wave-function deformation for general nonchiral topological phases that are described by string-net models. Finally, we discuss potential applications of wave-function deformation and conclude.

6.2   Example: Wen-plaquette model

It is instructive to first illustrate concretely our claim of extraction of universal edge information beginning from only the FPW in a specific model, before presenting the argument for general nonchiral topological phases. We will focus on the Wen-plaquettte model in this section.
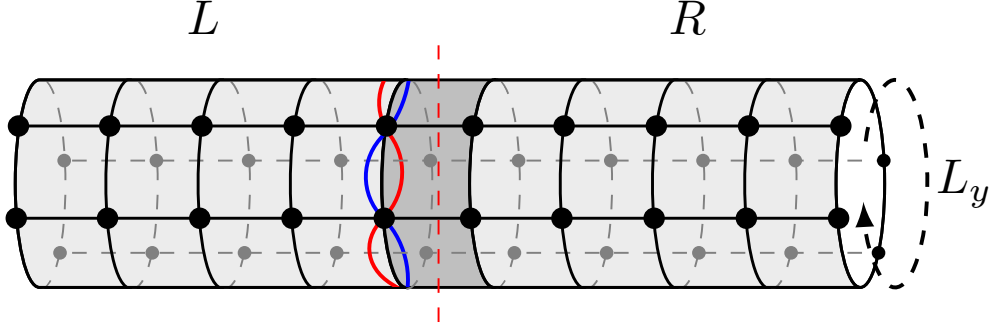
Figure 6.2.1: The infinite cylinder of width L_y on which the Wen-plaquette model is defined on, with the bipartition into two semi-infinite cylinders L and R. The red and blue strings acting on the row of spins adjacent to the entanglement cut are the two noncontractible Wilson loops wrapping around the cylinder, Γ^e and Γ^m.

6.2.1 Edge theories of Wen-plaquette model, revisited

We first review known results about the edge of the Wen-plaquette model using the Hamiltonian approach (mainly following Ref. [4]; see also Ref. [196] for a Projected Entangled Pairs States (PEPS) approach).

The Wen-plaquette model is a fixed-point Hamiltonian acting on a square lattice of spin-1/2s, comprised of mutually commuting plaquette-terms:

$$H = -\sum_p \mathcal{O}_p = -\sum_p \boxed{p}, \tag{6.3}$$

and its ground states(s) are FPWs. $\mathcal{O}_p = \boxed{p} = Z_1 X_2 Z_3 X_4$ is a plaquette-term, where $\{X_i, Y_i, Z_i\}$ are the Pauli-matrices acting on site i. The emergent TO is bosonic $\mathbb{Z}_2$-toric code, and so the system supports anyonic quasiparticle excitations labeled by $\{1, e, m, f\}$. The geometry we consider here is an infinite cylinder of circumference L_y ($L_y = 4n$ for some integer n), with a smooth bipartition dividing the infinite cylinder into two semi-infinite cylinders left (L) and right (R), mimicking the physical edge of a semi-infinite cylinder. On such a geometry, there are four topologically distinct FPWs, each of which carries an anyonic flux as measured by the two noncontractible Wilson loops $\Gamma^e = Z_1 X_2 \cdots Z_{L_y-1} X_{L_y}$ and $\Gamma^m = X_1 Z_2 \cdots X_{L_y-1} Z_{L_y}$ wrapping around the cylinder, which we choose to act on the circle of spins on L just adjacent to the entanglement cut, see Fig. 6.2.1.

On the left (L) semi-infinite cylinder, which has a boundary, we know from the work of Ref. [4] that the emergent degrees of freedom (DOF) which both the edge Hamiltonian (EdH) and the entanglement Hamiltonian (EH) act on are pseudospin-1/2s, composed each of two real spins on the boundary (see Fig. 6.2.2(a)). In addition, the algebra of boundary operators (i.e. operators which act on these emergent DOFs) is generated by the operators $Z_i X_{i+1}$, that each act on two boundary spins $(i, i+1)$ of L. In terms of the pseudospin-1/2s, a mapping to pseudospin operators that preserves the commutation relations of these boundary operators can be found as follows:

$$Z_{2n-1}X_{2n} \leftrightarrow \tau_n^x, \quad Z_{2n}X_{2n+1} \leftrightarrow \tau_n^z \tau_{n+1}^z, \tag{6.4}$$

where τ_n^α is an α-Pauli operator acting on the n-th pseudospin-1/2 (see also Fig. 6.2.2(a)). We see that these are $\mathbb{Z}_2$ symmetric, Ising-type terms τ_n^x and $\tau_n^z \tau_{n+1}^z$. There is a similar mapping for boundary operators on R. Thus, both the EdH and EH are made out of linear combinations of products of τ_n^x and $\tau_n^z \tau_{n+1}^z$, which are therefore both $\mathbb{Z}_2$ symmetric Hamiltonians.

What are the different gapped edge theories of the Wen-plaquette model? From the works of Refs. [89, 90, 91], we know that there are two known topologically distinct gapped edges in a system with a bosonic $\mathbb{Z}_2$-toric code TO, which are given by the Lagrangian subgroups $\{1, e\}$ and $\{1, m\}$. In the language of the pseudospin DOFs, τ, and the form of the edge Hamiltonian in terms of boundary operators, these two topologically distinct gapped edge theories can be easily understood as the paramagnetic and ferromagnetic phases of an emergent $\mathbb{Z}_2$ Ising-type Hamiltonian, with the two phases separated by a quantum phase transition described by a $(1+1)$-dimensional, $c = 1/2$ Ising CFT.

Let us now realize a clean, canonical, Ising model on a physical edge to the lowest nontrivial order in perturbation theory. Consider the following perturbation to the bulk Hamiltonian defined on the semi-infinite cylinder L, Eq. (6.3):

$$\epsilon V(h) = -\epsilon \sum_{i \in L} V_i(h), \ V_i(h) = \begin{cases} Z_i + hX_i, \ i \text{ even} \\ hZ_i + X_i, \ i \text{ odd} \end{cases}, \tag{6.5}$$

so that the full bulk Hamiltonian is $H + \epsilon V(h)$. Here, $\epsilon \ll 1$ (the bulk gap is 1), and h is a tunable parameter. It has been shown in Ref. [4] that to $\mathcal{O}(\epsilon^2)$, both the EdH on a semi-infinite cylinder L and the EH of the ground state of $H + \epsilon V(h)$ on an infinite cylinder are proportional to (up to a shift) the emergent Ising Hamiltonian:

$$H_{\text{Ising}} = -\sum_n \left(\tau_n^z \tau_{n+1}^z + h^2 \tau_n^x \right), \tag{6.6}$$

138
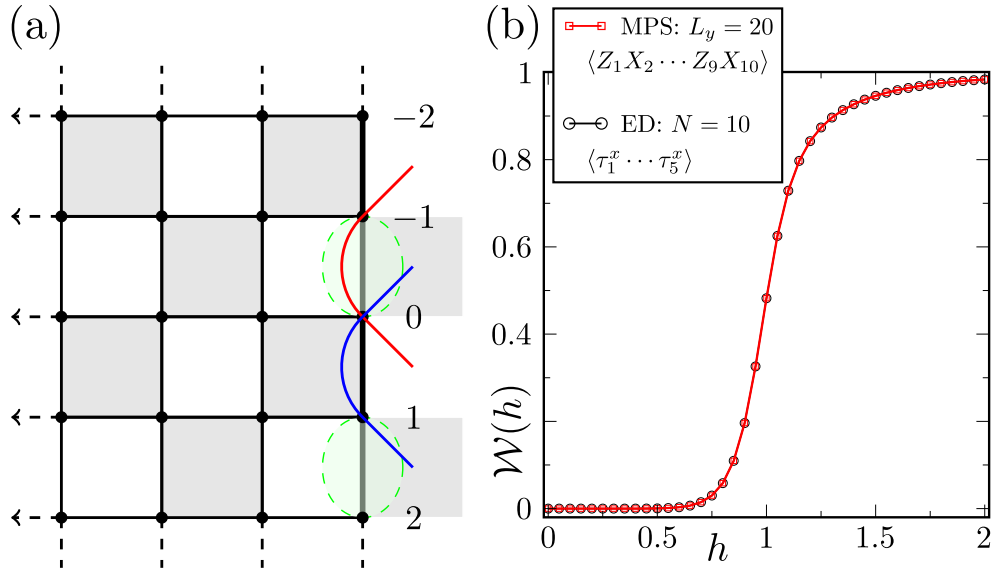
Figure 6.2.2: (a) The L semi-infinite cylinder with the boundary on the right. The numbers label rows of spins. The red boundary operators $Z_{2n-1}X_{2n}$ get mapped to τ_n^x, while the blue boundary operators $Z_{2n}X_{2n+1}$ get mapped to $\tau_n^z\tau_{n+1}^z$. τ_n^α is an α-Pauli operator acting on the emergent DOFs τ at the edge, a pseudospin-1/2, depicted by the green ellipse. (b) $\mathcal{W}(h)$ against h for an infinite cylinder of circumference $L_y = 20$ and $\epsilon = 0.001$. Red squares represent the numerical results obtained using the ground state of the EH on a semi-infinite cylinder, while black circles represent the exact diagonalization results of a bona fide Ising spin chain of length $N = 10$ – the agreement is virtually perfect. One can clearly see that $\mathcal{W}(h)$ distinguishes between the two phases, ferromagnetic for $h < 1$ and paramagnetic for $h > 1$, with the critical value at $h = 1$.

acting on the pseudospin DOFs. The different FPWs (with which to calculate the EdH and EH) give the boundary conditions on a circle (periodic/anti-periodic), and also the different $\mathbb{Z}_2$ symmetry sectors of $G = \prod_n \tau_n^x$ (see Ref. [4] for a more detailed explanation of the symmetry sectors corresponding to different FPWs).

If $h < 1$, the ground state of Eq. (6.6) realizes the ferromagnetic phase, while if $h > 1$, then it realizes the paramagnetic phase. When $h = 1$, so that there is full translational symmetry around the cylinder, the EdH and EH are both the critical Ising model, which realizes the $c = 1/2$ Ising CFT in the low-energy limit, as expected from Ref. [4] using arguments of Kramers-Wannier self-duality.

6.2.2 Edge theories of Wen-plaquette model from wave-function deformation

Our aim now is to recover the phase diagram of Eq. (6.6) starting from *only* the FPWs of the Wen-plaquette model, and to show how wave-function deformation can be used to extract this information.

To be precise, we work with $|\psi_{\text{FPW}}\rangle$ that has the identity flux, i.e. it is an eigenstate of both the Γ^e and Γ^m Wilson loops wrapping around the cylinder with eigenvalues $+1$. This choice of FPW selects for the $\mathbb{Z}_2$-symmetric sector of the Ising Hamiltonian with periodic boundary conditions[1]. Now, the FPWs of the model are defined by the flux-free conditions, $\mathcal{O}_p = +1$ for every plaquette p. Note that these conditions do not require the notion of a Hamiltonian, even though the states that satisfy these conditions are obviously realized as the ground states of Eq. (6.3). The unnormalized FPW with the identity flux is given by

$$|\psi_{\text{FPW}}\rangle = \prod_{a=e,m} \left(\frac{\mathbb{I} + \Gamma^a}{2} \right) \prod_p \left(\frac{\mathbb{I} + \mathcal{O}_p}{2} \right) |0\rangle_L |0\rangle_R, \qquad (6.7)$$

where $|0\rangle_L |0\rangle_R$ is a reference state. $\frac{1}{2}(\mathbb{I} + \mathcal{O}_p)$ is a projector onto the flux-free sector, and $\prod_{a=e,m} \frac{1}{2}(\mathbb{I} + \Gamma^a)$ projects onto the $+1$ eigenvalues of the noncontractible Wilson loops on the cylinder, Γ^e and Γ^m.

---

[1]If we had chosen to work with the other FPWs, then we get entanglement Hamiltonians which correspond to Ising models with different boundary conditions and symmetry sectors. Namely, the FPWs with the e or m anyonic flux give rise to entanglement Hamiltonians that are the periodic Ising model in the $G = -1$ symmetry sector or the antiperiodic Ising model in the $G = +1$ symmetry sector (the spectra of both are the same), while the FPW with the f anyonic flux gives rise to an entanglement Hamiltonian which is the antiperiodic Ising model in the $G = -1$ symmetry sector.

Now, to recover the edge physics of the Wen-plaquette model, we locally deform only the L half of the FPW given by Eq. (6.1), using $V_i = V_i(h)$ as in Eq. (6.5), so that $|\psi_{\mathrm{FPW}}\rangle \to |\psi'(h)\rangle$. We find, combining (1) a perturbative calculation in the representation of the FPW in terms of pseudospin variables τ (see the Appendix A for the details), and (2) the detailed calculations performed in Appendices B and C of Ref. [4], that

$$\rho'_L = \mathcal{N}' \exp\left(-4\epsilon^2 \mathbb{P}_{+1} H_{\mathrm{Ising}}^{\mathrm{PBC}}\right) + \mathcal{O}(\epsilon^3), \tag{6.8}$$

restricted to the $G = +1$ symmetry sector. That is, $H_{\mathrm{ent.}}$ is proportional to the $\mathbb{Z}_2$-symmetric periodic Ising model, Eq. (6.6), which is also proportional to the edge Hamiltonian. In contrast, for the (undeformed) FPW,

$$\rho_L = \mathcal{N} \mathbb{P}_{+1}. \tag{6.9}$$

Eq. (6.8) is an instance of the concrete expression of our claim – that the EH $H_{\mathrm{ent.}}$ in ρ'_L, obtained only from deformations to the wave function of the Wen-plaquette model, indeed informs us about the edge physics, given by Eq. (6.6). Note the striking contrast between ρ_L of the FPW and ρ'_L of the deformed FPW: the former has a flat ES and only tells us about the topological entanglement entropy of the topological phase, while the latter has an ES that gives us information about the edge.

However, if the EH of the deformed FPW not only reproduces the spectrum of the EdH, but is also proportional to it, then we should be able to directly obtain the phase diagram of Eq. (6.6) by measuring a suitable order parameter in the ground state $|\mathrm{GS}(h)\rangle_L$ of the EH. Typically, the order parameter that distinguishes between the ferromagnetic and paramagnetic phases in the Ising Hamiltonian is the local order parameter τ_n^z, which detects symmetry breaking. However, because Eq. (6.6) is actually an emergent Hamiltonian acting on pseudospin DOFs, certain emergent operators cannot be realized by the underlying, original, degrees of freedom. In particular, there is no way to realize the $\mathbb{Z}_2$-odd local operator τ_n^z (which one would typically measure to detect symmetry breaking in such a model) in terms of the local boundary operators $Z_i X_{i+1}$, as the latter all get mapped to $\mathbb{Z}_2$-even operators (see Eq. (6.4)). One therefore has to measure a nonlocal order parameter to distinguish between the two phases; two possible choices are the *open* string operators

$$
\begin{aligned}
W^e &= Z_1 X_2 \cdots Z_{L_y/2-1} X_{L_y/2} \leftrightarrow \tau_1^x \tau_2^x \cdots \tau_{L_y/4}^x, \\
W^m &= Z_2 X_3 \cdots Z_{L_y/2} X_{L_y/2+1} \leftrightarrow \tau_1^z \tau_{L_y/4}^z,
\end{aligned} \tag{6.10}
$$

acting on spins of L adjacent to the entanglement cut (they are *not* the closed string operators Γ^e or Γ^m). Intuitively, W^e and W^m measure the amount of anyonic condensation of e and m quasiparticles respectively on the boundary [89, 90]. Since these two operators

141

are Kramers-Wannier duals of each other, it suffices to measure only one; we choose to measure only W^e. The expectation value is then computed in the ground state of the EH:

$$\mathcal{W}(h) := \langle \mathrm{GS}(h)|_L W^e |\mathrm{GS}(h)\rangle_L. \tag{6.11}$$

When $L_y \to \infty$, the order parameter should show a kink at $h = 1$ where the quantum phase transition is. For $h < 1$, $\mathcal{W}(h)$ should be vanishing, signifying the ferromagnetic phase, while for $h > 1$, $\mathcal{W}(h)$ should increase as a power law $\mathcal{W}(h) \sim (h-1)^\beta$ with some critical exponent β, and saturate at $+1$, signifying the paramagnetic phase.

We implement this procedure and obtain the phase diagram numerically. We utilize an exact representation of $|\psi_{\mathrm{FPW}}\rangle$ on an infinite cylinder with circumference L_y, encoded in a matrix product state (MPS) that wraps around the cylinder in a snake-like fashion [107]. We deform the MPS according to Eq. (6.1) with deformations given by Eq. (6.5), and then extract the Schmidt vector corresponding to the largest singular value in the Schmidt decomposition, which gives us $|\mathrm{GS}(h)\rangle_L$.

Fig. 6.2.2(b) shows the plot of $\mathcal{W}(h)$ against the tuning parameter h, for $L_y = 20$ and $\epsilon = 0.001$ (the results are insensitive to the exact values of ϵ as long as $\epsilon \ll 1$). As expected, $\mathcal{W}(h)$ shows a sudden increase from 0 in the region $h < 1$ to $+1$ in the region $h > 1$, with the transition at $h = 1$. For comparison we have also plotted $\mathcal{W}(h)$ of a bona fide Ising spin chain of length $N = L_y/2 = 10$ with periodic boundary conditions, Eq. (6.6), obtained via exact diagonalization. The agreement is virtually perfect. This shows that we have successfully extracted the two known gapped edges in this system with $\mathbb{Z}_2$-toric code TO, by locally deforming only $|\psi_{\mathrm{FPW}}\rangle$. Note crucially that at no stage of the numerical illustration was there any optimization of the MPS tensors.

6.3 General argument for nonchiral topological phases

Having illustrated how wave-function deformation works in a concrete example, the Wen-plaquette model, we now make the case for the validity of wave-function deformation in general nonchiral topological phases. As seen from the preceding section, the crucial point was that both the EdH of the Wen-plaquette model and the EH obtained through just a local deformation of its FPW act on the same emergent DOFs and are generated by the same algebra of boundary operators. Thus, wave-function deformation of the FPW could be used to explore the space of edge theories and extract the desired universal edge information, which we did successfully.

Our aim in this section is to therefore argue that the same line of reasoning is true for general nonchiral topological phases. Concretely, we consider nonchiral topological

phases for which there is a string-net description, and perform a Schrieffer-Wolff(SW) transformation[199] to derive the edge Hamiltonian and entanglement Hamiltonian, beginning from a fixed-point Hamiltonian and its corresponding fixed-point wave function respectively. We will see that the forms of both the edge Hamiltonians of a given theory and the entanglement Hamiltonians of its deformed FPWs (given by Eqs. (6.1) or (6.2)) are the same, both being generated by the same algebra of boundary operators acting on the same emergent DOF. Thus, this would imply that the universal edge information of a topological phase is contained within the FPW and can be extracted by locally deforming the FPW and studying its EH. Note that since the arguments presented in this section are perturbative in nature, they do not constitute a mathematical proof of our claim; however, the calculation done for the specific case of the Wen-plaquette model in the previous section, together with the numerical evidence presented, constitute strong evidence for the validity of the line of reasoning below.

6.3.1   Edge Hamiltonian

The starting point is the fixed-point Hamiltonian of a generic nonchiral topological phase on a lattice, described by a string-net model [84]:

$$H = - \sum_{i \subset \mathcal{M}} P_i, \tag{6.12}$$

where P_i are commuting projectors, acting on a spatially local (not necessarily single-site) region i of a closed manifold $\mathcal{M}$, so that the ground state subspace consists of states that satisfy $P_i = +1$ for all i. The ground state subspace is typically degenerate, split into different topological sectors, differentiated by noncontractible Wilson loops around the manifold.

Note that the condition $P_i = +1$ for all i also precisely defines the fixed-point wave functions of the nonchiral topological phase, so that a Hamiltonian is actually not needed to describe these wave functions which characterizes this phase. However, we will use this fixed-point Hamiltonian to give meaning to the term 'edge theories' of a topological phase.

Consider now if the manifold $\mathcal{M}$ is instead open, so that it has a boundary $\partial \mathcal{M}$. Then, if Eq. (6.12) still describes the Hamiltonian on $\mathcal{M}$, in addition to the microscopic ground state degeneracy given by the different topological sectors, there will be a macroscopic ground state degeneracy within each topological sector, given by emergent local degrees of freedom (DOF) on the boundary. One can remove this degeneracy by imposing boundary conditions on $\partial \mathcal{M}$, which amounts to adding small ($\epsilon \ll 1$) *local* perturbations ϵV acting

near $\partial \mathcal{M}$, so that the full Hamiltonian is $H + \epsilon V$. The edge theory of the topological phase can then be understood as the low energy subspace of $H + \epsilon V$, which can be calculated, for example, using the Schrieffer-Wolff(SW) transformation:

$$H_{\text{edge}} = \mathbb{P}_0 H \mathbb{P}_0 + \epsilon \mathbb{P}_0 V \mathbb{P}_0 + \frac{1}{2}\epsilon^2 \sum_{j \neq 0} \frac{\mathbb{P}_0 V \mathbb{P}_j V \mathbb{P}_0}{E_j - E_0} + \cdots, \qquad (6.13)$$

where $\mathbb{P}_0$ is the projector onto the ground state subspace, and $\mathbb{P}_j$ is the projector onto the higher energy subspaces. We see from the above expansion that the only terms which contribute to the edge Hamiltonian are those that commute with all P_i, since they preserve the ground state condition $P_i = +1$. That is, $[\mathbb{P}_0 V \mathbb{P}_0, P_i] = 0$, $[\mathbb{P}_0 V \mathbb{P}_{j \neq 0} V \mathbb{P}_0, P_i] = 0$, and so on.

We define $\mathcal{A}$ as the maximal set of algebraically independent Hermitian operators that each acts locally on the manifold $\mathcal{M}$ and which commutes with all P_i. That is, $\mathcal{A}$ is comprised of algebraically independent operators a_j which satisfy

$$[a_j, P_i] = 0 \text{ for all } i, \qquad (6.14)$$

such that support(a_j) is in $\mathcal{M}$. Obviously, all P_i and the noncontractible Wilson loops are in $\mathcal{A}$, but on an open manifold, there will be typically many more local operators a_j, with support near the boundary $\partial \mathcal{M}$, localized around site j, that also satisfy this condition. We will hence call them 'boundary operators'. The boundary operators of $\mathcal{A}$ then generates (by virtue of being a maximal set of algebraically independent operators) the edge Hamiltonian – that is, H_{edge}, given by Eq. (6.13), must be a linear combination of products of a_j:

$$H_{\text{edge}} = \sum c_{i_1, \cdots, i_l} a_{i_1} \cdots a_{i_l}, \qquad (6.15)$$

where $c_{i_1, \cdots, i_l}$ is a coefficient denoting the weight of the string of boundary operators $a_{i_1} \cdots a_{i_l}$ and the sum is over such strings.

If the discussion above seems cryptic, it is instructive to go back to the example of the Wen-plaquette model considered in the previous section. There, the Hamiltonian Eq. (6.12) is given by Eq. (6.3), and an example of a boundary operator $a_i \in \mathcal{A}$ is $Z_i X_{i+1}$, which we see is both localized near the boundary and commutes with all plaquette operators $\mathcal{O}_p$ in the bulk. Furthermore, the set of all such boundary operators $Z_i X_{i+1}$ indeed generates H_{edge}, see Eqs. (6.4) and (6.6) (see also Ref. [4]).

Note that the boundary operators a_i in general obey nontrivial commutation relations between themselves, which give rise to an algebra $\mathcal{B}_{\mathcal{A}}$ that we will call the 'boundary

144

operator algebra' (c.f. Eq. (6.4) for the Wen-plaquette model). Because of this nontrivial algebra, the edge theory will have a nontrivial dispersion relation. Also, if the operators a_i are chosen as local as possible, then the condition that one adds *local* perturbations ϵV to H translates to the fact that the edge Hamiltonian will also obey some approximate sense of locality on $\partial \mathcal{M}$, since the support of the terms in the expansion of Eq. (6.13) can only grow linearly with the order of ϵ. Also, a local perturbation V ensures that the edge theory can be defined within each topological sector of the bulk theory without ambiguity, as mixing between topological sectors will be suppressed by an exponentially small factor $\sim \epsilon^L$, where L is the length scale associated with the boundary ∂M.

6.3.2 Entanglement Hamiltonian of deformed FPW

Now, we shift perspectives and start from the fixed-point wave functions of a topological phase defined on a closed manifold $\mathcal{M}$. We assume an entanglement cut of $\mathcal{M}$ into two parts L and R, mimicking the physical cut. Our aim in the following is to argue that the entanglement Hamiltonian that emerges from wave-function deformation of the FPW is also generated by $\mathcal{A}$, the maximal set of algebraically independent operators that act locally and which commutes with all P_i. If so, then that would imply that the space of EHs and the space of EdHs are equivalent (at least perturbatively), and so edge information of the topological phase can be extracted from wave-function deformation, thereby supporting our claim.

We have the following Schmidt decomposition of the FPW:

$$|\psi_{\mathrm{FPW}}\rangle = \Gamma \prod_{i \cap \partial M \neq 0} P_i |P_{j \subset L} = +1\rangle |P_{k \subset R} = +1\rangle, \qquad (6.16)$$

where $P_{j/k}$ are projectors that have support entirely in L/R, while projectors P_i are those that span the entanglement cut. Γ is some Wilson line/loop that chooses the FPW of a particular topological sector. Since $[P_i, P_{j/k}] = 0$, it must be that P_i can be decomposed into products of elements of $\mathcal{A}_L$ and $\mathcal{A}_R$. Here $\mathcal{A}_\xi$ is the set $\mathcal{A}$, defined previously, corresponding to the $\xi = L/R$ semi-infinite cylinder. That is, schematically, $P_i = \sum_\mu f_L^\mu(a_L) f_R^\mu(a_R)$, for some functions $f_{L/R}^\mu$. As an example, a plaquette term in the Wen-plaquette model that straddles the entanglement cut is $Z_{L,1} X_{R,1} Z_{R,2} X_{L,2}$ which can be written as $Z_{L,1} X_{L,2} \otimes X_{R,1} Z_{R,2}$, where the two terms of the tensor product belong to $\mathcal{A}_L$ to $\mathcal{A}_R$ respectively.

Thus, the Schmidt decomposition of the FPW must be

$$|\psi_{\mathrm{FPW}}\rangle = \frac{1}{\sqrt{N}} \sum_{\mu=1}^{N} |a_L^\mu\rangle \otimes |a_R^\mu\rangle, \qquad (6.17)$$

145

where N is the multiplicity that gives the correct topological entanglement entropy of the topological phase, and $|a_{L/R}^\mu\rangle$ are states in the ground state subspace of the *open* manifolds $\mathcal{M}_{L/R}$, schematically distinguished by the boundary operators $a_{L/R}^\mu \in \mathcal{A}_{L/R}$ (recall the macroscopic degeneracy in the case of open manifolds which can be resolved by the boundary operators). This gives the reduced density matrix on L:

$$\rho_L = \frac{1}{N}\mathbb{P}_0^\Gamma, \tag{6.18}$$

where $\mathbb{P}_0^\Gamma$ is the projector onto the ground state manifold (of H as in Eq. (6.12)) restricted to the topological sector chosen by Γ. We see from this that the ES is flat, as the ES of the FPW should be.

Next we deform the reduced density matrix as in Eq. (6.2). If we write $\bigotimes_i(\mathbb{1}_i + \epsilon V_i) \approx \bigotimes_i \exp(\epsilon V_i) \approx \exp(\sum_{n\geq 1}\epsilon^n S_n)$ (S_n is given by the Baker-Campbell-Hauserdoff formula; in particular, $S_1 = \sum_i V_i$), then we have the deformed reduced density matrix

$$\rho_L' \approx \frac{1}{N}\left(\underbrace{\mathbb{P}_0^\Gamma}_{h} + \underbrace{\epsilon\{S_1, \mathbb{P}_0^\Gamma\} + \mathcal{O}(\epsilon^2)}_{v}\right), \tag{6.19}$$

where $\{\cdot\}$ is the anticommuator and we have interpret Eq. (6.19) as a 'perturbation' v on a 'unperturbed' Hamiltonian h. We now apply the SW transformation to the Hamiltonian $h+v$, like before, but to instead obtain the 'higher-energy' subspace perturbatively. Here $||h|| = 1$ and $||v|| \sim \epsilon$ so the use of the SW transformation is justified. We have, to the two lowest orders in ϵ,

$$(\rho_L')_{\text{high}} = \frac{1}{N}\left(\mathbb{P}_0^\Gamma + \epsilon\mathbb{P}_0^\Gamma v\mathbb{P}_0^\Gamma + \frac{\epsilon^2}{2}\frac{\mathbb{P}_0^\Gamma v\mathbb{P}_1^\Gamma v\mathbb{P}_0^\Gamma}{1-0}\right). \tag{6.20}$$

Comparing the above to the perturbative expansion of the edge Hamiltonian given by Eq. (6.13), there is more than structural similarity of the expansions; there is also *algebraic* similarity. Since $\mathbb{P}_0^\Gamma$ is non other than the projector onto the ground state manifold of the fixed-point Hamiltonian H on $\mathcal{M}$, it follows that $(\rho_L')_{\text{high}}$ must also be generated by $\mathcal{A}$, the maximal set of local, algebraically independent operators in $\mathcal{M}$ that commute with all P_i, similar to H_{edge}. Furthermore, since the deformations of the FPW were local to begin with, $(\rho_L')_{\text{high}}$ is also approximately local on $\partial\mathcal{M}$. There is one more step to the entanglement Hamiltonian $H_{\text{ent.}}$: one has to take the logarithm of $(\rho_L')_{\text{high}}$, but it is clear that the entanglement Hamiltonian will also be generated by $\mathcal{A}$, although the notion of locality might be affected. However, to lowest order in ϵ, the entanglement Hamiltonian will

still be approximately local. An explicit example of the above calculations for a particular model, the Wen-plaquette model, can be found in Appendix A and also Ref. [4].

Thus, we have argued that the forms of both the edge and entanglement Hamiltonians are the same, both being generated by $\mathcal{A}$. This implies that the space of entanglement Hamiltonians obtained from a local deformation of the FPW is the same as the space of edge Hamiltonians obtained from various bulks, at least perturbatively. It is natural to assume then that for some local perturbation V to the *fixed-point Hamiltonian H* which gives some edge Hamiltonian, there exists a suitable choice of local deformations $\{V_i\}$ to the *FPW* such that the EH reproduces the edge Hamiltonian. Of course, our arguments above do not provide an explicit recipe for constructing this map; this map depends on the specific nonchiral topological phase in question, as one would have to find both the set of operators $\mathcal{A}$ and also the boundary operator algebra $\mathcal{B}_{\mathcal{A}}$ that these operators satisfy. However, we believe that we have managed to present convincing arguments for our claim: that universal edge information can be extracted solely from local deformations of the FPWs of a nonchiral topological phase.

6.4 Discussion and conclusion

In this chapter, we have argued through both analytical and numerical means that using wave-function deformation on the FPWs, one can extract the different edge theories that a nonchiral topological phases can support, at least perturbatively. We stress that this process does not require a bulk Hamiltonian, as firstly the FPW can be defined by local consistency relations, and secondly the deformation is done at the wave function level. Since the different edge theories that a topological phase can support is a universal piece of data of the TO, this lends support to the belief that TO is characterized solely by a set of quantum states.

Wave-function deformation can potentially be used to distinguish between systems with different TO. For example, two FPWs can have the same topological entanglement entropy (such as the $\mathbb{Z}_2$ Kitaev toric code and $\mathbb{Z}_2$ double semion which both have $\gamma = \log 2$), but extraction of the different edge theories they can host can be used to further differentiate between them. Furthermore, the study of edge theories using wave-function deformation can be readily applied to other nonchiral topological phases, especially since FPWs take simple representations in terms of tensor networks [222, 219, 223, 224] – in particular, this allows for a numerically relatively inexpensive way of exploring the space of edge theories as no numerical optimization is indeed. For instance, a study of the edge theories of the $\mathbb{Z}_3$ Wen-plaquette model has been conducted [225].

As a closing remark, we note that the analysis done in this chapter was perturbative in nature, controlled by the small parameter ϵ. Since we see that we can go from the FPW to any gapped or gapless boundary type, and since the local deformation is invertible, it follows that we can go from any boundary type to any boundary type of the topological phase, starting from a perturbative deformation of the FPW. This is likely to be true also for any nonperturbative deformation, as long as we do not destroy the TO. However, here one would potentially have to 'dress' the order parameter operators (Eq. (6.10)) appropriately, see Ref. [26]. It may thus be possible to explore the entire phase diagram of edge theories of a topological phase starting from a state $|\psi\rangle$ with a certain edge theory (i.e. not necessarily the FPW): one could move in this phase space of edge theories by locally deforming $|\psi\rangle$ (nonperturbatively) to produce another state $|\psi'\rangle$ with a different edge theory, even if the two edge theories are separated by a phase transition.

Appendices

Appendix: Perturbative calculation of entanglement Hamiltonian (EH)

First we rewrite the FPW of the Wen-plaquette model, Eq. (6.7), in terms of boundary pseudospin-1/2 degrees of freedom, τ, as explained in the main text and in Ref. [4]. This representation will also illustrate the pattern of entanglement ($\mathbb{Z}_2$-toric code TO) contained in the wave function.

The product over the plaquettes p in Eq. (6.7) splits into 3 sets: those that act on L, those that act on R, and those that act on the strip of spins where the entanglement cut is defined through. Define $|L\rangle$ as $\prod_{p \in L} \frac{1}{2}(\mathbb{I} + \mathcal{O}_p)|0\rangle_L$ and similarly for R. Here $|0\rangle_L|0\rangle_R$, the reference state in Eq. (6.7), is chosen in such a way that $(Z_{2n}X_{2n+1})_L|L\rangle|R\rangle = (X_{2n}Z_{2n+1})_R|L\rangle|R\rangle = |L\rangle|R\rangle$ for all n, where n labels the spins on both L and R adjacent to the entanglement cut (i.e. this fixes the gauge of the reference state).

With this choice of reference state, $|L\rangle$ can be represented as the state with pseudospin configuration $|\uparrow\uparrow \cdots \uparrow\uparrow\rangle_L$ (i.e. all τ_ns are pointing up), and there is a similar representation for $|R\rangle$. Furthermore, the mapping of boundary operators (e.g. Z_iX_i acting on L) to pseudospin operators is given by Eq. (6.4). Since the plaquettes acting on the strip (through which the entanglement cut is made) are comprised of a product of two boundary operators from the L and R cylinders, the FPW can be written as a superposition of pseudospin configurations on the L and R halves:

$$|\psi_{\text{FPW}}\rangle = \sum_\tau \mathbb{P}_{+1}|\tau\rangle_L|\tau\rangle_R = \sum_\tau |\tau_+\rangle_L|\tau\rangle_R, \qquad (6.21)$$

where $\mathbb{P}_{+1}$ is the projector on the $G = \prod_n \tau_n^x = +1$ symmetry sector, and $|\tau\rangle$ is a state with a certain pseudospin configuration (e.g. $|\uparrow\downarrow\downarrow \cdots \downarrow\uparrow\rangle$). Two different pseudospin configurations are orthogonal: $\langle\tau'|\tau\rangle = \delta_{\tau',\tau}$, and $|\tau_+\rangle = |\tau\rangle + |\bar{\tau}\rangle$, where $\bar{\tau}$ is the completely flipped configuration of τ. Ignoring the projector, one can intuitively see that this state is a loop quantum gas – it is an equal weight superposition of loops on the cylinder. The different configurations τ correspond to the different ways loops cross the entanglement cut; $|\tau\rangle_L$ must pair with only $|\tau\rangle_R$ or $|\bar{\tau}\rangle_R$ in order to form a closed loop.

We deform the FPW $|\psi_{\text{FPW}}\rangle$ of the Wen-plaquette model, Eq. (6.7) (or Eq. (6.21)), according to Eq. (6.1) with $V_i = V_i(h)$ as given by Eq. (6.5), and calculate the EH of the reduced density matrix ρ_L. Note that the manipulations here are formally similar to that

149

of Ref. [4], but the logic is fundamentally different: there, the perturbative calculation was performed for deformations to the Hamiltonian, while here, the perturbative calculation is performed for deformations to the wave function.

Now, we note that the V_is split into two sets – those that act on spins in the bulk of L (that is, away from the entanglement cut), and those that act on the circle of spins in L living adjacent to the entanglement cut. The former set simply renormalizes $|\tau\rangle_L \to |\tilde{\tau}\rangle_L$, which is still an orthogonal set, and so we drop the tilde label in our discussion. We therefore see that the change of the entanglement spectrum comes only from deformations to the wave function on spins next to the entanglement cut.

The deformed FPW, to $\mathcal{O}(\epsilon^2)$, is then

$$|\psi'(h)\rangle = \prod_{i \in L, \text{adj. to cut}} (\mathbb{1}_i + \epsilon V_i) \sum_\tau |\tau_+\rangle_L |\tau\rangle_R$$

$$= \left(\mathbb{1} + \epsilon \sum_i V_i + 2\epsilon^2 \sum_{i<j} V_i V_j \right) \sum_\tau |\tau_+\rangle_L |\tau\rangle_R. \tag{6.22}$$

Consider the $\mathcal{O}(\epsilon)$ effect of the deformation. This generates terms $|\alpha_+\rangle_L |\tau\rangle_R$ where $|\alpha\rangle_L$ is a new ket orthogonal to all the pseudospin configurations $|\tau\rangle_L$ (specifically it is a state describing an excitation in the bulk). Consider next the $\mathcal{O}(\epsilon^2)$ effect of the deformation. This generates two kinds of states. If V_i and V_j are not adjacent, then we also obtain a state $|\alpha_+\rangle_L |\tau\rangle_R$. But if $j = i + 1$ i.e. that V_i is next to V_j, then they can form boundary operators $Z_i X_{i+1}$, so that the deformed FPW contains new states $|\tau'\rangle_L |\tau\rangle_R$ for some τ', τ. The crucial point is that there is now additional coupling between states that are labeled only by pseudospin configurations which are beyond the diagonal $|\tau_+\rangle_L |\tau\rangle_R$ ones. These off-diagonal terms $|\tau'\rangle_L |\tau\rangle_R$ generate the EH.

Specifically, from the mapping given by Eq. (6.4), $V_{2n-1} V_{2n} |\tau_+\rangle_L |\tau\rangle_R \leftrightarrow h^2 \tau_n^x |\tau_+\rangle_L |\tau\rangle_R + \cdots$ and $V_{2n} V_{2n+1} |\tau_+\rangle_L |\tau\rangle_R + \leftrightarrow \tau_n^z \tau_{n+1}^z |\tau_+\rangle_L |\tau\rangle_R + \cdots$, so that the deformed FPW is

$$|\psi'(h)\rangle$$

$$= \sum_\tau \left(\mathbb{1} + 2\epsilon^2 \sum_n (\tau_n^z \tau_{n+1}^z + h^2 \tau_n^x) \right) |\tau_+\rangle_L |\tau\rangle_R + \cdots$$

$$= \sum_\tau \left(\mathbb{P}_{+1} - 2\epsilon^2 \mathbb{P}_{+1} H_{\text{Ising}}^{\text{PBC}} \right) |\tau\rangle_L |\tau\rangle_R + \cdots, \tag{6.23}$$

where $\cdots$ refer to terms such as $\mathcal{O}(\epsilon)|\alpha\rangle_L |\tau\rangle_R$. At this stage, we are done: from the detailed calculation performed in Appendices B and C of Ref. [4], we see the $\cdots$ terms do

not contribute to the EH at leading order, and so

$$\rho'_L = \mathrm{Tr}_R |\psi'(h)\rangle\langle\psi'(h)|$$
$$= \mathcal{N}' \exp\left(-4\epsilon^2 \mathbb{P}_{+1} H_{\mathrm{Ising}}^{\mathrm{PBC}}\right) + \mathcal{O}(\epsilon^3). \tag{6.24}$$

That is, the EH is proportional (up to a constant shift) to the periodic Ising Hamiltonian projected into the $G = \prod_n \tau_n^x = +1$ sector, which in turn is proportional to the edge Hamiltonian (EdH) of the Wen-plaquette model. This is Eq. (6.8) in the main text.

Chapter 7

Fermionic gapped edges in bosonic abelian topological states via fermion condensation

This chapter has not been published.

7.1 Introduction

Topologically ordered phases of matter in (2+1)-d are gapped many-body states with patterns of long-range entanglement [24]. These patterns of entanglement give rise to a host of universal features, which are protected from any local perturbations that do not close the bulk gap. Among these features include quasiparticle excitations with fractional statistics and charges, topology-dependent ground state degeneracies and interesting edge physics. The most famous examples of topological phases are the fractional quantum hall (FQH) states, which have been experimentally realized.

A universal quantity characterizing the edge of a gapped system is the so-called chiral central charge c_-. Systems with $c_- \neq 0$ are said to have chiral topological order and posses gapless modes which are impossible to gap out (modulo closing the bulk gap) and so they are maximally protected. Systems with $c_- = 0$ correspond to non-chiral topological order and one might ask whether these edges have any additional universal features, inherited from the bulk topological order.

In particular, an interesting question is the following: since the edge of a non-chiral topological phase is not intrinsically protected, how many different kinds of topological distinct gapped edges are there? Here a gapped edge is defined as a gapped domain wall between the topological phase and the vacuum (a topologically trivial gapped state). This question has been answered thoroughly in ref. [89, 88] for abelian topological states (see also [90, 91]). There it was found that the classification of topologically distinct gapped edges is completely given by Lagrangian subgroups $\mathcal{M}$ consisting of subsets of quasiparticles of the theory: the presence of each $\mathcal{M}$ is a necessary and sufficient condition for a gapped edge. Physically, each $\mathcal{M}$ corresponds to a maximal set of quasiparticles in the theory that can condense on the boundary, leading to a topologically distinct gapped edge. Therefore, the different kinds of edge theories is a universal feature constrained by the bulk topological physics. Interestingly there is the possibility of a non-chiral topological phase having no Lagrangian subgroups, which implies that it has gapless edge modes which are protected by something more subtle than symmetry or chirality [89].

However, there is a subtlety involved in defining a vacuum or 'topologically trivial gapped state'. Depending on the notion of locality in the vacuum – bosonic or fermionic, there can be two kinds of vacua. That is to say, the topologically trivial local excitations in the vacuum can be either bosonic or fermionic in nature, such as in a Ising paramagnet for the former and a trivial band insulator for the latter. In the works mentioned above, it was always implicitly assumed that a gapped edge of a bosonic topological phase implied a domain wall between a bosonic topological phase and a bosonic vacuum, and in particular, meant that the possibility of a fermionic vacuum was not considered.

A natural question is, does it even make sense to consider gapped boundaries between bosonic topological orders and fermionic vacua? We would like to argue that the answer is yes, one must consider this generalized scenario for computing the number of gapped boundary types if the bosonic topological order emerges from a system with local fermionic degrees of freedom (such as a system of electrons).

This can naturally happen if a system with local *fermionic* degrees of freedom is in a gapped phase where the local fermions are confined at low energies, and thus lead to a topological order with bosonic locality. An example is the large U limit of the Hubbard model, which can lead to gapped spin liquids with bosonic topological order [77]. Another example is a two-dimensional s-wave superconductor which, due to the Higgs mechanism and charge 2 of the Higgs field (Cooper pair), at low energy is described by a $\mathbb{Z}_2$ gauge theory and thus have topological order [76]. Therefore a case where a bosonic topological phase has a domain wall with a fermionic vacuum could occur, for example, between a two-dimensional superconductor and a band insulator.

In this chapter, we analyze the gapped edges that appear at the junction between a bosonic topological phase and a fermionic vacuum. In this scenario, we find new gapped edges, in principle beyond the ones found in [89, 90, 91], which we call *fermionic gapped edges*.

These new edges can be understood in two ways: 1) in the framework of Lagrangian subgroups $\mathcal{M}$ in Ref. [89], we show that the condition to find $\mathcal{M}$, which states that quasiparticles in $\mathcal{M}$ must be self-bosons, should be modified to allow self-fermions as well. We will see below that this condition arises from an allowed physical process of 'fermion condensation': if and only if a quasiparticle in the bosonic topological phase is a self-fermion, then it can combine with a real fermion on the boundary in a process reminiscent of 'Cooper pairing' to condense on the boundary. This leads to the new fermionic gapped edges. 2) We also provide a modular invariance argument and show that a relaxation of the modular invariance constraint on the partition function from $Z(\tau) = Z(\tau + 1)$ to $Z(\tau) = Z(\tau + 2)$ generates these new fermionic gapped edges.

To illustrate the presence of a fermionic gapped edge, we consider a system with bosonic $\mathbb{Z}_2$ topological order. The bosonic topological state hosts an array of topological quasiparticles $\{1, e, m, f\}$. It is well understood that there are two Lagrangian subgroups $\mathcal{M}_e = \{1, e\}$ and $\mathcal{M}_m = \{1, m\}$ which correspond to condensing the two self-boson quasiparticles, e and m respectively, leading to two topologically distinct gapped edges. However, if we consider the more general notion of gapped edge, we find that there will be an additional Lagrangian subgroup $\mathcal{M}_f = \{1, f\}$ corresponding to condensing the self-fermion quasiparticle – this leads to a new, topologically distinct fermionic gapped edge. We further demonstrate the process of fermion condensation explicitly in a microscopic model, the $\mathbb{Z}_2$ Wen-plaquette model [195] (unitarily equivalent to the Kitaev toric code model [69]) coupled to an array of Majorana fermions (the gapped fermionic vacuum), showing clearly the mechanism of condensation of the f-quasiparticle. We then explore the rich phase diagram of the edge theory of this model by mapping the edge theory to a modified Ashkin-Teller model. We show that there are critical lines of $c = 1$ $\mathbb{Z}_2$-orbifold boson CFTs separating the three gapped phases, including ones with exotic symmetries such as twisted $N = 2$ supersymmetry. Another feature is that the $\mathbb{Z}_2$ electro-magnetic duality of the $\mathbb{Z}_2$ topological order, is effectively extended to a full S_3 symmetry, corresponding to permutations of all quasiparticles. This implies that the boundary theory is equipped with a non-abelian Kramers-Wannier duality, constraining the phase diagram considerably. This is indeed directly observed in the study of the boundary theory.

The chapter is organized as follows. Sec. 7.2 presents a brief but necessary review of the formalism for characterizing abelian topological order using abelian Chern-Simons theory. Sec. 7.3 presents our work– we analyze the domain wall between a bosonic abelian

154

topological phase and a fermionic vacuum. We argue for the modification of the condition in the Lagrangian subgroups $\mathcal{M}$ that quasiparticles in $\mathcal{M}$ should be self-bosons to include self-fermions. We also provide a modular invariance argument. In sec. 7.4, we provide a few examples, and in particular illustrate the fermionic gapped edge in a system with bosonic $\mathbb{Z}_2$ topological order. We further explicitly construct a microscopic model realizing this topological order: the $\mathbb{Z}_2$ Wen-plaquette model coupled to an array of Majoranas fermions at the boundary. Sec. 7.5.3 analyzes the phase diagram of this model. We conclude with a discussion in sec. 7.6.

7.2 Topological order and gapped edges

7.2.1 Characterization of topological order

In this section, we briefly review (2+1)-d abelian Chern-Simons theory. The review in this section largely follows [90]. A systematic description of all abelian topological states is believed to given by (2+1)-d abelian Chern-Simons (CS) theory [105], described by a Lagrangian density with a non-singular, integer K-matrix

$$\mathcal{L} = \frac{1}{4\pi} K_{IJ} \epsilon^{\mu\nu\lambda} a_\mu^I \partial_\nu a_\lambda^J, \tag{7.1}$$

where a^I, $I = 1, \cdots, \mathrm{rank}(K)$ are compact $U(1)$ gauge fields, and μ, ν, λ are $(2+1)$-d space-time indices. The topologically non-trivial quasiparticles are described by integers vectors $\vec{l}$, where two integer vectors $\vec{l}$ and $\vec{l'}$ describe topologically equivalent quasiparticles if $\vec{l'} = \vec{l} + K\vec{\Lambda}$, where $\vec{\Lambda}$ is an integer vector. Therefore, the integer lattice in $\mathrm{rank}(K)$ dimensions, modulo this equivalence relation, defines a discrete group consisting of the quasiparticles, with the number of topologically distinct quasiparticles given by $|\mathrm{Det}(K)|$. Vectors $K\vec{\Lambda}$ describe local particles, which are always bosons or fermions.

If the K-matrix has all diagonal elements that are even integers, then the K-matrix is said to be even and all local particles are bosons – such a K-matrix describes bosonic topological order; otherwise, the K-matrix is said to be odd and the microscopic degrees of freedom must contain fermions (possibly in addition to bosons) – such a K-matrix describes fermionic topological order. The signature of the K-matrix is defined to be the number of positive eigenvalues minus the negative eigenvalues.

The mutual statistics of two quasiparticles labeled by $\vec{l}$ and $\vec{l'}$ are given by

$$\theta_{\vec{l}, \vec{l'}} = 2\pi \vec{l}^T K^{-1} \vec{l'} \mod 2\pi, \tag{7.2}$$
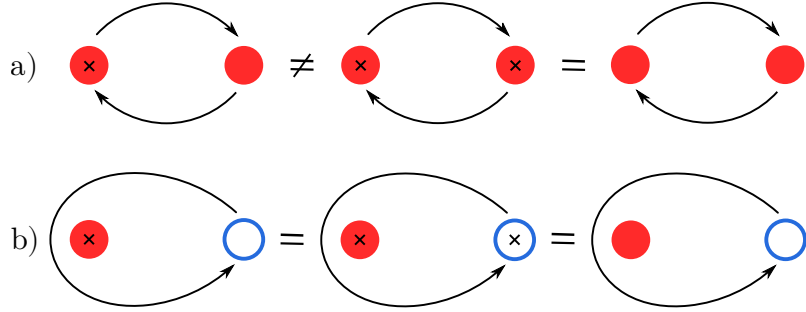
Figure 7.2.1: (a) Self-statistics and (b) mutual statistics of quasiparticles. Different colors and shadings correspond to different quasiparticle types, while $\times$ illustrates the presence of a local fermion. Only the self-statistics (a) will have an ambiguity of π in the presence of a local fermion, since in (b), any possible phase from the local fermion will cancel due to the double exchange in the mutual statistics.

while the self-statistics (also called exchange statistics) of a quasiparticle $\vec{l}$ is given by

$$\theta_{\vec{l}} = \pi \vec{l}^T K^{-1} \vec{l} \begin{cases} \text{mod } \pi \text{ for fermionic topological order,} \\ \text{mod } 2\pi \text{ for bosonic topological order.} \end{cases} \tag{7.3}$$

We can understand the difference in the condition for the self-statistics for fermionic and bosonic topological order as follows. In fermionic topological order, there exists local fermions which are topologically trivial, in the sense that the creation and removal of these local fermions are effected by local operators acting on the system. Hence, a non-trivial quasiparticle can come 'bound' together with an odd or even number of local fermions, and there is a sign ambiguity of π if one attempts to compute the self-statistics of a pair of quasiparticles. In order to achieve a consistent notion of self-statistics, one has to mod out this π phase ambiguity. No such ambiguity happens for the mutual statistics since there is a double exchange of quasiparticles, leading to a cancellation of the π phase of the fermions. This ambiguity is depicted in Fig. 7.2.1.

Note that different K-matrices can specify equivalent topological states if they have the same quasiparticle content. One such transformation is $K \rightarrow W^T KW$, where W is an integer matrix with $|\text{Det}(W)| = 1$, while another transformation is by extending an even (odd) K-matrix to $K' = K \oplus K_0$, where K_0 is an even (odd) even-dimensional, zero signature matrix with $|\text{Det}(K_0)| = 1$. Extending K to K' in this way does not add any topological quasiparticles, so K' and K describe the same topological order.

The abelian Chern-Simons theory in the bulk, eqn. 7.1, possesses gapless edge states

described by a (1+1)-d Luttinger liquid theory [105]:

$$\mathcal{L}_{\text{edge}} = \frac{K_{IJ}}{4\pi} \partial_x \phi_I \partial_t \phi_J - V_{IJ} \partial_x \phi_I \partial_x \phi_J, \tag{7.4}$$

where V_{IJ} is a positive-definite velocity matrix. The number of left and right moving bosons, n_L and n_R are set by the number of positive and negative eigenvalues of K respectively. The electron operators Ψ_I and quasiparticle operators $\chi_{\vec{l}}$ on the edge are given by

$$\Phi_I = e^{iK_{IJ}\phi_J}, \quad \chi_{\vec{l}} = e^{i\vec{l}^T \phi}, \tag{7.5}$$

where $\vec{l}$ is an integer vector labeling the quasiparticles and Φ_Is are real compact scalar fields: $\Phi_I \sim \Phi_I + 2\pi$. When Φ_I has integer scaling dimension, the "electron" is a boson, while if it has half-integer scaling dimension, it is a fermion.

This Luttinger liquid theory describing the edge, eqn. 7.4, is gapless. Local, backscattering terms can be added to the Lagrangian to generate an energy gap in the edge theory. Note that since backscattering terms gap out left and right moving modes in equal numbers, a K-matrix with non-vanishing signature can never be fully gapped. Hence, for an abelian topological phase to be possibly fully gapped, it is a necessary (but not sufficient) condition for the K-matrix to have vanishing signature.

In this chapter, we restrict ourselves to K-matrices that have non-vanishing signature and dimension $2N$ - in other words, systems with non-chiral, abelian topological order.

7.2.2   Gapped edges

In this section, we present the classification derived in [89, 90, 91] for all topologically distinct gapped edges an abelian topological state can support when placed next to a topologically trivial bosonic vacuum, in terms of the Langrangian subgroups $\mathcal{M}$ of topological quasiparticles in the theory.

A gapped edge in an abelian topological state next to a topologically trivial vacuum is possible if and only if there exists a subset of quasiparticle types, called a Lagrangian subgroup $\mathcal{M}$, such that

1. All quasiparticles in $\mathcal{M}$ have trivial mutual statistics, i.e. $e^{i\theta_{m,m'}} = 1$ for any $m, m' \in \mathcal{M}$,

2. Every quasiparticle that is not in $\mathcal{M}$ has nontrivial mutual statistics with at least one quasiparticle in $\mathcal{M}$, that is, if $l \notin \mathcal{M}$, then there exists an $m \in \mathcal{M}$ with $e^{i\theta_{l,m}} \neq 1$,

and for bosonic abelian topological order,

3. All quasiparticles in $\mathcal{M}$ must be self-bosons, i.e. $e^{i\theta_m} = 1$ for all $m \in \mathcal{M}$.

The proof of this involves going from this abstract Lagrangian subgroup language to null quasiparticles and then to adding local backscattering terms to the edge Lagrangian [89].

We give a physical picture as to what the set $\mathcal{M}$ describes: this is the set of quasiparticles that can be simultaneously condensed at the edge, consistently. Condensation is the idea that we can create a quasiparticle/quasihole pair $m, \bar{m}$ deep in the bulk from the vacuum state (not to be confused with the vacuum system!), adiabatically move them to two points a, b far away from each other using a Wilson line operator $W_{m,ab}$, but both near the boundary, and then annihilate them by two exponentially localized operators U_a, U_b at points a, b respectively, to return the system back to the vacuum state. That is,

$$U_a U_b W_{m,ab} |\psi_{\text{vac}}\rangle = |\psi_{\text{vac}}\rangle. \tag{7.6}$$

Intuively, the notion of a gap in the bulk and the edge is required to be able to adiabatically move the quasiparticles in the bulk, and also to be able to condense them by exponentially localized operators U_a and U_b at the edge.

However, not all quasiparticles can be consistently condensed on the boundary, which leads to the three conditions to find $\mathcal{M}$. Condition 1 in the definition of $\mathcal{M}$ can be understood as the statement that all quasiparticles of different types in $\mathcal{M}$ can be simultaneously condensed, regardless of the order in which they are condensed. If a pair of quasiparticles are not mutual bosons, then there is an inconsistency arising from the non-trivial mutual statistics– hence all quasiparticles in $\mathcal{M}$ must be mutual bosons . Condition 2 can be thought of as the statement to find the maximal set of quasiparticles that can be simultaneously condensed on the boundary in order to obtain a topologically distinct gapped edge. All other quasiparticles not in $\mathcal{M}$ must be confined after condensation of quasiparticles of $\mathcal{M}$, i.e. they must be able to be 'detected' through an Aharanov-Bohm type measurement. Otherwise, they can be added to $\mathcal{M}$ without leading to a new type of gapped edge. Condition 3 for bosonic abelian topological states is also a self-consistency condition for condensation of two pairs of quasiparticles of the same type but in different order. However, as we will argue later, this self-consistency condition relies on the fact the exponentially localized operators U_a and U_b are bosonic in nature (they mutually commute

if separated far apart), and should be relaxed if, at the boundary, U_a and U_b can acquire different commutation relations due to different notions of locality in the vacuum.

Now, one can also understand the domain wall between two different theories A_1 and A_2 harboring two different kinds of topological order using a simple and well-known trick called the folding trick. We can imagine folding A_2 back onto A_1, to obtain a boundary between the topological phase $A_1 \times \bar{A}_2$ and the topologically trivial gapped (bosonic) phase, thus reducing the analysis to the one we have presented above – finding the Lagrangian subgroups $\mathcal{M}$ of $A_1 \times \bar{A}_2$. Here $\bar{A}_2$ is the parity-reversed copy of A_2, which is necessary because the folding trick changes the parity of the state that is being folded.

7.3   Fermionic gapped edge

7.3.1   Lagrangian subgroup formalism and fermion condensation

In this section, we consider the topologically distinct gapped edges of a bosonic abelian topological phase interfaced with a fermionic vacuum. Luckily most of the analysis follows from a small modification of the arguments given in [89], however we will spell out some of the details and give a physical picture behind the processes leading to a fermionic gapped edge.

We can model this set-up as follows: let K_{TO} be the K-matrix corresponding to a bosonic abelian topological state living in the left half-plane, and let K_t describe K-matrix of the topologically trivial fermionic gapped system system living in the right half-plane. This condition requires K_{TO} to have only even numbers along the diagonal and vanishing sign. The fermionic vacuum can be easily characterized by the following K-matrix; $K_t = \begin{pmatrix} 1 & 0 \\ 0 & -1 \end{pmatrix}$, since $|K_t| = 0$, the sign vanishes and the diagonal contains odd numbers (thus there are local fermionic degrees of freedom).

Although this combined system of fermionic and bosonic locality seems strange, we can directly map into a problem we know how to deal with. We can attempt to use the folding trick, which instructs us to view the bilayer system $K_{TO} \oplus K_t$ as having fermionic topological order since the combined K-matrix is odd. We therefore have to use the fermionic version of finding Lagrangian subgroups in Sec. 7.2.2, which leads to possibly more Lagrangian subgroups and hence more gapped edges. However, the folding trick does not give much insight into the physics involved – clearly, the actual topological order (in the non-folded system) is still bosonic in nature, so what does it really mean to treat the

combined system as having fermionic topological order? We would like a physical reason as to the appearance of more gapped edges without reference to the folding trick. What precisely about the locality nature of the vacuum allows for more quasiparticles in the topological phase to condense?

The key point is that in the original, unfolded system, while the self and mutual statistics of the quasiparticles in the bosonic topological phase indeed remain unchanged, the commutation relations of the exponentially localized operators U_a and U_b in Eqn. 7.6 that annihilates the quasiparticles on the boundary at points a and b respectively can change if we pair each operator up with a localized fermionic operator from the vacuum near the boundary, such as χ, a Majorana fermion operator. Precisely, we can have

$$\tilde{U}_\xi := U_\xi \otimes \chi_\xi, \qquad \xi = a, b, \tag{7.7}$$

which is still an exponentially localized operator at the boundary that removes the quasi-particle and creates a real fermion in the vacuum at the same time. Also, more importantly, if $[U_a, U_b] = 0$, then $\{\tilde{U}_a, \tilde{U}_b\} = 0$. Using $\tilde{U}$, this change in the commutation relation does not affect condition 1 and condition 2 to find $\mathcal{M}$ as described in Sec. 7.2.2. However, it does affect condition 3. First let us understand condition 3 better. Let the self-statistics of the m particle be θ_m. We want the order in which we condense two pairs of m quasiparticles on the boundary to be irrelevant, so consider the following process:

$$\begin{matrix} \overset{\displaystyle U_b}{\underset{\displaystyle U_d}{\bigg\langle}} \end{matrix} \times \begin{matrix} \overset{\displaystyle U_a}{\underset{\displaystyle U_c}{\bigg\langle}} \end{matrix} = (U_b U_d W_{m,bd})(U_a U_c W_{m,ac}) \tag{7.8}$$

which should bring the system back to the vacuum state. Here $W_{m,ij}$ is a Wilson loop from point i to j on the boundary for the particle of type m. Then, Eq. (7.8) is equivalent to

$$(U_b U_d)(U_a U_c) \begin{matrix} a \\ b \\ c \\ d \end{matrix} = e^{i\theta_m}(U_a U_b)(U_c U_d) \begin{matrix} a \\ b \\ c \\ d \end{matrix}$$

$$= e^{i\theta_m} \begin{matrix} U_a \\ U_b \end{matrix} \times \begin{matrix} U_c \\ U_d \end{matrix} \tag{7.9}$$

160

However, there is a phase factor $e^{i\theta_m}$ due to the self-statistics of m, and so Eqn. (7.6) and (7.9) are inconsistent if $\theta_m \neq 0$ – that is, if they are not self-bosons. Now consider if we use $\tilde{U}$ instead of U to annihilate the quasiparticles on the boundary. Then we have

$$(\tilde{U}_b\tilde{U}_d)(\tilde{U}_a\tilde{U}_c) \begin{array}{c} a \\ b \\ c \\ d \end{array} = -e^{i\theta_m}(\tilde{U}_a\tilde{U}_b)(\tilde{U}_c\tilde{U}_d) \begin{array}{c} a \\ b \\ c \\ d \end{array} \tag{7.10}$$

$$\begin{array}{c} \tilde{U}_b \\ \tilde{U}_d \end{array} \times \begin{array}{c} \tilde{U}_a \\ \tilde{U}_c \end{array} = -e^{i\theta_m} \begin{array}{c} \tilde{U}_a \\ \tilde{U}_b \end{array} \times \begin{array}{c} \tilde{U}_c \\ \tilde{U}_d \end{array}$$

where once again $(\tilde{U}_a\tilde{U}_c W_{m,ac})$ is understood to happen before $(\tilde{U}_b\tilde{U}_d W_{m,bd})$. Crucially now, the RHS of Eqn. (7.10) now has a phase factor $(-1) \times e^{i\theta_m}$, which can made equal to unity if $\theta_m = \pi$ – that is, if the quasiparticles are self-fermions, they can self-consistently condense. We see that condition 3 should then be relaxed to allow both self-bosons and self-fermions in the Lagrangian subgroup.

In principle, this argument just shows that if the boundary between a bosonic topological order and a fermionic vacuum is gapped, it must satisfy the criterion of Lagrangian subgroups without the self-boson condition. One still needs to show that having a bosonic topological order with a fermionic Lagrangian subgroup, one will be able to gap out the edge modes. This part of the analysis is however identical to the purely fermionic case and shown in ref. [89].

It is not hard to see that the modification of condition 3 to allow both self-bosons and self-fermions to be in the Lagrangian subgroup is actually equivalent to the situation if we compute self-statistics in the bosonic TO using the fermionic version of Eqn. 7.3 – that is, if we consider the bosonic topological phase as having fermionic topological order instead. Therefore, the folding trick gives an equivalent result to our analysis, except that in our approach we have explicitly elucidated the process of fermion condensation as the physical mechanism for fermionic gapped edges.

7.3.2 Modular invariance formalism

In this section[1] we give an alternative argument for the presence of fermionic gapped edges, related to the discussion given in Ref. [216]. This description has the advantage that it works for non-abelian theories too and can be computed from properties that in principle are available from the ground states[1, 2]. More details regarding the bosonic case can be found in Ref. [226].

Imagine a domain wall between two gapped systems, each described by an effective Chern-Simons theory. It is well-known that the boundary theory will be a conformal field theory [61, 62], with conformal families labeled by each topological particle in the bulk. If there are $i_L = 1, \ldots, n_L$ topological excitations of the left and $i_R = 1, \ldots, n_R$ on the right, we have the corresponding characters $\chi_{i_L}^R$ and $\chi_{i_R}^L$. The first quasiparticles, $i_L = 1$ and $i_R = 1$, will always be taken to be the identity quasiparticles on the L or R part respectively.

In order to be able to gap the conformal field theory (and regularize it on a lattice), a necessary condition is that there are no global gravitational anomalies, i.e. there are no anomalies with respect to large diffeomorphims. In other words, the partition function on the torus

$$Z(\tau) = \sum_{i_L i_R} \mathcal{M}_{i_L i_R} \chi_{i_L}^L(\tau) \overline{\chi_{i_R}^R(\tau)}, \tag{7.11}$$

must be modular invariant[89], where $\mathcal{M}_{i_L i_R} \in \mathbb{N}_0$ and τ is the complex-valued modular parameter characterizing the torus. Under modular transformations $S : \tau \to -1/\tau$ and $T : \tau \to \tau + 1$, the characters transform as

$$\chi^L(-1/\tau) = S_L \chi^L(\tau), \qquad \qquad \chi^L(\tau + 1) = T_L \chi^L(\tau),$$
$$\overline{\chi^R(-1/\tau)} = S_R^{-1} \overline{\chi^R(\tau)}, \qquad \qquad \chi^L(\tau + 1) = T_R^{-1} \overline{\chi^R(\tau)},$$

where (S_L, T_L) and (S_R, T_R) are the modular matrices[56, 89] for the anyon theory on the left and right, respectively. The condition for modular invariance $Z(\tau) = Z(-1/\tau) = Z(\tau + 1)$ gives us the constraints

$$S_L \mathcal{M} = \mathcal{M} S_R, \qquad T_L \mathcal{M} = \mathcal{M} T_R, \qquad \mathcal{M}_{11} = 1. \tag{7.12}$$

The last condition comes from the fact that the theory must always contain the conformal family corresponding to the identity operator and that it must be unique [59]. These

---

[1]We would like to thank Huan He for insightful discussions about the modular invariance approach.

162

conditions are similar to the ones stated in Ref. [216]. Furthermore it was shown that these conditions are equivalent to the notion of Lagrangian subgroups for bosonic abelian topological order, and thus are also sufficient in this case. The discussion however changes for a theory containing fermions: the condition $Z(\tau) = Z(\tau + 1)$ must be replaced by the weaker condition $Z(\tau) = Z(\tau + 2)$[89, 227]. With these weaker conditions we arrive at the following constraints on $\mathcal{M}$:

$$S_L\mathcal{M} = \mathcal{M}S_R, \qquad T_L^2\mathcal{M} = \mathcal{M}T_R^2, \qquad \mathcal{M}_{11} = 1. \qquad (7.13)$$

Any solution $\mathcal{M}$ will correspond to a possible gapped boundary, solutions of Eqn. (7.12) correspond to bosonic gapped edges while the extra solutions of Eqn. (7.13) correspond to fermionic gapped edges.

Using these weaker conditions in the proof given in the appendix of Ref. [216] we conclude that for bosonic abelian topological order, these conditions for fermionic gapped edges are equivalent to the ones given in section 7.3.1.

7.4 Examples

7.4.1 $\mathbb{Z}_2$ topological order

We illustrate the presence of a fermionic gapped edge in a system with bosonic abelian $\mathbb{Z}_2$ topological order, described by the K-matrix $K_B = \begin{pmatrix} 0 & 2 \\ 2 & 0 \end{pmatrix}$. The Kitaev toric code model is an example of a system with such topological order.

We first use the Lagrangian subgroup formalism. From sec. 7.2.1, we see that this bosonic topological state hosts an array of four topological quasiparticles which can be labeled $\{1, e, m, f\}$. 1 is the trivial quasiparticle, e and m are the electric and magnetic quasiparticles respectively, which are both self bosons ($\theta_{ee} = \theta_{mm} = 0$) but mutual semions, i.e. having mutual braiding statistics ($\theta_{em} = \theta_{me} = \pi$), while f is the fermion quasiparticle which is a self-fermion ($\theta_{ff} = \pi$) and have semionic mutual statistics with both e and m ($\theta_{ef} = \theta_{mf} = \pi$).

If the vacuum is bosonic, there are two bosonic Lagrangian subgroups which are known: $\mathcal{M}_e = \{1, e\}$ and $\mathcal{M}_m = \{1, m\}$, corresponding to two topologically distinct bosonic gapped edges, and which physically correspond to being able to condense e and m quasiparticles respectively. However, if we allow for a fermionic vacuum, then from our prescription, the

self-fermion f can condense, which leads to one more Lagrangian subgroup $\mathcal{M}_f = \{1, f\}$, corresponding to a fermionic gapped edge.

We next consider the modular invariance approach for the same system. We have the following modular matrices (in the basis of quasiparticles $\{1, e, m, f\}$):

$$T_L = \begin{pmatrix} 1 & & & \\ & 1 & & \\ & & 1 & \\ & & & -1 \end{pmatrix}, \qquad S_L = \frac{1}{2}\begin{pmatrix} 1 & 1 & 1 & 1 \\ 1 & 1 & -1 & -1 \\ 1 & -1 & 1 & -1 \\ 1 & -1 & -1 & 1 \end{pmatrix}. \tag{7.14}$$

interfaced with a trivial vacuum $T_R = S_R = 1$. Since $T_L^2 = 1$, we just need to consider find the right eigenvectors of S_L with eigenvalues 1 with $\mathcal{M}_{11} = 1$. There are the following three solutions

$$\mathcal{M}_e = (1, 1, 0, 0), \quad \mathcal{M}_m = (1, 0, 1, 0), \quad \mathcal{M}_f = (1, 0, 0, 1). \tag{7.15}$$

$\mathcal{M}_e$ and $\mathcal{M}_m$ correspond to the two bosonic gapped boundaries, as they are also right eigenvectors of T_L with eigenvalue 1, while $\mathcal{M}_f$ is a fermionic gapped boundary as it is not a right eigenvector of T_L with eigenvalue 1, but only of T_L^2.

7.4.2 $\mathbb{Z}_N$ topological order

It is straightforward to generalize the Lagrangian subgroup analysis to systems with bosonic $\mathbb{Z}_N$ topological order. For odd N, there are no topological quasiparticles that are self-fermions, and so no new Lagrangian subgroups will be generated. Thus, no new topologically distinct gapped edges can be realized by coupling the odd N bosonic $\mathbb{Z}_N$ topological state to a system of topologically trivial fermions. However, for even N, the situation is much richer. For example consider taking a general fermion $f = \begin{pmatrix} q \\ \frac{N}{2q} \end{pmatrix}$, one can directly check that it cannot be detected through mutual statistics by a charge $b = \begin{pmatrix} 2q \cdot x \\ \frac{N}{q} \cdot y \end{pmatrix}$ for $x \in \mathbb{Z}_{\frac{N}{2q}}$ and $y \in \mathbb{Z}_q$. These extra charges are all bosons. Any fusion of these charges also have trivial mutual statistics with each other. Thus for a $q \in \mathbb{Z}$ such that $\frac{N}{q} \in \mathbb{Z}$ and $\frac{N}{2q} \in \mathbb{Z}$ the charges

$$\begin{pmatrix} q \\ \frac{N}{2q} \end{pmatrix} \qquad \text{and} \qquad \begin{pmatrix} 2q \cdot x \\ \frac{N}{q} \cdot y \end{pmatrix} \tag{7.16}$$

generate a fermionic Lagrangian subgroup corresponding to a fermionic gapped boundary.

7.4.3 Ising × $\overline{\text{Ising}}$

A more interesting example for the modular invariance formalism is to consider the Ising × $\overline{\text{Ising}}$ theory, which can be described by doubled non-abelian Chern-Simons theories[132]. This model is non-abelian and thus beyond the formalism discussed earlier. Furthermore it contains fermionic particles which mean it might have fermionic gapped boundaries. The modular S and T matrices are given by[216]

$$T_L = \text{Diag}\left(1, e^{-\frac{\pi i}{8}}, -1, e^{\frac{\pi i}{8}}, 1, -e^{\frac{\pi i}{8}}, -1, -e^{\frac{-\pi i}{8}}, 1\right),$$

$$S_L = \frac{1}{4}\begin{pmatrix} ,1 & \phi & 1 & \phi & 2 & \phi & 1 & \phi & 1 \\ \phi & 0 & -\phi & 2 & 0 & -2 & \phi & 0 & -\phi \\ 1 & -\phi & 1 & \phi & -2 & \phi & 1 & -\phi & 1 \\ \phi & 2 & \phi & 0 & 0 & 0 & -\phi & -2 & -\phi \\ 2 & 0 & -2 & 0 & 0 & 0 & -2 & 0 & 2 \\ \phi & -2 & \phi & 0 & 0 & 0 & -\phi & 2 & -\phi \\ 1 & \phi & 1 & -\phi & -2 & -\phi & 1 & \phi & 1 \\ \phi & 0 & -\phi & -2 & 0 & 2 & \phi & 0 & -\phi \\ 1 & -\phi & 1 & -\phi & 2 & -\phi & 1 & -\phi & 1 \end{pmatrix},$$

where $\phi = \sqrt{2}$. The vacuum is given by $S_R = 1$ and $T_R = 1$. One can readily find that there are two solutions to the conditions Eqn. (7.13) labeled by b:

$$\mathcal{M}_b = (1, 0, b, 0, 1 - b, 0, b, 0, 1), \quad b \in \{0, 1\}. \tag{7.17}$$

Here $b = 0$ corresponds to a bosonic gapped edge and was found in Ref. [216]. For $b = 1$ we have a fermionic gapped edge.

7.5 Microscopic model: $\mathbb{Z}_2$ Wen-plaquette model

So far all the arguments for a fermionic gapped edge have been at the level of the underlying field theory of the system. It will be helpful and enlightening to explicitly show the process of fermion condensation and the presence of a fermionic gapped edge in a microscopic model.

The model we consider in the remainder of the chapter is the $\mathbb{Z}_2$ Wen-plaquette model acting on spins on a square lattice (unitarily equivalent to the Kitaev toric code), which is a microscopic Hamiltonian realizing the bosonic $\mathbb{Z}_2$ topological order described in the
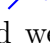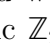
previous section, coupled to an array of Majorana fermions (the fermionic vacuum) on the boundary. We give a quick summary of the set-up and results: the full Hamiltonian is parameterized by two variables that change the coupling type between the spins and fermions, which produces all three topologically distinct edges. We find that the phase diagram in these two variables splits into three distinct gapped regions separated by continuous lines of $c = 1$ $\mathbb{Z}_2$–orbifold CFTs where the gap closes. Each gapped region in this phase diagram corresponds to a particular topologically distinct gapped edge theory in the topological phase.

7.5.1 Model

Consider the $\mathbb{Z}_2$ Wen-plaquette model on a semi-infinite plane. This is a model defined on a square lattice with spin-1/2 degrees of freedom living on the vertices (also called sites). The boundary of the lattice is taken to be 'smooth'–that is, the lattice is terminated beyond a certain line of spins. This line of spins forms an infinite 1d chain of spins that we will call the 'boundary spins'. Next, we will adorn the square lattice with a checkerboard coloring–white and grey. Such a choice of coloring is not unique, but in our analysis, we will always consistently work with one such choice. We label white plaquettes by a roman alphabet such as p, and grey plaquettes by an additional tilde label, such as $\tilde{p}$. Focusing our attention on the boundary spins, we label these spins with the set of integers (the choice of origin is arbitrary), but with the condition that two adjacent spins $(i, i+1)$ form a face of a grey plaquette in the bulk if i is even, while they form a face of a white plaquette in the bulk if i is odd. The coloring and labeling is made clear in Fig. 7.5.1.

Now, the Hamiltonian on this half of the system is given by

$$H_W = - \sum_{p \in \text{plaq.}} \mathcal{O}_p = - \sum_{p \in \text{plaq.}} \boxed{p}, \tag{7.18}$$

where $\mathcal{O}_p = \boxed{p} = Z_1 X_2 Z_3 X_4$ is a plaquette-operator acting on four spins around a plaquette as shown pictorally, with $\{X_i, Y_i, Z_i\}$ representing the Pauli-matrices on site i. The energy scale has been set to 1. Here we find it useful to introduce the following graphical notation: we represent the Pauli operator Z_i as a blue (red) string operator $\diagup_i$ ($\diagup_i$) and X_i as $\diagdown_i$ ($\diagdown_i$) if the strings live on white (grey) plaquettes, and we color the string black if the coloring does not matter. This model realizes the bosonic $\mathbb{Z}_2$ topological order we wish to consider.
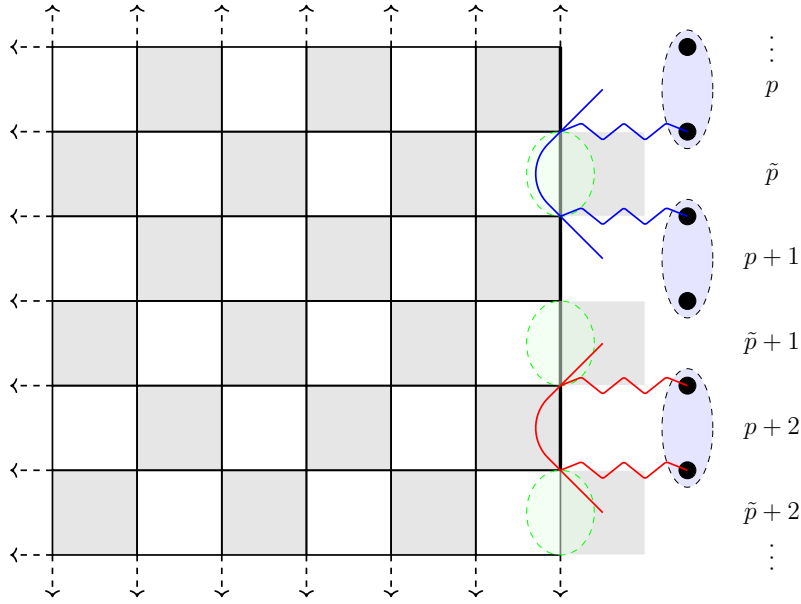
Figure 7.5.1: The semi-infinite square lattice on the left with a chain of Majorana fermions (big black dots) on the right. A checkerboard coloring (white $[p]$ and grey $[\tilde{p}]$) has been made on the square lattice, and we have also colored the 'plaquettes' outside the lattice. A labeling of the boundary spins has been made such that two adjacent spins $(i, i+1)$ form a face of a grey plaquette in the bulk if i is even, while they form a face of a white plaquette in the bulk if i is odd. Boundary string terms $Z_i X_{i+1}$ are represented as non-wavy open blue and red string operators if i is even or odd respectively, with end-points outside the lattice. Notice that the blue(red) boundary operators live entirely on white(grey) plaquettes. The wavy lines represent the coupling between the boundary terms to Majorana operators χ_i. The two composite operators shown here are both terms in $H_f : Z_i X_{i+1} \otimes i\chi_i\chi_{i+1}$. The green ellipses represent pseudo-spins of two real spins and the blue ellipses represent pairing of Majorana fermions, defined in the main text.

On the other semi-infinite plane, let us duplicate the square lattice of the Wen-plaquette model, but replace each spin-1/2 degree of freedom living on the vertices of the lattice with a Majorana fermion site χ. Any two Majorana modes χ_a and χ_b obey the anticommutation relations $\{\chi_a, \chi_b\} = 2\delta_{ab}$. In our model, we will only couple the spin-system to Majorana fermions that live directly adjacent to it; thus, we can simply treat the combined system as the semi-infinite Wen-plaquette model coupled to an infinite 1d chain of Majorana fermions, and discard the other Majorana fermions. Each Majorana fermion in this chain can therefore be labeled with the same label as its neighboring boundary spin. Then, the

167

full Hamiltonian is given by

$$H(\theta_1, \theta_2) = H_W + \epsilon H_\partial(\theta_1, \theta_2), \tag{7.19}$$

where $\epsilon < 1$, the energy gap in the bulk, and $H_\partial(\theta_1, \theta_2)$ represents the local boundary (denoted by ∂) terms coupling together the spins living adjacent to the Majorana fermions (to be specified below), parameterized by (θ_1, θ_2), where both $\theta_1, \theta_2 \in [0, \pi/2]$.

The boundary terms in H_∂ are given by

$$\begin{aligned} H_\partial(\theta_1, \theta_2) = {} & \cos\theta_1 H_e + \sin\theta_1 \cos\theta_2 H_m \\ & + \sin\theta_1 \sin\theta_2 H_f, \end{aligned} \tag{7.20}$$

where as the labeling suggests, H_e, H_m and H_f represent couplings that realize a particular edge theory corresponding to e, m and f quasiparticles respectively, and only affect the spins and Majorana fermions that live next to each other. They are given as follows:

$$\begin{aligned} H_e &= -\sum_{i\in\text{even}} Z_i X_{i+1} - \sum_{i\in\text{odd}} i\chi_i\chi_{i+1}, \\ H_m &= -\sum_{i\in\text{odd}} Z_i X_{i+1} - \sum_{i\in\text{even}} i\chi_i\chi_{i+1}, \\ H_f &= -\sum_{i} Z_i X_{i+1} \otimes i\chi_i\chi_{i+1}. \end{aligned} \tag{7.21}$$

Using the graphical notation introduced above, the term $Z_i X_{i+1}$ is a red (blue) boundary string operator with end-points outside the lattice that lives on grey(white) plaquettes if i is even(odd). See Fig. 7.5.1 for an illustration of these operators.

The parameters (θ_1, θ_2) tune the strengths of the various edge theories. At the special points $(\theta_1, \theta_2) = (0, 0)$, H_∂ gives a pure H_e edge theory, where e-quasiparticles are condensed on the boundary but m and f ones are confined, while $(\theta_1, \theta_2) = (\pi/2, 0)$ gives a pure H_m edge theory, where m-quasiparticles are condensed on the boundary but e and f ones are confined, and lastly $(\theta_1, \theta_2) = (\pi/2, \pi/2)$ gives a pure H_f edge theory, where f-quasiparticles are condensed on the boundary but e and m ones are confined – this is the fermionic gapped edge, which we will analyze below. Note also that at these special points, the full Hamiltonian is exactly solvable because all terms commute.

It is expected that the edge theory remains in the same phase (i.e. the gap does not close) as these special edge theories upon tuning (θ_1, θ_2) away from these special points (thus, the special points can be understood as fixed points in the RG sense), until the values of (θ_1, θ_2) are such that the strengths of two boundary theories are comparable and

the system undergoes a phase transition. We will thoroughly analyze the phase diagram of this model below, and also study the nature of the phase transition between the different topological gapped edges.

7.5.2 Rationale for model

Before proceeding to the analysis, let us explain how the Hamiltonian in (7.19) was obtained. To begin we must understand a few key properties of the Wen-plaquette model. The knowledgeable reader can skip the discussion of these properties and continue with the text after Eqn. (7.24).

Firstly, the Wen-plaquette model is an exactly solvable model as the plaquette terms $\mathcal{O}_p$ mutually commute. Thus, the ground state subspace is spanned by states which satisfy all $\mathcal{O}_p = +1$, the so-called flux-free condition, while excitations above the ground state subspace are because of plaquette violations: some $\mathcal{O}_p = -1$.

Secondly, plaquette violations come in pairs and they are generated by the generalized string operators acting on the ground state, also called Wilson line/string operators:

$$|\psi_{\text{exc.}}\rangle = W_{\gamma_{p,p'}}|\psi_{\text{g.s.}}\rangle. \tag{7.22}$$

Here $W_{\gamma_{p,p'}}$ is a string γ of neighboring Z_as and X_bs (a and b are sites in the bulk) that connect plaquettes p and p'. Only the end points of a string are physical, i.e. two strings γ, γ', with the same end points p, p' give rise to the same excited state $W_{\gamma_{p,p'}}|\psi_{\text{g.s.}}\rangle = W_{\gamma'_{p,p'}}|\psi_{\text{g.s.}}\rangle$. The plaquette violations live at the end points of the string, at the plaquettes p and p', and we can understand these plaquette violations as the presence of a quasiparticle–anti-quasiparticle pair. Note that these string operators live entirely on either the white or grey plaquettes (i.e. they can only connect p with p', or $\tilde{p}$ with $\tilde{p}'$, and not p with $\tilde{p}$).

Thirdly, there are four different kinds of quasiparticles $\{1, e, m, f\}$ in this model and they are anyons with statistics as described in sec. 7.4. They can be understood as follows. Two e-quasiparticles at $\tilde{p}, \tilde{p}'$ are created by a white string operator $W_{\gamma_{\tilde{p},\tilde{p}'}}$, while two m-quasiparticles at p, p' are created by a grey string operator $W_{\gamma_{p,p'}}$. An f-quasiparticle can be understood as a bound state of an e and m and is hence created by a bound string of e and m type. A canonical ordering of the application of $W_{\gamma_{\tilde{p},\tilde{p}'}}$ and $W_{\gamma_{p,p'}}$ type strings that creates e and m quasiparticles respectively has to be chosen in this case.

Fourthly, a quasiparticle is unconfined in the bulk. This means that there is no energy cost to moving a quasiparticle. If $|\psi_{m-m}\rangle$ is an excited state with two m-quasiparticles at p, p', then we can move one of the m quasiparticles to a neighboring white plaquette (say,

169
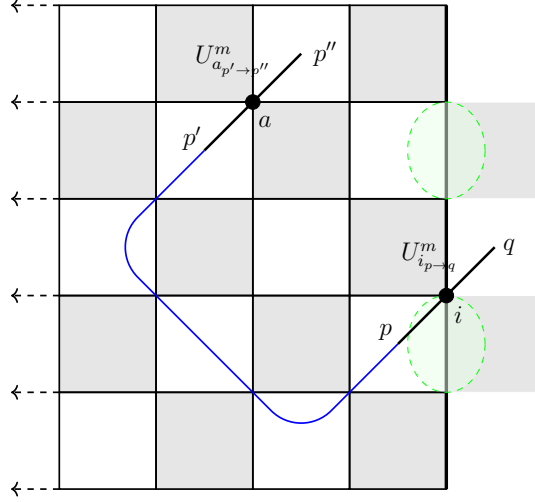
Figure 7.5.2: Movement and condensation of quasiparticles. The blue string operator initially depicts a state with two m-quasiparticle excitations at the plaquettes p, p'. To move an m-quasiparticle from p' to p'' in the bulk, we act on it with $U^m_{a_{p'\to p''}}$, where a is the bulk site that connects the plaquettes p' and p''. In this case, $U^m_{a_{p'\to p''}} = Z_a$. Condensation of a quasiparticle so that it ends up outside the boundary involves applying the same movement operators. In the diagram, the local operator $U^m_{i_{p\to q}} = Z_i$ acting on the boundary site i condenses an m-quasiparticle that initially lived inside the bulk (at p) to a plaquette outside the bulk (at q). The green ellipses represent pseudo-spins, defined in the main text.

$p' \to p''$) by the action of a local unitary operator $U^m_{a_{p'\to p''}}$ acting on site a, either Z_a or X_a, that connects the two white plaquettes p' and p''. This is simply nothing but the shortest m-Wilson string possible.

More precisely, the move is given as

$$
\begin{aligned}
|\psi_{m-m}\rangle := W_{\gamma_{p,p'}} |\psi_{\text{g.s.}}\rangle &\overset{\text{move}}{\to} U^m_{a_{p'\to p''}} |\psi_{m-m}\rangle \\
&\equiv W_{\gamma'_{p,p''}} |\psi_{\text{g.s.}}\rangle.
\end{aligned}
\tag{7.23}
$$

Both states before and after the move have similar energy. Fig. 7.5.2 shows such a movement.

Similarly, moves can be defined for the other quasiparticles, and they are given as follows.

1. Moving an e quasiparticle from $\tilde{p}'$ to $\tilde{p}''$: Acting by $U^e_{a_{\tilde{p}'\to \tilde{p}''}}$, where a is the site that connects $\tilde{p}'$ and $\tilde{p}''$, and $U^e_{a_{\tilde{p}'\to \tilde{p}''}} = Z_a$ or X_a depending on the orientation.

170

2. Moving an m quasiparticle from p' to p'': Acting by $U^m_{a_{p' \to p''}}$, where a is the site that connects p' and p'', and $U^m_{a_{p' \to p''}} = Z_a$ or X_a depending on the orientation.

3. Moving an f quasiparticle from $(p', \tilde{p}')$ to $(p'', \tilde{p}'')$: Acting by $U^e_{a_{\tilde{p}' \to \tilde{p}''}} U^m_{a_{p' \to p''}}$, where a is the common site connecting $(p', \tilde{p}')$ with $(p'', \tilde{p}'')$, and the local unitaries are defined as in the e and m move case.

By successively applying the local movement operators, we can move a quasiparticle anywhere in the system. In particular, if the Wen-plaquette model is defined on a system with a boundary, we can move a quasiparticle to the boundary by applying the local unitaries so that the resulting string γ has an end-point living on a 'plaquette' outside the system. The last local unitary U_a that effects this move is the 'exponentially localized' operator in Eqn. (7.6) that effects condensation. See Fig. 7.5.2 for an illustration of condensation.

Fifthly, for the Wen-plaquette model on a manifold with a boundary, there will be a macroscopic ground-state degeneracy as the plaquette conditions ($\mathcal{O}_p = +1$) do not uniquely define a microscopic number of ground-states. As shown in Ref. [4], one can further distinguish the states in this macroscopic ground-state subspace by the set of boundary terms $Z_i X_{i+1}$ (the set of operators which maximally commute is if we take all $i \in$ even or all $i \in$ odd) that act on two adjacent spins $(i, i+1)$ on the boundary, which all commute with $\mathcal{O}_p$. It is clear from our previous discussion then that the $Z_i X_{i+1}$s, depending on their coloring, are the shortest e or m Wilson strings that have two end-points outside the boundary. To be precise, say that $i \in$ odd, then,

$$Z_i X_{i+1} = W_{\tilde{p}, \tilde{p}+1}|_\partial, \tag{7.24}$$

where $\tilde{p}, \tilde{p} + 1$ are 'plaquettes' outside the Wen-plaquette model. See fig. 7.5.3 for an illustration of these operators. A ground state that satisfies $Z_i X_{i+1} = +1$ for some $i \in$ odd can then be understood as having some e-quasiparticles condensed at the boundary. Thus, the large number of ground states in the ground-state manifold for the Wen-plaquette model on a system with a boundary can be distinguished by the different configurations of condensed quasiparticles at the boundary.

We are now in a position to understand the rationale behind the boundary terms in Eqn. (7.21) that realizes the different topologically distinct gapped edges. If we have the Hamiltonian $H_W + H_e$, the ground state, in addition to being flux-free (given by H_W), is then also a condensate of e-quasiparticles (given by H_e, and furthermore we can ignore the Majorana part of the system for now as it decouples from the spins). Importantly, the theory is gapped as excitations are given by violations to the conditions $\mathcal{O}_p = +1$ or
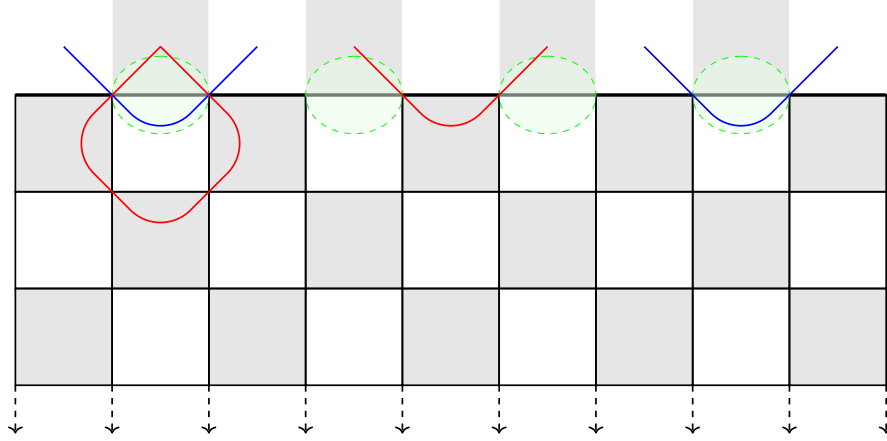
Figure 7.5.3: Boundary operators that measure condensation of quasiparticles. Left: an example of the shortest f-Wilson string operator on the boundary. The red string forms a loop which is a plaquette operator and is $+1$ in the ground state subspace. Middle: an example of the shortest e-Wilson string operator on the boundary. Right: an example of the shortest m-Wilson string operator on the boundary. The green ellipses represnt pseudo-spins, defined in the main text.

$Z_i X_{i+1} = +1$ which are finite in magnitude. Similarly, $H_W + H_m$ gives a gapped theory with the ground state being a condensate of m-quasiparticles. So, we see that the two boundary terms H_e and H_m give rise to the topologically distinct gapped edges labeled by the Lagrangian subgroups $\mathcal{M}_e = \{1, e\}$ and $\mathcal{M}_m = \{1, m\}$ respectively.

In order to realize the fermionic gapped edge we must condense the f-quasiparticle. Hence, we need to redefine the exponentially localized operator that annihilates the f-quasiparticle on the boundary as in Eqn. (7.7). That is, we need to redefine the f-quasiparticle move defined below Eqn. (7.23) on the boundary. There, we allow the f quasiparticle to pair up with the Majorana fermion. Thus, the move of an f-quasiparticle from a bulk plaquette pair $(p', \tilde{p}')$ to a boundary plaquette pair $(p'', \tilde{p}'')$ is now given by

$$U_i^f = U_{i_{\tilde{p}' \to \tilde{p}''}}^e U_{i_{p' \to p''}}^m \otimes e^{i\pi/4} \chi_i, \qquad (7.25)$$

(the phase factor is chosen to produce a factor of (i) in the Wilson loop below) where i is the boundary site that connects the pairs. This operator U_i^f is still unitary, and more importantly, is a local operator. This is important because it means that the condensation of one f-quasiparticle can be performed locally. Now, using this local move and forming

the shortest f Wilson string W^f on the boundary, we arrive at

$$W^f_{p,p+1}|_\partial = Z_i X_{i+1} \otimes i\chi_i\chi_{i+1} \text{ if } i \in \text{odd,}$$
$$W^f_{\tilde{p},\tilde{p}+1}|_\partial = Z_i X_{i+1} \otimes i\chi_i\chi_{i+1} \text{ if } i \in \text{even.}$$
(7.26)

Amazingly, all $W^f|_\partial$, even neighboring ones, commute. Therefore, the ground state of $H_W + H_f = H_W - \sum_i Z_i X_{i+1} \otimes i\chi_i\chi_{i+1}$ is now both flux free and a condensate of f-quasiparticles, and the theory is gapped! This is an example of the fermionic gapped edge alluded to in this chapter, corresponding to the Lagrangian subgroup $\mathcal{M}_f = \{1, f\}$.

7.5.3 Analysis of model

Having given the rationale behind the model, we now analyze the phase diagram of the Hamiltonian which realizes mixed boundary conditions,

$$H(\theta_1, \theta_2) = H_W + \epsilon H_\partial(\theta_1, \theta_2),$$
(7.27)

in full detail, given by equations (7.19), (7.20), and (7.21), and where $\epsilon < 1$. Specifically, we look at the phase diagram in the parameter range $\theta_1, \theta_2 \in [0, \pi/2]$.

Low energy effective Hamiltonian

We wish to only analyze the ground state of $H(\theta_1, \theta_2)$. Assuming that $\epsilon < 1$ so that the boundary term H_∂ does not close the gap of the ground state manifold of H_W to the excited states, we can simply look at the effective low energy Hamiltonian of $H(\theta_1, \theta_2)$, which can be calculated by the Schrieffer-Wolff transformation, as used in Ref. [4].

In essence, we look at the algebra of the operators of H_∂: $W^e|_\partial, W^m|_\partial, W^f|_\partial$ and $i\chi_i\chi_{i+1}$, acting in the flux-free sector of H_W. Now, boundary Wilson string operators of the same type commute with each other, and clearly, Wilson string operators, even of different types, commute if they have disjoint support. The same is true for the $i\chi_i\chi_{i+1}$ operators: if such an operator has disjoint support with any other operator, the two operators commute. Otherwise, they might give rise to non-trivial commutation relations. We thus only have to worry about boundary terms that have overlapping support (on either spins or Majorana fermions). Then we have the following non-trivial commutation/anticommutation relations

for operators with overlapping support:

$$\{W^m_{p,p+1}|_\partial, W^e_{\tilde{p},\tilde{p}+1}|_\partial\} = 0,$$
$$\{W^m_{p,p+1}|_\partial, W^f_{\tilde{p},\tilde{p}+1}|_\partial\} = 0,$$
$$\{W^f_{p,p+1}|_\partial, W^e_{\tilde{p},\tilde{p}+1}|_\partial\} = 0,$$
$$\{W^f_{p,p+1}|_\partial, i\chi_i\chi_{i+1}|_{i\in\text{even}}\} = 0,$$
$$\{W^f_{\tilde{p},\tilde{p}+1}|_\partial, i\chi_i\chi_{i+1}|_{i\in\text{odd}}\} = 0, \qquad (7.28)$$
$$[W^f_{\tilde{p},\tilde{p}+1}|_\partial, i\chi_i\chi_{i+1}|_{i\in\text{even}}] = 0,$$
$$[W^f_{p,p+1}|_\partial, i\chi_i\chi_{i+1}|_{i\in\text{odd}}] = 0,$$
$$[W^m_{p,p+1}|_\partial, W^f_{p,p+1}|_\partial] = 0,$$
$$[W^e_{\tilde{p},\tilde{p}+1}|_\partial, W^f_{\tilde{p},\tilde{p}+1}|_\partial] = 0.$$

We can find a representation of this algebra using two sets of spin-1/2 variables, σ and τ, each obeying the Pauli algebra, by the following identification:

$$W^e_{\tilde{p},\tilde{p}+1}|_\partial \to \sigma^z_n\sigma^z_{n+1},$$
$$W^m_{p,p+1}|_\partial \to \sigma^x_n,$$
$$W^f_{\tilde{p},\tilde{p}+1}|_\partial \to \sigma^z_n\sigma^z_{n+1}\tau^z_n\tau^z_{n+1}, \qquad (7.29)$$
$$W^f_{p,p+1}|_\partial \to \sigma^x_n\tau^x_n,,$$
$$i\chi_i\chi_{i+1}|_{i\in\text{odd}} \to \tau^x_n$$
$$i\chi_i\chi_{i+1}|_{i\in\text{even}} \to \tau^z_n\tau^z_{n+1},$$

where the σ_n operator acts on a pseudo-spin (n) comprised of two adjacent real spins, and the τ_n operator acts on pairs (labeled also by n) of adjacent Majorana fermions (see Fig. 7.5.1).

Then, the low energy effective Hamiltonian of $H_W + \epsilon H_\partial(\theta_1, \theta_2)$ simply becomes a Hamiltonian acting on a spin-ladder system:

$$
H_{\text{eff}}(\theta_1, \theta_2) = \epsilon \left(-\cos\theta_1 \sum_n \left(\sigma^z_n\sigma^z_{n+1} + \tau^x_n \right) \right.
$$
$$
-\sin\theta_1 \cos\theta_2 \sum_n \left(\sigma^x_n + \tau^z_n\tau^z_{n+1} \right) \qquad (7.30)
$$
$$
\left. -\sin\theta_1 \sin\theta_2 \sum_n \left(\sigma^z_n\sigma^z_{n+1}\tau^z_n\tau^z_{n+1} + \sigma^x_n\tau^x_n \right) \right).
$$

174

Here we can drop the constant ϵ for the rest of the analysis because it is an overall multiplicative factor. Written in this form, this is nothing but a variant of the Ashkin-Teller model, which has been well studied. However, the Hamiltonian usually studied in the literature is when the model is parameterized as such:

$$H_{\text{AT}} = -\sum_n \left(\sigma_n^z \sigma_{n+1}^z + \sigma_n^x + \tau_n^z \tau_{n+1}^z + \tau_n^x \right)$$
$$- \lambda \sum_n \left(\sigma_n^z \sigma_{n+1}^z \tau_n^z \tau_{n+1}^z + \sigma_n^x \tau_n^x \right). \tag{7.31}$$

There, it is known that the model is critical for all values of $\lambda \in [-\sqrt{2}/2, 1)$, and is described by a $c = 1$ $\mathbb{Z}_2$-orbifold CFT with orbifold radius given by

$$R_O^2 = \frac{\pi}{2} \frac{1}{\cos^{-1}(-\lambda)}. \tag{7.32}$$

To translate the parameter range to our model, we have $\cos \theta_1 = \sin \theta_1 \cos \theta_2 > 0$, while $\lambda = \tan \theta_2$.

Phase diagram, order parameters and dualities

Phase diagram. – The parameters (θ_1, θ_2) tune the relative strengths of the various edge theories, and lie in $\theta_1, \theta_2 \in [0, \pi/2]$. As such, the vector $(\sin \theta_1 \cos \theta_2, \sin \theta_1 \sin \theta_2, \cos \theta_1)$ is a unit vector pointing in the upper quadrant of the sphere S^2, and so the phase diagram of this model is the 2-d suface area of the upper quadrant of S^2. For simplicity, we can project this surface onto the plane defined by $x + y + z = 1$, by shooting rays from the origin to the surface of the upper quadrant. Each ray will hit the plane and surface of the upper quadrant at only one point each and is thus an invertible mapping. The projection onto the plane of the surface of the upper quadrant will then be an equilateral triangle, with the three corners given by the special points $(\theta_1, \theta_2) = (0, 0)$, $(\pi/2, 0)$ and $(\pi/2, \pi/2)$. Fig. 7.5.4 shows the projection of the upper quadrant of the unit sphere S^2 onto the plane $x + y + z = 1$ which gives an equilateral triangle.

At the corners of the triangle, the edge theories are gapped and are purely H_e, H_m or H_f corresponding to $(\theta_1, \theta_2) = (0, 0)$, $(\pi/2, 0)$ and $(\pi/2, \pi/2)$ respectively. The effective Hamiltonians there are exactly solvable because all terms commute. In a finite region away from these special points, it is expected that the gap will not close and the edge theory remains in the same phase as the phase defined by the closest corner of the triangle (in some sense, the corners are the fixed points of the RG flow). This will be made precise
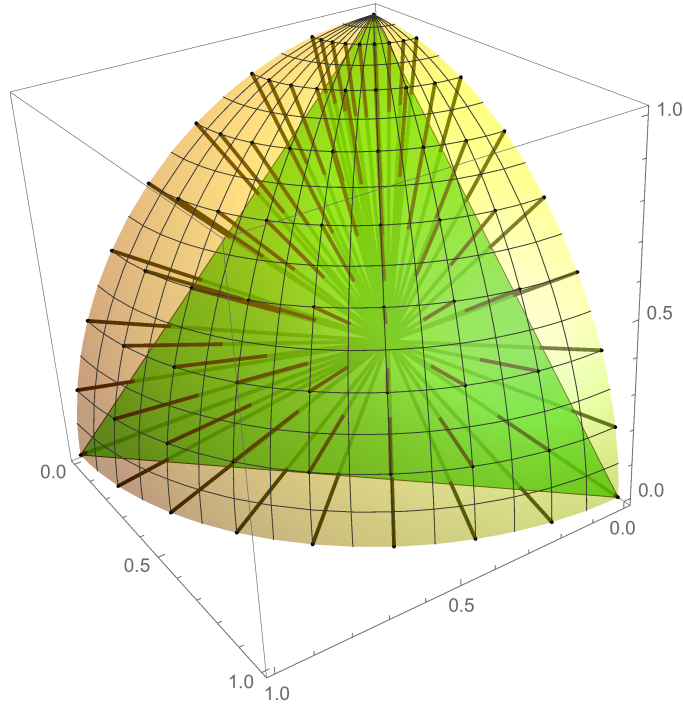
Figure 7.5.4: Projection of upper quadrant of the unit sphere S^2 onto the plane $x+y+z = 1$ which gives an equilateral triangle.

below by defining suitable order parameters that show a phase transition between the different phases. We will find from using the order parameters that the equilateral triangle is divided into three regions separated by three critical lines meeting at a common point in the middle of the triangle. One of these critical lines is the known critical line of the Ashkin-Teller model corresponding to $\cos\theta_1 = \sin\theta_1 \cos\theta_2$ alluded to before. Because of our restrictions on the range of $\theta_1, \theta_2, \lambda$, as defined in the previous section, which governs the orbifold radius for this critical line, only ranges from $[0, 1]$. Fig. 7.5.5 shows the resulting phase diagram on the equilateral triangle.

Order parameters and dualities.–We define order parameters that produce the phase diagram shown in fig. 7.5.5. To detect the $\mathcal{M}_e$ phase, we wish to find an order parameter that measures the presence of a condensate of e-quasiparticles, i.e. that it takes non-zero values in the $\mathcal{M}_e$ phase and is vanishing outside it. This implies that the order parameter must be non-local; indeed, from (7.29), the order parameter for detecting an e-condensate

176
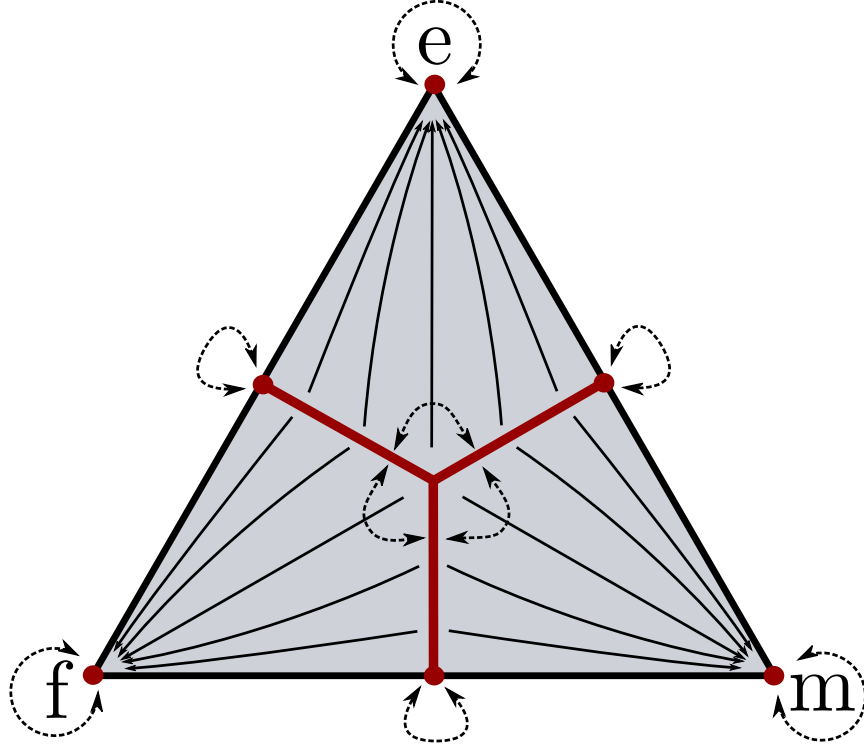
Figure 7.5.5: Projected phase diagram of Eqn. (7.30). The phase diagram is split into 3 different regions corresponding to the 3 gapped edge theories labeled by $\mathcal{M}_e$, $\mathcal{M}_m$, and $\mathcal{M}_f$. The gapped regions are separated by critical lines. Red lines are the critical lines, while red points are the fixed points of the RG flow. Black solid arrows in the triangle depict RG flow lines schematically, while dotted arrows indicate dualities. The three corners correspond to $(\theta_1, \theta_2) = (0, 0)$, which realizes a pure H_e edge theory, $(\theta_1, \theta_2) = (\pi/2, 0)$, which realizes a pure H_m edge theory, and $(\theta_1, \theta_2) = (\pi/2, \pi/2)$, which realizes a pure H_f edge theory.

should be

$$\langle \mathcal{O}_e \rangle := \lim_{m \to \infty} \langle \sigma_n^z \sigma_{n+m}^z \rangle, \tag{7.33}$$

where n is some arbitrary pseudospin, and the expectation is taken in the ground state. By similar reasoning the order parameter for detecting an m-condensate should be

$$\langle \mathcal{O}_m \rangle := \lim_{m \to \infty} \langle \prod_{k=1}^{m} \sigma_{n+k}^x \rangle, \tag{7.34}$$

177

and for an f-condensate the order parameters should be

$$\langle \mathcal{O}_{f_1} \rangle := \lim_{m \to \infty} \langle \sigma_n^z \sigma_{n+m}^z \tau_n^z \tau_{n+m}^z \rangle,$$

$$\langle \mathcal{O}_{f_2} \rangle := \lim_{m \to \infty} \langle \prod_{k=1}^m \sigma_{n+k}^x \tau_{n+k}^x \rangle. \tag{7.35}$$

One might worry about the presence of two different order parameters for the $\mathcal{M}_f$ phase: these came about because we arbitrarily subdivided our square lattice into grey and white plaquettes, and so the order parameters measure condensation of 'different' f-quasiparticles residing at different sites at the boundary. However, this division is arbitrary and not physical, and we expect that $\langle \mathcal{O}_{f_1} \rangle = \langle \mathcal{O}_{f_2} \rangle$.

Indeed, this is guaranteed by the many Kramers-Wannier dualities that the effective Hamiltonian (7.30) possesses. Consider the line L_{em} that bisects the line that connects the $\mathcal{M}_e$ and $\mathcal{M}_f$ points on the phase diagram (see fig. 7.5.5). Two points on the phase diagram which are related by the reflection about L_{em} are equivalent–that is, the two theories are the same. The reflection is effected by the simultaneous local unitary mappings on both chains

$$\begin{aligned} \sigma_n^z \sigma_{n+1}^z &\leftrightarrow \sigma_n^x \\ \tau_n^x &\leftrightarrow \tau_n^z \tau_{n+1}^z, \end{aligned} \tag{7.36}$$

each one of which is the usual $\mathbb{Z}_2$ Kramers-Wannier duality mapping that is encountered in, for example, the transverse field Ising model. Accepting the phase diagram of fig. 7.5.5 for now, this implies that the gapped phase of $\mathcal{M}_e$ gets swapped with $\mathcal{M}_m$, while $\mathcal{M}_f$ maps to itself. There is also another way to effect this duality: one can perform a swap of the two spin chains $\sigma \leftrightarrow \tau$.

Consider next the line L_{ef}. Two points on the phase diagram of the model are also equal under reflections about this line, and the local unitary mapping is given by

$$\begin{aligned} \sigma_n^z \sigma_{n+1}^z &\leftrightarrow \sigma_n^z \sigma_{n+1}^z \tau_n^z \tau_{n+1}^z \\ \tau_n^x &\leftrightarrow \sigma_n^x \tau_{n+1}^x. \end{aligned} \tag{7.37}$$

Here $\mathcal{M}_e \leftrightarrow \mathcal{M}_f$, while $\mathcal{M}_m$ maps to itself. Lastly, the same is true for the line L_{mf}. The mapping is

$$\begin{aligned} \sigma_n^x &\leftrightarrow \sigma_n^x \tau_n^x \\ \tau_n^z \tau_{n+1}^z &\leftrightarrow \sigma_n^z \sigma_{n+1}^z \tau_n^z \tau_{n+1}^z. \end{aligned} \tag{7.38}$$

We have $\mathcal{M}_m \leftrightarrow \mathcal{M}_f$, while $\mathcal{M}_e$ maps to itself.

The lines L_{em}, L_{ef}, L_{mf}, are self-dual under their respective mappings - this implies for example, for a fixed value of $\sin\theta_1 \sin\theta_2$, if the theory has a phase transition it must be along the line L_{em}. Note that however this does not imply that the line is guaranteed to be critical. The same analysis also holds for the lines L_{ef} and L_{mf}.

Using the dualities, we can understand how the order parameters are related. The order parameter $\langle \mathcal{O}_e \rangle$ is equal to the value of $\langle \mathcal{O}_m \rangle$ under a reflection across L_{em}. Also, applying the two different ways to effect L_{em} in succession leaves the model invariant; however, we have that $\mathcal{O}_{f_1} \leftrightarrow \mathcal{O}_{f_2}$ so $\langle \mathcal{O}_{f_1} \rangle = \langle \mathcal{O}_{f_2} \rangle$, as expected.

It is interesting that the critical lines contain very interesting theories with emergent symmetries, such as twisted $\mathcal{N} = 2$ superconformal symmetry [227]. One can also, starting from the Ising decoupling point, explicitly construct the marginal operators on the lattice that deforms the conformal field theory. Actually this is exactly how the Ashkin-Teller model can be constructed.

7.5.4 Numerics

We perform numerics to confirm the phase diagram of fig. 7.5.5. Using DMRG[228] we solve for the ground states of the effective model given by Eqn. (7.30) (setting $\epsilon = 1$), for a system size of $L = 200$ (for each spin chain), with open boundary conditions (OBC). We have also added weak pinning fields $\eta(\sigma_1^z + \sigma_L^z + \tau_1^z + \tau_L^z)$ ($\eta = 0.05 \ll 1$) at the ends of the chains to explicitly break the $\mathbb{Z}_2 \times \mathbb{Z}_2$ symmetry that the model has, in order to avoid obtaining a cat state as the ground state in the symmetry breaking phase. We do not expect the weak pinning fields to alter the analysis of the model as argued in the previous sections.

In the definition of the order parameters, the limit $m \to \infty$ is just an idealization, and for finite systems, m is necessary finite. In our numerics, we choose $n = 10$ and $n + m = 190$, which we find offers a very good balance between avoiding boundary effects from the OBC and m being large enough to simulate the thermodynamic limit. Deep in the expected gapped regions we find essentially exact results (truncation error $< 10^{-12}$), while nearer the expected critical lines the DMRG slows down significantly indicating the presence of criticality.

Fig. 7.5.6 shows the contour plot of the order parameter $\mathcal{O}_e$. One can quite clearly see that the order parameter is non-zero and in fact almost maximal in the region of the triangle that encompasses the point $\mathcal{M}_e$, while it is vanishing outside of it. This region defines the region of the phase diagram that belongs to the gapped phase $\mathcal{M}_e$.
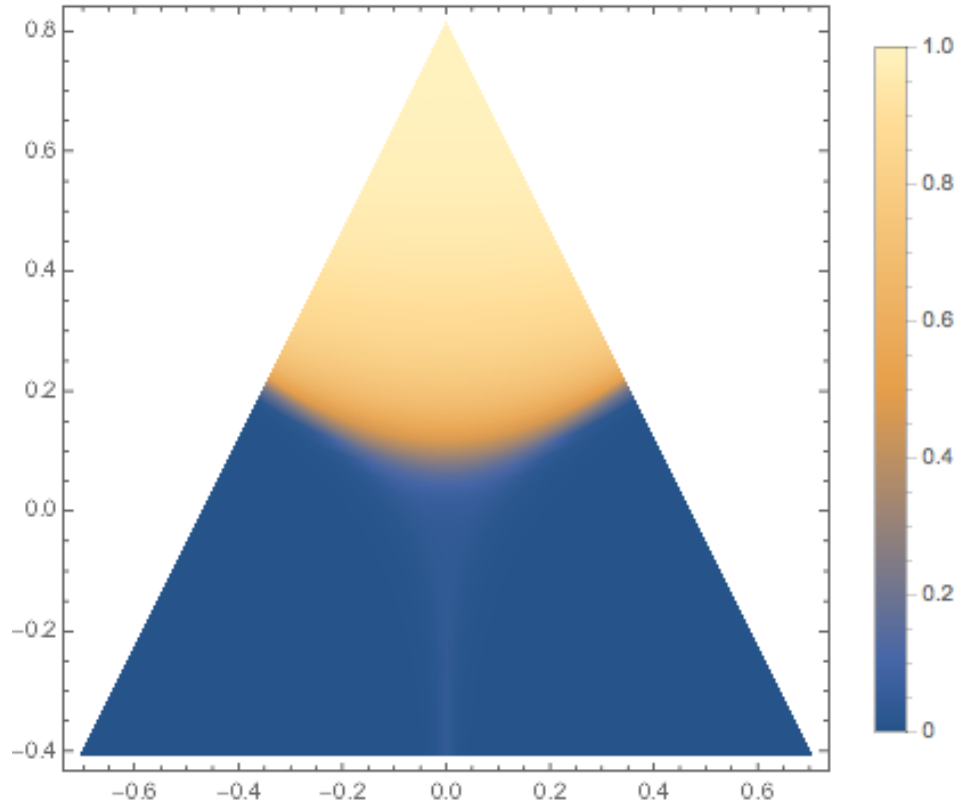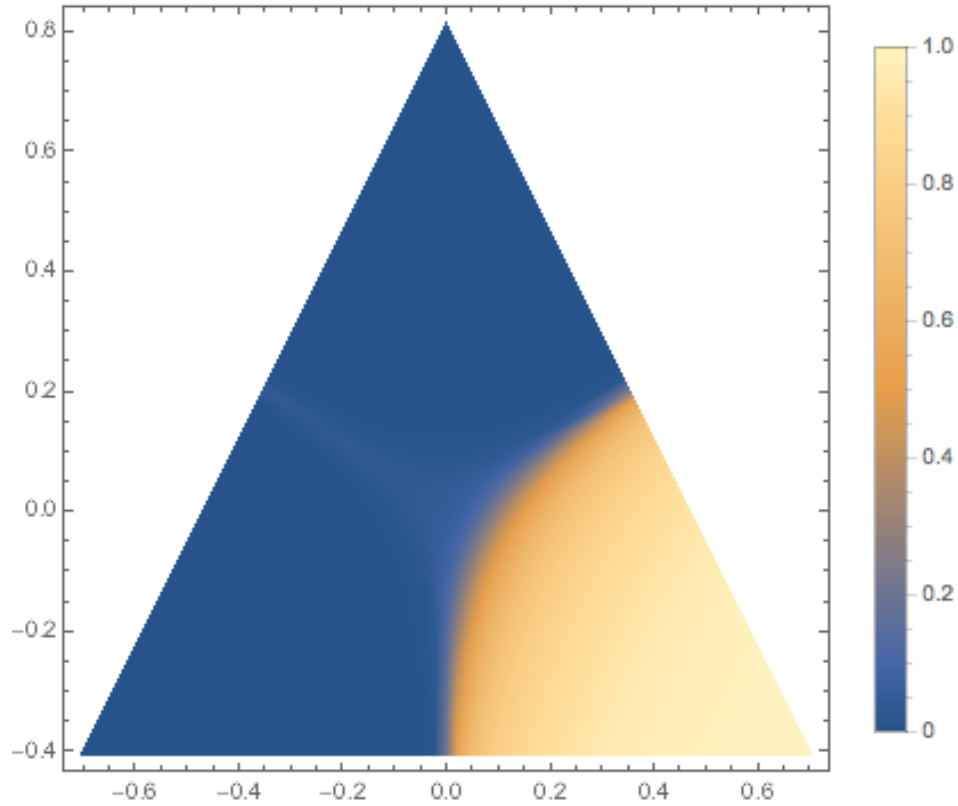
Figure 7.5.6: Contour plot of the order parameter $\langle \mathcal{O}_e \rangle$ for a system with open boundary conditions. Here the length of each chain is $L = 200$. One can see clearly that the order parameter is non-zero and in fact almost maximal in the region of the triangle that encompasses the point $(\theta_1, \theta_2) = (0, 0)$, while it is vanishing outside of it. This defines the gapped phase $\mathcal{M}_e$. The thin, light blue region emanating from the middle of the triangle to the bottom is an artifact of the system being at criticality there–the numerical error from the exact results to the result from the DMRG approach is large, and is expected to vanish upon taking the maximum bond dimension allowed in the simulations to ∞, which is impossible to achieve in practice.

We next plot the order parameter $\mathcal{O}_{f_1}$. We find that the order parameter is non-zero and in fact almost maximal in the region of the triangle that encompasses the point $(\theta_1, \theta_2) = (\pi/2, \pi/2)$. This defines the region of the phase diagram that belongs to the gapped phase $\mathcal{M}_f$. We also find numerically that the order parameter $\mathcal{O}_{f_2}$ gives the same result as $\mathcal{O}_{f_2}$, in agreement with our analysis.

Figure 7.5.7: Contour plot of the order parameter $\langle \mathcal{O}_{f_1} \rangle$ for a system with open boundary conditions, which we find (not shown) is equivalent to $\langle \mathcal{O}_{f_2} \rangle$. Here the length of each chain is $L = 200$. The region of the phase diagram where the order parameter is non-zero and in fact maximal defines the gapped phase $\mathcal{M}_f$.

For the last phase $\mathcal{M}_m$, we again obtain similar results using the order parameter $\mathcal{O}_m$.

Criticality, central charge and entanglement entropy

To confirm that the red lines of fig. 7.5.5 are in fact critical, we use DMRG to study periodic systems of size $L = 50$ along these critical lines and compute the entanglement entropy $S_L(x)$ of a subregion of size x. From there, we can extract the central charge c from the
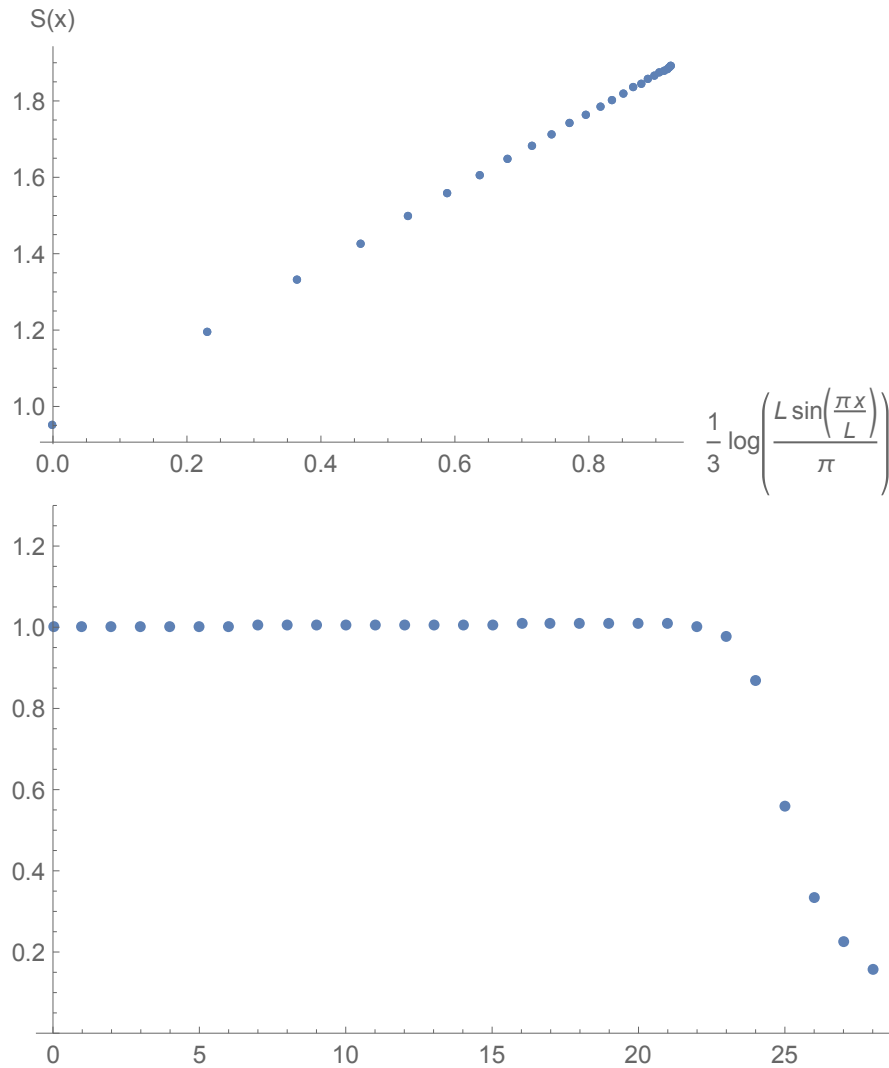
Figure 7.5.8: (a). Entanglement scaling $S_L(x)$ for a length-x subregion of a periodic system with $L = 50$ for one point along the critical line. By fitting to the CFT prediction, we extract a central charge $c = 1$, consistent with known results from the Ashkin-Teller model that the theory is described by a $\mathbb{Z}_2$-orbifold CFT. (b). Extracted central charge values along the line L_{em}. The extracted central charge is essentially constant at $c = 1$ from the beginning of L_{em} to the middle of the triangle, beyond which it quickly decays, indicating a loss of criticality.

entanglement scaling given by CFT calculations [229, 230]

$$S_L(x) = \frac{c}{3} \ln \left[\frac{L}{\pi} \sin \left(\frac{\pi x}{L} \right) \right]. \tag{7.39}$$

Fig. 7.5.8 shows the results. We see from the scaling results that extracted central charge is indeed $c = 1$, consistent with the known results that the Ashkin-Teller model is described by a $\mathbb{Z}_2$-orbifold CFT at the critical line. Beyond the midpoint of the triangle, the extracted central charge quickly decays, indicating a loss of criticality.

Putting the numerical results from the order parameters and entanglement scaling together, we therefore obtain the phase diagram of fig. 7.5.5.

7.5.5 Anyonic symmetry and Kramers-Wannier dualities

In this section we will give a short discussion regarding an observation of an interesting, but usually overlooked, universal feature of the boundary phase diagram.

The boundary of a chiral topological order is always gapless, where the gap is protected against any local perturbation not closing the bulk gap, and characterized by a universal number c_-, the chiral central charge. In the case of a non-chiral topological order we have $c_- = 0$, however the boundary still contain universal features. One feature, as discussed in [89, 90, 91] and this chapter, is that the number of distinct gapped boundary types is directly related to the bulk topological order, either through the notion of Lagrangian subgroups or S and T matrices.

Here we will explore another interesting feature related to anyonic symmetries and (potentially non-abelian) Kramers-Wannier dualities.

An *anyonic symmetry group* $\mathcal{A}$ is a subgroup of the permutation group S_N, permuting the anyons in a given topological order while leaving the statistics and fusion rules invariant. For an abelian topological order, this is given by[231]

$$\mathcal{N}_{\sigma(i)\sigma(j)}^{\sigma(k)} = N_{ij}^k \qquad \text{(Fusion rules)},$$
$$\theta_{\sigma(i)} = \theta_i \mod \pi \text{ or } 2\pi \qquad \text{(Self-statistics)},$$
$$\theta_{\sigma(i)\sigma(j)} = \theta_{ij} \qquad \text{(Mutual-statistics)},$$

where σ is an element of the subgroup $\mathcal{A}$ of the permutation group S_N, for a system with N anyons. Here the modulo 2π is for a system with bosonic topological order and

modulo π is for fermionic topological order. We can define the action of this symmetry on a Lagrangian subgroup $\sigma(\mathcal{M}_i)$, by its action on individual anyons in the subgroup. An immediate consequence of the above invariance properties is that if $\mathcal{M}_i$ is a Lagrangian subgroup, then $\sigma(\mathcal{M}_i)$ will also be. In other words, it will leave the set of Lagrangian subgroups $\mathcal{M} = \{\mathcal{M}_1, \mathcal{M}_2, \ldots, \mathcal{M}_n\}$ invariant

$$\sigma(\mathcal{M}_i) = \mathcal{M}_{\tilde{\sigma}(i)},$$

where $\tilde{\sigma}$ is a permutation of the Lagrangian subgroups, induced from σ, the anyonic symmetry of the anyons.

This implies that the bulk anyonic symmetry gives rise to some sort generalized Kramers-Wannier duality on the boundary, constraining the phase diagram of the boundary theory. This can be considered as another universal feature of topological order, the bulk anyonic statistics, through the anyonic symmetries, constrain the global structrue of the boundary phase diagram. Or in other words, anyonic symmetries in the bulk implies generalized Kramers-Wannier dualities on the boundary.

An example of this is the $\mathbb{Z}_N$ topological order which has a $\mathbb{Z}_2$ anyonic symmetry corresponding to the electro-magnetic duality. In ref. [4] we showed that this symmetry gives rise to the usual Kramers-Wannier duality of a Ising spin chain. This correspondence can be seen in more details when considering periodic boundary conditions and twist defects [4].

As argued in this chapter, if we allow for fermionic gapped edges we need to take the self-statistics to be defined only modulo π. This enhances the effective anyonic symmetry from $\mathbb{Z}_2$ to the full permutation groups S_3. As discussed in section 7.5.3, we indeed saw that the phase diagram is constrained by a non-abelian S_3 Kramers-Wannier duality. We can also understand each critical line in the phase diagram as having a Kramers-Wannier self-duality $(\mathcal{M}_e \leftrightarrow \mathcal{M}_m)$, $(M_e \leftrightarrow M_f)$ and $(M_m \leftrightarrow M_f)$ corresponding to a subgroup $\mathbb{Z}_2 \subset S_3$ of the anyonic symmetry, while the tricritical point where all three critical lines meet as realizing the full S_3 symmetry.

Another signature of this duality can be seen when considering periodic boundary conditions and twist defects, where different symmetry sectors and conformal defects are mapped to each other in non-trivial ways under the action of the bulk anyonic symmetry or boundary Kramers-Wannier duality. We examples of this in chapter 5. The relation between anyonic symmetries and generalized Kramers-Wannier dualities and their generalizations will be discussed in an upcoming work [92].

The model discussed here is closely related to the fermionic model discussed in [232], where the anyonic symmetries are realized as lattice symmetries. In this realization one can

explicitly construct Kramers-Wannier self-dual boundary conditions protected by lattice symmetries (similar to [4]) [233].

Another interesting aspect of this observation is that Kramers-Wannier dualities, and other aspects of spin-chains, can be understood from a holographic point-of-view as boundary theories of TQFT's. This opens up a route to study non-abelian Kramers-Wannier dualities [92] more systematically using (2+1)-dimensional topological order.

7.6 Conclusion

In this chapter, we have argued for the presence of a new topological gapped edge, the fermionic gapped edge, supported at the junction between a bosonic abelian topological state and a topologically trivial fermionic vacuum. We have presented two approaches to understanding this edge theory: one, through the Lagrangian subgroup formalism developed by [89, 90, 91], and two, through the modular invariance formalism. The presence of fermionic modes on the boundary implies that for the first case, the self-statistics of the quasiparticles must change, thereby possibly giving new Lagrangian subgroups which correspond to a topologically distinct gapped edge; while for the second case, the condition for modular invariance must be relaxed from $Z(\tau) = Z(\tau + 1)$ to $Z(\tau) = Z(\tau + 2)$, thereby offering potentially more solutions to the condition of gapping the CFT on the boundary. Physically, the fermionic gapped edge can be understood as a condensate of fermionic quasiparticles at the boundary.

To illustrate and substantiate our arguments, we have also explicitly constructed a microscopic model, the $\mathbb{Z}_2$ Wen-plaquette model coupled to an array of Majorana fermions on the boundary, and showed how fermionic condensation occurs in this model by redefining the microscopic moves for the fermionic quasiparticles. We have thoroughly analyzed the low energy effective Hamiltonian of this model through both analytic and numerical means, and showed that the phase diagram is indeed divided into three regions corresponding to the three topologically distinct gapped edges of the underlying bosonic topological order.

In upcoming work [92] we will discuss the relation between anyonic symmetries in Topological Quantum Field theories in $d+1$-dimensions and generalized Kramers-Wannier dualites in d-dimensions. In another work [96] we classify gapped boundaries and generalize the notion of lagrangian subgroups to $3 + 1$-dimensional topological order.

References

[1] H. Moradi and X.-G. Wen, "Universal Wave Function Overlap and Universal Topological Data from Generic Gapped Ground States," *Phys. Rev. Lett.* **115** no. 3, (2015) 036802, arXiv:1401.0518 [cond-mat.str-el].

[2] H. He, H. Moradi, and X.-G. Wen, "Modular matrices as topological order parameter by a gauge-symmetry-preserved tensor renormalization approach," *Physical Review B* **90** no. 20, (Nov., 2014) 205114, arXiv:1401.5557 [cond-mat.str-el].

[3] H. Moradi and X.-G. Wen, "Universal Topological Data for Gapped Quantum Liquids in Three Dimensions and Fusion Algebra for Non-Abelian String Excitations," *Phys.Rev.* **B91** no. 7, (2015) 075114, arXiv:1404.4618 [cond-mat.str-el].

[4] W. W. Ho, L. Cincio, H. Moradi, D. Gaiotto, and G. Vidal, "Edge-entanglement spectrum correspondence in a nonchiral topological phase and Kramers-Wannier duality," *Physical Review B* **91** no. 12, (Mar., 2015) 125119, arXiv:1411.6932 [cond-mat.str-el].

[5] W. W. Ho, L. Cincio, H. Moradi, and G. Vidal, "Universal edge information from wave-function deformation," *Phys. Rev.* **B95** no. 23, (2017) 235110, arXiv:1510.02982 [cond-mat.str-el].

[6] W. W. Ho and H. Moradi, "Fermionic gapped edges in bosonic abelian topological states via fermion condensation," *Unpublished* .

[7] P. W. Anderson, "More Is Different," *Science* **177** (1972) 393–396.

[8] L. D. Landau, "On the theory of phase transitions," *Zh. Eksp. Teor. Fiz.* **7** (1937) 19–32. [Ukr. J. Phys.53,25(2008)].

[9] L. D. Landau, "Theory of phase transformations I," *Phys. Z. Sowjetunion* **11** (1937) 26.

[10] L. D. Landau, "Theory of phase transformations II," *Phys. Z. Sowjetunion* **11** (1937) 545.

[11] L. D. Landau and E. M. Lifschitz, *Statistical Physics - Course of Theoretical Physics Vol 5*. Pergamon, London, 1958.

[12] J. Goldstone, A. Salam, and S. Weinberg, "Broken Symmetries," *Phys. Rev.* **127** (1962) 965–970.

[13] N. D. Mermin, "The topological theory of defects in ordered media," *Rev. Mod. Phys.* **51** (Jul, 1979) 591–648.
https://link.aps.org/doi/10.1103/RevModPhys.51.591.

[14] L. D. Landau, "The theory of a Fermi liquid," *Sov. Phys. JETP* **3** (1956) 920.

[15] R. Shankar, "Renormalization-group approach to interacting fermions," *Reviews of Modern Physics* **66** (Jan., 1994) 129–192, cond-mat/9307009.

[16] K. v. Klitzing, G. Dorda, and M. Pepper, "New Method for High-Accuracy Determination of the Fine-Structure Constant Based on Quantized Hall Resistance," *Phys. Rev. Lett.* **45** (Aug, 1980) 494–497.
https://link.aps.org/doi/10.1103/PhysRevLett.45.494.

[17] D. C. Tsui, H. L. Stormer, and A. C. Gossard, "Two-Dimensional Magnetotransport in the Extreme Quantum Limit," *Phys. Rev. Lett.* **48** (May, 1982) 1559–1562. https://link.aps.org/doi/10.1103/PhysRevLett.48.1559.

[18] R. B. Laughlin, "Anomalous Quantum Hall Effect: An Incompressible Quantum Fluid with Fractionally Charged Excitations," *Phys. Rev. Lett.* **50** (May, 1983) 1395–1398. https://link.aps.org/doi/10.1103/PhysRevLett.50.1395.

[19] X. G. Wen, "Topological Order in Rigid States," *Int. J. Mod. Phys.* **B4** (1990) 239.

[20] B. Zeng and X.-G. Wen, "Gapped quantum liquids and topological order, stochastic local transformations and emergence of unitarity," *Physical Review B* **91** no. 12, (Mar., 2015) 125121, arXiv:1406.5090 [cond-mat.str-el].

[21] R. Movassagh, "Generic Local Hamiltonians are Gapless," *Physical Review Letters* **119** no. 22, (Dec., 2017) 220504, arXiv:1606.09313 [quant-ph].

[22] T. S. Cubitt, D. Perez-Garcia, and M. M. Wolf, "Undecidability of the spectral gap," *Nature* **528** (Dec., 2015) 207–211, `arXiv:1502.04573 [quant-ph]`.

[23] T. Cubitt, D. Perez-Garcia, and M. M. Wolf, "Undecidability of the Spectral Gap (short version)," *ArXiv e-prints* (Feb., 2015) , `arXiv:1502.04135 [quant-ph]`.

[24] X. Chen, Z.-C. Gu, and X.-G. Wen, "Local unitary transformation, long-range quantum entanglement, wave function renormalization, and topological order," *Physical Review B* **82** no. 15, (Oct., 2010) 155138, `arXiv:1004.3835 [cond-mat.str-el]`.

[25] B. Swingle and J. McGreevy, "Renormalization group constructions of topological quantum liquids and beyond," *Physical Review B* **93** no. 4, (Jan., 2016) 045127, `1407.8203 [cond-mat.str-el]`.

[26] M. B. Hastings and X.-G. Wen, "Quasiadiabatic continuation of quantum states: The stability of topological ground-state degeneracy and emergent gauge invariance," *Physical Review B* **72** no. 4, (July, 2005) 045141, `cond-mat/0503554`.

[27] S. Bravyi, M. B. Hastings, and S. Michalakis, "Topological quantum order: Stability under local perturbations," *Journal of Mathematical Physics* **51** no. 9, (Sept., 2010) 093512–093512, `arXiv:1001.0344 [quant-ph]`.

[28] A. Kitaev, "Periodic table for topological insulators and superconductors," in *American Institute of Physics Conference Series*, V. Lebedev and M. Feigel'Man, eds., vol. 1134 of *American Institute of Physics Conference Series*, pp. 22–30. May, 2009. `arXiv:0901.2686 [cond-mat.mes-hall]`.

[29] J. Haah, "Local stabilizer codes in three dimensions without string logical operators," *Physical Review A* **83** no. 4, (Apr., 2011) 042330, `arXiv:1101.1962 [quant-ph]`.

[30] S. Vijay, J. Haah, and L. Fu, "A new kind of topological quantum order: A dimensional hierarchy of quasiparticles built from stationary excitations," *Physical Review B* **92** no. 23, (Dec., 2015) 235136, `arXiv:1505.02576 [cond-mat.str-el]`.

[31] S. Vijay, J. Haah, and L. Fu, "Fracton topological order, generalized lattice gauge theory, and duality," *Physical Review B* **94** no. 23, (Dec., 2016) 235157, `arXiv:1603.04442 [cond-mat.str-el]`.

[32] H. Ma, E. Lake, X. Chen, and M. Hermele, "Fracton topological order via coupled layers," *Physical Review B* **95** no. 24, (June, 2017) 245126, `arXiv:1701.00747 [cond-mat.str-el]`.

[33] K. Slagle and Y. B. Kim, "Quantum field theory of X-cube fracton topological order and robust degeneracy from geometry," *Physical Review B* **96** no. 19, (Nov., 2017) 195139, `arXiv:1708.04619 [cond-mat.str-el]`.

[34] A. Kitaev and J. Preskill, "Topological entanglement entropy," *Phys.Rev.Lett.* **96** (2006) 110404, `arXiv:hep-th/0510092 [hep-th]`.

[35] M. Levin and X.-G. Wen, "Detecting Topological Order in a Ground State Wave Function," *Phys.Rev.Lett.* **96** (2006) 110405, `arXiv:cond-mat/0510613 [cond-mat]`.

[36] J. Eisert, M. Cramer, and M. B. Plenio, "Colloquium: Area laws for the entanglement entropy," *Reviews of Modern Physics* **82** (Jan., 2010) 277–306, `arXiv:0808.3773 [quant-ph]`.

[37] D. N. Page, "Average entropy of a subsystem," *Physical Review Letters* **71** (Aug., 1993) 1291–1294, `gr-qc/9305007`.

[38] I. H. Kim, "Long-range entanglement is necessary for a topological storage of quantum information," *Phys. Rev. Lett.* **111** (2013) 080503, `arXiv:1304.3925 [quant-ph]`.

[39] H. Li and F. D. M. Haldane, "Entanglement Spectrum as a Generalization of Entanglement Entropy: Identification of Topological Order in Non-Abelian Fractional Quantum Hall Effect States," *Physical Review Letters* **101** no. 1, (July, 2008) 010504, `arXiv:0805.0332`.

[40] X.-L. Qi, H. Katsura, and A. W. W. Ludwig, "General Relationship between the Entanglement Spectrum and the Edge State Spectrum of Topological Quantum States," *Physical Review Letters* **108** no. 19, (May, 2012) 196402, `arXiv:1103.5437 [cond-mat.mes-hall]`.

[41] T. Grover, A. M. Turner, and A. Vishwanath, "Entanglement entropy of gapped phases and topological order in three dimensions," *Physical Review B* **84** no. 19, (Nov., 2011) 195120, `arXiv:1108.4038 [cond-mat.str-el]`.

[42] Y. Zheng, H. He, B. Bradlyn, J. Cano, T. Neupert, and B. A. Bernevig, "Structure of the entanglement entropy of (3+1)-dimensional gapped phases of matter," *Physical Review B* **97** no. 19, (May, 2018) 195118, `arXiv:1710.01747 [cond-mat.str-el]`.

[43] S. Dong, E. Fradkin, R. G. Leigh, and S. Nowling, "Topological entanglement entropy in Chern-Simons theories and quantum Hall fluids," *Journal of High Energy Physics* **5** (May, 2008) 016, `arXiv:0802.3231 [hep-th]`.

[44] B. Bradlyn and N. Read, "Topological central charge from Berry curvature: Gravitational anomalies in trial wave functions for topological phases," *Physical Review B* **91** no. 16, (Apr., 2015) 165306, `arXiv:1502.04126 [cond-mat.mes-hall]`.

[45] H.-H. Tu, Y. Zhang, and X.-L. Qi, "Momentum polarization: An entanglement measure of topological spin and chiral central charge," *Physical Review B* **88** no. 19, (Nov., 2013) 195412, `arXiv:1212.6951 [cond-mat.str-el]`.

[46] F. Cohen and J. Wu, "On braid groups and homotopy groups," *ArXiv e-prints* (Apr., 2009) , `arXiv:0904.0783 [math.AT]`.

[47] S. Doplicher, R. Haag, and J. E. Roberts, "Local observables and particle statistics I," *Commun. Math. Phys.* **23** (1971) 199–230.

[48] S. Doplicher, R. Haag, and J. E. Roberts, "Local observables and particle statistics. II," *Commun. Math. Phys.* **35** (1974) 49–85.

[49] M. Freedman, M. B. Hastings, C. Nayak, X.-L. Qi, K. Walker, and Z. Wang, "Projective ribbon permutation statistics: A remnant of non-Abelian braiding in higher dimensions," *Physical Review B* **83** no. 11, (Mar., 2011) 115132, `arXiv:1005.0583 [cond-mat.mes-hall]`.

[50] F. Wilczek, "Projective Statistics and Spinors in Hilbert Space," *ArXiv High Energy Physics - Theory e-prints* (June, 1998) , `hep-th/9806228`.

[51] N. Read, "Non-Abelian braid statistics versus projective permutation statistics," *Journal of Mathematical Physics* **44** (Feb., 2003) 558–563, `hep-th/0201240`.

[52] J. C. Y. Teo and C. L. Kane, "Majorana Fermions and Non-Abelian Statistics in Three Dimensions," *Physical Review Letters* **104** no. 4, (Jan., 2010) 046401, `arXiv:0909.4741 [cond-mat.mes-hall]`.

[53] J. M. Leinaas and J. Myrheim, "On the theory of identical particles," *Nuovo Cim.* **B37** (1977) 1–23.

[54] F. Wilczek, "Quantum Mechanics of Fractional Spin Particles," *Phys. Rev. Lett.* **49** (1982) 957–959.

[55] T. Lan and X.-G. Wen, "Topological quasiparticles and the holographic bulk-edge relation in 2+1D string-net models," `arXiv:1311.1784`.

[56] A. Kitaev, "Anyons in an exactly solved model and beyond," *Annals of Physics* **321** (Jan., 2006) 2–111, `cond-mat/0506438`.

[57] M. Levin and X.-G. Wen, "Fermions, strings, and gauge fields in lattice spin models," *Physical Review B* **67** no. 24, (June, 2003) 245316, `cond-mat/0302460`.

[58] E. Rowell, R. Stong, and Z. Wang, "On classification of modular tensor categories," *ArXiv e-prints* (Dec., 2007) , `arXiv:0712.1377 [math.QA]`.

[59] G. W. Moore and N. Seiberg, "Polynomial Equations for Rational Conformal Field Theories," *Phys. Lett.* **B212** (1988) 451.

[60] G. W. Moore and N. Seiberg, "LECTURES ON RCFT," in *1989 Banff NATO ASI: Physics, Geometry and Topology Banff, Canada, August 14-25, 1989*, pp. 1–129. 1989. [,1(1989)].

[61] E. Witten, "Quantum Field Theory and the Jones Polynomial," *Commun. Math. Phys.* **121** (1989) 351–399.

[62] S. Elitzur, G. W. Moore, A. Schwimmer, and N. Seiberg, "Remarks on the Canonical Quantization of the Chern-Simons-Witten Theory," *Nucl. Phys.* **B326** (1989) 108.

[63] E. P. Verlinde, "Fusion Rules and Modular Transformations in 2D Conformal Field Theory," *Nucl. Phys.* **B300** (1988) 360–376.

[64] M. Mignard and P. Schauenburg, "Modular categories are not determined by their modular data," *ArXiv e-prints* (Aug., 2017) , `arXiv:1708.02796 [math.QA]`.

[65] P. Bonderson, C. Delaney, C. Galindo, E. C. Rowell, A. Tran, and Z. Wang, "On invariants of Modular categories beyond modular data," *ArXiv e-prints* (May, 2018) , `arXiv:1805.05736 [math.QA]`.

[66] C. Delaney and A. Tran, "A systematic search of knot and link invariants beyond modular data," *ArXiv e-prints* (June, 2018) , `arXiv:1806.02843 [math.QA]`.

[67] J. Preskill, "Lecture Notes for Physics 219: Quantum Computation." `http://www.theory.caltech.edu/~preskill/ph219/topological.pdf`, June, 2014.

[68] C. Kassel, *Quantum Groups*. Graduate Texts in Mathematics. Springer New York, 1994.

[69] A. Y. Kitaev, "Fault tolerant quantum computation by anyons," *Annals Phys.* **303** (2003) 2–30, `arXiv:quant-ph/9707021 [quant-ph]`.

[70] C. Nayak, S. H. Simon, A. Stern, M. Freedman, and S. Das Sarma, "Non-Abelian anyons and topological quantum computation," *Reviews of Modern Physics* **80** (July, 2008) 1083–1159, `arXiv:0707.1889 [cond-mat.str-el]`.

[71] M. H. Freedman, A. Kitaev, M. J. Larsen, and Z. Wang, "Topological Quantum Computation," *eprint arXiv:quant-ph/0101025* (Jan., 2001) , `quant-ph/0101025`.

[72] A. Abrikosov, "The magnetic properties of superconducting alloys," *Journal of Physics and Chemistry of Solids* **2** no. 3, (1957) 199 – 208. `http://www.sciencedirect.com/science/article/pii/0022369757900835`.

[73] H. B. Nielsen and P. Olesen, "Vortex Line Models for Dual Strings," *Nucl. Phys.* **B61** (1973) 45–61. [,302(1973)].

[74] J. C. Baez, D. K. Wise, and A. S. Crans, "Exotic Statistics for Strings in 4d BF Theory," *ArXiv General Relativity and Quantum Cosmology e-prints* (Mar., 2006) , `gr-qc/0603085`.

[75] C. Wang and M. Levin, "Topological invariants for gauge theories and symmetry-protected topological phases," *Physical Review B* **91** no. 16, (Apr., 2015) 165119, `arXiv:1412.1781 [cond-mat.str-el]`.

[76] T. H. Hansson, V. Oganesyan, and S. L. Sondhi, "Superconductors are topologically ordered," *Annals of Physics* **313** (Oct., 2004) 497–538, `cond-mat/0404327`.

[77] X. G. Wen, "Mean-field theory of spin-liquid states with finite energy gap and topological orders," *Phys. Rev. B* **44** (Aug, 1991) 2664–2672. `http://link.aps.org/doi/10.1103/PhysRevB.44.2664`.

[78] B. I. Halperin, "Quantized Hall conductance, current-carrying edge states, and the existence of extended states in a two-dimensional disordered potential," *Phys. Rev. B* **25** (Feb, 1982) 2185–2190. http://link.aps.org/doi/10.1103/PhysRevB.25.2185.

[79] X.-G. Wen, "Theory of the edge states in fractional quantum Hall effects," *Int. J. Mod. Phys.* **B6** (1992) 1711–1762.

[80] X.-G. Wen, "Topological orders and edge excitations in fractional quantum Hall states," *Advances in Physics* **44** (Sept., 1995) 405–473, cond-mat/9506066.

[81] N. Read and D. Green, "Paired states of fermions in two dimensions with breaking of parity and time-reversal symmetries and the fractional quantum Hall effect," *Physical Review B* **61** (Apr., 2000) 10267–10297, cond-mat/9906453.

[82] J. Callan, Curtis G. and J. A. Harvey, "Anomalies and Fermion Zero Modes on Strings and Domain Walls," *Nucl.Phys.* **B250** (1985) 427.

[83] A. Bilal, "Lectures on Anomalies," *ArXiv e-prints* (Feb., 2008) , arXiv:0802.0634 [hep-th].

[84] M. A. Levin and X.-G. Wen, "String-net condensation: A physical mechanism for topological phases," *Physical Review B* **71** no. 4, (Jan., 2005) 045110, cond-mat/0404617.

[85] E. Plamadeala, M. Mulligan, and C. Nayak, "Short-range entangled bosonic states with chiral edge modes and T duality of heterotic strings," *Physical Review B* **88** no. 4, (July, 2013) 045131, arXiv:1304.0772 [cond-mat.str-el].

[86] J. Polchinski, *String Theory: Volume 1, An Introduction to the Bosonic String*. Cambridge Monographs on Mathematical Physics. Cambridge University Press, 1998. https://books.google.ca/books?id=jbM3t_usmX0C.

[87] J. Polchinski, *String Theory: Volume 2, Superstring Theory and Beyond*. Cambridge Monographs on Mathematical Physics. Cambridge University Press, 1998. https://books.google.ca/books?id=WKatSc5pjOgC.

[88] A. Kapustin and N. Saulina, "Topological boundary conditions in abelian Chern-Simons theory," *Nucl. Phys. B* **845** (2011) 393 – 435, arXiv:1008.0654.

[89] M. Levin, "Protected Edge Modes without Symmetry," *Physical Review X* **3** no. 2, (Apr., 2013) 021009, arXiv:1301.7355 [cond-mat.str-el].

[90] M. Barkeshli, C.-M. Jian, and X.-L. Qi, "Theory of defects in Abelian topological states," *Phys. Rev. B* **88** (Dec, 2013) 235103. http://link.aps.org/doi/10.1103/PhysRevB.88.235103.

[91] M. Barkeshli, C.-M. Jian, and X.-L. Qi, "Classification of topological defects in Abelian topological states," *Phys. Rev. B* **88** (Dec, 2013) 241103. http://link.aps.org/doi/10.1103/PhysRevB.88.241103.

[92] H. Moradi *To be published* (2018) .

[93] L. Kong and X.-G. Wen, "Braided fusion categories, gravitational anomalies, and the mathematical framework for topological orders in any dimensions," *ArXiv e-prints* (May, 2014) , arXiv:1405.5858 [cond-mat.str-el].

[94] L. Kong, X.-G. Wen, and H. Zheng, "Boundary-bulk relation for topological orders as the functor mapping higher categories to their centers," *ArXiv e-prints* (Feb., 2015) , arXiv:1502.01690 [cond-mat.str-el].

[95] T. Lan, L. Kong, and X.-G. Wen, "Classification of (3 +1)D Bosonic Topological Orders: The Case When Pointlike Excitations Are All Bosons," *Physical Review X* **8** no. 2, (Apr., 2018) 021074, arXiv:1704.04221 [cond-mat.str-el].

[96] H. Moradi, A. Tiwari, and F. Moosavian *To be published* (2018) .

[97] V. Kalmeyer and R. B. Laughlin, "Equivalence of the resonating-valence-bond and fractional quantum Hall states," *Phys. Rev. Lett.* **59** (1987) 2095–2098.

[98] X.-G. Wen, F. Wilczek, and A. Zee, "Chiral Spin States and Superconductivity," *Phys. Rev. B* **39** (1989) 11413.

[99] X.-G. Wen, "Vacuum Degeneracy of Chiral Spin State in Compactified Spaces," *Phys. Rev. B* **40** (1989) 7387.

[100] X.-G. Wen and Q. Niu, "Ground State Degeneracy of the FQH States in Presence of Random Potentials and on High Genus Riemann Surfaces," *Phys. Rev. B* **41** (1990) 9377.

[101] E. Keski-Vakkuri and X.-G. Wen, "Ground state structure of hierarchical QH states on torus and modular transformation," *Int. J. Mod. Phys. B* **7** (1993) 4227.

[102] X.-G. Wen, "Modular transformation and bosonic/fermionic topological orders in Abelian fractional quantum Hall states," arXiv:1212.5121.

[103] Z. Wang, *Topological Quantum Computation*. CBMS Regional Conference Series in Mathematics, 2010.

[104] X.-G. Wen, "Theory of the Edge Excitations in FQH effects," *Int. J. Mod. Phys. B* **6** (1992) 1711.

[105] X.-G. Wen, "Topological Orders and Edge Excitations in FQH States," *Advances in Physics* **44** (1995) 405.

[106] Y. Zhang, T. Grover, A. Turner, M. Oshikawa, and A. Vishwanath, "Quasi-particle Statistics and Braiding from Ground State Entanglement," *Phys. Rev. B* **85** (2012) 235151, arXiv:1111.2342.

[107] L. Cincio and G. Vidal, "Characterizing topological order by studying the ground states of an infinite cylinder," *Phys. Rev. Lett.* **110** (2013) 067208, arXiv:1208.2623.

[108] M. P. Zaletel, R. S. K. Mong, and F. Pollmann, "Topological characterization of fractional quantum Hall ground states from microscopic Hamiltonians," arXiv:1211.3733.

[109] L.-Y. Hung and X.-G. Wen, "Universal symmetry-protected topological invariants for symmetry-protected topological states," arXiv:1311.5539.

[110] N. Read and S. Sachdev, "Large-N expansion for frustrated quantum antiferromagnets," *Phys. Rev. Lett.* **66** (1991) 1773.

[111] X.-G. Wen, "Mean-field theory of spin-liquid states with finite energy gap and topological orders," *Phys. Rev. B* **44** (1991) 2664.

[112] S. S. Bullock and G. K. Brennen, "Qudit surface codes and gauge theory with finite cyclic groups," *J. Phys. A* **A40** (2007) 3481–3505, arXiv:quant-ph/0609070 [quant-ph].

[113] M. D. Schulz, S. Dusuel, R. Orús, J. Vidal, and K. P. Schmidt, "Breakdown of a perturbed \boldsymbol{m{Z}}_N topological phase," *New Journal of Physics* **14** no. 2, (Feb., 2012) 025005, arXiv:1110.3632 [cond-mat.stat-mech].

[114] Y.-Z. You and X.-G. Wen, "Projective non-Abelian Statistics of Dislocation Defects in a Z_N Rotor Model," *Phys. Rev. B* **86** (2012) 161107, arXiv:1204.0113.

[115] M. B. Hastings, "An area law for one-dimensional quantum systems," *Journal of Statistical Mechanics: Theory and Experiment* **8** (Aug., 2007) 24, `arXiv:0705.2024 [quant-ph]`.

[116] L. Masanes, "An Area law for the entropy of low-energy states," *Phys.Rev.* **A80** (2009) 052104, `arXiv:0907.4672 [quant-ph]`.

[117] X. Chen, B. Zeng, Z.-C. Gu, I. L. Chuang, and X.-G. Wen, "Tensor product representation of a topological ordered phase: Necessary symmetry conditions," *Physical Review B* **82** no. 16, (Oct., 2010) 165119, `arXiv:1003.1774 [cond-mat.str-el]`.

[118] B. Swingle and X.-G. Wen, "Topological Properties of Tensor Network States From Their Local Gauge and Local Symmetry Structures," *ArXiv e-prints* (Jan., 2010) , `arXiv:1001.4517 [cond-mat.str-el]`.

[119] N. Schuch, I. Cirac, and D. Pérez-García, "PEPS as ground states: Degeneracy and topology," *Annals of Physics* **325** (Oct., 2010) 2153–2192, `arXiv:1001.3807 [quant-ph]`.

[120] O. Buerschaper, "Twisted Injectivity in PEPS and the Classification of Quantum Phases," `arXiv:1307.7763 [cond-mat.str-el]`.

[121] R. Dijkgraaf and E. Witten, "Topological Gauge Theories and Group Cohomology," *Commun.Math.Phys.* **129** (1990) 393.

[122] F. Liu, Z. Wang, Y.-Z. You, and X.-G. Wen, "Quantum fidelity, modular transformations, and topological orders in two dimensions," *ArXiv e-prints* (Mar., 2013) , `arXiv:1303.0829 [cond-mat.str-el]`.

[123] S. M. Trott, "A pair of generators for the unimodular group," *Canadian Mathematical Bulletin* **5** (1962) 245–252.

[124] X.-G. Wen, "Topological Orders in Rigid States," *Int. J. Mod. Phys. B* **4** (1990) 239.

[125] F. Verstraete, J. I. Cirac, J. I. Latorre, E. Rico, and M. M. Wolf, "Renormalization-Group Transformations on Quantum States," *Phys. Rev. Lett.* **94** (2005) 140601.

[126] G. Vidal, "Entanglement renormalization," *Phys. Rev. Lett.* **99** (2007) 220405.

[127] R. Moessner and S. L. Sondhi, "Resonating Valence Bond Phase in the Triangular Lattice Quantum Dimer Model," *Phys. Rev. Lett.* **86** (2001) 1881.

[128] G. Moore and N. Read, "Nonabelions in the fractional quantum hall effect," *Nucl. Phys. B* **360** (1991) 362.

[129] X.-G. Wen, "Non-Abelian Statistics in the FQH states," *Phys. Rev. Lett.* **66** (1991) 802.

[130] R. Willett, J. P. Eisenstein, H. L. Strörmer, D. C. Tsui, A. C. Gossard, and J. H. English *Phys. Rev. Lett.* **59** (1987) 1776.

[131] I. P. Radu, J. B. Miller, C. M. Marcus, M. A. Kastner, L. N. Pfeiffer, and K. W. West, "Quasiparticle Tunneling in the Fractional Quantum Hall State at $\nu = 5/2$," *Science* **320** (2008) 899.

[132] M. Freedman, C. Nayak, K. Shtengel, K. Walker, and Z. Wang, "A class of P, T-invariant topological phases of interacting electrons," *Annals of Physics* **310** (Apr., 2004) 428–492, `cond-mat/0307511`.

[133] Z.-C. Gu, Z. Wang, and X.-G. Wen, "A classification of 2D fermionic and bosonic topological orders," `arXiv:1010.1517`.

[134] Z.-C. Gu, Z. Wang, and X.-G. Wen, "Lattice Model for Fermionic Toric Code," `arXiv:1309.7032`.

[135] B. Blok and X.-G. Wen, "Many-body Systems with Non-abelian Statistics," *Nucl. Phys. B* **374** (1992) 615.

[136] X.-G. Wen and Y.-S. Wu, "Chiral operator product algebra hidden in certain FQH states," *Nucl. Phys. B* **419** (1994) 455, `cond-mat/9310027`.

[137] Y.-M. Lu, X.-G. Wen, Z. Wang, and Z. Wang, "Non-Abelian Quantum Hall States and their Quasiparticles: from the Pattern of Zeros to Vertex Algebra," *Phys. Rev. B* **81** (2010) 115124, `arXiv:0910.3988`.

[138] X.-G. Wen and Z. Wang, "Classification of symmetric polynomials of infinite variables: Construction of Abelian and non-Abelian quantum Hall states," *Phys. Rev. B* **77** (2008) 235108, `arXiv:0801.3291`.

[139] X.-G. Wen and Z. Wang, "Topological properties of Abelian and non-Abelian quantum Hall states from the pattern of zeros," *Phys. Rev. B* **78** (2008) 155109, arXiv:0803.1016.

[140] M. Barkeshli and X.-G. Wen, "Structure of Quasiparticles and Their Fusion Algebra in Fractional Quantum Hall States," *Phys. Rev. B* **79** (2009) 195132, arXiv:0807.2789.

[141] A. Seidel and D.-H. Lee, "Abelian and Non-abelian Hall Liquids and Charge Density Wave: Quantum Number Fractionalization in One and Two Dimensions," *Phys. Rev. Lett.* **97** (2006) 056804.

[142] E. J. Bergholtz, J. Kailasvuori, E. Wikberg, T. H. Hansson, and A. Karlhede, "The Pfaffian quantum Hall state made simple–multiple vacua and domain walls on a thin torus," *Phys. Rev. B* **74** (2006) 081308.

[143] A. Seidel and K. Yang, "Halperin (m, m',n) bilayer quantum Hall states on thin cylinders," arXiv:0801.2402.

[144] B. A. Bernevig and F. D. M. Haldane, "Fractional Quantum Hall States and Jack Polynomials," *Phys. Rev. Lett.* **100** (2008) 246802, arXiv:0707.3637.

[145] B. A. Bernevig and F. D. M. Haldane, "Generalized Clustering Conditions of Jack Polynomials at Negative Jack Parameter α," *Phys. Rev. B* **77** (2008) 184502, arXiv:0711.3062.

[146] B. A. Bernevig and F. D. M. Haldane, "Properties of Non-Abelian Fractional Quantum Hall States at Filling nu=k/r," arXiv:0803.2882.

[147] B. Blok and X.-G. Wen, "Effective theories of Fractional Quantum Hall Effect: Hierarchical Construction," *Phys. Rev. B* **42** (1990) 8145.

[148] N. Read, "Excitation structure of the hierarchy scheme in the fractional quantum Hall effect," *Phys. Rev. Lett.* **65** (1990) 1502.

[149] J. Fröhlich and T. Kerler, "Universality in quantum Hall systems," *Nucl. Phys. B* **354** (1991) 369.

[150] X.-G. Wen and A. Zee, "A Classification and Matrix Formulation of the abelian FQH states," *Phys. Rev. B* **46** (1992) 2290.

[151] D. Belov and G. W. Moore, "Classification of abelian spin Chern-Simons theories," arXiv:hep-th/0505235.

[152] Z.-C. Gu, M. Levin, B. Swingle, and X.-G. Wen, "Tensor-product representations for string-net condensed states," *Phys. Rev. B* **79** (2009) 085118, arXiv:0809.2821.

[153] O. Buerschaper, M. Aguado, and G. Vidal, "Explicit tensor network representation for the ground states of string-net models," *Phys. Rev. B* **79** (2009) 085119, arXiv:0809.2393.

[154] X. Chen, B. Zeng, Z.-C. Gu, I. L. Chuang, and X.-G. Wen, "Tensor product representation of topological ordered phase: necessary symmetry conditions," *Phys. Rev. B* **82** (2010) 165119, arXiv:1003.1774.

[155] X.-G. Wen and B. Swingle, "Topological Properties of Tensor Network States From Their Local Gauge and Local Symmetry Structures," arXiv:1001.4517.

[156] Z.-C. Gu, M. Levin, and X.-G. Wen, "Tensor-entanglement renormalization group approach as a unified method for symmetry breaking and topological phase transitions," *Phys. Rev. B* **78** (2008) 205116.

[157] Y. Hu, Y. Wan, and Y.-S. Wu, "Twisted Quantum Double Model of Topological Phases in Two–Dimension," arXiv:1211.3695 [cond-mat.str-el].

[158] F. Liu, Z. Wang, Y.-Z. You, and X.-G. Wen, "Quantum fidelity, modular transformations, and topological orders in two dimensions," arXiv:1303.0829.

[159] H. He, Z. Wang, C. Li, Y. Han, and G. Guo, "A Study of Highly Frustrated Spin Systems with mixed PEPS in Infinite Honeycomb Lattice," *ArXiv e-prints* (Mar., 2013) , arXiv:1303.2431 [cond-mat.str-el].

[160] M. Burak Şahinoğlu, D. Williamson, N. Bultinck, M. Mariën, J. Haegeman, N. Schuch, and F. Verstraete, "Characterizing Topological Order with Matrix Product Operators," *ArXiv e-prints* (Sept., 2014) , arXiv:1409.2150 [quant-ph].

[161] S. Jiang, A. Mesaros, and Y. Ran, "Generalized modular transformations in 3+1D topologically ordered phases and triple linking invariant of loop braiding," *ArXiv e-prints* (Apr., 2014) , arXiv:1404.1062 [cond-mat.str-el].

[162] J. Wang and X.-G. Wen, "Non-Abelian String and Particle Braiding in Topological Order: Modular SL(3,Z) Representation and 3+1D Twisted Gauge Theory," *ArXiv e-prints* (Apr., 2014) , arXiv:1404.7854 [cond-mat.str-el].

[163] J.-W. Mei, J.-Y. Chen, H. He, and X.-G. Wen, "Gapped spin liquid with Z_2 topological order for the kagome Heisenberg model," *Physical Review B* **95** no. 23, (June, 2017) 235107, `arXiv:1606.09639 [cond-mat.str-el]`.

[164] K. Walker and Z. Wang, "(3+1)-TQFTs and Topological Insulators," `arXiv:1104.2632`.

[165] C. Wang and M. Levin, "Braiding statistics of loop excitations in three dimensions," `arXiv:1403.7437`.

[166] S. Jiang, A. Mesaros, and Y. Ran, "Generalized modular transformations in 3+1D topologically ordered phases and triple linking invariant of loop braiding," `arXiv:1404.1062`.

[167] Y. Hu, Y. Wan, and Y.-S. Wu, "Twisted Quantum Double Model of Topological Phases in Two–Dimension," *Phys. Rev. B* **87** (2013) 125114, `arXiv:1211.3695`.

[168] J. Wang and X.-G. Wen, "Non-Abelian String and Particle Braiding in Topological Order: Modular SL(3,Z) Representation and 3+1D Twisted Gauge Theory," *ArXiv e-prints* (Apr., 2014) , `arXiv:1404.7854 [cond-mat.str-el]`.

[169] A. M. Läuchli, E. J. Bergholtz, J. Suorsa, and M. Haque, "Disentangling Entanglement Spectra of Fractional Quantum Hall States on Torus Geometries," *Physical Review Letters* **104** no. 15, (Apr., 2010) 156404, `arXiv:0911.5477 [cond-mat.mes-hall]`.

[170] N. Regnault, B. A. Bernevig, and F. D. M. Haldane, "Topological Entanglement and Clustering of Jain Hierarchy States," *Physical Review Letters* **103** no. 1, (July, 2009) 016801, `arXiv:0901.2121`.

[171] R. Thomale, A. Sterdyniak, N. Regnault, and B. A. Bernevig, "Entanglement Gap and a New Principle of Adiabatic Continuity," *Physical Review Letters* **104** no. 18, (May, 2010) 180502, `arXiv:0912.0523 [cond-mat.str-el]`.

[172] J. Dubail, N. Read, and E. H. Rezayi, "Real-space entanglement spectrum of quantum Hall systems," *Physical Review B* **85** no. 11, (Mar., 2012) 115321, `arXiv:1111.2811 [cond-mat.mes-hall]`.

[173] I. D. Rodríguez, S. H. Simon, and J. K. Slingerland, "Evaluation of Ranks of Real Space and Particle Entanglement Spectra for Large Systems," *Physical Review Letters* **108** no. 25, (June, 2012) 256806, `arXiv:1111.3634 [cond-mat.str-el]`.

[174] A. Sterdyniak, A. Chandran, N. Regnault, B. A. Bernevig, and P. Bonderson, "Real-space entanglement spectrum of quantum Hall states," *Physical Review B* **85** no. 12, (Mar., 2012) 125308, `arXiv:1111.2810 [cond-mat.mes-hall]`.

[175] A. Chandran, M. Hermanns, N. Regnault, and B. A. Bernevig, "Bulk-edge correspondence in entanglement spectra," *Physical Review B* **84** no. 20, (Nov., 2011) 205136, `arXiv:1102.2218 [cond-mat.str-el]`.

[176] H. Yao and X.-L. Qi, "Entanglement Entropy and Entanglement Spectrum of the Kitaev Model," *Physical Review Letters* **105** no. 8, (Aug., 2010) 080501, `arXiv:1001.1165 [cond-mat.str-el]`.

[177] T. H. Hsieh and L. Fu, "Bulk Entanglement Spectrum Reveals Quantum Criticality within a Topological State," *Physical Review Letters* **113** no. 10, (Sept., 2014) 106801, `arXiv:1305.1949 [cond-mat.str-el]`.

[178] L. Fidkowski, "Entanglement Spectrum of Topological Insulators and Superconductors," *Physical Review Letters* **104** no. 13, (Apr., 2010) 130502, `arXiv:0909.2654 [cond-mat.str-el]`.

[179] A. M. Turner, Y. Zhang, and A. Vishwanath, "Band Topology of Insulators via the Entanglement Spectrum," *ArXiv e-prints* (Sept., 2009) , `arXiv:0909.3119 [cond-mat.str-el]`.

[180] E. Prodan, T. L. Hughes, and B. A. Bernevig, "Entanglement Spectrum of a Disordered Topological Chern Insulator," *Physical Review Letters* **105** no. 11, (Sept., 2010) 115501, `arXiv:1005.5148 [cond-mat.mes-hall]`.

[181] N. Regnault and B. A. Bernevig, "Fractional Chern Insulator," *Physical Review X* **1** no. 2, (Oct., 2011) 021014, `arXiv:1105.4867 [cond-mat.str-el]`.

[182] F. Pollmann, E. Berg, A. M. Turner, and M. Oshikawa, "Symmetry protection of topological phases in one-dimensional quantum spin systems," *Physical Review B* **85** no. 7, (Feb., 2012) 075125, `arXiv:0909.4059 [cond-mat.str-el]`.

[183] W.-J. Rao, X. Wan, and G.-M. Zhang, "Critical-entanglement spectrum of one-dimensional symmetry-protected topological phases," *Physical Review B* **90** no. 7, (Aug., 2014) 075151, `arXiv:1406.7113 [cond-mat.str-el]`.

[184] B. Nienhuis, M. Campostrini, and P. Calabrese, "Entanglement, combinatorics and finite-size effects in spin chains," *Journal of Statistical Mechanics: Theory and Experiment* **2** (Feb., 2009) 63, `arXiv:0808.2741 [cond-mat.stat-mech]`.

[185] R. Thomale, D. P. Arovas, and B. A. Bernevig, "Nonlocal Order in Gapless Systems: Entanglement Spectrum in Spin Chains," *Physical Review Letters* **105** no. 11, (Sept., 2010) 116805, `arXiv:0912.0028 [cond-mat.str-el]`.

[186] G. De Chiara, L. Lepori, M. Lewenstein, and A. Sanpera, "Entanglement Spectrum, Critical Exponents, and Order Parameters in Quantum Spin Chains," *Physical Review Letters* **109** no. 23, (Dec., 2012) 237208, `arXiv:1104.1331 [cond-mat.stat-mech]`.

[187] G. Torlai, L. Tagliacozzo, and G. De Chiara, "Dynamics of the entanglement spectrum in spin chains," *ArXiv e-prints* (Nov., 2013) , `arXiv:1311.5509 [cond-mat.stat-mech]`.

[188] D. Poilblanc, "Entanglement Spectra of Quantum Heisenberg Ladders," *Physical Review Letters* **105** no. 7, (Aug., 2010) 077202, `arXiv:1005.2123 [cond-mat.str-el]`.

[189] A. J. A. James and R. M. Konik, "Understanding the entanglement entropy and spectra of 2D quantum systems through arrays of coupled 1D chains," *Physical Review B* **87** no. 24, (June, 2013) 241103, `arXiv:1208.4033 [cond-mat.stat-mech]`.

[190] A. M. Läuchli and J. Schliemann, "Entanglement spectra of coupled S=(1)/(2) spin chains in a ladder geometry," *Physical Review B* **85** no. 5, (Feb., 2012) 054403, `arXiv:1106.3419 [cond-mat.str-el]`.

[191] X. Chen and E. Fradkin, "Quantum entanglement and thermal reduced density matrices in fermion and spin systems on ladders," *Journal of Statistical Mechanics: Theory and Experiment* **8** (Aug., 2013) 13, `arXiv:1305.6538 [cond-mat.str-el]`.

[192] R. Lundgren, Y. Fuji, S. Furukawa, and M. Oshikawa, "Entanglement spectra between coupled Tomonaga-Luttinger liquids: Applications to ladder systems and topological phases," *Physical Review B* **88** no. 24, (Dec., 2013) 245137, `arXiv:1310.0829 [cond-mat.str-el]`.

[193] S. Tanaka, R. Tamura, and H. Katsura, "Entanglement Spectra of the quantum hard-square model: Holographic minimal models," *Phys. Rev.* **A86** (2012) 032326, `arXiv:1207.6752 [cond-mat.stat-mech]`.

[194] A. Chandran, V. Khemani, and S. L. Sondhi, "How Universal Is the Entanglement Spectrum?," *Physical Review Letters* **113** no. 6, (Aug., 2014) 060501, `arXiv:1311.2946 [cond-mat.str-el]`.

[195] X.-G. Wen, "Quantum Orders in an Exact Soluble Model," *Physical Review Letters* **90** no. 1, (Jan., 2003) 016803, `quant-ph/0205004`.

[196] S. Yang, L. Lehman, D. Poilblanc, K. Van Acoleyen, F. Verstraete, J. I. Cirac, and N. Schuch, "Edge Theories in Projected Entangled Pair State Models," *Phys. Rev. Lett.* **112** (Jan, 2014) 036402. `http://link.aps.org/doi/10.1103/PhysRevLett.112.036402`.

[197] J. Lou, S. Tanaka, H. Katsura, and N. Kawashima, "Entanglement spectra of the two-dimensional Affleck-Kennedy-Lieb-Tasaki model: Correspondence between the valence-bond-solid state and conformal field theory," *Physical Review B* **84** no. 24, (Dec., 2011) 245128, `arXiv:1107.3888 [cond-mat.str-el]`.

[198] Y. Zhang, T. Grover, A. Turner, M. Oshikawa, and A. Vishwanath, "Quasiparticle statistics and braiding from ground-state entanglement," *Physical Review B* **85** no. 23, (June, 2012) 235151, `arXiv:1111.2342 [cond-mat.str-el]`.

[199] J. R. Schrieffer and P. A. Wolff, "Relation between the Anderson and Kondo Hamiltonians," *Phys. Rev.* **149** (Sep, 1966) 491–492. `http://link.aps.org/doi/10.1103/PhysRev.149.491`.

[200] S. Bravyi, D. P. DiVincenzo, and D. Loss, "Schrieffer-Wolff transformation for quantum many-body systems," *Annals of Physics* **326** (Oct., 2011) 2793–2826, `arXiv:1105.0675 [quant-ph]`.

[201] W. Zheng, C. J. Hamer, R. R. P. Singh, S. Trebst, and H. Monien, "Linked cluster series expansions for two-particle bound states," *Phys. Rev. B* **63** (Mar, 2001) 144410. `http://link.aps.org/doi/10.1103/PhysRevB.63.144410`.

[202] S. Sachdev, *Quantum Phase Transitions*. Troisième Cycle de la Physique. Cambridge University Press, 2011.

[203] I. S. Tupitsyn, A. Kitaev, N. V. Prokof'ev, and P. C. E. Stamp, "Topological multicritical point in the phase diagram of the toric code model and three-dimensional lattice gauge Higgs model," *Phys. Rev. B* **82** (Aug, 2010) 085114. `http://link.aps.org/doi/10.1103/PhysRevB.82.085114`.

[204] J. Yu, X.-H. Zhang, and S.-P. Kou, "Majorana edge states for $\mathbb{Z}_2$ topological orders of the Wen plaquette and toric code models," *Phys. Rev. B* **87** (May, 2013) 184402. http://link.aps.org/doi/10.1103/PhysRevB.87.184402.

[205] J. Vidal, S. Dusuel, and K. P. Schmidt, "Low-energy effective theory of the toric code model in a parallel magnetic field," *Phys. Rev. B* **79** (Jan, 2009) 033109. http://link.aps.org/doi/10.1103/PhysRevB.79.033109.

[206] V. B. Petkova and J.-B. Zuber, "Generalised twisted partition functions," *Physics Letters B* **504** (Apr., 2001) 157–164, hep-th/0011021.

[207] J. Fröhlich, J. Fuchs, I. Runkel, and C. Schweigert, "Kramers-Wannier Duality from Conformal Defects," *Phys. Rev. Lett.* **93** (Aug, 2004) 070601. http://link.aps.org/doi/10.1103/PhysRevLett.93.070601.

[208] C. Chui, C. Mercat, W. P. Orrick, and P. A. Pearce, "Integrable lattice realizations of conformal twisted boundary conditions," *Physics Letters B* **517** no. 3–4, (2001) 429 – 435. http://www.sciencedirect.com/science/article/pii/S0370269301009820.

[209] I. McCulloch, " Infinite size density matrix renormalization group, revisited," *ArXiv e-prints* (Apr., 2008) , arXiv:0804.2509 [cond-mat.str-el].

[210] H. Bombin, "Topological Order with a Twist: Ising Anyons from an Abelian Model," *Phys. Rev. Lett.* **105** (Jul, 2010) 030403. http://link.aps.org/doi/10.1103/PhysRevLett.105.030403.

[211] U. Grimm, "Duality and conformal twisted boundaries in the Ising model," *ArXiv High Energy Physics - Theory e-prints* (Sept., 2002) , hep-th/0209048.

[212] J. Fjelstad, J. Fuchs, and C. Stigner, "{RCFT} with defects: Factorization and fundamental world sheets," *Nuclear Physics B* **863** no. 1, (2012) 213 – 259. http://www.sciencedirect.com/science/article/pii/S055032131200260X.

[213] X. G. Wen, "Vacuum degeneracy of chiral spin states in compactified space," *Phys. Rev. B* **40** (Oct, 1989) 7387–7390. http://link.aps.org/doi/10.1103/PhysRevB.40.7387.

[214] X. G. Wen and Q. Niu, "Ground-state degeneracy of the fractional quantum Hall states in the presence of a random potential and on high-genus Riemann surfaces," *Phys. Rev. B* **41** (May, 1990) 9377–9396. http://link.aps.org/doi/10.1103/PhysRevB.41.9377.

[215] Y. Zhang, T. Grover, and A. Vishwanath, "General procedure for determining braiding and statistics of anyons using entanglement interferometry," *Phys. Rev. B* **91** (Jan, 2015) 035127.
http://link.aps.org/doi/10.1103/PhysRevB.91.035127.

[216] T. Lan, J. C. Wang, and X.-G. Wen, "Gapped Domain Walls, Gapped Boundaries, and Topological Degeneracy," *Physical Review Letters* **114** no. 7, (Feb., 2015) 076402, arXiv:1408.6514 [cond-mat.str-el].

[217] H. Li and F. D. M. Haldane, "Entanglement Spectrum as a Generalization of Entanglement Entropy: Identification of Topological Order in Non-Abelian Fractional Quantum Hall Effect States," *Phys. Rev. Lett.* **101** (Jul, 2008) 010504.
http://link.aps.org/doi/10.1103/PhysRevLett.101.010504.

[218] X.-L. Qi, H. Katsura, and A. W. W. Ludwig, "General Relationship between the Entanglement Spectrum and the Edge State Spectrum of Topological Quantum States," *Phys. Rev. Lett.* **108** (May, 2012) 196402.
http://link.aps.org/doi/10.1103/PhysRevLett.108.196402.

[219] M. Aguado and G. Vidal, "Entanglement Renormalization and Topological Order," *Phys. Rev. Lett.* **100** (Feb, 2008) 070404.
http://link.aps.org/doi/10.1103/PhysRevLett.100.070404.

[220] R. König, B. W. Reichardt, and G. Vidal, "Exact entanglement renormalization for string-net models," *Phys. Rev. B* **79** (May, 2009) 195123.
http://link.aps.org/doi/10.1103/PhysRevB.79.195123.

[221] S. T. Flammia, A. Hamma, T. L. Hughes, and X.-G. Wen, "Topological Entanglement Rényi Entropy and Reduced Density Matrix Structure," *Phys. Rev. Lett.* **103** (Dec, 2009) 261601.
http://link.aps.org/doi/10.1103/PhysRevLett.103.261601.

[222] G. Vidal, "Entanglement Renormalization," *Phys. Rev. Lett.* **99** (Nov, 2007) 220405. http://link.aps.org/doi/10.1103/PhysRevLett.99.220405.

[223] G. Vidal, "Class of Quantum Many-Body States That Can Be Efficiently Simulated," *Phys. Rev. Lett.* **101** (Sep, 2008) 110501.
http://link.aps.org/doi/10.1103/PhysRevLett.101.110501.

[224] N. Schuch, D. Poilblanc, J. I. Cirac, and D. Pérez-García, "Topological Order in the Projected Entangled-Pair States Formalism: Transfer Operator and Boundary

Hamiltonians," *Phys. Rev. Lett.* **111** (Aug, 2013) 090501.
http://link.aps.org/doi/10.1103/PhysRevLett.111.090501.

[225] L. Cincio and G. Vidal Unpublished work.

[226] H. He *To be published* (2015) .

[227] P. Ginsparg, "Applied Conformal Field Theory," *ArXiv High Energy Physics - Theory e-prints* (Nov., 1991) , hep-th/9108028.

[228] S. R. White, "Density matrix formulation for quantum renormalization groups," *Phys. Rev. Lett.* **69** (Nov, 1992) 2863–2866.
http://link.aps.org/doi/10.1103/PhysRevLett.69.2863.

[229] P. Calabrese and J. L. Cardy, "Entanglement entropy and quantum field theory," *J. Stat. Mech.* **0406** (2004) P06002, arXiv:hep-th/0405152 [hep-th].

[230] P. Calabrese and J. L. Cardy, "Entanglement entropy and quantum field theory: A Non-technical introduction," *Int. J. Quant. Inf.* **4** (2006) 429, arXiv:quant-ph/0505193 [quant-ph].

[231] M. Barkeshli, P. Bonderson, M. Cheng, and Z. Wang, "Symmetry, Defects, and Gauging of Topological Phases," *ArXiv e-prints* (Oct., 2014) , arXiv:1410.4540 [cond-mat.str-el].

[232] S. Vijay, T. H. Hsieh, and L. Fu, "Majorana Fermion Surface Code for Universal Quantum Computation," *Phys. Rev.* **X5** no. 4, (2015) 041038, arXiv:1504.01724 [cond-mat.mes-hall].

[233] H. Moradi and B. Yoshida *Unpublished notes* .